Quantum scalar field theory on anti-de Sitter space

Carl Kent

School of Mathematics and Statistics

Submitted in partial fulfilment for the degree of PhD

December 2013

Supervisor: Prof. Elizabeth Winstanley

University of Sheffield

Abstract

This thesis considers a real massive free quantum scalar field propagating with arbitrary coupling to n-dimensional anti-de Sitter space.

Analytical expressions are found for the field modes and Feynman Green function. The condition for the equivalence of rotational vacuum states is also established. The rotational and thermal anti-commutator functions are then derived.

A method is developed for computing the Hadamard renormalised vacuum and thermal expectation values of the quadratic field fluctuations and the stress-energy tensor. Results are obtained for $n = 2$ to $n = 11$, satisfying Wald's axioms and exhibiting the trace anomaly.

Contents

Figures

Preface

The review of the geometry of n-dimensional anti-de Sitter space (AdS_n) in chapter 2 draws heavily on material from a number of authors in the discussions of: conformal structure [9] [77]; maximal symmetry [67]; extremisation of path length [10]; the theory of hyperspherical harmonics [37] [61]; and the hypergeometric function [2].

Chapters 3 and 4 involve the independent verification of the scalar field modes [16] [25] and propagator [4] [16]. The explicit construction of the Hadamard form in section 4.4 applies the general method of [31]. Much of the introductory material on the Hadamard renormalisation of the stress-energy tensor in section 5.2.1, as well as the discussion of its ambiguity in section 5.2.3 is also adapted from [31].

For the case of vacuum expectation values (see chapter 5), the original contributions of the author are: the generalisation of Camporesi's expression for the $n = 4$ scalar field propagator [19] to $n \geq 2$; the Hadamard renormalisation of the quadratic fluctuations and the stress-energy tensor for $n \geq 2$ with explicit analytical results obtained for $n = 2$ to $n = 11$.

The author has also: established the condition for the AdS_n vacuum state of a rigidly rotating observer to coincide with that of an inertial observer in chapter 6; and in chapter 7, obtained thermal expectation values of the quadratic fluctuations and the stress-energy tensor for $n \geq 2$ with explicit numerical results for $n = 3$ to $n = 11$.

The author would like to acknowledge the help and support of his supervisor, Prof. E. Winstanley, as well as the financial support of the EPSRC.

1 Introduction

1.1 Quantum gravity

One of the main goals of theoretical physics is to establish a self-consistent framework describing all four fundamental interactions. Currently, there are essentially two extremely successful physical theories of fundamental interactions. On the one hand, the interactions of the standard model of particle physics: the electromagnetic, the weak and the strong nuclear interactions, are described by quantum field theories (QFTs). On the other hand, the gravitational interaction is described by general relativity which is a classical field theory. Both theories have consistently demonstrated immense predictive power.

There are many examples of this ability. Among them, in the case of quantum electrodynamics (QED), the fine structure constant $\boldsymbol{\alpha}$, can be derived from other experimental measurements and is found to agree with theory with an accuracy of 10^{-9} [40]. The mass of the Z-boson (a particle that mediates the weak interaction) matches predictions and has been determined to an accuracy of 3×10^{-3} (see for example [1]). The predictions of the quark model by Gell-Mann [44] and Zweig [80] continue to be observationally confirmed. Very recently, the predictions of Brout, Englert, Guralnik, Hagen, Higgs and Kibble concerning the Higgs boson, the symmetry-breaking agent responsible for endowing gauge bosons, (and thus other particles) with mass has been famously verified [8].

In the case of general relativity, a topical yet often understated point is that theoretical predictions concerning the gravitational redshift are essential considerations

in the design of the Global Positioning System (GPS) (see [7] for more). Another predictive success of general relativity is highlighted by the observed decay of the Hulse-Taylor binary pulsar system's orbital period. Theoretically, this decrease arises from energy loss due to gravitational wave emission and agrees with observations to within 2×10^{-3} [69].

Despite many efforts to construct a single theory in which all four interactions can be represented, it is not yet reality. Gravity is notoriously difficult to quantise. It is also a challenge to accommodate gravity within a universal framework because traditionally, it is inextricably connected with the very space-time on which QFTs are defined.

A fully quantised theory of gravity implies a description of nature where microscopic, relativistic and gravitational effects are all equally signficant. The appropriate regime for such a theory is defined in a natural way at the Planck scale, in terms of the fundamental constants implicit in the very theories that decribe these effects. These are respectively: Planck's reduced constant, $\hbar$; the speed of light *in vacuo*, c; and Newton's gravitational constant, G_{N}. Accordingly, the Planck scale corresponds to masses (and equivalently energies) of the order of the Planck mass,

$$m_{\mathrm{P}} := \sqrt{\frac{\hbar c}{G_{\mathrm{N}}}} = 2.18 \times 10^{-8}\ \mathrm{kg} = 1.99 \times 10^{19}\ \mathrm{GeV\,c^{-2}}, \tag{1.1}$$

and sizes of the order of the Planck length,

$$l_{\mathrm{P}} := \sqrt{\frac{\hbar G_{\mathrm{N}}}{c^3}} = 1.62 \times 10^{-35}\ \mathrm{m}. \tag{1.2}$$

The most developed and widely accepted formulation of a full quantum theory of gravity is string theory (see e.g. [65] for an introductory review). As well as quantising gravity, it describes the four fundamental interactions as facets of a single

unified interaction. This is a fundamental theory of nature in which the most basic physical entities are one-dimensional extended objects referred to as 'strings'. String theory is an umbrella term comprising several variants, in particular its modern-day incarnation M-theory [65].

A relatively small proportion of the research effort in quantum gravity focuses on non-stringy approaches. Perhaps the most well-known of these is loop quantum gravity (see [64] for an in-depth review) which is constructed using the canonical quantisation scheme.

Another route involves theories where the gravitational interaction remains classical. The justification in trying to construct a physical theory that admits all fundamental interactions consistently while not requiring gravity to be quantised is twofold.

Firstly, even if gravity were quantisable, it is unlikely that the predictions of such a theory could be observationally verified in the foreseeable future (barring the existence of extra dimensions – see section 1.3 below). This is due to the current highest collider energies (~ 8 TeV) lagging some fifteen orders of magnitude below the Planck scale.

Secondly, the expectation that gravity be quantised is largely due to a desire for consistency and unification. It is natural to consider the successful microscopic description of the standard model interactions as a template for the gravitational interaction. More generally, there is a pervading sense in theoretical physics that progressively fundamental theories will not only look increasingly elegant, but also the mathematical forms describing them will tend towards simpler and more generic forms. However strictly speaking, past experience aside, this expectation is naïve, given that there is no *a priori* requirement that suggests gravity *should* be quantised.

1.2 Quantum field theory on curved space-time

A framework that includes all fundamental interactions while not requiring that gravity be quantised is generically referred to as a QFT on a curved space-time.

A defining trait of these theories is that the concept of a vacuum state is somewhat abstruse, which inevitably affects any subsequent quantisation procedure. As pointed out in [60], the idea of a vacuum state is ambiguous and it follows therefore that the idea of a particle is too. However, it is not only the ambiguity of the vacuum state that poses a difficulty for the development of QFTs on curved space-times. The expectation values of operators quadratic in the fields and their derivatives with respect to the vacuum state are formally divergent at short distances. Unlike QFT in flat space, these divergences cannot be removed by a straightforward redefinition of the vacuum through normal-ordering. Instead, in the case of QFTs on curved space-times, a more sophisticated class of techniques is required in order to extract the physically meaningful *renormalised* expectation values.

The dynamics of such theories are encoded in the semi-classical Einstein equations

$$\mathcal{G}_{\mu\nu}(x) = \frac{8\pi G_{\mathrm{N}}}{c^4} \langle \boldsymbol{\psi} | \, T_{\mu\nu}(x) \, | \boldsymbol{\psi} \rangle_{\mathrm{ren}} \,, \tag{1.3}$$

where $\mathcal{G}_{\mu\nu}(x)$ is the Einstein tensor, representing the geometry of the background space-time, and $\langle \boldsymbol{\psi} | \, T_{\mu\nu}(x) \, | \boldsymbol{\psi} \rangle_{\mathrm{ren}}$ is the renormalised expectation value of the stress-energy tensor, embodying the matter content associated with some quantum state $|\boldsymbol{\psi}\rangle$. A feature of these renormalised expectation values is that they consist of a purely geometry-dependent part and a state-dependent part [31], a property evident from the classical-quantum split apparent on either side of (1.3).

A number of interesting predictions using QFT on curved space-times have already

been made, most notably the thermal emission from a black hole known as Hawking radiation [49] [50]. This hypothetical phenomenon is currently experimentally relevant, as it forms the basis for simulating the expected detection signatures of microscopic black holes in high-energy collisions (see section 1.3). There are other physical effects such as the Unruh effect (described by Fulling [42], Davies [27] and Unruh [72]), the Casimir effect [21], and various negative energy conditions (see as an example [41]) which are used for instance to constrain models of wormholes (see for example [39]).

QFT on curved space-time requires a physical regime in which the influence of gravity on the propagation of quantum fields is significant but its own microscopic description is irrelevant. The domain of applicability of such a theory would be in regions of extremely high spatial curvature such as in the vicinity of a black hole or in the very early stages of the universe. Such a regime would occur when the characteristic length-scale of a highly curved space-time becomes comparable to the wavelength of quantum modes propagating on it [11].

As a result QFT on curved space-times is not a fundamental physical theory but a higher-level approximation valid in a particular regime. Its rôle complements fundamental theories such as string theory through its capacity to predict and describe emergent phenomena that are not otherwise directly addressed. String theory is intended as a fundamental theory building from the foundations upwards. However, QFTs on curved space-times look at the problem from the other end, and can potentially inform the development of fundamental theories and validate other approaches.

Generally speaking the construction of semi-classical quantum theories singles out a particular type of quantum field (representing the matter content) on a particular space-time (representing the geometry) with a particular coupling between the two.

The research and associated background theory presented in this thesis relate to a quantum field of the simplest type, namely a free, electrically-neutral scalar field. This is a field that represents non-interacting spin-0 particles. Moreover, the background space-time involved is *pure* therefore the scalar field corresponds to vacuum fluctuations predicted by Heisenberg's uncertainty principle.

1.3 Extra dimensions

The motivation for considering space-times of n dimensions stems from an open question in particle physics. It is a particular 'hierarchy problem' and is the absence of a physical explanation for the extreme relative weakness of gravity, some 10^{32} times weaker than the weak nuclear interaction.

There are currently several frameworks investigating possible explanations for this anomaly that invoke the existence of extra dimensions.

One such approach is the ADD model (due to Arkani–Hamed, Dimopoulos and Dvali [6]) . It proposes that the electroweak scale is, in fact, the fundamental energy scale and accounts for the hierarchy phenomenon by positing the existence of d_{c} additional spatial dimensions of a characteristic scale r_{c}. This scale is sufficiently large that it also allows gravitational interactions to take place within these extra dimensions, but sufficiently small that the effect of other interactions are excluded – see [53] for a nice introduction. As a result, in the $n-d_{\mathrm{c}} = 3+1$ space-time dimensions of everyday experience, gravity appears extremely weak as it is effectively diluted in these hidden dimensions whereas other interactions retain their true intensity.

In this model, assuming a gravitational interaction between two test masses over a

distance $r \gg r_{\mathrm{c}}$, the gravitational potential

$$V_{\mathrm{grav}} \propto \left(m_{\mathrm{P}\,(n)}^{d_{\mathrm{c}}+2} r_{\mathrm{c}}^{d_{\mathrm{c}}} r \right)^{-1}, \tag{1.4}$$

using Gauss' law and (1.1), which should appear as

$$V_{\mathrm{grav}} \propto \left(m_{\mathrm{P}}^{2} r \right)^{-1}, \tag{1.5}$$

in four dimensions.

Following [6], a simple constraint on the value of d_{c} and that of r_{c} can be found by setting

$$m_{\mathrm{P}\,(n)}^{d_{\mathrm{c}}+2} \simeq m_{\mathrm{EW}}, \tag{1.6}$$

where m_{EW} is the electroweak energy scale,and demanding that m_{P} retain its usual value. The key result of this approach is that $d_{\mathrm{c}} \geq 2$ for $r_{\mathrm{c}} < 1$ mm.

As far as the ability to test models of hidden extra dimensions is concerned, given the Planck scale (1.1) and (1.2), and the fact that the Schwarzschild radius is given by

$$r_{\mathrm{S}} := \frac{2 G_{\mathrm{N}} m_{\mathrm{P}}}{c^2}, \tag{1.7}$$

quantum gravitational effects are expected to arise when the Compton wavelength of a particle

$$\lambda_{\mathrm{C}} = \frac{\hbar}{m_{\mathrm{P}} c}, \tag{1.8}$$

i.e. when $\lambda_{\mathrm{C}} \simeq r_{\mathrm{S}}$.

Thus the existence of extra dimensions could enable the signatures of transient microscopic black holes in collider experiments with beam energies $\sim$ TeV to be detectable [52]. As mentioned in section 1.2, simulations of microscopic black hole

events in the Large Hadron Collider (LHC) experiment at CERN rely on *higher*-dimensional QFT on curved space-times in order to accurately compute the corresponding Hawking radiation signatures.

1.4 Anti-de Sitter space

In principle, research on the behaviour of quantum fields coupled to any curved space-time could be attempted. At first glance, AdS_n looks a bit risky though. On the one hand, it is off-putting as it does not naturally respect causality [36] (see section 2.2). But on the other hand it has the promising practical feature of maximal symmetry (see section 2.3).

Perhaps the most compelling reason to study AdS_n is that it is of great interest to high-energy physics. In particular, it features in a remarkable result arising from string theory called the AdS/CFT correspondence [55]. This is a conjecture that a theory of quantum gravity on AdS_n is equivalent to a conformal field theory; that is, a QFT *without* gravity on its $(n-1)$-dimensional conformal boundary (see section 2.2 for more). Given the difficulties in integrating the gravitational interaction into a full quantum theory, a duality between a QFT with gravity and one without offers a potentially insightful perspective on the problem.

In the past, particularly in the 1970s and 1980s, research into QFT on curved space-times boomed. As Padmanabhan [62] points out '*there was a large industry computing* [*a suitable* $\langle\psi| T_{\mu\nu}(x) |\psi\rangle$] *in the hope that it has something to do with quantum gravity*'. However, with the advent of more modern approaches such as string theory, it became a less popular area of research.

This evolution has resulted in the establishment of fundamental and conceptual frameworks for developing matter content, but leaving many calculations unat-

tempted. Anti-de Sitter space is a case in point as solid foundations have already been laid [9] for the understanding and management of the causal structure of AdS_n, such that subject to certain restrictions (also discussed in section 2.2), it is a viable background for QFT.

Reflecting this state of affairs, although there is much guidance in the literature on how to compute objects such as $\langle \boldsymbol{\psi} | \, T_{\mu\nu}(x) \, | \boldsymbol{\psi} \rangle_{\text{ren}}$, in the case of AdS_n at least, published results tend to have focused on special cases. In addition, higher-dimensional calculations have only come into vogue relatively recently.

The study of AdS_n in general is therefore an important aspect of the research effort into quantum gravity. More specifically, in the context of QFT on curved space-time, although AdS_n is 'badly-behaved', its behaviour is well-understood and manageable, and as space-times go, it is relatively straightforward to work with. As the ingredients for rigorously calculating more general, and higher-dimensional cases of $\langle \boldsymbol{\psi} | \, T_{\mu\nu}(x) \, | \boldsymbol{\psi} \rangle_{\text{ren}}$ exist (see [31] for an excellent recipe), the symmetry of AdS_n provides an excellent testbed for explicit higher-dimensional Hadamard renormalisation (see chapter 5).

Finally, although QFT on AdS_n has inherent points of interest, the choice of AdS_n is also partly due to at least one ulterior motive. The results of this work are expected to contribute to ongoing research [12] into the behaviour of the analytical part of scalar field modes at spatial infinity in Schwarzschild-anti-de Sitter space ($SAdS$).

1.5 Outline

In broad terms, the goal of the research presented in this thesis is to determine some specific expectation values of the stress-energy tensor. The vacuum expectation value is the first to be investigated as it is from the vacuum state $|\mathbf{0}\rangle$ that other quantum

states can be constructed. Vacuum expectation values of QFTs on curved space-times exhibit the characteristic short-distance singularity structure (mentioned in section 1.2) that calls for renormalisation techniques. Determining the renormalised vacuum expectation value of the stress-energy tensor $\langle \mathbf{0}| T_{\mu\nu}(x) |\mathbf{0}\rangle_{\text{ren}}$ is a little involved. Accordingly, its computation hogs much of the material in this report, and rightly so. The scheme for developing the matter content relating to vacuum fluctuations is summarised in figure 1.1 below.

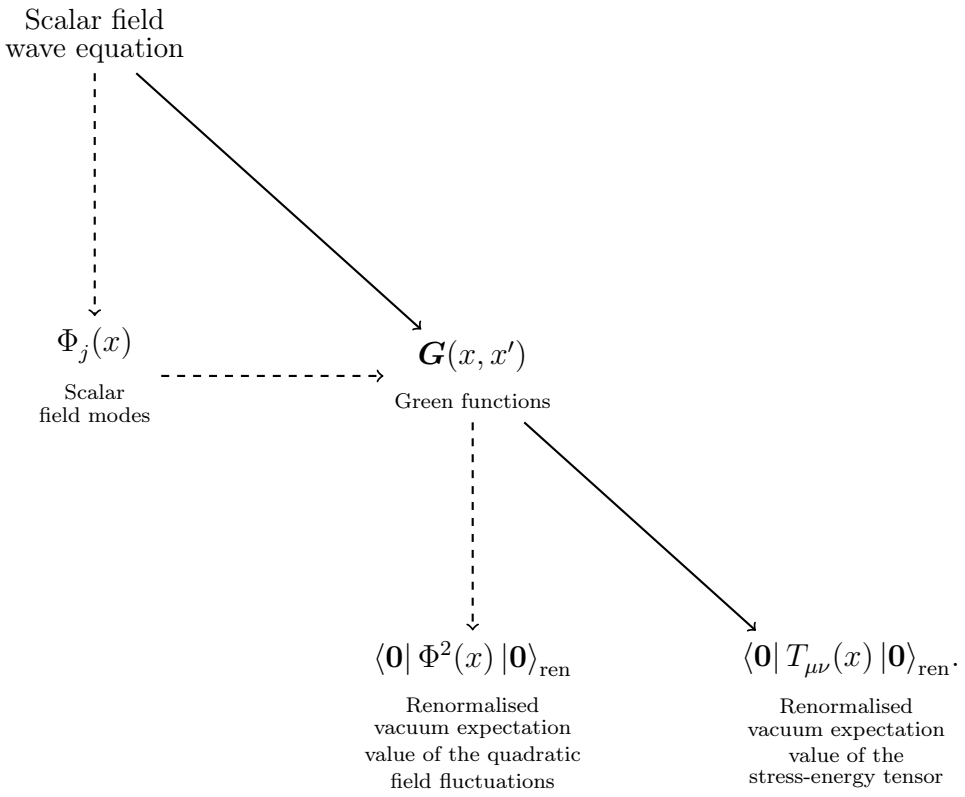

Figure 1.1 – Order of vacuum state calculations from field dynamics to matter content

The essential progression is depicted by the solid arrows running diagonally. One begins with the equations of motion, obtains a Green function solution $\boldsymbol{G}(x, x')$ whose form exposes its singularity structure readily, and then implements a renormalisation procedure culminating in an expression for the renormalised vacuum expectation

value of the stress-energy tensor.

The dashed arrows represent optional detours one may take, either to derive an expression for the Green function solution $\boldsymbol{G}(x, x')$ from expressions obtained for the field modes, or to study renormalisation in the simpler context of the vacuum expectation value of the quadratic field fluctuations $\langle \mathbf{0} | \, \Phi^2(x) \, | \mathbf{0} \rangle_{\text{ren}}$.

The scheme illustrated in 1.1 is dealt with in chapters 3 – 5.

Finding the Green function and extracting its divergences is not only necessary for the computation of $\langle \mathbf{0} | \, T_{\mu\nu}(x) \, | \mathbf{0} \rangle_{\text{ren}}$, but also provides the starting-point for determining rotational and thermal expectation values of the field. These are discussed in chapters 6 and 7.

The particular method studied in this thesis is known as Hadamard renormalisation. It is important to point out that Caldarelli [17] has already obtained expressions for $\langle \mathbf{0} | \, \Phi^2(x) \, | \mathbf{0} \rangle_{\text{ren}}$ and $\langle \mathbf{0} | \, T_{\mu\nu}(x) \, | \mathbf{0} \rangle_{\text{ren}}$ using the zeta function method. Futhermore, Wald [76] has shown the equivalence between these two methods. It is therefore *expected* that the results obtained in this thesis should agree with those published in [17]. In addition, Moretti [58] has shown this equivalence is a general result for finite-temperature field states and for compact spatial sections of a static space-time.[1]

The chapter-by-chapter development of this thesis is summarised below.

- Following this outline, having already motivated the research presented in this thesis, **Chapter 1** ends by introducing some notation conventions. The next two chapters explain some relevant background theory.

- **Chapter 2** is devoted to the geometry of the background space-time. After

[1] The author is grateful to A. Higuchi and V. Moretti for respectively bringing the references [76] and [58] to his attention.

a basic description of AdS_n, two of its properties that unavoidably affect the mathematical treatment of systems coupled to it are discussed: peculiarities in its causal structure and its behaviour at spatial infinity. Following this, its symmetries are discussed. Lastly, in preparation for appropriately handling the scalar field and its propagation, elements of the theory of hyperspherical harmonics and properties of the hypergeometric function are also covered.

- **Chapter 3** sets about solving the scalar field equations of motion. An expression for the normalised field modes is then independently verified, settling a source of disagreement in the literature.

- **Chapter 4** considers the propagation of the field with respect to $|\mathbf{0}\rangle$ in terms of Green functions. Two methods for computing the *Feynman* Green function $G_{\mathrm{F}}(x, x')$ (representing the scalar field propagator) are reviewed. Its Hadamard form $G_{\mathrm{H}}(x, x')$ is also constructed. The divergences of both G_{F} and G_{H} are then both carefully uncovered.

- **Chapter 5** addresses the Hadamard renormalisation of the expectation values of the quadratic field fluctuations and the stress-energy tensor, detailing the method of computation. The results for the renormalised vacuum expectation values, $\langle \mathbf{0}| \Phi^2(x) |\mathbf{0}\rangle_{\mathrm{ren}}$ and $\langle \mathbf{0}| T_{\mu\nu}(x) |\mathbf{0}\rangle_{\mathrm{ren}}$ can be found here as algebraic expressions and various plots.

- **Chapter 6** studies the consequences of introducing rotation into the theory developed previously for vacuum states. The states of interest are the *rotational* vacuum states $|\mathbf{0}\rangle_{\boldsymbol{\Omega}}$, corresponding to the irrotational vacuum state seen from the point of view of a rigidly-rotating observer with some fixed angular speed $\boldsymbol{\Omega} \neq 0$.

- **Chapter 7** looks at the thermal states $|\boldsymbol{\beta}\rangle$ examining the effects of the presence of an inverse temperature $\boldsymbol{\beta}$ on expectation values. Calculations are carried

out numerically and plots of the thermal expectation values, $\langle \boldsymbol{\beta} | \, \Phi^2(x) \, | \boldsymbol{\beta} \rangle$ and $\langle \boldsymbol{\beta} | \, T_{\mu\nu}(x) \, | \boldsymbol{\beta} \rangle$ appear in this chapter.

- **Chapter 8** briefly summarises what has been covered in this thesis and what has been achieved by the associated research. In addition, some ongoing unfinished business is mentioned as well as potential directions for this work.

1.6 Notation

For simplicity, the system of units used throughout the remainder of this thesis is the *Planck* unit system. It amounts to setting the constants

$$\hbar = c = G_{\mathrm{N}} = k_{\mathrm{B}} = 1, \tag{1.9}$$

where k_{B} is Boltzmann's constant.

On occasions it will also be helpful to use a notation distinguishing clearly between the numbers of space-time dimensions n, and the numbers of purely spatial and temporal dimensions d and d_0 respectively, via the simple relation

$$n = d + d_0, \tag{1.10}$$

with $n \geq 2$ and where (thankfully) $d_0 = 1$ in AdS_n.

The metric signature convention used in this thesis is *spacelike*: see Misner, Thorne and Wheeler [56] for details. This choice corresponds to the d space-space eigenvalues of a metric tensor taking on a plus sign and its d_0 time-time eigenvalues assuming a

minus sign as follows:

$$\operatorname{sgn}\operatorname{diag} g_{\mu\nu} = (\underbrace{+,+,\ldots,+}_{d \text{ entries}},\underbrace{-,-,\ldots,-}_{d_0 \text{ entries}}). \tag{1.11}$$

The signature itself is then given by $d - d_0$ [36] which is $n - 2$ for $g_{\mu\nu}$, the metric tensor on AdS_n.

The following notation conventions have been adopted:

- The set of natural numbers, strictly positive natural numbers, and strictly negative integers are respectively

$$\mathbb{N} := \{0, 1, 2, \ldots\}, \tag{1.12}$$

$$\mathbb{N}_0 := \{1, 2, \ldots\}, \tag{1.13}$$

$$\mathbb{Z}^- := \{0, -1, -2, \ldots\}. \tag{1.14}$$

- The symbols i, j, h, l, p and q; x and z; f and b; are reuseable placeholders, respectively denoting: integer indices; real and complex variables; a scalar function of one or more variables and a biscalar function.

- x also denotes a general space-time coordinate, $\underline{x}$ a general spatial coordinate and t a general time coordinate. Coordinates are distinguished using primes e.g. x, x'.

- Lowercase Greek letters are used to indicate the space-time index of a coordinate e.g. x^μ where $\mu = 0, 1, \ldots, n$. Lowercase Latin letters are used to indicate the spatial index of a coordinate e.g. x^i where $i = 1, 2, \ldots d$.

- The appearance of the same space-time or spatial index as a subscript and a superscript in a product implies the Einstein summation convention. This is a

summation over the repeated index, for example:

$$x_\mu x'^\mu := \sum_\mu x_\mu x'^\mu = x_0 x'^0 + x_1 x'^1 + \cdots + x_n x'^n. \tag{1.15}$$

- The ordinary and partial derivative operators are respectively denoted as follows:

$$\begin{aligned} d_z^k &:= \frac{d^k}{dz^k}, \\ \partial_z^k &:= \frac{\partial^k}{\partial z^k}. \end{aligned} \tag{1.16}$$

- To avoid confusion with the usage of primes to distinguish coordinates, the prime notation for derivatives is *not* used. Instead, partial and covariant derivatives appear respectively in the forms:

$$f_{,\mu} := \partial_\mu f := \frac{\partial f}{\partial x^\mu}, \tag{1.17}$$

$$V^\sigma{}_{;\mu} := \nabla_\mu V^\sigma = V^\sigma{}_{,\mu} + \Gamma^\sigma_{\mu\nu} V^\nu, \tag{1.18}$$

$$V_{\sigma;\mu} := \nabla_\mu V_\sigma = V_{\sigma,\mu} - \Gamma^\nu_{\sigma\mu} V_\nu. \tag{1.19}$$

- As is commonplace, the tilde is used to indicate an object that has undergone some transformation, e.g.

$$f \to \tilde{f}. \tag{1.20}$$

  The exact transformation will be clear from the context in which the tilde appears. Its main use is in chapter 6 to denote the coordinate transformation appropriate for a rigidly-rotating observer.

- Many of the calculations presented here rely on the application of formulae from external references. These formulae are cited using their native formula number prefixed by the symbol §.

- The symbols α, β, γ and ε are reserved as reusable placeholders for the orders and degrees of special functions. This notation has been introduced in a spirit of kerbing the population of an already abundant nomenclature. In tandem with this reuse, the binary relation

$$z \overset{(\mathrm{N})}{\longmapsto} z', \tag{1.21}$$

signifying that a correspondence has been made from the z in equation number N to z' appearing elsewhere, allows this without the need for a later redefinition of z.

By way of illustration, consider the application of the definition of the Pochhammer symbol in terms of gamma functions (§6.1.22 in [2]),

$$(\alpha)_j = \frac{\Gamma(\alpha + j)}{\Gamma(\alpha)}, \qquad \alpha \in \mathbb{C}\backslash\mathbb{Z}^-,\, j \in \mathbb{N}, \tag{1.22}$$

to some expression

$$\left(\mu + \frac{n-1}{2}\right)_k, \qquad \mu > 0,\, n \geq 2,\, k \in \mathbb{N}, \tag{1.23}$$

implies the application of the mappings

$$\begin{aligned} \alpha &\mapsto \mu + \frac{n-1}{2}, \\ j &\mapsto k, \end{aligned} \tag{1.24}$$

leading to the expression

$$\frac{\Gamma\left(\mu + \frac{n-1}{2} + k\right)}{\Gamma\left(\mu + \frac{n-1}{2}\right)}. \tag{1.25}$$

As there are many quite separate operations of this kind appearing in this work,

rather than making the *definitions*,

$$\begin{aligned} \alpha &:= \mu + \frac{n-1}{2}, \\ j &:= k, \end{aligned} \tag{1.26}$$

(meaning that a further set of symbols (or adornments to existing ones) will be required for the application of any subsequent formulae), allowing the reuse of α and j, the notation (1.21) applied to the above example gives

$$\begin{aligned} \alpha &\overset{(1.22)}{\longmapsto} \mu + \frac{n-1}{2}, \\ j &\overset{(1.22)}{\longmapsto} k, \end{aligned} \tag{1.27}$$

translating as 'the α and j in (1.22) correspond [respectively] to $\mu + \frac{n-1}{2}$ and k'. The relations (1.27) therefore imply

$$\left(\mu + \frac{n-1}{2}\right)_k = \frac{\Gamma\left(\mu + \frac{n-1}{2} + k\right)}{\Gamma\left(\mu + \frac{n-1}{2}\right)}. \tag{1.28}$$

- The study of the singularity structure of Green functions goes hand-in-hand with the renormalisation prescribed in sections 5.1 and 5.2. Typically, once expanded these functions contain a formal Laurent series (FLS).

Consider, for example the FLS

$$f(z) = \sum_{j=p}^{+\infty} X_{p-j} z^j, \qquad z > 0,\, p < 0. \tag{1.29}$$

Then as $z \to 0$, $f(z)$ diverges. In later calculations, it will be necessary to isolate the terms of $f(z)$ that do *not* vanish as $z \to 0$. Accordingly, the *non-vanishing*

part of $f(z)$ as $z \to 0$ is defined as

$$f^{\bigstar}(z) := \sum_{j=p}^{0} X_{p-j} z^j, \qquad z > 0,\, p < 0. \tag{1.30}$$

- By the same token, in later calculations, it is also helpful to introduce a way of denoting a truncation of a FLS to a second-order polynomial

$$f^{\mathbf{II}}(z) := \sum_{j=p}^{2} X_{p-j} z^j, \qquad z > 0,\, p < 0. \tag{1.31}$$

2 | Geometry of AdS_n

An anti-de Sitter space of n-dimensions (AdS_n) can be understood as the isometric immersion of a single-sheeted n-dimensional hyperboloid (see figure 2.1 in section 2.1) in some $(n+1)$-dimensional Euclidean space [10], [36], [59]. The embedding space is represented by the set of coordinates

$$\mathbb{E}^{(2,\,n-1)} = \{\zeta^\alpha\}, \qquad \alpha = 0, 1, 2, \ldots, n, \tag{2.1}$$

with the metric

$$\eta_{\alpha\beta} = \mathrm{diag}(-1, 1, 1, \ldots, 1, -1). \tag{2.2}$$

Coordinates on AdS_n are given by the constraint

$$\{x^\mu\} = \{\zeta^\alpha\}, \qquad \eta_{\alpha\beta}\zeta^\alpha\zeta^\beta = -a^2, \tag{2.3}$$

with

$$a > 0 \tag{2.4}$$

being the radius of curvature of AdS_n corresponding to the radius of the 'waist' of the hyperboloid.

The notation for the coordinates $\{x;\zeta\}$ and index labels $(\mu, \nu, \ldots; \alpha, \beta, \ldots)$ is a deliberate choice designed to distinguish between events restricted to AdS_n and *anywhere* within $\mathbb{E}^{(2,\,n-1)}$ respectively.

A suitable set of intrinsic *dimensionless* coordinates for AdS_n and their respective

domains is the set of hyperspherical coordinates,

$$\begin{aligned}
&\tau, \text{ a timelike coordinate,} && -\pi \leq \tau \leq \pi, \\
&\rho, \text{ a radial coordinate,} && 0 \leq \rho < \tfrac{\pi}{2}, \\
&\theta_j, \text{ polar coordinates,} && 0 \leq \theta_j \leq \pi, \qquad j = 1, 2, \ldots, n-3, \\
&\varphi, \text{ an azimuthal coordinate,} && 0 \leq \varphi < 2\pi,
\end{aligned} \tag{2.5}$$

where for later convenience the following definition has been made:

$$\varphi := \theta_{n-2}. \tag{2.6}$$

Coordinates in the embedding space of points in AdS_n are then parametrised as follows:

$$\begin{aligned}
x^0 &= a \cos\tau \sec\rho, \\
x^1 &= a \tan\rho \cos\theta_1, \\
x^2 &= a \tan\rho \sin\theta_1 \cos\theta_2, \\
&\vdots \\
x^{n-2} &= a \tan\rho \sin\theta_1 \sin\theta_2 \cdots \sin\theta_{n-3} \cos\varphi, \\
x^{n-1} &= a \tan\rho \sin\theta_1 \sin\theta_2 \cdots \sin\theta_{n-3} \sin\varphi, \\
x^n &= a \sin\tau \sec\rho.
\end{aligned} \tag{2.7}$$

The metric induced on AdS_n is

$$g_{\mu\nu} x^\mu x^\nu = -a^2 (\sec\rho)^2 \left[d\tau^2 - d\rho^2 - (\sin\rho)^2 \, dS^2 \right], \tag{2.8}$$

where

$$dS^2 = d\theta_1^2 + \sum_{i=2}^{n-2} \prod_{j=1}^{i-1} \left(\sin\theta_j\right)^2 d\theta_i^2 \tag{2.9}$$

is the square of the line element on a *unit* $(n-2)$-sphere, S. Equivalently,

$$g_{\mu\nu} = a^2 \left(\sec\rho\right)^2 \times \operatorname{diag}\left\{-1, 1, \left(\sin\rho\right)^2 \left[1, \left(\sin\theta_1\right)^2, \left(\sin\theta_1 \sin\theta_2\right)^2, \ldots, \left(\sin\theta_1 \cdots \sin\theta_{n-3}\right)^2\right]\right\}. \tag{2.10}$$

The non-zero Christoffel connections, $\Gamma^{\lambda}_{\mu\nu}$, are found to be

$$\lambda = \tau, \qquad \Gamma^{\tau}_{\rho\tau} = \tan\rho, \tag{2.11}$$

$$\lambda = \rho, \qquad \Gamma^{\rho}_{\tau\tau} = \Gamma^{\rho}_{\rho\rho} = \tan\rho, \tag{2.12}$$

$$\Gamma^{\rho}_{\theta_i\theta_j} = -\delta_{ij} \tan\rho \prod_{l=1}^{j-1} \left(\sin\theta_l\right)^2, \tag{2.13}$$

$$\lambda = \theta_i, \qquad \Gamma^{\theta_i}_{\rho\theta_j} = \delta_{ij} \sec\rho \operatorname{cosec}\rho, \tag{2.14}$$

$$\Gamma^{\theta_i}_{\theta_i\theta_j} = \cot\theta_j, \tag{2.15}$$

$$\Gamma^{\theta_i}_{\theta_j\theta_j} = -\cot\theta_i \prod_{l=i}^{j-1} \left(\sin\theta_l\right)^2. \tag{2.16}$$

The space-times $\mathbb{E}^{(2,n-1)}$ and AdS_n are *pseudo-Riemannian* spaces as their metrics contain both spacelike and timelike directions. The metric of AdS_n is a special case of pseudo-Riemannian metrics as it has a *single* timelike direction. Such metrics are known as *Lorentzian* metrics and naturally give rise to three classes of event separations:

$$
\begin{aligned}
g_{\mu\nu}\Delta x^\mu \Delta x^\nu < 0, &\qquad \text{timelike,} \\
g_{\mu\nu}\Delta x^\mu \Delta x^\nu = 0, &\qquad \text{lightlike or null,} \\
g_{\mu\nu}\Delta x^\mu \Delta x^\nu > 0, &\qquad \text{spacelike,} \qquad\qquad \Delta x^\mu := x_2^\mu - x_1^\mu.
\end{aligned} \tag{2.17}
$$

2.1 Basic geometry and topology

A careful consideration of figure 2.1 below is a useful starting point in appreciating the nature and subsequent peculiarities of AdS_n. Several key ideas that arise from this discussion are treated more rigorously a little later in the sections on conformal structure (section 2.2) and maximal symmetry (section 2.3).

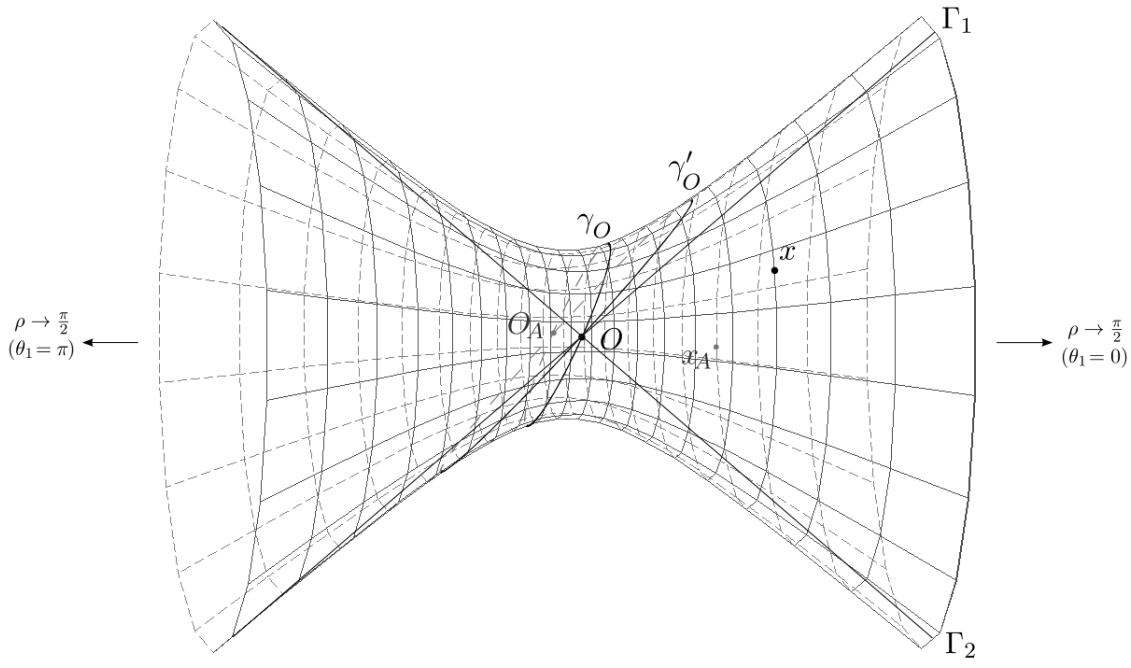

Figure 2.1 – A single-sheeted 2-hyperboloid representing AdS_n

For a fixed radius a, with $\theta_1 = 0$ for example, and suppressing $x^1, \ldots, x^{n-1}$, the local coordinate system (2.7) reduces to just x^0, x^1 and x^n and describes the upper half of a single-sheeted 2-hyperboloid. On this surface the transverse sections are parameterised by τ, and the longitudinal sections are parameterised by ρ. These appear as the fine grey lines in figure 2.1.

The suppressed local coordinates θ_j and φ are hyperspherical coordinates on the $(n-2)$-sphere of unit radius, S. These label the $n-3$ angles of inclination and the azimuthal angle respectively. As a result AdS_n is affected by $n-2$ possible coordinate singularities associated with the degeneracy at $\rho = 0$ and the $n-3$ possible polar degeneracies. For $n \geq 4$ each point on the hyperboloid corresponds to a hyperhemisphere of radius $a \tan \rho$ with positive θ_j to the right of the waist in figure 2.1 and negative θ_j to the left. Sign aside, the values of these variables are not detectable from figure 2.1 as these dimensions have been suppressed. For$n = 3$, the only angular variable is the azimuth φ, meaning that there is no notion of 'left' or 'right' of the waist in this case. For $n = 2$, as there are no angular variables, $\rho \gtrless 0$ corresponds respectively to the left and right of the waist.[1]

The topology of this space-time is $\mathbb{S}^1 \times \mathbb{R}^{n-1}$ which means the space-time has closed timelike curves. This periodicity is reflected in the parameterisation of the time coordinate τ and equivalently by the circular symmetry of the hyperboloid. The remedy to this is discussed in section 2.2. The choice of parametrisation of the radial coordinate allows spatial infinity to be represented by a finite value of ρ. These features are scrutinised in the next section.

For the time being, the consideration of AdS_n is restricted to spatially finite regions with a single natural period of 2π. Here, *purely* timelike geodesics trace out circles in the embedding space, and can be imagined as the transverse sections of the

[1]The author is grateful to A. Higuchi for clarification regarding the $n = 2$ and $n = 3$ cases.

hyperboloid in figure 2.1. Null geodesics are the only straight lines of the embedding space shared with AdS_n. The pair of null geodesics (Γ_1, Γ_2) passing through the origin O appears in figure 2.1. Such pairs mark out the light cones of events on the space-time. Timelike geodesics emanating from any point on the space-time appear as ellipses in the embedding space and are represented by the set of all sections passing through the hyperboloid at the point of origin and the corresponding antipode, defined by

$$x_{\text{A}} := x_{\text{A}}(\tau + \pi, \rho, \pi - \theta_j, \varphi + \pi) \text{ for } x = x(\tau, \rho, \theta_j, \varphi). \tag{2.18}$$

Two such geodesics γ_{O} and γ'_{O} are shown in figure 2.1. These pass through the origin O and its antipode O_{A}.

Equation (2.18) is one indication of the homogeneity of AdS_n. In particular, one may (without loss of any generality) fix the origin at *any* point of the space-time. Equivalently there are no privileged events in AdS_n (see section 2.3 for more details).

An interesting physical feature is suggested by the space-time topology. Given an initial point on the space-time and some initial velocity in a fixed direction, there is a corresponding maximum radial value for timelike geodesics. This is reminiscent of the influence of gravity on the trajectory of a projectile fired vertically away from the surface of a massive body. As such a null geodesic would correspond to a projectile with escape velocity. This comparison is consistent at least over a half-period. In any case the analogy hints at gravity-like effects induced by the topology on timelike geodesics.

2.2 Conformal structure

As mentioned previously in section 2.1, AdS_n is periodic in time which discounts it as a physically viable space-time. Visually, AdS_n may be thought of as space-time that has been 'rolled up' along a timelike dimension of infinite extent. Points on the surface of the roll relate to points on the embedding space. However, each such point is also identified with an infinity of other points in AdS_n each sitting in consecutive layers of the roll.

This multi-valued nature of time in AdS_n can be avoided by moving to the universal covering space of AdS_n [9] [36]. This space-time is denoted by $CAdS_n$ and has topology $\mathbb{R}^n$. As a result, the domain of the timelike coordinate of $CAdS_n$ is now $-\infty < \tau < +\infty$. This corresponds to effectively 'unrolling' AdS_n, and removing the closed timelike curves inherent to AdS_n in the process.

The parameterisation (2.5) allows both spatial and temporal infinity of AdS_n to be represented by a finite value [9] [46]. It follows that the entire space-time can therefore be represented by a region of finite extent. However, for such a representation to be physically meaningful, the *global* causal structure of the space-time would also need to be preserved [46]. Geometrically, this requires that the angle of the light-cone be the same throughout the representation without exception.

An equivalent requirement is that the metric of AdS_n be *conformal* everywhere to the metric of some other space-time with metric $g_{c\mu\nu}$, which is possible for any space-time [46]. Stated mathematically:

$$g_{c\mu\nu} = \Omega^2(x) g_{\mu\nu}, \tag{2.19}$$

where Ω is an arbitrary function known as the *conformal factor*. For (2.19) to be

valid at spatial infinity,

$$\Omega(\rho) \to 0, \qquad \rho \to \tfrac{\pi}{2}. \tag{2.20}$$

In this particular context, spatial infinity is referred to as *conformal infinity* and denoted by $\mathcal{I}$ [36].

The equations (2.19) and (2.20) now allow AdS_n to be 'conformally compactified', that is to be represented as a finite region while preserving its global causal structure. Such representations are referred to as Carter-Penrose (CP) diagrams.

Figure 2.2 shows a CP diagram of AdS_n where θ_1 and φ have been suppressed [9], which is the conformally compactified version of the space-time represented in figure 2.1. By convention, the timelike direction in these diagrams is vertical on the page. Conformal infinity (conventionally denoted by $\mathcal{I}$) is represented by the two vertical lines. The spacelike hypersurfaces at $\tau = 0$ and $\tau = 2\pi$ are identified. Causal trajectories emanating from $\rho = 0$ are confined to the diamonds shown. Their outline is defined by null geodesics from $\rho = 0$.

As discussed in section 2.1, a peculiarity of AdS_n is that an initially radially outward trajectory from $\rho = 0$ will begin to reconverge to its starting point following a period of $\frac{\pi}{2}$. Two timelike geodesics γ, and γ' are also shown in figure 2.2 to demonstrate this.

Figure 2.2 also shows the same trajectories on $CAdS_n$. It serves to reinforce the fact that although the problem of the multi-valued nature of time in AdS_n has been cured, a '*residual effect of the time periodicity*' persists [9].

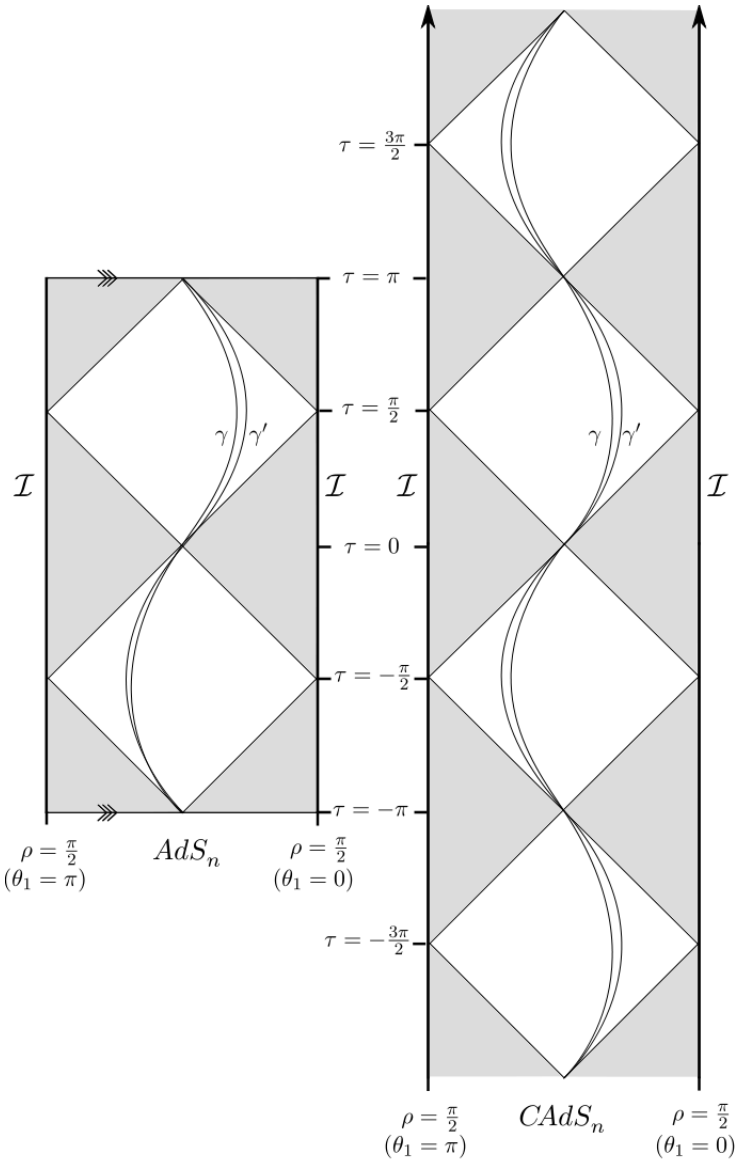

Figure 2.2 – CP diagram of AdS_n and $CAdS_n$ with θ_1 and φ suppressed

Despite this, $CAdS_n$ is still not a physically acceptable space-time. To explain why, it is necessary to introduce some background theory on the causal structure of space-times. The following theory can be found in [77].

Two distinct events $\{x, x'\}$ in a space-time are *causally related* if one event lies in or on the light-cone of the other. If x' is causally related to x and occurs in the future of x then x' is said to lie in the causal future of x, denoted by $\mathcal{J}^+(x)$. Similarly, if

x' is causally related to x and occurs in the past of x, then x' is said to lie in the causal past of x denoted by $\mathcal{J}^-(x)$.

For an arbitrary spacelike hypersurface $H \subset AdS_n$, the set of all events in AdS_n that are causally related to events on H is the union of past and future light-cones of all events on H.

$$\mathcal{J}(H) = \mathcal{J}^-(H) \cup \mathcal{J}^-(H). \tag{2.21}$$

It is worth pointing out that although an event in $\mathcal{J}^{\pm}(H)$ *may* be causally influenced by or causally influence events on H, there are possible pasts and futures of these events which may not be.

Fortunately, there is a more restricted causal region relating to the hypersurface H which defines those events in AdS_n which are *entirely* causally related to events on H. By *entirely*, it is meant that all possible causal pasts of an event in the causal future of H intersect with H. Similarly, all possible causal futures of an event in the causal past of H intersect with H.

These causal regions are respectively defined as the *future domain of dependence* of H, denoted by $\mathcal{D}^+(H)$, and the *past domain of dependence* of H, denoted by $\mathcal{D}^-(H)$. The future domain of dependence therefore is a region of the space-time in which events are *inevitably* causally influenced by events on H. As a result, events on H form a set of initial data from which events in $\mathcal{D}^+(H)$ may *always* be predicted. Likewise, the past domain of dependence is a region of the space-time whose events *inevitably* causally influence any event on H. As a result, events on H form a set of final data from which events in $\mathcal{D}^-(H)$ may *always* be 'retrodicted'.

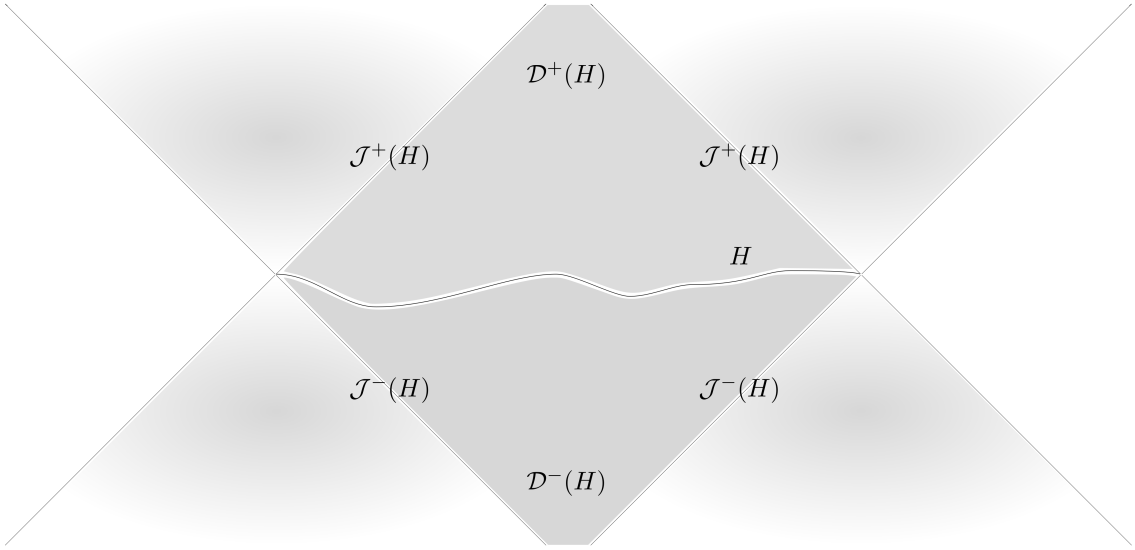

Figure 2.3 – Causally-dependent regions associated with the spacelike hypersurface H

Figure 2.3 illustrates a spacelike hypersurface H of *finite* extent and the accompanying causal regions $\mathcal{J}^-(H)$, $\mathcal{J}^+(H)$, $\mathcal{D}^-(H)$ and $\mathcal{D}^+(H)$.

The set of events that is entirely determined by events on H is

$$\mathcal{D}(H) := \mathcal{D}^-(H) \cup \mathcal{D}^+(H), \tag{2.22}$$

and is called the *full domain of dependence* of H.

If H determines *all* events in AdS_n then $\mathcal{D}(H) = AdS_n$ and H is called a *Cauchy hypersurface*, H_{C}. A space-time that admits a Cauchy hypersurface is called *globally hyperbolic*.

Having set out the theory from Wald [77], from figures 2.2 and 2.3, it can be gleaned that for the spacelike hypersurface at $\tau = 0$, there are events occuring at future times which are not influenced by any event in H. There are therefore future regions in AdS_n for which a knowledge of events in H does not allow any prediction. These

regions are shown in figure 2.2 for a geodesic emanating from $\rho = 0$ as the four shaded triangles surrounding a single unshaded diamond between some τ and $\tau + \pi$. Therefore, $CAdS_n$ remains unphysical as it is not globally hyperbolic. The reason for this is that spatial infinity in AdS_n and $CAdS_n$ is a *timelike* hypersurface.

Given this feature, any photon emitted from H in AdS_n will reach spatial infinity in a finite parameter time τ. Consequently, once the photon reaches spatial infinity, its past can no longer be traced back to H (as it no longer lies in $\mathcal{D}^+(H)$). In this way, information has been 'lost' from H to spatial infinity.

Equally, AdS_n allows information to be *introduced* from spatial infinity. A lone, radially inward photon will eventually strike H, and its past would then be retrodictable up to spatial infinity. This lack of global hyperbolicity remains following the move to $CAdS_n$ and can be attributed to the 'leakage' of information to and from spatial infinity.

Heuristically, the leak can be sealed by patching this conformal boundary with particular conditions. These need to ensure that given knowledge on some spacelike hypersurface H, all futures and pasts of events on H are determinable. As futures and pasts lose their respective predictability and retrodictability on reaching $\mathcal{I}$, a *reflection* is recommended. These reflective boundary conditions are discussed in detail for the $n = 4$ case in [9] and amount to requiring that there is '*no net flux across* [*spatial infinity*]' [9]. They are given as

$$\Phi_j^2(x) = \Phi_j^2(x_{\text{A}}), \tag{2.23}$$

implying that

$$\Phi_j^2(x) \sec\rho \to 0, \qquad \rho \to \tfrac{\pi}{2}, \tag{2.24}$$

where $\Phi_j^2(x)$ are the modes of the scalar field (introduced in section 3.5), and x_{A} is

the antipodal point to x on AdS_n defined in (2.18).

2.3 Maximal symmetry

A space-time can be pictured as being interwoven by families of integral curves associated with vector fields. If the metric of the space-time is invariant along the direction of such a curve, then the related vector field χ is called a Killing vector field. An arbitrary space-time will have a (possibly empty) set of N_χ Killing vector fields

$$\{\chi_q^\mu\}, \qquad q = 1, 2, \ldots, N_\chi, \tag{2.25}$$

with

$$N_\chi = 0, 1, \ldots, N_{\chi,\max}. \tag{2.26}$$

These Killing vectors are the tangent vectors along directions associated with isometries (i.e. distance-preserving symmetries) of the space-time.

Stephani [67] expresses this idea in a more rigorous way, as follows. Consider the infinitesimal coordinate transformation

$$\tilde{x}^\mu = x^\mu + \delta x^\mu. \tag{2.27}$$

The infinitesimal change has been made along the vector field χ at x^μ and is directed toward x^ν. This is given by

$$\delta x^\mu := \chi^\mu \left(x^\nu\right) dp, \tag{2.28}$$

where p is a parameter along the integral curve of χ through x^μ.

Similarly, the change of the metric with respect to the coordinate transformation

along this curve is given by

$$\delta g_{\mu\nu} = \frac{\partial g_{\mu\nu}}{\partial x^\rho} \chi^\rho dp. \tag{2.29}$$

Then, for distance to remain unchanged between x^μ and $\tilde{x}^\mu$,

$$\begin{aligned} \delta s^2 &= \delta \left(g_{\mu\nu} dx^\mu dx^\nu \right) \\ &= \left(g_{\mu\nu,\rho} \chi^\rho + g_{\rho\nu} \chi^\rho{}_{,\mu} + g_{\mu\rho} \chi^\rho{}_{,\nu} \right) dx^\mu dx^\nu dp \\ &= 0, \end{aligned} \tag{2.30}$$

which gives rise to the condition

$$g_{\mu\nu,\rho} \chi^\rho + g_{\rho\nu} \chi^\rho{}_{,\mu} + g_{\mu\rho} \chi^\rho{}_{,\nu} = 0. \tag{2.31}$$

Therefore any vector field that satisfies this condition is a Killing vector field of the space-time. The condition (2.31) is covariant, and the promotion of partial derivatives to covariant derivatives allows the isometry of the metric to be neatly encapsulated in the form

$$\boldsymbol{\pounds}_\chi g_{\mu\nu} := \chi_{\mu;\nu} - \chi_{\nu;\mu} = 0, \tag{2.32}$$

known as Killing's equation, where $\boldsymbol{\pounds}_\chi g_{\mu\nu}$ is the Lie derivative of the metric along the Killing vector field χ^μ.

From the Killing equation (2.32), exploiting the symmetries of the Riemann tensor, it can be shown [67] that in an n-dimensional space, the maximum possible number of linearly independent Killing vectors is

$$N_{\chi,\,\max} = \frac{n(n+1)}{2}. \tag{2.33}$$

A space possessing $N_{\chi,\max}$ Killing vectors is known as a *maximally symmetric* space. A defining feature of such a space is that the Riemann tensor may be expressed in the following way [67]:

$$\mathcal{R}_{\mu\nu\rho\sigma} = a^{-2}\left(g_{\nu\sigma}g_{\mu\rho} - g_{\nu\rho}g_{\mu\sigma}\right), \tag{2.34}$$

where a is the radius of curvature in (2.3) and

$$\mathcal{R} = a^{-2}n(n-1). \tag{2.35}$$

It follows that the radius of curvature of a maximally symmetric space is given by

$$a = \sqrt{\frac{n(n-1)}{\mathcal{R}}}. \tag{2.36}$$

Classically AdS_n is a solution to the vacuum Einstein equations, that is

$$\mathcal{G}_{\mu\nu}(x) = \mathcal{R}_{\mu\nu}(x) - \frac{1}{2}\mathcal{R}(x)g_{\mu\nu}(x) + \Lambda g_{\mu\nu}(x) = 0, \tag{2.37}$$

where $\mathcal{R}_{\mu\nu}(x)$ is the Ricci tensor, $\mathcal{R}(x)$ is the Ricci scalar and Λ is the cosmological constant.

Using (2.37) the Ricci scalar can be found by contracting with the metric tensor yielding

$$\mathcal{R} = \frac{n\Lambda}{\frac{n}{2} - 1}, \tag{2.38}$$

where Λ may be positive, zero or negative. These cases correspond respectively to n-dimensional de Sitter space-time (dS_n), Minkowski space-time ($\mathbb{M}^n$) and *anti*-de Sitter space-time (AdS_n). Thus, in view of (2.36), AdS_n is the vacuum solution to Einstein's equations of constant *negative* scalar curvature.

Many quantities of interest to studies of QFT on general space-times involve series expansions containing Riemann tensor polynomials. This a collective term for combinations of products, contractions and derivatives of the Riemann tensor and its contractions with the metric. Detailed studies have been carried out on the properties of these objects; see in particular [26] and also [30]. The most basic of the quantities involving Riemann tensor polynomials are the Hadamard series involved in renormalising the vacuum expectation value of the quadratic field fluctuations discussed in section 5.1. One benefit of maximal symmetry is that the relation (2.34) simplifies such expansions significantly, for example the covariant derivatives of all curvature tensors vanish. There are two Riemann tensor polynomials of direct relevance to later calculations. These are the Kretschmann scalar

$$\mathcal{K} := \mathcal{R}_{\mu\nu\rho\sigma}\mathcal{R}^{\mu\nu\rho\sigma}, \tag{2.39}$$

and the contraction of the Ricci tensor with itself

$$\mathcal{R}_{\mu\nu}\mathcal{R}^{\mu\nu}. \tag{2.40}$$

These are calculated here for later reference. Firstly,

$$\begin{aligned}
\mathcal{R}_{\mu\nu\rho\sigma}\mathcal{R}^{\mu\nu\rho\sigma} &= a^{-4}\left(g_{\mu\rho}g_{\nu\sigma} - g_{\mu\sigma}g_{\nu\rho}\right)\left(g^{\mu\rho}g^{\nu\sigma} - g^{\mu\sigma}g^{\nu\rho}\right) \\
&= a^{-4}\left(g_{\mu\rho}g^{\mu\rho}g_{\nu\sigma}g^{\nu\sigma} - g_{\mu\sigma}g_{\nu\rho}g^{\mu\rho}g^{\nu\sigma} - g_{\mu\rho}g_{\nu\sigma}g^{\mu\sigma}g^{\nu\rho} + g_{\mu\sigma}g^{\mu\sigma}g_{\nu\rho}g^{\nu\rho}\right) \\
&= 2a^{-4}\left(g_{\mu\rho}g^{\mu\rho}g_{\nu\sigma}g^{\nu\sigma} - g_{\mu\sigma}g_{\nu\rho}g^{\mu\rho}g^{\nu\sigma}\right) \\
&= 2a^{-4}n(n-1),
\end{aligned} \tag{2.41}$$

where the indices ρ and σ have been swapped in the third and fourth terms of the

second line. Similarly,

$$\begin{aligned}\mathcal{R}_{\nu\sigma}g^{\mu\rho}\mathcal{R}_{\mu\nu\rho\sigma} \Rightarrow \mathcal{R}_{\nu\sigma}\mathcal{R}^{\nu\sigma} &= a^{-4}\left(\delta^{\rho}{}_{\rho}g_{\nu\sigma} - \delta^{\rho}{}_{\sigma}g_{\nu\rho}\right)\left(\delta_{\lambda}{}^{\lambda}g^{\nu\sigma} - \delta_{\lambda}{}^{\sigma}g^{\nu\lambda}\right) \\ &= a^{-4}\left(\delta^{\rho}{}_{\rho}\delta_{\lambda}{}^{\lambda}\delta_{\nu}{}^{\nu} - 2\delta_{\lambda}{}^{\lambda}\delta_{\rho}{}^{\rho} + \delta^{\rho}{}_{\lambda}\delta^{\lambda}{}_{\rho}\right) \\ &= a^{-4}n(n-1)^2. \end{aligned} \tag{2.42}$$

2.4 Geodetic interval — $s(x, x')$

A further key simplification due to the maximal symmetry of AdS_n arises in the computation of the geodetic interval. Given a pair of distinct events $\{x, x'\}$ sharing a geodesic in a maximally symmetric space, any invariant biscalar quantity $b(x, x')$ dependent on this event-pair may be expressed without loss of generality as $b(0, s)$ where

$$s = s(x, x') \tag{2.43}$$

is the *geodetic* interval separating events x and x'. In particular biscalars are reducible to scalars in such settings [4]. Equivalently,

$$b(x, x') \xrightarrow{\text{maximal symmetry}} b(s). \tag{2.44}$$

It is commonplace in the literature to use a related quantity

$$\sigma(x, x') = \frac{1}{2}\left[s(x, x')\right]^{\frac{1}{2}}. \tag{2.45}$$

This is also an invariant distance originally due to Synge [68] which he named the 'world function'. Authors use the term 'geodetic interval' interchangeably between the two. Confusingly, some authors, e.g. [19] use σ to denote s.

Both AdS_n and $\mathbb{E}^{(2,n-1)}$ are maximally symmetric. Consequently, a geodetic interval separating points on AdS_n may be associated with a geodesic lying in either space. When exploiting maximal symmetry in AdS_n, it is therefore advisable to carefully distinguish in which space the geodesics in question lie.

Below, distances along geodesics in the embedding space s_{e} and σ_{e}, are treated first. Following this, the approach required to constrain geodesics to lie in AdS_n

is discussed. Expressions for distances along these geodesics *locally*, s and σ are then derived. Finally, the relationship between geodesic distances in both spaces is defined.

To begin with, consider a geodesic γ in $\mathbb{E}^{(2,n-1)}$ parametrised by p, and passing through two distinct points ζ^α and ζ'^α. The geodesic distance, $s_{\mathrm{e}}(\zeta^\alpha, \zeta'^\alpha)$, between these points is the interval along γ separating them. It is given by the integral of the line element between these points along γ. Accordingly

$$s_{\mathrm{e}} = \int_{\zeta'^\alpha}^{\zeta^\alpha} ds_{\mathrm{e}} = \int_0^1 \left(\eta_{\alpha\beta}\zeta^\alpha{}_{,p}\zeta^\beta{}_{,p}\right)^{\frac{1}{2}} dp, \tag{2.46}$$

where

$$\begin{aligned} \zeta^\alpha &:= \zeta(0), \\ \zeta'^\alpha &:= \zeta(1). \end{aligned} \tag{2.47}$$

Given (2.46), the equation (2.45) is written

$$\sigma_{\mathrm{e}}(\zeta, \zeta') = \frac{1}{2}\eta_{\alpha\beta}\left(\zeta'^\alpha - \zeta^\alpha\right)\left(\zeta'^\beta - \zeta^\beta\right). \tag{2.48}$$

Specialising to events lying on AdS_n, the geodetic interval on the embedding space is now

$$\sigma_{\mathrm{e}}(x, x') = \frac{1}{2}\eta_{\mu\nu}\left(x^\mu - x'^\mu\right)\left(x^\nu - x'^\nu\right). \tag{2.49}$$

In order to describe the geodetic interval in terms of the coordinates intrinsic to AdS_n, it is helpful to define the decomposition,

$$\sigma_{\mathrm{e}}(x, x') := \sum_\mu \sigma_\mu, \tag{2.50}$$

where

$$\sigma_0 + \sigma_n = a^2 \left\{ \sec\rho \, \sec\rho' \left(\cos\tau \, \cos\tau' + \sin\tau \, \sin\tau' \right) - \frac{1}{2} \left[(\sec\rho)^2 + (\sec\rho')^2 \right] \right\} \tag{2.51}$$

and

$$\sigma_k := a^2 \left[\frac{\left(x^k\right)^2}{2} + \frac{\left(x'^k\right)^2}{2} - x^k x'^k \right], \qquad k = 1, 2, \ldots, n-1. \tag{2.52}$$

Therefore

$$\sum_{k=1}^{n-1} \sigma_k = a^2 \Bigg[\frac{(\tan\rho)^2 + (\tan\rho')^2}{2} + \tan\rho \, \tan\rho' \times \left(\sum_{i=1}^{n-2} \left[\cos\theta_i \cos\theta_i' \prod_{j=1}^{i-1} \sin\theta_j \sin\theta_j' \right] + \prod_{l=1}^{n-2} \sin\theta_l \sin\theta_l' \right) \Bigg]. \tag{2.53}$$

Combining (2.51) and (2.53) using (2.50) results in

$$\sigma_{\mathrm{e}}(x, x') = a^2 \Bigg[\sec\rho \, \sec\rho' \left(\cos\tau \, \cos\tau' + \sin\tau \, \sin\tau' \right) - 1 + \tan\rho \, \tan\rho' \times \left(\sum_{i=1}^{n-2} \left[\cos\theta_i \cos\theta_i' \prod_{j=1}^{i-1} \sin\theta_j \sin\theta_j' \right] + \prod_{l=1}^{n-2} \sin\theta_l \sin\theta_l' \right) \Bigg], \tag{2.54}$$

and hence

$$\sigma_{\mathrm{e}}(x, 0) = a^2 \left(\sec\rho \cos\tau - 1 \right). \tag{2.55}$$

which is in agreement with [9] and [16].

Following Bengtsson's treatment in [10], suitable geodesics on the *embedded* space

AdS_n can be found by extremising the path length in $\mathbb{E}^{(2,\,n-1)}$ subject to the constraint (2.3). The method of finding the form of these geodesics is a straightforward variational problem where the action is the path length. The definition of the embedded hyperboloid appears as an undetermined Lagrange multiplier term constraining the extremisation to paths on AdS_n.

Using the coordinates $\{\zeta^\alpha\}$ of the embedding space of an appropriate Lagrangian for this treatment is [10], with and p a geodetic parametrisation,

$$\mathcal{L}_{\mathrm{B}} := \frac{1}{2}\left(\zeta_{,p}\right)^{\,2} + \boldsymbol{\kappa}_{\mathrm{B}}\left(\zeta^2 + a^2\right), \tag{2.56}$$

where

$$\begin{aligned} \zeta^2 &= \zeta_\alpha \zeta^\alpha, \\ \left(\zeta_{,p}\right)^{\,2} &= -\frac{1}{2}\left(\zeta_\alpha \zeta_{\beta,p} - \zeta_\beta \zeta_{\alpha,p}\right)\left(\zeta^\alpha \zeta^\beta{}_{,p} - \zeta^\beta \zeta^\alpha{}_{,p}\right), \end{aligned} \tag{2.57}$$

and where $\boldsymbol{\kappa}_{\mathrm{B}}$ is the undetermined constant Lagrange multiplier.

Applying the Euler-Lagrange equations

$$\frac{\partial \mathcal{L}_{\mathrm{B}}}{\partial \zeta_\alpha} = \partial_p \frac{\partial \mathcal{L}_{\mathrm{B}}}{\partial\left(\zeta_{\alpha,p}\right)} \tag{2.58}$$

to (2.56), the following equations of motion for the coordinates and their derivatives with respect to x^μ are obtained:

$$\zeta_{\alpha,pp} = 2\boldsymbol{\kappa}_{\mathrm{B}} \zeta_\alpha. \tag{2.59}$$

Now that these equations are confined to AdS_n using (2.3), equation (2.59) may be written as

$$x_{\mu,pp} = 2\boldsymbol{\kappa}_{\mathrm{B}} x_\mu. \tag{2.60}$$

It can be shown [10] that the Lagrange multiplier of (2.56) is determined as

$$\boldsymbol{\kappa}_{\mathrm{B}} = \frac{1}{2a^2}\left(x_{,p}\right)^2, \tag{2.61}$$

and so the equation of motion to be solved is reduced to the set of second order linear differential equations

$$x_{\mu,pp} = \left(x_{,p}\right)^2 x_{\mu}, \tag{2.62}$$

with *constant* coefficients.

The solutions to (2.62) are [10]

$$\begin{aligned} x_{\mu} &= \boldsymbol{\kappa}_{1\,\mu}\exp\left(\boldsymbol{i}\sqrt{\left(x_{,p}\right)^2}\,\varsigma\right) + \boldsymbol{\kappa}_{2\,\mu}\exp\left(-\boldsymbol{i}\sqrt{\left(x_{,p}\right)^2}\,\varsigma\right), \qquad \text{for timelike geodesics,} \\ x_{\mu} &= \boldsymbol{\kappa}_{1\,\mu}\exp\left(\sqrt{\left(x_{,p}\right)^2}\,\tau\right) + \boldsymbol{\kappa}_{2\,\mu}\exp\left(-\sqrt{\left(x_{,p}\right)^2}\,\tau\right), \qquad \text{for spacelike geodesics,} \end{aligned} \tag{2.63}$$

at a fixed spatial location $\varsigma := \varsigma(\rho, \theta_j, \varphi)$ and fixed time τ respectively, and where the constants $\boldsymbol{\kappa}_{1\,\mu}$ and $\boldsymbol{\kappa}_{2\,\mu}$ satisfy the following conditions [10]:

$$\begin{aligned} \boldsymbol{\kappa}_{1\,\mu}\,\boldsymbol{\kappa}_1{}^{\mu} &= \boldsymbol{\kappa}_{2\,\mu}\,\boldsymbol{\kappa}_2{}^{\mu} = 0, \\ \boldsymbol{\kappa}_{1\,\mu}\,\boldsymbol{\kappa}_2{}^{\mu} &= -\frac{1}{2}. \end{aligned} \tag{2.64}$$

The solution for null separations [10] is simply

$$x_{\mu,pp} = 0, \tag{2.65}$$

which describes straight lines in Euclidean spaces.

In this treatment, the vectors x^{μ} are most usefully thought of as vectors pointing to

some location on AdS_n. Distances along geodesics restricted to lie in AdS_n between events x^μ and x'^μ can then be found by applying the scalar product

$$g_{\mu\nu}x^\mu x'^\nu, \tag{2.66}$$

to (2.63), where

$$\begin{aligned} &x^\mu := x^\mu(\varsigma), \quad x'^\mu := x^\mu(\varsigma'), && \text{for timelike separations,} \\ &x^\mu := x^\mu(\tau), \quad x'^\mu := x^\mu(\tau'), && \text{for spacelike separations.} \end{aligned} \tag{2.67}$$

Bearing in mind that for events confined to AdS_n there is now an analogous equation to (2.46) which may be expressed as

$$s = \int_\gamma ds = \sqrt{\left(x_{,p}\right)^2}(\varsigma' - \varsigma), \tag{2.68}$$

for timelike separations, and as

$$s = \int_\gamma ds = \sqrt{\left(x_{,p}\right)^2}(\tau' - \tau), \tag{2.69}$$

for spacelike separations, the expression (2.66) equates to

$$g_{\mu\nu}x^\mu x'^\nu = \begin{cases} -\cos\left(\dfrac{s}{a}\right) & \text{for timelike separations,} \quad (2.70a) \\ -\cosh\left(\dfrac{s}{a}\right) & \text{for spacelike separations.} \quad (2.70b) \end{cases}$$

Therefore, both timelike and spacelike separations may be expressed as (2.70b) if the separation s is purely imaginary for timelike separations.

The classification of event separations along geodesics in AdS_n may now be sum-

marised in terms of criteria involving the value of s. In particular

$$\begin{aligned} s^2 < 0, &\qquad \text{timelike,} \\ s^2 = 0, &\qquad \text{lightlike or null,} \\ s^2 > 0, &\qquad \text{spacelike.} \end{aligned} \tag{2.71}$$

Geometrically, the invariant distances s_{e} and σ_{e} may be thought of as chordal distances between points in AdS_n through $\mathbb{E}^{(2,\,n-1)}$ subtended by the angle $\frac{s}{a}$. Similarly, from the point of view of the embedding space, s and σ may be thought of as arc lengths separating events on the embedded surface.

Recalling (2.49), (2.50) and (2.3), the world-function on the embedding space can be expressed as:

$$\sigma_{\mathrm{e}} = -a^2 \left(1 + \eta_{\alpha\beta}\zeta^{\alpha}\zeta'^{\beta}\right). \tag{2.72}$$

Given (2.70b) and (2.45) the invariant measures of distance s and σ between events in AdS_n along geodesics in both $\mathbb{E}^{(2,\,n-1)}$ and AdS_n are related as follows:

$$\begin{aligned} \cosh\left(\frac{s}{a}\right) &= 1 + \frac{s_{\mathrm{e}}^2}{2a^2} \\ \cosh\left(\frac{\sqrt{2\sigma}}{a}\right) &= 1 + \frac{\sigma_{\mathrm{e}}}{a^2}. \end{aligned} \tag{2.73}$$

Events in any pseudo-Riemannian space are not necessarily geodetically separated [4]. Given an event at the origin $x = 0$, and defining $H(0)$ to be the spacelike hypersurface at $\tau = 0$, then the set of all events x' that are not geodetically separated

from x is given for

$$AdS_n \text{ by } x' \in \{AdS_n - [\mathcal{J}(H(0)) \cup H(0+2\pi k)]\}\,, \qquad k \in \mathbb{Z},$$
$$CAdS_n \text{ by } x' \in \{AdS_n - [\mathcal{J}(H(0)) \cup H(0)]\}\,. \tag{2.74}$$

In other words, $\{x'\}$ in these circumstances is the set of all events *outside* $\mathcal{J}(H(0))$ and *off* $H(0)$. It appears in figure 2.2 as the shaded areas of AdS_n and $CAdS_n$.

Despite this, non-geodetic event separations can be described via analytic continuation [4]. Defining a dimensionless parameter

$$z_1 := \left[\cosh\left(\frac{s}{2a}\right)\right]^2, \tag{2.75}$$

specifically for separations along a geodesic, allows the description of *any* event separation [4] to be written as

$$z_1 = \frac{1}{2}\left[1 + \cosh\left(\frac{s}{a}\right)\right]. \tag{2.76}$$

Finally, for completeness, the explicit relation between $\sigma_{\rm e}$ and σ is as follows:

$$\sigma_{\rm e} = a^2\left[\cosh\left(\frac{1}{a}\sqrt{\frac{\sigma}{2}}\right) - 1\right], \tag{2.77}$$

2.5 Hyperspherical harmonics — $Y_\ell(\theta,\varphi)$

The theory of hyperspherical harmonics is covered in depth by Erdélyi in [37] and by Müller in [61]. A basic knowledge of hyperspherical harmonics is relevant to three aspects of the research presented in this thesis:

- The separation and normalisation of scalar field modes (in sections 3.3 and 3.6).
- The study of the effect of rotation on the vacuum in $CAdS_n$ (in chapter 6).
- The study of the effect of thermal radiation (in chapter 7).

To begin with, the unit hypersphere S is defined here for $n \geq 3$ as the $(n-2)$-sphere of unit radius, of area

$$A_S = \frac{2\pi^{\frac{n-1}{2}}}{\Gamma\left(\frac{n-1}{2}\right)}. \tag{2.78}$$

Each of the $n-2$ angular coordinates, θ_j, φ, $(j = 1, 2, \ldots, n-3)$ is exclusively associated with one of the $n-2$ angular quantum numbers,

$$m_i = m_0, m_1, \ldots, m_{n-3}, \qquad m_0 \geq m_1 \geq \ldots \geq m_{n-3} \geq 0. \tag{2.79}$$

It is convenient to single out the quantum number associated with the polar angle θ_1, which is present in the definition of S for *all* $n \geq 3$, with the label

$$\ell := m_0, \tag{2.80}$$

as well as the azimuthal quantum number with the label,

$$m := m_{n-3}. \tag{2.81}$$

The degree ℓ labelling the harmonics collectively, actually denotes a *set* of values of m_j, with the understanding that for a given ℓ there is more than one possible set of corresponding values. For completeness, the multiplicity of ℓ [25] [37] [61] is given by

$$\mathfrak{M}_\ell = (2\ell + n - 3)\frac{(\ell + n - 4)!}{\ell!(n-3)!}. \tag{2.82}$$

The $\breve{Y}_\ell(\theta,\phi)$ are the complex *unnormalised* hyperspherical harmonics of order $n-2$ and degree $\ell = 0,1,\ldots n-2$. They form a complete set $\{\breve{Y}_\ell^p(\theta,\phi)\}$, with $p = 1,2,\ldots \mathfrak{M}_\ell$.

Any two distinct $\breve{Y}_\ell^p(\theta,\varphi)$ are orthogonal on S, i.e.

$$\int_S dS\ \breve{Y}_\ell^p(\theta,\varphi)\breve{Y}_\ell^q(\theta,\varphi) = 0, \qquad \forall\, p \neq q, \tag{2.83}$$

unless they are complex conjugate, in which case

$$\int_S dS \left|\breve{Y}_\ell^p(\theta,\varphi)\right|^2 = N_{m_i}. \tag{2.84}$$

Therefore, the hyperspherical harmonics of degree ℓ on S, *normalised to unity* are

$$Y_\ell^p(\theta,\varphi) := \frac{1}{\sqrt{N_{m_i}}}\breve{Y}_\ell^p(\theta,\varphi). \tag{2.85}$$

A form of these normalised harmonics expressed explicitly in terms of all the $n-2$ angular coordinates is useful in the study of rotational and thermal states considered in chapters 6 and 7 respectively. The expression used is given in [37] by

$$Y_\ell(\theta,\varphi) = \frac{1}{\sqrt{N_{m_i}}} e^{\pm i m\varphi} \prod_{j=0}^{n-4} \left(\sin\theta_{j+1}\right)^{m_{j+1}} C_{m_j-m_{j+1}}^{m_{j+1}+\frac{n-j-3}{2}}\left(\cos\theta_{j+1}\right), \tag{2.86}$$

where $C_{m_j-m_{j+1}}^{m_{j+1}+\frac{n-j-3}{2}}\left(\cos\theta_{j+1}\right)$ are Gegenbauer polynomials [2] [45], and where

$$N_{m_i} := 2\pi \prod_{j=0}^{n-4} E_{j+1}\left(m_j, m_{j+1}\right), \tag{2.87}$$

with

$$E_{j+1}\left(m_j, m_{j+1}\right) = \frac{\pi 4^{-\left(m_{j+1}+\frac{n-3-j}{2}-\frac{1}{2}\right)}\Gamma\left(m_j + m_{j+1} + n - 3 - j\right)}{\left(m_j + \frac{n-j-3}{2}\right)\left(m_j - m_{j+1}\right)!\left[\Gamma\left(m_{j+1}+\frac{n-j-3}{2}\right)\right]^2}. \tag{2.88}$$

Temporarily dropping the arguments of the harmonics for clarity, a *real* orthonormal basis can be constructed from the Y_ℓ^p by defining the set of real hyperspherical harmonics of unit norm on S,

$$\bar{Y}_\ell = \left\{ \bar{Y}_\ell^q \in \mathbb{R},\, q = 1, 2, \ldots \tfrac{1}{2}\mathfrak{M}_\ell \right\}, \tag{2.89}$$

to be for example,

$$\bar{Y}_\ell^q := \frac{1}{\sqrt{2}} \left\{ Y_\ell^q + (Y_\ell^q)^* \right\} = \sqrt{2}\, \mathrm{Re}\, Y_\ell^p, \qquad m > 0, \tag{2.90}$$

or as another example,

$$\hat{\bar{Y}}_\ell^q := \frac{\boldsymbol{i}}{\sqrt{2}} \left\{ (Y_\ell^q)^* - Y_\ell^q \right\} = \sqrt{2}\, \mathrm{Im}\, Y_\ell^p, \qquad m > 0, \tag{2.91}$$

remarking that,

$$\bar{Y}_\ell^q = \hat{\bar{Y}}_\ell^q = Y_\ell^q = (Y_\ell^q)^*, \qquad m = 0. \tag{2.92}$$

It is convenient in what follows to define the further shorthand notation,

$$\bar{Y}^q := \bar{Y}_\ell^q(\theta, \varphi), \qquad \bar{Y}^{q'} := \bar{Y}_\ell^q(\theta', \varphi'), \qquad Y^q := Y_\ell^q(\theta, \varphi), \qquad Y^{q'} := Y_\ell^q(\theta', \varphi'), \tag{2.93}$$

such that (2.92) leads to

$$\bar{Y}^q \bar{Y}^{q'} = \frac{1}{2} \left\{ Y^q (Y^{q'})^* + (Y^q)^*\, Y^{q'} \right\}, \qquad m = 0, \tag{2.94}$$

and (2.90) gives

$$\bar{Y}^q \bar{Y}^{q'} = \frac{1}{2} \left\{ Y^q Y^{q'} + Y^q (Y^{q'})^* + (Y^q)^*\, Y^{q'} + (Y^q)^*\, (Y^{q'})^* \right\}, \qquad m > 0. \tag{2.95}$$

Then it follows that

$$\sum_{q=1}^{\frac{1}{2}\mathfrak{M}_\ell} \bar{Y}^q \bar{Y}^{q'} = \frac{1}{2} \sum_{q=1}^{\frac{1}{2}\mathfrak{M}_\ell} \left\{ Y^q (Y^{q'})^* + (Y^q)^* Y^{q'} \right\}, \qquad m = 0, \tag{2.96}$$

and

$$\begin{aligned} \sum_{q=1}^{\frac{1}{2}\mathfrak{M}_\ell} \bar{Y}^q \bar{Y}^{q'} &= \sum_{q=1}^{\frac{1}{2}\mathfrak{M}_\ell} \left\{ \bar{Y}^q \bar{Y}^{q'}|_{m>0} + \bar{Y}^q \bar{Y}^{q'}|_{m=0} \right\} \\ &= \sum_{q=1}^{\frac{1}{2}\mathfrak{M}_\ell} \left\{ Y^q (Y^{q'})^* + (Y^q)^* Y^{q'} \right\}, \end{aligned} \tag{2.97}$$

by adding (2.94) and (2.95) resulting in the disappearance of the first and last terms in braces in (2.95).

Therefore

$$\sum_{q=1}^{\frac{1}{2}\mathfrak{M}_\ell} \bar{Y}^q \bar{Y}^{q'} = \sum_{q=1}^{\frac{1}{2}\mathfrak{M}_\ell} \epsilon_m \left\{ Y^q (Y^{q'})^* + (Y^q)^* Y^{q'} \right\}, \qquad \forall m, \tag{2.98}$$

where

$$\epsilon_m := \begin{cases} \frac{1}{2}, & m = 0, \quad (2.99a) \\ 1, & m > 0. \quad (2.99b) \end{cases}$$

Now,

$$\sum_{q=1}^{\frac{1}{2}\mathfrak{M}_\ell} \bar{Y}^q \bar{Y}^{q'} = \sum_{m_1=0}^{\ell} \sum_{m_2=0}^{m_1} \cdots \sum_{m_{n-5}=0}^{m_{n-4}} \sum_{m=0}^{m_{n-4}} \epsilon_m \left\{ e^{\boldsymbol{i} m(\varphi-\varphi')} + e^{-\boldsymbol{i} m(\varphi-\varphi')} \right\} \Theta_{m_i} \Theta'_{m_i} \tag{2.100}$$

$$= \sum_{m_1=0}^{\ell} \sum_{m_2=0}^{m_1} \cdots \sum_{m_{n-5}=0}^{m_{n-4}} \sum_{m=0}^{m_{n-4}} \epsilon_m e^{\pm \boldsymbol{i} m(\varphi-\varphi')} \Theta_{m_i} \Theta'_{m_i} \tag{2.101}$$

$$= \sum_{m_i} e^{\boldsymbol{i} m(\varphi-\varphi')} \Theta_{m_i} \Theta'_{m_i}, \tag{2.102}$$

where

$$\Theta_{m_i} := \frac{1}{\sqrt{N_{m_i}}} \prod_{j=0}^{n-4} \left(\sin\theta_{j+1}\right)^{m_{j+1}} C_{m_j - m_{j+1}}^{m_{j+1}+\frac{n-j-3}{2}} \left(\cos\theta_{j+1}\right), \tag{2.103}$$

such that (2.86) may be written as

$$Y_\ell^p(\theta,\varphi) = e^{\pm i m\varphi}\Theta_{m_i}(\theta), \tag{2.104}$$

and where

$$\sum_{m_i} f = \sum_{m_1=0}^{\ell} \sum_{m_2=0}^{m_1} \cdots \sum_{m_{n-5}=0}^{m_{n-4}} \sum_{m=-m_{n-4}}^{m_{n-4}} f. \tag{2.105}$$

Therefore,

$$\sum_{q=1}^{\frac{1}{2}\mathfrak{M}_\ell} \bar{Y}^q \bar{Y}^{q'} = \sum_{p=1}^{\mathfrak{M}_\ell} Y^p (Y^{p'})^*. \tag{2.106}$$

For $n \geq 4$, the addition theorem for real normalised hyperspherical harmonics $\bar{Y}_\ell^q(\theta,\varphi)$ (§11.4.2 and §11.4.3 in [37]) states that

$$\frac{C_\ell^{\frac{n-3}{2}}(\hat{x}\cdot\hat{x}')}{C_\ell^{\frac{n-3}{2}}(1)} = A_S \mathfrak{M}_\ell \sum_{q=1}^{\frac{1}{2}\mathfrak{M}_\ell} \bar{Y}_\ell^q(\theta,\varphi)\bar{Y}_\ell^q(\theta',\varphi'), \tag{2.107}$$

where $\hat{x}, \hat{x}'$ are unit vectors on S.

Using (2.106), equation (2.107) is given by

$$\sum_{p=1}^{\mathfrak{M}_\ell} Y_\ell^p(\theta,\varphi)\Big(Y_\ell^p(\theta',\varphi')\Big)^* = \frac{\mathfrak{M}_\ell}{A_S}\frac{C_\ell^{\frac{n-3}{2}}(\hat{x}\cdot\hat{x}')}{C_\ell^{\frac{n-3}{2}}(1)}. \tag{2.108}$$

From §11.1.28 in [37] and §22.4.2 in [2],

$$C_\ell^{\frac{n-3}{2}}(1) = \frac{(\ell+n-4)!}{\ell!(n-4)!}, \qquad n \geq 4. \tag{2.109}$$

Therefore, from (2.82)

$$\sum_{p=1}^{\mathfrak{M}_\ell} Y_\ell^p(\theta,\varphi)\Big(Y_\ell^p(\theta',\varphi')\Big)^* = \frac{1}{A_S}\frac{2\ell+n-3}{n-3}C_\ell^{\frac{n-3}{2}}(\hat{x}\cdot\hat{x}')\,, \qquad n\geq 4, \tag{2.110}$$

which reduces to

$$\sum_{p=1}^{\mathfrak{M}_\ell} Y_\ell^p(\theta,\varphi)\Big(Y_\ell^p(\theta',\varphi')\Big)^* = \frac{1}{A_S}(2\ell+1)P_\ell\,(\hat{x}\cdot\hat{x}')\,, \qquad n=4, \tag{2.111}$$

where $P_\ell\,(\hat{x}\cdot\hat{x}')$ is a Legendre polynomial. The addition theorem (2.108) extends to $n=3$ [61], using $\mathfrak{M}_\ell = 2$. From §22.5.28 in [2],

$$C_\ell^0(\hat{x}\cdot\hat{x}') = \frac{2}{\ell}T_\ell\,(\hat{x}\cdot\hat{x}')\,, \qquad \ell>0, \tag{2.112}$$

where $T_\ell\,(\hat{x}\cdot\hat{x}')$ is a Chebyshev polynomial, and from §22.2.3 in [2] where,

$$C_\ell^0(1) = \frac{2}{\ell}, \qquad \ell>0, \tag{2.113}$$

and

$$C_0^0(z) = 1, \qquad \forall\, z\in\mathbb{R}, \tag{2.114}$$

it follows that,

$$\sum_{p=1}^{2} Y_\ell^p(\theta,\varphi)\Big(Y_\ell^p(\theta',\varphi')\Big)^* = \frac{1}{\pi}T_\ell\,(\hat{x}\cdot\hat{x}')\,, \qquad n=3. \tag{2.115}$$

The result (2.115) is therefore true for $\ell>0$ using (2.113) and (2.112) and for $\ell=0$ using (2.114). Moreover, from §22.3.15 in [2],

$$T_\ell(\hat{x}\cdot\hat{x}') = \cos\left(\ell\theta_1\right). \tag{2.116}$$

2.6 The hypergeometric function — $F[\alpha, \beta; \gamma; z]$

Owing to its frequent use throughout this thesis, it is worthwhile stating the basic features of the Gaussian hypergeometric function that are relevant to later calculations. The hypergeometric function plays a significant rôle in the construction of the radial scalar field modes in section 3.4 and also in the study of Green functions in section 4.1. The following description is heavily adapted from chapter 15 in [2].

The hypergeometric *series* is given by [2]

$$F[\alpha, \beta; \gamma; z] := \frac{\Gamma(\gamma)}{\Gamma(\alpha)\Gamma(\beta)} \sum_{j=0}^{+\infty} \frac{\Gamma(\alpha+j)\Gamma(\beta+j)}{\Gamma(\gamma+j)} \frac{z^j}{j!}. \tag{2.117}$$

The series (2.117) can also be expressed in terms of Pochhammer symbols $(z)_j$, given by §6.1.22 [2]

$$\begin{aligned} (z)_0 &:= 1 \\ (z)_j &:= z(z+1)(z+2)\cdots(z+j-1) = \frac{\Gamma(z+j)}{\Gamma(z)}, \qquad j \in \mathbb{N}_0, \end{aligned} \tag{2.118}$$

as

$$F[\alpha, \beta; \gamma; z] := \sum_{j=0}^{+\infty} \frac{(\alpha)_j (\beta)_j}{(\gamma)_j} \frac{z^j}{j!}. \tag{2.119}$$

The convergence criteria of the hypergeometric function $F(z)$ generated by the hypergeometric series, are determined by the behaviour of its series representation on the latter's circle of convergence of radius $|z| = 1$.

Accordingly, if:

$$|z| < 1, \qquad F \text{ converges } \textit{absolutely}; \tag{2.120}$$

$$|z| = 1,\ z = 1, \quad F \text{ converges } \textit{absolutely}, \qquad 0 < \mathrm{Re}(\gamma - \alpha - \beta),\ \gamma \notin \mathbb{Z}^{-}; \tag{2.121}$$

$$|z| = 1,\ z \neq 1, \quad F \text{ converges } \textit{absolutely}, \qquad 0 < \mathrm{Re}(\gamma - \alpha - \beta), \tag{2.122a}$$

$$F \text{ converges } \textit{conditionally}, \quad -1 < \mathrm{Re}(\gamma - \alpha - \beta) \leq 0, \tag{2.122b}$$

$$F \text{ diverges}, \qquad \mathrm{Re}(\gamma - \alpha - \beta) \leq -1; \tag{2.122c}$$

$$|z| > 1, \qquad F \text{ diverges}. \tag{2.123}$$

A point of interest concerning the analyticity of the hypergeometric function (2.117), visible from (2.120) is that F is *cut* in the complex plane along $z \leq 1$.

Solutions $\boldsymbol{F}(z)$ to the hypergeometric differential equation [2]

$$z(z-1)\boldsymbol{F}_{,zz} + [\gamma - (\alpha + \beta + 1)z]\boldsymbol{F}_{,z} - \alpha\beta\boldsymbol{F} = 0, \tag{2.124}$$

are comprised of many possible linear pairings of hypergeometric functions. The specific form of these solutions depends partly on the the properties of α, β and γ and how these parameters interrelate. In addition, equation (2.124) possesses three regular singular points at $z = 0, 1, \infty$, the vicinity of which also characterises the choice of solutions – see section 15.5 in [2] for details of the make-up of $\boldsymbol{F}$.

3 | Scalar QFT coupled to AdS_n

3.1 Field dynamics

The action for a free, real quantum scalar field $\Phi(x)$ coupled to AdS_n is,

$$\mathcal{S}[\Phi, g_{\mu\nu}] = -\frac{1}{2}\int_{AdS_n} d^n x \sqrt{g}\left(g^{\mu\nu}\Phi_{;\mu}\Phi_{;\nu} + m_\xi^2\Phi^2\right), \tag{3.1}$$

where g is defined as

$$g := \left|\det g_{\mu\nu}\right|, \tag{3.2}$$

with the effective mass-squared term

$$m_\xi^2(x) := m^2 + \xi\mathcal{R}(x), \tag{3.3}$$

where m is the mass of the field quanta, the constant ξ is the coupling strength between the scalar and classical gravitational fields and $\mathcal{R}(x)$ is the Ricci scalar curvature of the background space-time.

The related equation of motion is the Klein-Gordon equation,

$$\left(\Box - m_\xi^2(x)\right)\Phi(x) = 0, \tag{3.4}$$

where $\Box$ is the Laplace-Beltrami operator.

The equation (3.4) admits a complete set of solutions $\Phi_j(x)$ that obey the Klein-

Gordon inner product [11]

$$\langle \Phi_j, \Phi_{j'} \rangle_{\mathrm{KG}} = -\int_H d^{n-1}\underline{x}\sqrt{g}g^{00}\Phi_j^* \overleftrightarrow{\partial_0} \Phi_{j'} = \delta_{jj'}, \tag{3.5}$$

evaluated on some spacelike hypersurface of simultaneity H.

Therefore the field may be represented by

$$\Phi(x) = \sum_j a_j \Phi_j + a_j^\dagger \Phi_j^*, \tag{3.6}$$

where j labels the field mode operators and a_j and $a_j^\dagger$ are the expansion coefficients of the field modes and their hermitian conjugates respectively.

The construction of the QFT associated with the equation of motion (3.4) relies on a vacuum state, a state of lowest energy, *defined* as

$$a_j \left|\mathbf{0}\right\rangle := 0, \tag{3.7}$$

from which a Fock space may be populated through the operations of the expansion coefficients $a_j^\dagger$ and a_j corresponding to creation and annihilation operators respectively.

The field modes Φ_j and their complex conjugates Φ_j^* are said to be *positive* and *negative* frequency modes, $\Phi_j^{(\pm)}$ respectively, if

$$\omega \gtrless 0 \quad \Leftrightarrow \quad \|\Phi_j^{(\pm)}\|_{\mathrm{KG}} \gtrless 0. \tag{3.8}$$

In general, the possibility of distinguishing the field modes $\Phi_j^{(\pm)}$ relies on the symmetries of the background space-time, if indeed there are any. Fortunately, the

symmetries of AdS_n do admit a timelike Killing vector ∂_0 such that

$$\partial_0 \Phi_j^{(\pm)} \propto \mp i\omega \Phi_j^{(\pm)}, \qquad \omega > 0, \tag{3.9}$$

thus constraining the distinction of modes $\Phi_j^{(\pm)}$ unambiguously (see section 3.3 for the explicit form of these field modes). Obtaining this split is fundamental to this research as its existence ensures the usual commutation relations, allowing in turn for a QFT to be defined on the background. This is particularly relevant in the case of the vacuum state from the point of view of a rigidly-rotating observer. These rotational vacuum states are the subject of later research, presented in chapter 6.

Returning now to the equation of motion, there are some special cases of (3.4) that are of interest for any smooth, globally hyperbolic, pseudo-Riemannian, space-time [36] primarily due to the fact that they give rise to certain simplifying features. These are:

- The minimally-coupled case

$$\xi = 0 \Rightarrow \left(\Box - m^2\right) \Phi(x) = 0. \tag{3.10}$$

- The conformally-coupled case, characterised by the value of the conformal coupling, given by:

$$\xi = \xi_{\mathrm{c}} := \frac{(n-1)}{4(n-2)} \Leftrightarrow m_\xi^2 = m^2 + \frac{n(n-1)}{2}\Lambda. \tag{3.11}$$

  It is possible for $CAdS_n$ to be conformally mapped into a region of a globally hyperbolic space-time known as the Einstein static universe (ESU) [36] via the transformation

$$g_{\mu\nu}^{\mathrm{ESU}} = \Omega^2 g_{\mu\nu}, \tag{3.12}$$

where

$$\Omega = \cos\rho, \qquad 0 \leq \rho < \tfrac{\pi}{2}. \tag{3.13}$$

In addition, when a scalar field is present, the subsequent equations of motion are conformally invariant for $m = 0$ and with the field taking on the conformal weight of -1 [9]:

$$\Phi^{\text{ESU}} = \Omega^{-1}\Phi. \tag{3.14}$$

As ESU is globally hyperbolic, quantisation is well-established and therefore the field theory can be done there in a more straightforward manner. Avis, Isham and Storey [9] first studied this case for $n = 4$ and then mapped the results back to AdS_4 as a way of avoiding dealing with the problems associated with the 'leaks' in AdS_4 (described in section 2.2) directly.

- For any coupling to the curvature, the massless, i.e. $m = 0$ case may also be considered.

The focus of the work detailed in this thesis is on a *massive* field with a *general* coupling.

3.2 The Laplace-Beltrami operator — $\Box(x)$

The Laplace-Beltrami operator in (3.4) can now be recast in terms of the local hyperspherical coordinates $(\tau, \rho, \theta, \varphi)$ where

$$\theta := \{\theta_j\}, \qquad j = 1, 2, \ldots, n-3. \tag{3.15}$$

The coordinate transformation is most usefully applied by taking into account the following dependencies from the metric (2.10):

$$\begin{aligned} &g_{\tau\tau},\ g_{\rho\rho} \text{ and } g_{\theta_1\theta_1} \text{ depend on } \rho \text{ only, whereas} \\ &g_{\theta_i\theta_i} \text{ (with } i = 2, 3, \ldots, n-2) \text{ depends on } \rho \text{ and } \theta \text{ only, and} \\ &g_{\varphi\varphi} \text{ does } \textit{not} \text{ depend on } \varphi; \end{aligned} \tag{3.16}$$

and also that from (3.2), $\sqrt{g}$ is given by

$$\sqrt{g} = a^n \left(\sec\rho\right)^n \left(\sin\rho\right)^{n-2} \prod_{j=1}^{n-3} \left(\sin\theta_j\right)^{n-2-j}. \tag{3.17}$$

The action of the box operator on a scalar field on a general space is equivalent to that of the Laplace-Beltrami operator. It is given by the identity:

$$\Box\Phi = \frac{1}{\sqrt{g}} \left(\sqrt{g} g^{\mu\nu} \Phi_{,\nu}\right)_{,\mu}. \tag{3.18}$$

This allows the box operator acting on the scalar field in (3.4) to be written as

$$\Box\Phi = \left\{ g^{\tau\tau}\partial_\tau^2 + \frac{1}{\sqrt{g}} \left[\partial_\rho \left(\sqrt{g} g^{\rho\rho} \partial_\rho\right) + \underbrace{\partial_{\theta_j} \left(\sqrt{g} g^{\theta_j\theta_j} \partial_{\theta_j}\right)}_{\text{sum over } n-3 \text{ terms}} \right] + g^{\varphi\varphi}\partial_\varphi^2 \right\} \Phi. \tag{3.19}$$

The terms in τ and θ_j can be found in a straightforward manner by using (2.10). However the evaluation of the terms in ρ and φ is complicated by the action of the derivatives on $\sqrt{g}$. In the case of the ρ-indexed term

$$\frac{1}{\sqrt{g}} \left[\partial_\rho \left(\sqrt{g} g^{\rho\rho} \partial_\rho\right)\right] \Phi = \left[\Gamma^\mu_{\rho\,\mu} g^{\rho\rho} + \partial_\rho g^{\rho\rho} + g^{\rho\rho}\partial_\rho\right] \partial_\rho \Phi, \tag{3.20}$$

where the connections $\Gamma^{\mu}_{\rho\,\mu}$ are given by

$$\Gamma^{\mu}_{\rho\,\mu} = \Gamma^{\tau}_{\rho\,\tau} + \Gamma^{\rho}_{\rho\,\rho} + \underbrace{\Gamma^{\theta_k}_{\rho\,\theta_k}}_{\text{sum over } n\text{-2 terms}}, \tag{3.21}$$

as only the diagonal elements of the metric contribute. An expression for $\Gamma^{\theta_k}_{\rho\,\theta_k}$ in n-dimensions is obtained using

$$g_{\theta_k\theta_k} = a^2 \left(\tan\rho\right)^2 \prod_{j=1}^{k-1} \left(\sin\theta_j\right)^2 \tag{3.22}$$

$$\Rightarrow \partial_\rho g_{\theta_k\theta_k} = 2a^2 \left(\sec\rho\right)^2 \tan\rho \prod_{j=1}^{k-1} \left(\sin\theta_j\right)^2, \tag{3.23}$$

resulting in

$$\frac{1}{\sqrt{g}}\left[\partial_\rho\left(\sqrt{g}g^{\rho\rho}\partial_\rho\right)\right]\Phi = (n-2)\cot\rho\,\partial_\rho\Phi + \left(\cos\rho\right)^2\,\partial^2_\rho\Phi. \tag{3.24}$$

The transformation of the θ_j-indexed terms into local coordinates follows the same procedure as for the ρ-indexed terms. Hence

$$\frac{1}{\sqrt{g}}\left[\partial_{\theta_j}\left(\sqrt{g}g^{\theta_j\theta_j}\partial_{\theta_j}\right)\right]\Phi = \left[\Gamma^{\mu}_{\theta_j\,\mu}g^{\theta_j\theta_j} + \partial_{\theta_j}g^{\theta_j\theta_j} + g^{\theta_j\theta_j}\partial_{\theta_j}\right]\partial_{\theta_j}\Phi. \tag{3.25}$$

The connections over the index $\Gamma^{\theta_i}_{\theta_j\,\theta_i}$ are

$$\Gamma^{\theta_i}_{\theta_j\,\theta_i} = \frac{1}{2}g^{\theta_i\theta_i}\partial_{\theta_j}g_{\theta_i\theta_i}. \tag{3.26}$$

Thus the full scalar field wave equation on AdS_n (3.4) can be written in terms of

the local coordinates as follows:

$$\begin{aligned}
&\left(\Box - m^2 - \xi\mathcal{R}\right)\Phi \\
&= -a^{-2}\Bigg\{ \left(\cot\rho\right)^2 \Bigg[\left(\sin\rho\right)^2 \partial_\tau^2 - (n-2)\tan\rho\,\partial_\rho^2 - (n-2)\sum_{j=1}^{n-3}\cot\theta_j\,\partial_{\theta_j} \\
&\qquad\qquad - \sum_{j=1}^{n-3}\prod_{p=1}^{j-1}\left(\operatorname{cosec}\theta_p\right)^2 \partial_{\theta_j}^2 - \prod_{j=1}^{n-3}\left(\operatorname{cosec}\theta_j\right)^2 \partial_\varphi^2 \Bigg] \Bigg\}\Phi - \left(m^2 + \xi\mathcal{R}\right)\Phi.
\end{aligned} \tag{3.27}$$

3.3 Separation of the scalar field wave equation

Owing to the maximal symmetry of the space-time, the solutions to (3.27) are hyperspherically separable. Setting

$$\Phi(\tau,\rho,\theta,\varphi) = T(\tau)\widetilde{R}(\rho)Y(\theta,\varphi), \tag{3.28}$$

the following expression is obtained:

$$\begin{aligned} -(\cos\rho)^2\ T^{-1}d_\tau^2 T + (n-2)\cot\rho\,\widetilde{R}^{-1}d_\rho\widetilde{R} \\ + (\cos\rho)^2\ \widetilde{R}^{-1}d_\rho^2\widetilde{R} + (\cot\rho)^2\ Y^{-1}\Delta_S\, Y - a^2\left(m^2+\xi\mathcal{R}\right) = 0, \end{aligned} \tag{3.29}$$

where (3.27) was multiplied through by $a^2\Phi^{-1}$ and where

$$\Delta_S = (n-2)\sum_{j=1}^{n-3}\cot\theta_j\,\partial_{\theta_j} + \sum_{j=1}^{n-3}\prod_{p=1}^{j-1}\left(\operatorname{cosec}\theta_p\right)^2\ \partial_{\theta_j}^2 + \prod_{j=1}^{n-3}\left(\operatorname{cosec}\theta_j\right)^2\ \partial_\varphi^2, \tag{3.30}$$

is the Laplace-Beltrami operator on the *unit* $(n-2)$-sphere.

The separation of variables is achieved by isolating τ-dependent terms first and keeping angular variables together. This procedure yields the following ordinary differential equations:

$$\begin{aligned} &\omega^2 = -T^{-1}T_{,\tau\tau}\,; \\ &\lambda = -(n-2)\,(\tan\rho)\,\widetilde{R}^{-1}\widetilde{R}_{,\rho} - (\sin\rho)^2\,\widetilde{R}^{-1}\widetilde{R}_{,\rho\rho} + a^2(m^2+\xi\mathcal{R})\,(\tan\rho)^2 - \omega^2\,(\sin\rho)^2\,; \\ &\lambda = Y^{-1}\Delta_S\, Y; \end{aligned} \tag{3.31}$$

where ω^2 and λ are separation constants.

The solutions for $T(\tau)$ and $Y(\theta, \varphi)$ can be found in a straightforward manner. Hence,

$$T(\tau) = e^{\pm i\omega\tau}, \tag{3.32}$$

corresponding respectively to the negative and positive frequency parts of the field $\Phi(x)$.

The field modes considered in this research are chosen to be just the positive-frequency solutions, i.e.

$$\Phi_j := \Phi_j^{(+)} \propto e^{-i\omega\tau}, \qquad \omega > 0. \tag{3.33}$$

In the case of the angular part, having identified Δ_S, then

$$\lambda := -\ell(\ell + n - 3), \qquad \ell = 0, 1, 2, \ldots. \tag{3.34}$$

3.4 Radial modes — $R_{r\ell}(\rho)$

There are three sources in the literature for an expression for the full scalar field modes on AdS_n. The first result published by Avis, Isham and Storey [9] gives an expression for $n = 4$. Burgess and Lütken in [16] extended this to general $n > 2$. More recently however, Cotăescu [25] derived a slightly different expression for the full n-dimensional modes to that published in [16]. Moreover, Cotăescu's expression reduces to the earlier result in [9] for $n = 4$ whereas Burgess and Lütken's does not. The source of the discrepancy detailed in [25] lies in the form of the *radial* functions and that of the normalisation constant of the full field modes.

Having an accurate expression for the full modes is very important for this research.

As indicated in figure 1.1, the field modes can be used to construct Green functions directly (see section 4.2.1) that are fundamental to the calculation of other objects relating to the matter content of QFTs on curved space-times.

The general method for deriving the radial modes is not explicitly stated in [9] or [16]. In [25] it is mentioned that the final expression for the radial modes relies on recognising that the radial equation is in fact a hypergeometric differential equation (2.124). However, establishing this equivalence is not immediately obvious. Fortunately, in [24], Cotăescu highlights the main steps in this method which have guided the development presented below.

To begin with, the form of the radial equation obtained immediately after separation in (3.31) is a second order linear differential equation with varying coefficients. Muliplying through by $-\left(\operatorname{cosec}\rho\right)^2$ yields

$$\widetilde{R}_{,\rho\rho} + \mathcal{A}\widetilde{R}_{,\rho} + \mathcal{B}\widetilde{R} = 0. \tag{3.35}$$

The coefficients

$$\mathcal{A} := (n-2)\sec\rho\operatorname{cosec}\rho, \tag{3.36}$$

$$\mathcal{B} := -a^2 m_\xi^2 \left(\sec\rho\right)^2 + \lambda\left(\operatorname{cosec}\rho\right)^2 + \omega^2, \tag{3.37}$$

have been temporarily included for simplicity and result in (3.35) being singular for $\rho = 0$.

The form of (3.35) can be rendered into a Schrödinger equation by eliminating the coefficient of the first-derivate term via the substitution

$$\widetilde{R} := R_{\check{\mathrm{C}}} R. \tag{3.38}$$

This yields

$$R_{,\rho\rho} + \left(2\frac{R_{\breve{\mathrm{C}},\rho}}{R_{\breve{\mathrm{C}}}} + \mathcal{A}\right) R_{,\rho} + \left(\frac{R_{\breve{\mathrm{C}},\rho\rho}}{R_{\breve{\mathrm{C}}}} + \mathcal{A}\frac{R_{\breve{\mathrm{C}},\rho}}{R_{\breve{\mathrm{C}}}} + \mathcal{B}\right) R = 0. \tag{3.39}$$

Setting

$$2\frac{R_{\breve{\mathrm{C}},\rho}}{R_{\breve{\mathrm{C}}}} + \mathcal{A} = 0 \tag{3.40}$$

gives

$$R_{\breve{\mathrm{C}}} = (\cot\rho)^{\frac{n-2}{2}} \tag{3.41}$$

and the canonical form

$$R_{,\rho\rho} + \mathcal{B}R - \left(\frac{\mathcal{A}^2}{4} + \frac{\mathcal{A}_{,\rho}}{2}\right) R = 0. \tag{3.42}$$

Reinstating $\mathcal{A}$ and $\mathcal{B}$, the radial equation is now

$$\left\{ d_\rho^2 - \lambda\,(\mathrm{cosec}\,\rho)^2 - a^2 m_\xi^2\,(\sec\rho)^2 + \omega^2 - \frac{(n-2)^2}{4}\,(\sec\rho\,\mathrm{cosec}\,\rho)^2 \right.$$
$$\left. + \frac{(n-2)}{2}\left[(\mathrm{cosec}\,\rho)^2 - (\sec\rho)^2\right] \right\} R = 0. \tag{3.43}$$

Expressing the fourth term as

$$-\frac{(n-2)^2}{4}\frac{\left[(\cos\rho)^2 + (\sin\rho)^2\right]}{(\cos\rho\sin\rho)^2}, \tag{3.44}$$

gives

$$R_{,\rho\rho} - \left[\frac{P}{(\sin\rho)^2} + \frac{Q}{(\cos\rho)^2}\right] R = -\omega^2, \tag{3.45}$$

with

$$P := -\lambda - \frac{(n-2)}{2} + \frac{(n-2)^2}{4},$$
$$Q := m_\xi^2 a^2 + \frac{(n-2)}{2} + \frac{(n-2)^2}{4}, \tag{3.46}$$

such that

$$P, Q > 0. \tag{3.47}$$

The form of the coefficient of R on the left-hand side of (3.45), i.e.

$$\frac{P}{(\sin\rho)^2} + \frac{Q}{(\cos\rho)^2} \tag{3.48}$$

defines a Pöschl-Teller potential [63].

The method of solution of such Pöschl-Teller problems (see for example [70]) typically involves introducing a change of variable such as

$$z_2 := (\sin\rho)^2 \tag{3.49}$$

which recasts the radial equation as

$$4(1-z_2) R_{,z_2 z_2} + 2(1-2z_2) R_{,z_2} - \left[P(z_2)^{-1} + Q(1-z_2)^{-1} - \omega^2\right] R = 0. \tag{3.50}$$

Next, the method of solution involves the substitution

$$R(z_2) = (z_2)^p (1-z_2)^q \mathcal{F}(z_2), \qquad p, q \in \mathbb{R}. \tag{3.51}$$

Applying (3.51) to (3.50) yields the expression

$$z_2\,(1-z_2)\,\mathcal{F}_{,z_2z_2}+\left[2p+\frac{1}{2}+(2q-2p-1)z_2\right]\mathcal{F}_{,z_2}+\left(2pq-p^2-q^2+\frac{\omega^2}{4}\right)\mathcal{F}=0, \tag{3.52}$$

which follows from setting

$$\begin{aligned} P &= 2p\,(2p-1),\\ Q &= 2q\,(2q-1). \end{aligned} \tag{3.53}$$

The form of the equation (3.52) is now readily identifiable with that of the hypergeometric equation (2.124) in $\mathcal{F}\,(z_2)$. An appropriate choice of solution is the following linear combination of Gaussian hypergeometric functions [2], $F\,[\alpha,\beta;\gamma;z]$:

$$\mathcal{F}\,(z_2)=C_{\mathcal{F}}F\,[\alpha,\beta;\gamma;z_2]+D_{\mathcal{F}}\,(z_2)^{1-\gamma}\,F\,[\alpha-\gamma+1,\beta-\gamma+1;2-\gamma;z_2] \tag{3.54}$$

(see §15.5.3 and §15.5.4 in [2]), where

$$\begin{aligned} \alpha &\overset{(3.54)}{\longmapsto} p+q-\frac{\omega}{2},\\ \beta &\overset{(3.54)}{\longmapsto} p+q+\frac{\omega}{2},\\ \gamma &\overset{(3.54)}{\longmapsto} 2p+\frac{1}{2}, \end{aligned} \tag{3.55}$$

and where $C_{\mathcal{F}}$ and $D_{\mathcal{F}}$ are arbitrary constants.

As a result of the associations (3.55), the general solution for the radial equation

(3.43) is now

$$R(\rho) = C_{\mathcal{F}} (\sin\rho)^{2p} (\cos\rho)^{2q} \; F\left[p+q-\frac{\omega}{2}, p+q+\frac{\omega}{2}; 2p+\frac{1}{2}; (\sin\rho)^2\right] \\ + D_{\mathcal{F}} (\sin\rho)^{1-2p} (\cos\rho)^{2q} \; F\left[\frac{1}{2}-p+q-\frac{\omega}{2}, \frac{1}{2}-p+q+\frac{\omega}{2}; \frac{3}{2}-2p\,; (\sin\rho)^2\right]. \tag{3.56}$$

Given that $n \geq 2$ in this treatment, a regular solution to (3.43) at $\rho = 0$ requires the *positive* solutions to (3.53), that is

$$2p = \ell + \frac{n-2}{2}, \\ 2q = \mu + \frac{1}{2}, \tag{3.57}$$

where

$$\mu := \sqrt{m^2 a^2 + \xi\mathcal{R} + \frac{(n-1)^2}{4}}. \tag{3.58}$$

Consequently, a singularity at $\rho = 0$ arises in the second term of (3.56) due to the $(\sin\rho)^{1-2p}$ factor. This applies for $n > 2$, $\forall \ell$ and for $n = 2$, $\forall \ell > 1$. For these cases, setting

$$D_{\mathcal{F}} := 0 \tag{3.59}$$

eliminates this unphysical term.

Recalling that $CAdS_n$ is globally hyperbolic subject to the reflective boundary conditions (2.23), it follows that the radial modes should also die off at spatial infinity. This is rather like a wavefunction spanning an infinitely wide potential well. However, the criteria (2.120) reveal there is a branch point at $z_2 = 1$ for the remaining hypergeometric function. To avoid this singularity, the series can be terminated by fixing α or β to take on a negative integer value. Following Cotăescu, a suitable

quantisation condition is established, namely

$$\omega := 2(p + q + r), \qquad r = 0, 1, 2, \ldots, \tag{3.60}$$

where r is the 'radial quantum number' [16].

The periodic nature of time in AdS_n affects the modes despite (2.23) as in general the full field modes are multivalued. Setting ω to an integer w (ensuring a consistent notation for quantised variables) cures this problem. This extra quantisation condition is reserved for AdS_n and is obtained by defining

$$\kappa := \mu + \frac{n-1}{2}, \qquad \kappa \in \mathbb{N}_0, \tag{3.61}$$

where κ is known is the 'conformal dimension of the field theory on $\mathbb{M}^{n-1}$' [79] (cited in [24]). The quantisation condition is

$$w = \kappa + \ell + 2r, \tag{3.62}$$

and implies that

$$m_\xi^2 a^2 = \kappa(\kappa - n - 1). \tag{3.63}$$

For 'regular modes' [14], i.e. solutions to (3.4) where the mass term respects the condition

$$m_\xi^2 > \left(1 - \frac{(n-1)^2}{4}\right) m^2, \tag{3.64}$$

and requiring that κ is an integer, such that $\kappa > n - 1$ results in a 'discrete mass spectrum' [9] being induced from the quantisation condition (3.62).

In the remainder of this thesis, unless stated otherwise, AdS_n can be taken to mean $CAdS_n$, with the understanding that when this is assumed the condition in (3.61) is

relaxed such that

$$\mathcal{k} \to k := \mu + \frac{n-1}{2}, \qquad k \in \mathbb{R}_0. \tag{3.65}$$

For AdS_n, for $n > 2$, it is now possible to convert the remaining hypergeometric function of the radial mode to a Jacobi polynomial using §15.4.6 [2]. Accordingly,

$$F\left[-r, 2p+2q+r; 2p+\frac{1}{2}; (\sin\rho)^2\right] = \frac{r!}{\left(\ell+\frac{n-3}{2}\right)_r} P_r^{\left(\ell+\frac{n-3}{2}, \mathcal{k}-\frac{n-1}{2}\right)}(\cos 2\rho), \tag{3.66}$$

where the Pochhammer notation (2.118) has been used.

The physically acceptable solution to (3.43) is now

$$R_{r\ell}(\rho) = N_{r\ell} (\sin\rho)^{2p} (\cos\rho)^{2q} \, P_r^{\left(\ell+\frac{n-3}{2}, \mathcal{k}-\frac{n-1}{2}\right)}(\cos 2\rho) \tag{3.67}$$

where

$$N_{r\ell} := C_{\mathcal{F}} \frac{r!}{\left(\ell+\frac{n-3}{2}\right)_r}, \tag{3.68}$$

is a normalisation constant and is to be determined in section 3.6.

3.5 Field modes — $\Phi_{n\ell}(x)$

In order to label the individual overall quantum modes, Cotăescu [25] defines the *main* quantum number

$$n := 2r + \ell. \tag{3.69}$$

This combines the radial quantum number r and the angular quantum number ℓ into a total quantum number and allows a numbering of field modes $n = 0, 1, 2, \ldots$ such that the parity of n and ℓ always match.

In addition, given (3.60) a total energy level naturally arises:

$$w_n = \mathcal{k} + n, \tag{3.70}$$

albeit generally degenerate owing to the multiplicity of ℓ in (2.82).

Finally, using the results (3.32), (3.41) and (3.67), the full (positive frequency) modes can now be stated as:

$$\Phi^{(+)}_{n\ell}(x) = N_{r\ell} e^{-\boldsymbol{i} w_n \tau} Y_\ell(\theta, \varphi) \left(\sin\rho\right)^\ell \left(\cos\rho\right)^{\mathcal{k}} P_r^{\left(\ell + \frac{d-2}{2}, \mathcal{k} - \frac{d}{2}\right)} \left(\cos 2\rho\right), \tag{3.71}$$

where for convenience in the following section, the expression is given in terms of the number of spatial dimensions d, where $d = n - 1$ and n is the number of space-time dimensions.

For completeness, it is worthwhile mentioning that the overall multiplicity of energy levels [25] is the sum over the multiplicity of each angular quantum number, hence

$$\mathfrak{M}_n = \sum_\ell \mathfrak{M}_\ell = \frac{(n + d - 1)!}{n!(d-1)!}. \tag{3.72}$$

3.6 Normalisation

Bearing in mind (3.33) and (3.64), to ensure the modes (3.71) form an orthonormal basis of a Hilbert space [9], they are subject to the relativistic scalar product (3.5)

$$\langle \Phi_{n\ell}, \Phi_{n'\ell'} \rangle_{\mathrm{KG}} = -\int_H d^d\underline{x} \sqrt{g} g^{00} \Phi^*_{n\ell} \overleftrightarrow{\partial_0} \Phi_{n'\ell'} = \delta_{nn'}, \qquad \Phi_{n\ell} = \Phi_{n\ell}(\underline{x}, t), \tag{3.73}$$

evaluated on some spacelike hypersurface of simultaneity H.

To compute (3.73) it is useful to try and convert the integrand into a purely spatially-

dependent expression. This can be achieved via the following steps.

Defining,

$$\begin{aligned}\Phi_{n\ell}(x) &:= e^{-i w_n \tau} R_{\check{\mathrm{C}}}(\rho)\phi_{n\ell}(\rho,\theta,\varphi),\\ \phi_{n\ell}(\underline{x}) &:= R_{r\ell}(\rho)Y_\ell(\theta,\varphi),\end{aligned} \tag{3.74}$$

for a given ℓ, suppressing arguments, and using (3.41) gives

$$\begin{aligned}\Phi_n^* \overleftrightarrow{\partial_0} \Phi_{n'} &= \Phi_n^*(\partial_0\Phi_{n'}) - (\partial_0\Phi_n^*)\Phi_{n'}\\ &= -\left(w_n + w_{n'}\right) e^{i(w_n - w_{n'})\tau} \left(\cot\rho\right)^{d-1} \phi_n^*\phi_{n'}.\end{aligned} \tag{3.75}$$

From (3.17),

$$g = a^{2d+2}\left(\tan\rho\right)^{2d-2}\left(\sec\rho\right)^4 g_S, \tag{3.76}$$

where g_S is the determinant of the purely *angular* part of the metric on the unit $(d-1)$-sphere given by

$$g_S := \left|\det g_{\theta_i\theta_i}\right| = \left(\sin\theta_1\right)^{2d-4}\left(\sin\theta_2\right)^{2d-6}\cdots\left(\sin\theta_{d-2}\right)^2. \tag{3.77}$$

Therefore, on the hypersurface

$$\sqrt{g}g^{00} = -a^{d-1}\left(\tan\rho\right)^{d-1}\sqrt{g_S}. \tag{3.78}$$

Using the expressions (3.74–3.77) yields

$$\langle \Phi_{n\ell}, \Phi_{n'\ell}\rangle_{\mathrm{KG}} = a^{d-1}(w_n + w_{n'})e^{i(w_n - w_{n'})\tau}\int_H d^d\underline{x}\sqrt{g_S}\phi_{n\ell}^*\phi_{n'\ell} = \delta_{nn'}. \tag{3.79}$$

Recalling that the spatial modes are separable in the hyperspherical variables, it is reasonable to seek to recast (3.73) in terms of a product of scalar products over each integration variable.

This is achieved by defining

$$d\theta := d\theta_1 d\theta_2 \cdots d\theta_{d-2}, \tag{3.80}$$

where for notational simplicity

$$d^d\underline{x} := a\sqrt{g_S}\, d\rho\, d\theta\, d\varphi. \tag{3.81}$$

Suppressing arguments the integral (3.73) now becomes

$$a^{d-1}(w_n + w_{n'})e^{i(w_n - w_{n'})\tau} \int_0^{2\pi} d\varphi \int_0^{\pi} d\theta\, g_S Y_\ell^* Y_\ell \int_0^{\frac{\pi}{2}} d\rho\, R_{r\ell}^* R_{r'\ell} = \delta_{nn'}. \tag{3.82}$$

The normalisation of the radial functions can be achieved by introducing the change of variable

$$y = \cos 2\rho. \tag{3.83}$$

As a result,

$$(\sin\rho)^q = \left(\frac{1-y}{2}\right)^{\frac{q}{2}} \text{ and } (\cos\rho)^q = \left(\frac{1+y}{2}\right)^{\frac{q}{2}}, \tag{3.84}$$

for any q and therefore

$$d\rho = -(1+y)^{-\frac{1}{2}}(1-y)^{-\frac{1}{2}}\, dy. \tag{3.85}$$

The integral of the radial functions is now

$$\int_0^{\frac{\pi}{2}} d\rho\, R^*_{r\ell} R_{r'\ell} = \frac{|N_{r\ell}|^2}{2^{\kappa+\ell}} \times \int_{-1}^{1} dy\, (1-y)^{\ell+\frac{d}{2}-1}(1+y)^{\kappa-\frac{d}{2}} P_r^{\left(\ell+\frac{d-2}{2},\kappa-\frac{d}{2}\right)}(y)\, P_{r'}^{\left(\ell+\frac{d-2}{2},\kappa-\frac{d}{2}\right)}(y)\,, \tag{3.86}$$

which is the form required for the normalisation formula for Jacobi polynomials, §22.2.1 in [2]. Applying this and reinserting in (3.82) gives the following equality

$$|N_{r\ell}|^2 = a^{1-d}\,\frac{2r+\ell+\kappa}{\omega_n}\frac{r!\,\Gamma(r+\ell+\kappa)}{\Gamma\left(r+\ell+\frac{d}{2}\right)\Gamma\left(r+\kappa-\frac{d-2}{2}\right)}. \tag{3.87}$$

Finally, simplifying by inspection and using (3.70), the expression for the normalisation constant of the full modes is found to be

$$N_{r\ell} = a^{\frac{1-d}{2}}\sqrt{\frac{r!\,\Gamma(r+\ell+\kappa)}{\Gamma\left(r+\ell+\frac{d}{2}\right)\Gamma\left(r+\kappa-\frac{d-2}{2}\right)}} \tag{3.88}$$

which is in exact agreement with Cotăescu's result [25] for the full modes (3.71) and for the associated normalisation constant (3.88). In addition, the results reduce in the $n = 4$ case to the expressions given in [9]. There is a misprint in the results published in [16] for the expression for these modes.

4 | Scalar field propagation on AdS_n

4.1 Green functions

The matter content of QFTs on curved space-times is described by expectation values of operators that are quadratic in the fields and their derivatives evaluated at the same space-time point. However, these objects are not simply expectation values of originally classical expressions whose field variables have been promoted to operators, as such operator-valued expressions are formally divergent and therefore make no physical sense.

The central practical question facing QFTs on curved space-times seems therefore to be how to uncover sensible physics from physical nonsense (in a mathematically justifiable way).

In simple terms, these formally divergent expectation values have a part that is regular when $x' \to x$ (the 'coincidence limit'), and a part that is singular. The latter is construed as unphysical and therefore to be discarded. In curved space-time, the normal-ordering prescription of flat-space QFT is no longer applicable. The reason for this failure, and the methods used to renormalise on curved space-times are discussed in more detail in chapter 5.

The method used to resolve these regular and singular parts is known as *regularisation* in the context of QFT. A pragmatic regularisation approach is to first consider a version of the divergent operator of interest whose constituent operators are evaluated at *nearby* points $\{x, x'\}$ along a geodesic. By way of a simple example, consider

the relationship between the following *formal* equalities,

$$\langle \mathbf{0}| \Phi(x)\Phi(x') |\mathbf{0}\rangle \to \langle \mathbf{0}| \Phi^2(x) |\mathbf{0}\rangle , \qquad x' \to x, \tag{4.1}$$

$$\Rightarrow \qquad \langle \mathbf{0}| \Phi^2(x) |\mathbf{0}\rangle = \langle \mathbf{0}| \Phi^2(x) |\mathbf{0}\rangle_{\text{reg}} + \langle \mathbf{0}| \Phi^2(x) |\mathbf{0}\rangle_{\text{sing}} , \tag{4.2}$$

$$\Leftrightarrow \quad \langle \mathbf{0}| \Phi(x)\Phi(x') |\mathbf{0}\rangle = \langle \mathbf{0}| \Phi(x)\Phi(x') |\mathbf{0}\rangle_{\text{reg}} + \langle \mathbf{0}| \Phi(x)\Phi(x') |\mathbf{0}\rangle_{\text{sing}} , \quad x' \to x. \tag{4.3}$$

This method is originally due to DeWitt [33] and is known as the 'covariant geodesic point-separation' method, or more simply as 'point-splitting'. In this approach therefore, the matter content of QFTs on curved space-times relies fundamentally on a knowledge of the interplay between the background and the *propagation* of the fields on it. The essence of point-splitting is that this information can be borne out of the study of the singularity structure of two-point correlation functions of field operators and their derivatives.

To this end, it is reasonable to consider members of the set of two-point Green function solutions $\boldsymbol{G}(x, x')$ of (3.4) and the inhomogeneous scalar field wave equation

$$\left(\Box_x - m_\xi^2(x)\right) \boldsymbol{G}(x, x') = -\delta^n(x, x'), \tag{4.4}$$

where

$$\delta^n(x, x') = -\frac{1}{\sqrt{g(x)}} \delta^n \left(x - x'\right) . \tag{4.5}$$

The vacuum state on curved space-time is ambiguous (see e.g. sections 3.2 and 3.3 of [11] for a detailed explanation), and the final step in order to obtain a physically acceptable expectation value of the stress-energy tensor with respect to this state involves 'bringing the split-points back together', the Green functions of relevance to the development of the matter content of a QFT are the *state-dependent* Green

functions. These are the Wightman functions,

$$G_+(x,x') := \langle \mathbf{0}| \, \Phi(x)\Phi(x') \, |\mathbf{0}\rangle \,, \tag{4.6}$$

$$G_-(x,x') := \langle \mathbf{0}| \, \Phi(x')\Phi(x) \, |\mathbf{0}\rangle \,, \tag{4.7}$$

the anti-commutator function,

$$G_{(1)}(x,x') := \langle \mathbf{0}| \, \{\Phi(x), \Phi(x')\} \, |\mathbf{0}\rangle \,, \tag{4.8}$$

and the Feynman Green function,

$$G_{\mathrm{F}}(x,x') := \boldsymbol{i} \, \langle \mathbf{0}| \, \mathcal{T} \left(\Phi(x)\Phi(x')\right) |\mathbf{0}\rangle \,, \tag{4.9}$$

where $\mathcal{T}$ denotes the time-ordering of the application of the field operators. Explicitly, this requirement corresponds to

$$\mathcal{T} \left(\Phi(x)\Phi(x')\right) := \begin{cases} \Phi(x)\Phi(x'), & t < t', \\ \\ \Phi(x')\Phi(x), & t > t'. \end{cases} \tag{4.10}$$

As a result of (4.10), (4.9) can be written as

$$G_{\mathrm{F}}(x,x') = \boldsymbol{i} \, \langle \mathbf{0}| \, \left[\Theta(t-t')\Phi(x)\Phi(x') + \Theta(t'-t)\Phi(x')\Phi(x)\right] |\mathbf{0}\rangle \,, \tag{4.11}$$

where $\Theta(t-t')$ is the Heaviside or 'step' function

$$\Theta(t-t') := \begin{cases} 0, & t < t', \\ \\ 1, & t > t'. \end{cases} \tag{4.12}$$

The Feynman Green function is the sole vacuum-state-dependent Green function to satisfy (4.4); the others satisfy (3.4). Explicit expressions for the Feynman Green

function can be found using Schwinger's 'proper time' method [66], later generalised by Feynman and DeWitt (see e.g. [32]) to curved space-times [20] [22].

Accordingly, for timelike separations, the Feynman Green function $G_{\rm F}(x,x')$ can be thought of as representing the probability amplitude for a virtual scalar particle to propagate from x' to x, i.e. to be created at one event x' and then annihilated at another event x within the space-time. In the case of spacelike separations, $G_{\rm F}(x,x') \neq 0$ either and so it should br pointed out that its interpretation as a probability amplitude in this case breaks down as it would imply a violation of causality.

A crucial point is that the fact that these state-dependent Green functions are solutions to one or both of the scalar field wave equations (3.4) or (4.4) does not automatically lead to a specification of the vacuum state [11] [20] [43] (unlike in Minkowski space). Thus more information than just the choice of contour deformation needs to be supplied in order to specify the vacuum or equivalently to define a Green function $\boldsymbol{G}(x,x')$ to be $G_{\rm F}(x,x')$, $G_{(1)}(x,x')$, or $G_{\pm}(x,x')$.

The Wightman functions are the building blocks of the anti-commutator and Feynman Green functions and crucially, all four are constructed from the modes of the field with respect to the vacuum state. These modes are constrained by the way in which their field operator is decomposed into positive and negative-frequency modes (3.8) as well as any boundary conditions.

In AdS_n this latter requirement is especially pertinent in view of its reflective boundary conditions (2.23). Mathematically, the modes are sensitive to the metric through the definition of the Laplace-Beltrami operator (3.18) and through the coupling ξ [20].

The field modes are therefore global objects as they are defined everywhere on the

space-time. Through this chain of associations, the state-dependent Green functions are themselves global objects.

Physically, sealing the timelike boundary of $CAdS_n$ allows it to admit a Cauchy surface ensuring the space-time's status as a globally hyperbolic. This in turn permits a notion of causality and therefore time-ordering on which the definition (4.9) of the Feynman Green function relies.

The 'proper-time' method [32] is based on a matrix representation of $G_{\rm F}(x,x')$. Both the reason that $G_{\rm F}(x,x')$ is undefined in the coincidence limit and its natural interpretation as a transition amplitude can be understood from intermediate steps in the method. In particular, defining,

$$0^+ := \lim_{\epsilon\to 0}\epsilon, \qquad \epsilon > 0, \tag{4.13}$$

Therefore, there is a tacit understanding that the Feynman Green function $G_{\rm F}(\sigma)$ is actually the limiting case of a function that is analytic in the upper complex half-plane of σ so that $G_{\rm F}(\sigma) := G_{\rm F}(\sigma + \boldsymbol{i}0^+)$.

The matter content developed in the research presented here exploits the point-split nature of $G_{\rm F}(x,x')$ and $G_{(1)}(x,x')$. Any of the remaining three state-dependent Green functions can be obtained from $G_{\rm F}(x,x')$. The Feynman Green function is used here as a tool for the purposes of renormalisation, and the anti-commutator function in the analysis of thermal states.

The Feynman Green function is related to the anti-commutator function via the relation

$$G_{\rm F}(x,x') = \frac{1}{2}[\Theta(t-t') - \Theta(t'-t)]G(x,x') + \frac{\boldsymbol{i}}{2}G_{(1)}(x,x'), \tag{4.14}$$

where $G(x, x')$ is the *commutator* function, given by

$$G(x, x') = \langle \mathbf{0} | \left[\Phi(x), \Phi(x') \right] | \mathbf{0} \rangle = \left[\Phi(x), \Phi(x') \right]. \tag{4.15}$$

This is state-*in*dependent as the commutation relations for the free scalar field mean that the associated commutator function is a c-number. With this in mind, the relation (4.14) gives the first glimpse of a characteristic division of expectation values in QFTs in curved space-times into state-independent and state-dependent parts.

Since it is the study of the singularity structure of these functions that is of relevant interest here, note that as $x' \to x$, G is finite, therefore

$$G_{\mathrm{F}}(x, x') \sim \frac{\boldsymbol{i}}{2} G_{(1)}(x, x'), \qquad x' \to x. \tag{4.16}$$

In the case of the Feynman Green function on AdS_n, the maximal symmetry of the background allows (4.4) to be written as

$$\left(\Box - m_\xi^2 \right) G_{\mathrm{F}}(s) = -\delta^n(s), \tag{4.17}$$

without any loss of generality.

4.2 Feynman Green function — $G_{\mathrm{F}}(x, x')$

There are two methods for deriving an expression of the Feynman Green function in the literature. One technique involves summing over the expression for the full field modes (3.71) which is dealt with in section 4.2.1 below. The alternative technique, detailed in section 4.2.2, solves (4.17) directly.

4.2.1 Mode sum construction

The self-confessed 'brute force' sum-over-modes approach by Burgess and Lütken appears in [16]. Their method [16] begins with the standard definition of the Feynman Green function (4.11). Bearing this definition in mind, for some $G_{\rm F}(x',x'')$, the maximal symmetry of AdS_n means that if $s(x',x'') = s(x,0)$ then this property can be exploited by translating $x' \mapsto x, x'' \mapsto 0$. Thus by translating one of its points to the origin, and recalling both the split (3.6) and the definition of the vacuum state (3.7), it follows that

$$G_{\rm F}(x,0) = \boldsymbol{i}\left(\Theta(x,0)\sum_{n\ell}\Phi_{n\ell}(x)\Phi_{n\ell}(0) + \Theta(0,x)\sum_{n\ell}\Phi_{n\ell}(0)\Phi_{n\ell}(x)\right). \tag{4.18}$$

Given the $(\sin\rho)^{\ell}$ factor in the radial mode expression (3.67), for $\rho = 0$, the only non-zero contribution from the radial modes at the origin will be from the $\ell = 0$ mode. Bearing this in mind,the misprint in Burgess & Lütken's expression for the field modes does not affect their construction of the propagator. Hence

$$G_{\rm F}(x,0) = \boldsymbol{i}\frac{\Gamma\left(\frac{1}{2}(n-1)\right)}{2\pi^{\frac{1}{2}(n-1)}}e^{-\boldsymbol{i}\mathcal{k}|\tau|}\sum_{r}R_{{\rm BL}r0}(\rho)R_{{\rm BL}r0}(0)e^{-2\boldsymbol{i}r|\tau|}, \tag{4.19}$$

where the overall factor comes from the $\ell = 0$ hyperspherical harmonic and is effectively the normalised density of the $(n-2)$-sphere (i.e. the inverse area, A_S^{-1} of the unit $(n-2)$-sphere), and where

$$R_{{\rm BL}r\ell}(\rho) = N_{r\ell}P_r^{\left(\ell+\frac{n-3}{2},\mathcal{k}-\frac{n-1}{2}\right)}(\cos 2\rho), \tag{4.20}$$

using (3.38) with (3.41) and (3.67). For $\ell = 0$

$$|N_{r0}|^2 = a^{2-n}\frac{r!\,\Gamma(\mathcal{k}+r)}{\Gamma\left(r+\frac{1}{2}(n-1)\right)\Gamma\left(\mathcal{k}-\frac{1}{2}(n-3)+r\right)}, \tag{4.21}$$

and when $\rho = 0$

$$R_{\mathrm{BL}r0}(0) = N_{r0} P_r^{\left(\frac{n-3}{2}, \mathcal{k}-\frac{n-1}{2}\right)}(1)\,. \tag{4.22}$$

Applying the formula §22.4.1 from [2] on the Jacobi polynomial gives

$$P_r^{\left(\frac{n-3}{2}, \mathcal{k}-\frac{n-1}{2}\right)}(1) = \binom{r+\frac{n-3}{2}}{r}. \tag{4.23}$$

This can then be transformed into an expression involving gamma functions, which is useful for later simplification. This is done using the formulae §6.1.21 and then §6.1.15 from [2] and yields,

$$P_r^{\left(\frac{n-3}{2}, \mathcal{k}-\frac{n-1}{2}\right)}(1) = \frac{\Gamma\left(r+\frac{1}{2}(n-1)\right)}{r!\,\Gamma\left(\frac{1}{2}(n-1)\right)}. \tag{4.24}$$

The Feynman Green function (4.19) can now be written as the sum

$$\begin{aligned} G_{\mathrm{F}}(x,0) = {} & \boldsymbol{i}\frac{a^{2-n}}{2\pi^{\frac{1}{2}(n-1)}} e^{-\boldsymbol{i}\mathcal{k}|\tau|}\,(\cos\rho)^{\mathcal{k}} \\ & \times \sum_r \frac{\Gamma(\mathcal{k}+r)}{\Gamma\left(\mathcal{k}+r-\frac{1}{2}(n-3)\right)} e^{-2\boldsymbol{i}r|\tau|} P_r^{\left(\frac{n-3}{2}, \mathcal{k}-\frac{n-1}{2}\right)}(\cos 2\rho)\,. \end{aligned} \tag{4.25}$$

The final summation can be performed as directed in [16] using formula §45.1.4 from Hansen [48]:

$$\begin{aligned} & \sum_{j=0}^{+\infty} \frac{(\alpha+\beta+1)_j}{(\alpha+\beta)_j} \varepsilon^j P_j^{(\alpha,\beta)}(y) \\ & = (1+\varepsilon)^{-(\alpha+\beta+1)} F\left[\frac{\alpha+\beta+1}{2}, \frac{\alpha+\beta+2}{2}; \beta+1; 2\varepsilon(y+1)(1+\varepsilon)^{-2}\right], \end{aligned} \tag{4.26}$$

recalling (3.83), and having made the associations:

$$\begin{aligned}
\alpha &\overset{(4.26)}{\longmapsto} \frac{n-3}{2},\\
\beta &\overset{(4.26)}{\longmapsto} \mathcal{k} - \frac{n-1}{2},\\
\varepsilon &\overset{(4.26)}{\longmapsto} e^{-2\boldsymbol{i}|\tau|},\\
j &\overset{(4.26)}{\longmapsto} \mathcal{r}.
\end{aligned} \tag{4.27}$$

Therefore applying (2.118) to the Pochhammer quotient term of the summation in (4.26) gives

$$\frac{(\alpha+\beta+1)_j}{(\beta+1)_j} \overset{(4.26)}{\longmapsto} \frac{\Gamma\left(\mathcal{k}-\frac{n-3}{2}\right)}{\Gamma(\mathcal{k})} \frac{\Gamma(\mathcal{k}+\mathcal{r})}{\Gamma\left(\mathcal{k}+\mathcal{r}-\frac{n-3}{2}\right)}. \tag{4.28}$$

Considering next the right-hand side of (4.26):

$$(1+\varepsilon)^{-(\alpha+\beta+1)} \overset{(4.26)}{\longmapsto} \left(1+e^{-2\boldsymbol{i}|\tau|}\right)^{-\mathcal{k}}, \tag{4.29}$$

which, multiplied with the $e^{-\boldsymbol{i}\mathcal{k}|\tau|}$ outside the summation in (4.25) gives

$$e^{-\boldsymbol{i}\mathcal{k}|\tau|}\left(1+e^{-2\boldsymbol{i}|\tau|}\right)^{-\mathcal{k}} = 2^{-\mathcal{k}}(\sec\tau)^{\mathcal{k}}. \tag{4.30}$$

The remaining $(\cos\rho)^{\mathcal{k}}$ factor outside the summation in (4.25) yields

$$2^{-\mathcal{k}}(\cos\rho)^{\mathcal{k}}\,(\sec\tau)^{\mathcal{k}} = (2z_0)^{-\mathcal{k}}. \tag{4.31}$$

where,

$$z_0 := \left[\cosh\left(\frac{s}{a}\right)\right]^2, \tag{4.32}$$

the Feynman Green function is then found to be:

$$G_{\mathrm{F}}(s) = \boldsymbol{i}\frac{a^{2-n}}{2^{\mathcal{k}+1}\pi^{\frac{1}{2}(n-1)}}\frac{\Gamma(\mathcal{k})}{\Gamma\left(\mathcal{k}-\frac{1}{2}(n-3)\right)}(z_0)^{-\mathcal{k}}F\left[\frac{1}{2}\mathcal{k},\frac{1}{2}(\mathcal{k}+1);\mathcal{k}-\frac{1}{2}(n-3);(z_0)^{-1}\right], \tag{4.33}$$

based on Cotăescu's results for the normalised mode expansions (3.71).

4.2.2 Direct solution of the inhomogeneous wave equation

There are two key sources in the literature that derive an expression for the Feynman Green function by solving (4.17) directly. Allen & Jacobson [4] published such a method allowing $G_{\mathrm{F}}(s)$ to be calculated for $n > 2$. Later, Camporesi [19] specialised to $n = 4$ following a slight variation of the approach set out in [4]. This section begins by reviewing the general method of solution set out by these authors. Camporesi's method is then generalised to $n \geq 2$ in a straightforward manner, agreeing with Allen & Jacobson's results for $n > 2$.

I. Allen & Jacobson's method

Allen & Jacobson show that the inhomogeneous scalar field wave equation (4.17) is a function of s only. The resulting ordinary differential equation for the Feynman Green function is

$$G_{\mathrm{F},ss} + \frac{(n-1)}{a}\coth\left(\frac{s}{a}\right)G_{\mathrm{F},s} - m_\xi^2 G_{\mathrm{F}} = 0, \qquad s^2 < 0. \tag{4.34}$$

The result (4.34) then identified with a hypergeometric differential equation (2.124)

$$z_1(1-z_1)G_{\mathrm{F},z_1z_1} - n\left(z_1 - \frac{1}{2}\right)G_{\mathrm{F},z_1} + m_\xi^2 a^2 G_{\mathrm{F}} = 0, \qquad 0 \leq z_1 < 1, \tag{4.35}$$

where

$$z_1 := \left[\cosh\left(\frac{s}{2a}\right)\right]^2, \tag{4.36}$$

The linearly independent solutions to (4.34) in the vicinity of $z_1 = \infty$ are given by §15.5.7 and §15.5.8 in [2]. Accordingly, applying §15.5.7 from [2] to (4.35) yields,

$$\begin{aligned} G_{\mathrm{F}}(s) = J\,(z_1)^{-\alpha}\,F\left[\alpha, \alpha-\gamma+1; \alpha-\beta+1; (z_1)^{-1}\right] \\ +K\,(z_1)^{-\beta}\,F\left[\beta, \beta-\gamma+1; \beta-\alpha+1; (z_1)^{-1}\right], \end{aligned} \tag{4.37}$$

where the associations

$$\begin{aligned} \alpha &\overset{(4.37)}{\longmapsto} \frac{n-1}{2} + \mu, \\ \beta &\overset{(4.37)}{\longmapsto} \frac{n-1}{2} - \mu, \\ \gamma &\overset{(4.37)}{\longmapsto} \frac{n}{2}, \end{aligned} \tag{4.38}$$

have been made and where J and K are arbitrary constants.

For $G_{\mathrm{F}}(s)$ to represent a physically reasonable propagator, it must remain finite as $s \to \infty$. However, $z_1 \to \infty$ as $s \to \infty$, leading the second term in (4.37) to diverge. To ensure a physically acceptable solution, this boundary condition requires that

$$K = 0. \tag{4.39}$$

Therefore,

$$G_{\mathrm{F}}(s) = J\,(z_1)^{-\alpha}\,F\left[\alpha, \alpha-\gamma+1; \alpha-\beta+1; (z_1)^{-1}\right]. \tag{4.40}$$

As $s \to 0$ (and therefore as $z_1 \to 1$), the expression (4.40) is singular. However, an infinitessimally small region of AdS_n will be isomorphic to an infinitessimally

small region of *any* maximally symmetric space. Accordingly, the flat-space Feynman Green function $G_{\mathrm{F}}^{\mathbb{M}^n}$, shares the same singular behaviour in this region, and a comparison of the two expressions is used to determine the constant J in [4].

An alternative approach to determining J is used here, and the result matches those of [4]. The exact singularity structure of any Feynman Green function in a general space-time of arbitrary dimension is given by its 'Hadamard form' $G_{\mathrm{H}}(s)$, (4.156), discussed in detail in section 4.4.1. Considering (4.156) and bearing in mind the boundary conditions (4.167 – 4.168b),

$$G_{\mathrm{H}}^{n=2}(s) \sim -\frac{\boldsymbol{i}}{2\pi} \ln \bar{s}, \qquad s \to 0, \tag{4.41}$$

$$G_{\mathrm{H}}^{n>2}(s) \sim \frac{\boldsymbol{i}}{4\pi^{\frac{n}{2}}} \Gamma\left(\tfrac{n}{2} - 1\right) s^{2-n}, \qquad s \to 0, \tag{4.42}$$

where

$$\bar{s} := Ms, \tag{4.43}$$

is a version of the geodetic interval that is *dimensionless* due to the presence of a parameter of this theory known as the 'mass renormalisation scale', M, in its definition. Similarly, other quantities have dimensionless versions appearing later as logarithmic arguments. These are

$$\bar{\sigma} := M^2 \sigma, \tag{4.44}$$

and

$$\bar{a} := Ma. \tag{4.45}$$

This freedom of choice is a manifestation of a fundamental feature of QFTs on curved space-times in general, and is discussed in sections 5.1 and 5.2.

To verify that this leading-order behaviour matches that of $G_{\mathrm{F}}^{n>2}(s)$, it is necessary

to transform (4.40) using §15.3.3 in [2]. This yields

$$G_{\mathrm{F}}(s) = J\,(z_1)^{-\alpha}\,(1-z_1)^{\gamma-\beta-\alpha}\,F\left[1-\beta,\gamma-\beta;\alpha-\beta+1;(z_1)^{-1}\right]. \tag{4.46}$$

As $s \to 0$, $(z_1)^{-1} \to 1$. Using §15.1.20 from [2] gives

$$F\left[1-\beta,\gamma-\beta;\alpha-\beta+1;1\right] = \frac{\Gamma\left(\alpha-\beta+1\right)\Gamma\left(\alpha+\beta-\gamma\right)}{\Gamma\left(\alpha\right)\Gamma\left(\alpha-\gamma+1\right)}, \tag{4.47}$$

which from (2.120) is valid as $\mathrm{Re}\left(\alpha+\beta-\gamma\right) \overset{(4.37)}{\longmapsto} \frac{n-2}{2} > 0$, $n > 2$.

Recalling that separations z_1 are described by (2.75), and bearing in mind that given

$$(z_1)^{-\alpha}\,(1-z_1)^{\gamma-\beta-\alpha} = \left[\mathrm{sech}\left(\frac{s}{2a}\right)\right]^{n-1+2\mu}\left\{-\left[\sinh\left(\frac{s}{2a}\right)\right]^2\right\}^{1-\frac{n}{2}}, \tag{4.48}$$

then

$$(z_1)^{-\alpha}\,(1-z_1)^{\gamma-\beta-\alpha} \sim (-1)^n\frac{s^{2-n}}{2^{2-n}a^{2-n}}, \qquad s \to 0. \tag{4.49}$$

Matching the leading-order divergent behaviour of $G_{\mathrm{F}}^{n>2}(s)$ to that of $G_{\mathrm{H}}^{n>2}(s)$ fixes

$$J = \boldsymbol{i}(-1)^n\frac{a^{2-n}}{\pi^{\frac{n}{2}}2^n}\frac{\Gamma\left(\alpha\right)\Gamma\left(\alpha-\gamma+1\right)}{\Gamma\left(\alpha-\beta+1\right)}. \tag{4.50}$$

Therefore (for $n > 2$), the Feynman Green function resulting from Allen & Jacobson's treatment [4] is thus

$$G_{\mathrm{F}}(s) = \boldsymbol{i}\frac{a^{2-n}}{\pi^{\frac{n}{2}}2^n}\frac{\Gamma\left(\alpha\right)\Gamma\left(\alpha-\gamma+1\right)}{\Gamma\left(\alpha-\beta+1\right)}\,(z_1)^{-\alpha}\,F\left[\alpha,\alpha-\gamma+1;\alpha-\beta+1;(z_1)^{-1}\right]. \tag{4.51}$$

Explicitly, using (4.38) the expression is:

$$G_{\mathrm{F}}(s) = \boldsymbol{i}\frac{a^{2-n}}{\pi^{\frac{n}{2}}2^n}\frac{\Gamma\left(\frac{n-1}{2}+\mu\right)\Gamma\left(\frac{1}{2}+\mu\right)}{\Gamma\left(2\mu+1\right)} \times\left[\operatorname{sech}\left(\frac{s}{2a}\right)\right]^{n-1+2\mu} F\left[\frac{n-1}{2}+\mu,\frac{1}{2}+\mu;2\mu+1;\left[\operatorname{sech}\left(\frac{s}{2a}\right)\right]^2\right]. \tag{4.52}$$

II. Camporesi's method

Camporesi [19] follows Allen & Jacobson's approach [4] specialising to $n = 4$. Accordingly, a matching form for the equation (4.34) is obtained for $n = 4$. Its identification with the hypergeometric differential equation (4.35) also follows naturally. However the change of variable used by Camporesi to achieve this is

$$z_3 := -\left[\sinh\left(\frac{s}{2a}\right)\right]^2, \tag{4.53}$$

rather than (2.75).

Observing that in (4.38)

$$\alpha+\beta+1 = 2\gamma, \tag{4.54}$$

an acceptable solution to the hypergeometric equation in $z = z(s)$ near $z = 0$ for any $n \geq 2$ can be found from §9.153.7 of [45] to be

$$G_{\mathrm{F}}(s) = G_{\mathrm{F}(C)}(s) + G_{\mathrm{F}(D)}(s), \tag{4.55}$$

where

$$G_{\mathrm{F}(C)}(s) := CF\left[\frac{n-1}{2}+\mu,\frac{n-1}{2}-\mu;\frac{n}{2};z\right], \tag{4.56}$$

is the 'C-term' of the Feynman Green function,

$$G_{\mathrm{F}(D)}(s) := DF\left[\frac{n-1}{2}+\mu, \frac{n-1}{2}-\mu; \frac{n}{2}; 1-z\right], \tag{4.57}$$

is the 'D-term' of the Feynman Green function, with C and D undetermined coefficients.

A useful examination of (4.55) as $s \to \infty$ is achieved by the successive use of the pair of linear transformations

$$\begin{aligned} F[\alpha,\beta;\gamma;z] = &\frac{\Gamma(\gamma)\Gamma(\beta-\alpha)}{\Gamma(\beta)\Gamma(\gamma-\alpha)}(-z)^{-\alpha}F\left[\alpha,\alpha+1-\gamma;\alpha+1-\beta;z^{-1}\right] \\ &+\frac{\Gamma(\gamma)\Gamma(\alpha-\beta)}{\Gamma(\beta)\Gamma(\gamma-\beta)}(-z)^{-\beta}F\left[\beta,\beta+1-\gamma;\beta+1-\alpha;z^{-1}\right], \end{aligned} \tag{4.58}$$

(§2.10.2 in [38]) and

$$F\left[\alpha,\beta;\gamma;z^{-1}\right] = \left(1-z^{-1}\right)^{-\alpha}F\left[\alpha,\gamma-\beta;\gamma;\frac{z^{-1}}{z^{-1}-1}\right], \tag{4.59}$$

(§2.9.3 in [38]), on both the C and D-terms (equations (4.56) and (4.57) respectively), where

$$\begin{aligned} \alpha &\overset{(4.59)}{\longmapsto} \alpha, \\ \beta &\overset{(4.59)}{\longmapsto} \alpha+1-\gamma, \\ \gamma &\overset{(4.59)}{\longmapsto} \alpha+1-\beta, \end{aligned} \tag{4.60}$$

for the first term in (4.58) and

$$\begin{aligned}
\alpha &\overset{(4.59)}{\longmapsto} \beta, \\
\beta &\overset{(4.59)}{\longmapsto} \beta + 1 - \gamma, \\
\gamma &\overset{(4.59)}{\longmapsto} \beta + 1 - \alpha,
\end{aligned} \tag{4.61}$$

for the second term in (4.58).

The result of the application of (4.58) to (4.55), further transformed by (4.59) yields the expression

$$\begin{aligned}
G_{\mathrm{F}}(s) = (C + (-1)^{\frac{n-1}{2}+\mu} D) & \frac{\Gamma\left(\frac{n}{2}\right)\Gamma\left(-2\mu\right)}{\Gamma\left(\frac{n-1}{2}-\mu\right)\Gamma\left(\frac{1}{2}-\mu\right)} (-z)^{-\frac{n-1}{2}-\mu} \\
& \times F\left[\frac{n-1}{2}+\mu, \frac{1}{2}+\mu; 2\mu+1; (z)^{-1}\right] \\
+(C + (-1)^{\frac{n-1}{2}-\mu} D) & \frac{\Gamma\left(\frac{n}{2}\right)\Gamma\left(2\mu\right)}{\Gamma\left(\frac{n-1}{2}+\mu\right)\Gamma\left(\frac{1}{2}+\mu\right)} (-z)^{-\frac{n-1}{2}+\mu} \\
& \times F\left[\frac{n-1}{2}-\mu, \frac{1}{2}-\mu; 1-2\mu; (z)^{-1}\right].
\end{aligned} \tag{4.62}$$

Following [4], the behaviour of $G_{\mathrm{F}}(s)$ is considered at spatial infinity and then in the coincidence limit.

As $s \to \infty$, for $z = z_3$, the first term of (4.62) tends to zero whereas the second term is divergent. For a physically reasonable propagator, finite as $s \to \infty$,

$$C + (-1)^{\frac{n-1}{2}-\mu} D = 0. \tag{4.63}$$

Therefore

$$G_{\mathrm{F}}(s) = \boldsymbol{\kappa} DE\,(-z_3)^{-\frac{n-1}{2}-\mu}\,F\left[\frac{n-1}{2}+\mu, \frac{1}{2}+\mu; 2\mu+1; (z_3)^{-1}\right], \tag{4.64}$$

where

$$\boldsymbol{\kappa} := (-1)^{\frac{n-1}{2}-\mu+1} + (-1)^{\frac{n-1}{2}+\mu} \tag{4.65}$$

$$= 2\boldsymbol{i}^n \sin(\pi\mu), \tag{4.66}$$

and

$$E := \frac{\Gamma\left(\frac{n}{2}\right)\Gamma(-2\mu)}{\Gamma\left(\frac{n-1}{2}-\mu\right)\Gamma\left(\frac{1}{2}-\mu\right)}. \tag{4.67}$$

In the case of the 'C-term', for some $z(s) \to 0$ as $s \to 0$, only the zeroth summation index of the hypergeometric series expansion (2.117) contributes, hence

$$\lim_{s\to 0} G_{\mathrm{F}(C)}(s) = C. \tag{4.68}$$

In the case of the hypergeometric function in the 'D-term', the convergence criteria (2.120) for $z = 0$ require that

$$1 - \frac{n}{2} > 0, \tag{4.69}$$

which means that

$$G_{\mathrm{F}(D)}(s) \text{ diverges}, \qquad s \to 0,\ n \geq 2. \tag{4.70}$$

Therefore, the singularity structure of $G_{\mathrm{F}}(s)$ as $s \to 0$ lies only *within* the D-term, $G_{\mathrm{F}(D)}(s)$. It follows that to extract the singularity structure of $G_{\mathrm{F}(D)}(s)$ as $s \to 0$, it is necessary to determine the factor D.

Following [4], and abbreviating the hypergeometric function appearing in (4.64)

momentarily to $F(z)$, it is desirable to apply a linear transformation

$$F(z) \mapsto h(z) F\left(\tilde{z}(z)\right), \tag{4.71}$$

such that

$$\begin{cases} \tilde{z} \to 1, & s \to 0, \quad (4.72a) \\ F\left(\tilde{z}\right) \text{ converges}, & s \to 0, \quad (4.72b) \end{cases}$$

in order to make use of the relation §15.1.20 [2], allowing the result to be expressed independently of $\tilde{z}$ and solely in terms of gamma functions of n and μ.

This step is intended to displace the source of divergences to a hyperbolic function $h(z)$ in the prefactor of the resulting transformation, allowing the divergent structure to be subsequently exposed via a straightforward series expansion in s.

To achieve this, applying the transformation §15.3.4 [2] to the hypergeometric function in (4.64) gives

$$F\left[\frac{n-1}{2}+\mu, \frac{1}{2}+\mu; 2\mu+1; z^{-1}\right] = \left(1-z^{-1}\right)^{-\frac{n-1}{2}-\mu} \times F\left[\frac{n-1}{2}+\mu, \frac{1}{2}+\mu; 2\mu+1; \tilde{z}\right], \tag{4.73}$$

where

$$\tilde{z} := \frac{z^{-1}}{z^{-1}-1}. \tag{4.74}$$

However the convergence criteria (2.120) show that although $\tilde{z} \to 1$ as $s \to 0$ as desired in (4.72a), $F(\tilde{z})$ remains undefined for $\tilde{z} = 1$ for all $n \geq 2$.

A further linear transformation overcomes this remaining obstacle. Applying the transformation §15.3.3 from [2] to the hypergeometric function on the right-hand

side of (4.73) gives

$$F\left[\frac{n-1}{2}+\mu,\frac{1}{2}+\mu;2\mu+1;\tilde{z}\right]=(1-\tilde{z})^{1-\frac{n}{2}}\,F\left[\mu-\frac{n-3}{2},\frac{1}{2}+\mu;2\mu+1;\tilde{z}\right], \tag{4.75}$$

where $F\left[\mu-\frac{n-3}{2},\frac{1}{2}+\mu;2\mu+1;\tilde{z}\right]$ is convergent for all $n>2$.

Therefore, for $z=z_3$, combining (4.64), (4.73) and (4.75), gives

$$\begin{aligned}G_{\mathrm{F}}^{n>2}(s)=\boldsymbol{\kappa}DE&\left[\operatorname{sech}\left(\frac{s}{2a}\right)\right]^{n-1+2\mu}\left[\tanh\left(\frac{s}{2a}\right)\right]^{2-n}\\&\times F\left[\mu-\frac{n-3}{2},\frac{1}{2}+\mu;2\mu+1;\left[\operatorname{sech}\left(\frac{s}{2a}\right)\right]^{2}\right].\end{aligned} \tag{4.76}$$

Now the singularity structure of $G_{\mathrm{F}}^{n>2}(s)$ is contained within the $\left[\tanh\left(\frac{s}{2a}\right)\right]^{2-n}$ factor. This will allow a direct way of determining the coefficient D for $n>2$ as the leading-order divergence exhibited by the Hadamard form for separations approaching coincidence in (given by (4.42)) is identical.

Turning now to the $n=2$ case, the equation (4.52) yields the associations

$$\frac{n-1}{2}+\mu\overset{(4.52)}{\longmapsto}\alpha, \tag{4.77}$$

$$\frac{1}{2}+\mu\overset{(4.52)}{\longmapsto}\beta, \tag{4.78}$$

$$2\mu+1\overset{(4.52)}{\longmapsto}\gamma, \tag{4.79}$$

$$\Rightarrow\qquad \alpha\overset{(4.52)}{\longleftrightarrow}\beta, \tag{4.80}$$

$$\gamma\overset{(4.52)}{\longleftrightarrow}\alpha+\beta. \tag{4.81}$$

These relations allow the transformation §15.3.10 from [2] to be applied to the hy-

pergeometric function on the right-hand side of (4.73) yielding

$$F\left[\frac{1}{2}+\mu,\frac{1}{2}+\mu;2\mu+1;\tilde{z}\right] = \frac{\Gamma(2\mu+1)}{\left[\Gamma\left(\frac{1}{2}+\mu\right)\right]^2}\sum_{k=0}^{+\infty}\left[\frac{\left(\frac{1}{2}+\mu\right)_k}{k!}\right]^2\left[\Psi_{(1)}^{n=2}(\mu,k)-\ln(1-\tilde{z})\right](1-\tilde{z})^k, \tag{4.82}$$

where:

$$\Psi_{(1)}^{n=2}(\mu,k) := 2\left[\psi(k+1)-\psi\left(\tfrac{1}{2}+\mu+k\right)\right], \tag{4.83}$$

(with the subscript (1) distinguishing this function from another object also involving sums of psi functions appearing in the following section); and is valid because $|1-\tilde{z}|\to 0$ as $s\to 0$.

So, given (4.82) and (4.73), equation (4.64) becomes

$$G_{\mathrm{F}}^{n=2}(s) = \boldsymbol{\kappa}DE\left[\operatorname{sech}\left(\frac{s}{2a}\right)\right]^{2\mu+1}\frac{\Gamma(2\mu+1)}{\left[\Gamma\left(\frac{1}{2}+\mu\right)\right]^2} \times\sum_{k=0}^{+\infty}\left[\frac{\left(\frac{1}{2}+\mu\right)_k}{k!}\right]^2\left(\Psi_{(1)}^{n=2}(\mu,k)-\ln\left\{\left[\tanh\left(\frac{s}{2a}\right)\right]^2\right\}\right)\left[\tanh\left(\frac{s}{2a}\right)\right]^{2k}. \tag{4.84}$$

The behaviour of the expressions (4.84) and (4.76) are now examined respectively for separations approaching coincidence and then compared with their Hadamard-form counterparts (4.41) and (4.42) in order to determine D in each case.

The following useful relations between gamma and trigonometric functions are used

in the calculations for D.

$$\Gamma\left(\tfrac{1}{2}+\mu\right)\Gamma\left(\tfrac{1}{2}-\mu\right) = \pi\sec(\pi\mu), \qquad \text{§1.2.7 [38]}, \tag{4.85}$$

$$\Gamma\left(-2\mu\right)\Gamma\left(2\mu+1\right) = -\frac{\pi}{2}\sec(\pi\mu)\operatorname{cosec}(\pi\mu), \qquad \text{§6.1.17 [2]}. \tag{4.86}$$

$D^{n=2}$

For $n = 2$, as the $k = 0$ terms are the only contributors to the summation in (4.84) when $s = 0$, the form of the sum tends to $-\ln\left\{\left[\tanh\left(\frac{s}{2a}\right)\right]^2\right\}$ as $s \to 0$. Furthermore,

$$\ln\left\{\left[\tanh\left(\frac{s}{2a}\right)\right]^2\right\} \sim 2\ln\bar{s}, \qquad s \to 0, \tag{4.87}$$

Combining (4.41), (4.84) and (4.87),

$$D = D^{n=2}(\mu) = -\frac{\boldsymbol{i}}{8\pi\sin(\pi\mu)}\frac{\left[\Gamma\left(\frac{1}{2}+\mu\right)\Gamma\left(\frac{1}{2}-\mu\right)\right]^2}{\Gamma\left(-2\mu\right)\Gamma\left(2\mu+1\right)} \tag{4.88}$$

is obtained.

This expression is further simplified using (4.85) on the numerator, and (4.86) on the denominator, allowing (4.88) to be written as

$$D^{n=2}(\mu) = \frac{\boldsymbol{i}}{4}\sec(\pi\mu). \tag{4.89}$$

$D^{n>2}$

When $n > 2$, $D = D^{n>2}$, and the leading-order divergence of $G_{\rm F}(s)$ as $s \to 0$ is that of the $\left[\tanh\left(\frac{s}{2a}\right)\right]^{2-n}$ factor in (4.76) and so

$$\begin{aligned} G_{\rm F}^{n>2}(s) = 2\boldsymbol{i}^n \sin(\pi\mu) D^{n>2}(\mu) \\ \times \frac{\Gamma\left(\frac{n}{2}\right)\Gamma\left(-2\mu\right)}{\Gamma\left(\frac{n-1}{2}-\mu\right)\Gamma\left(\frac{1}{2}-\mu\right)} \frac{\Gamma\left(\frac{n}{2}-1\right)\Gamma\left(2\mu+1\right)}{\Gamma\left(\frac{n-1}{2}+\mu\right)\Gamma\left(\frac{1}{2}+\mu\right)} \\ \times (2a)^{n-2} s^{2-n} + \mathcal{O}(s^n)\,, \qquad s \to 0, \end{aligned} \tag{4.90}$$

as the criteria (2.120) for the hypergeometric function in (4.76) show that convergence is satisfied for $n > 2$.

The comparison of (4.90) with the leading-order divergence of the corresponding Hadamard form (4.42), yields

$$\begin{aligned} D^{n>2}(\mu) = \frac{\boldsymbol{i}^{1-n}}{2^{n+1}\pi^{\frac{n}{2}+1}a^{n-2}} \\ \times \frac{\Gamma\left(\frac{n-1}{2}-\mu\right)\Gamma\left(\frac{n-1}{2}+\mu\right)\Gamma\left(\frac{1}{2}-\mu\right)\Gamma\left(\frac{1}{2}+\mu\right)\Gamma\left(\mu\right)\Gamma\left(1-\mu\right)}{\Gamma\left(\frac{n}{2}\right)\Gamma\left(-2\mu\right)\Gamma\left(2\mu+1\right)}, \end{aligned} \tag{4.91}$$

where the $\sin(\pi\mu)$ has been converted into gamma functions using (4.86).

It is convenient for later calculations to split the result (4.91) into versions for n odd and n even. For $p=1,2,\ldots$, these expressions are:

$$D^{n=2p+1}(\mu)=\frac{(-1)^p}{4^{p+1}\pi^{p+\frac{3}{2}}a^{2p-1}}\frac{\Gamma\left(p-\mu\right)\Gamma\left(p+\mu\right)\Gamma\left(\frac{1}{2}-\mu\right)\Gamma\left(\frac{1}{2}+\mu\right)\Gamma\left(\mu\right)\Gamma\left(1-\mu\right)}{\Gamma\left(p+\frac{1}{2}\right)\Gamma\left(-2\mu\right)\Gamma\left(2\mu+1\right)}; \tag{4.92}$$

$$D^{n=2p+2}(\mu)=\frac{\boldsymbol{i}(-1)^{p+1}}{4^{p+\frac{3}{2}}\pi^{p+2}a^{2p}} \times\frac{\Gamma\left(p+\frac{1}{2}-\mu\right)\Gamma\left(p+\frac{1}{2}+\mu\right)\Gamma\left(\frac{1}{2}-\mu\right)\Gamma\left(\frac{1}{2}+\mu\right)\Gamma\left(\mu\right)\Gamma\left(1-\mu\right)}{\Gamma\left(p+1\right)\Gamma\left(-2\mu\right)\Gamma\left(2\mu+1\right)}, \tag{4.93}$$

respectively.

The remaining step in Camporesi's treatment applies (4.91) for $n=4$ to the hypergeometric function in (4.64) and then transforms the result using §2.11.4 from [38]:

$$F\left[\alpha,\beta;2\beta;z\right]=\left(1-\frac{z}{2}\right)^{-\alpha}F\left[\frac{\alpha}{2},\frac{\alpha+1}{2};\beta+\frac{1}{2};\left(\frac{z}{z-2}\right)^2\right], \tag{4.94}$$

together with §6.1.18 from [2] to yield

$$G_{\mathrm{F}}^{n=4}(s)=\boldsymbol{i}\frac{a^{-2}\Gamma(\mu+\frac{3}{2})}{\pi^{\frac{3}{2}}2^{\mu+\frac{5}{2}}\Gamma(\mu+1)}\left[\operatorname{sech}\left(\frac{s}{a}\right)\right]^{\frac{3}{2}+\mu} \times F\left[\frac{1}{2}\left(\mu+\frac{3}{2}\right),\frac{1}{2}\left(\mu+\frac{5}{2}\right);\mu+1;\left[\operatorname{sech}\left(\frac{s}{a}\right)\right]^2\right], \tag{4.95}$$

where from (3.58),

$$\mu=\sqrt{\frac{9}{4}+m_\xi^2a^2}, \tag{4.96}$$

which is in agreement with the result in [19] and also agrees with (4.52) (for $n=4$).

4.2.3 Comparison of results

The expressions for the n-dimensional Feynman Green functions using the mode sum method of Burgess & Lütken (4.33) and the Green function method of Allen & Jacobson (4.52) are found to agree. In addition, for the $n = 4$ case Camporesi's expression (4.95) also matches (4.33) and (4.52).

A further check was carried out on another independently derived expression for the n-dimensional Feynman Green function by Burges, Davis, Freedman & Gibbons [15], and this was also found to agree.

In summary, an expression for the n-dimensional Feynman Green function on AdS_n is given by:

$$G_{\mathrm{F}}(s) = \boldsymbol{i}\frac{a^{2-n}\Gamma(\mu+\frac{n-1}{2})}{\pi^{\frac{n-1}{2}}2^{\mu+\frac{n+1}{2}}\Gamma(\mu+1)}\left[\operatorname{sech}\left(\frac{s}{a}\right)\right]^{\frac{n-1}{2}+\mu} \times F\left[\frac{1}{2}\left(\mu+\frac{n-1}{2}\right),\frac{1}{2}\left(\mu+1+\frac{n-1}{2}\right);\mu+1;\left[\operatorname{sech}\left(\frac{s}{a}\right)\right]^2\right]. \tag{4.97}$$

4.3 Singularity structure of $G_{\mathrm{F}}(x, x')$

4.3.1 Introduction

Having calculated expressions for the Feynman Green function in section 4.2, the next quantity to be calculated following the scheme in figure 1.1 is the renormalised vacuum expectation value of the quadratic field fluctuations,

$$\langle \Phi^2(x) \rangle_{\mathrm{ren}} := \langle \mathbf{0} | \, \Phi^2(x) \, | \mathbf{0} \rangle_{\mathrm{ren}} \, . \tag{4.98}$$

In simple terms, renormalisation is a procedure that removes divergent parts of mathematical objects in order to allow them a physical interpretation. The nature of the divergences that characterise QFTs on curved space-times, and the subject of renormalisation in such theories is discussed in more detail later on, in sections 5.1 and 5.2.

The object $\langle \Phi^2(x) \rangle_{\mathrm{ren}}$ is the simplest renormalised object of a QFT. For this reason, and as renormalisation is somewhat tricky, computing $\langle \Phi^2(x) \rangle_{\mathrm{ren}}$ first makes for a very insightful precursor to renormalising expectation values of the stress-energy tensor.

In order to renormalise, it is first necessary to *regularise*. Recalling from section 4.1, regularisation is the identification of convergent and divergent terms within an expression. Bearing in mind the definition of the Feynman Green function (4.9), the *unrenormalised* vacuum expectation value of the quadratic field fluctuations may be defined as

$$\text{“}\langle \Phi^2(x) \rangle := -\boldsymbol{i} \lim_{x' \to x} G_{\mathrm{F}}(x, x')\text{”}, \tag{4.99}$$

using DeWitt's point-splitting method [33]. In keeping with the related discussion in

section 4.1, the equation (4.99) represents a formally divergent object, as $G_{\rm F}(x,x')$ is undefined in the limit involved, hence the quotation marks.

Accordingly, the focus of this section is the extraction of the singularity structure of the Feynman Green function (4.55) as $s \to 0$. In principle, alternative expressions such as (4.97) could be used as a starting-point for this treatment. However, as highlighted in (4.70), it is only the D-term that harbours the divergences sought. Therefore, the very definition (4.55) affords a clear separation into a known regular part (4.56) and a known singular part (4.57) from the outset.

Exploiting properties of the hypergeometric functions in (4.55) and expressions of the coefficient D in (4.88), (4.92) and (4.93), section 4.3.2 expands the 'D-term' of the Feynman Green function (4.57) exposing both its singularity structure in $z = z_3$ *and* any finite terms present. In a similar way, section 4.3.3 expands the purely regular 'C-term' of the Feynman Green function (4.56). Section 4.3.4 then reconstructs the full Feynman Green function (4.55) as an expansion in $z = z_3$.

Finally, section 4.3.5 examines the behaviour of the newly expanded Feynman Green function as an explicit function of s as $s \to 0$. Recalling (1.30), it is convenient for later calculations of $\langle \Phi^2(x) \rangle_{\rm ren}$ to also define a *non-vanishing* regular part, $G^{\bigstar}_{\rm F,\,reg}(s)$ of the Feynman Green function as $s \to 0$; and a non-vanishing singular part, $G^{\bigstar}_{\rm F,\,sing}(z)$ as $s \to 0$. As discussed later in section 5.1, when calculating $\langle \Phi^2(x) \rangle_{\rm ren}$, it is crucial to not lose sight of the fact that for even n with $n > 2$, the non-vanishing singular part $G^{n=2p+2\,\bigstar}_{\rm F,\,sing}(s)$, $p = 1, 2, \ldots$, $s \to 0$, also contains *finite* terms.

It turns out that for $n > 2$, there is no obvious way to express $G^{\bigstar}_{\rm F,\,reg}(s)$ and $G^{\bigstar}_{\rm F,\,sing}(s)$ as closed-forms, either for arbitrary n, or for n even and n odd separately. As a result, such expressions are computed using code for specific numbers of space-time dimensions. This step and the renormalisation of $G_{\rm F}(s)$ as $s \to 0$ are dealt with in section 5.1.

4.3.2 The 'D-term' — $G_{\mathrm{F}(D)}(x,x')$

Having derived expressions for the coefficient D in equations (4.88), (4.92) and (4.93), it is necessary to expand the hypergeometric function in (4.57) that houses the divergent behaviour of the Feynman Green function with the aim of exposing its singularity structure for later renormalisation.

Expansions of the D-term of $G_{\mathrm{F}}(z)$ for $n=2$, $n=2p+2$ and $n=2p+1$ (with $p=1,2,\ldots$) are respectively given below using the definition (4.57).

I. ——— $\boldsymbol{n=2}$ ———

In this case, the hypergeometric function present in (4.57),

$$F\left[\frac{n-1}{2}+\mu,\frac{n-1}{2}-\mu;\frac{n}{2};1-z\right]=F\left[\frac{1}{2}+\mu,\frac{1}{2}-\mu;1;1-z\right]. \tag{4.100}$$

Therefore, formula §15.3.10 from [2] can be applied to (4.100) yielding

$$F\left[\frac{1}{2}+\mu,\frac{1}{2}-\mu;1;1-z\right]=\frac{1}{\Gamma\left(\frac{1}{2}+\mu\right)\Gamma\left(\frac{1}{2}-\mu\right)} \times\sum_{k=0}^{+\infty}\frac{\left(\frac{1}{2}+\mu\right)_k\left(\frac{1}{2}-\mu\right)_k}{(k!)^2}\left[\Psi_{(2)}^{n=2}(\mu,k)-\ln z\right]z^k, \tag{4.101}$$

where

$$\Psi_{(2)}^{n=2}(\mu,k):=2\psi(k+1)-\psi\left(\tfrac{1}{2}+\mu+k\right)-\psi\left(\tfrac{1}{2}-\mu+k\right), \tag{4.102}$$

and where equation (4.101) is valid as $s\to 0$.

The results (4.88) and (4.101) yield

$$G^{n=2}_{\mathrm{F}(D)}(z) = \frac{\boldsymbol{i}}{4\pi}\sum_{k=0}^{+\infty}\frac{\left(\frac{1}{2}+\mu\right)_k\left(\frac{1}{2}-\mu\right)_k}{(k!)^2}\left[\Psi^{n=2}_{(2)}(\mu,k)-\ln z\right]z^k, \tag{4.103}$$

revealing a logarithmic singularity as $s \to 0$.

II. $n > 2$, n EVEN

When $n = 2p+2$ with $p = 1, 2, \ldots$, the hypergeometric function present in (4.57),

$$F\left[\frac{n-1}{2}+\mu, \frac{n-1}{2}-\mu; \frac{n}{2}; 1-z\right] = F\left[p+\frac{1}{2}+\mu, p+\frac{1}{2}-\mu; p+1; 1-z\right]. \tag{4.104}$$

Therefore, formula §15.3.12 from [2] can be applied to (4.104) yielding

$$\begin{aligned} &F\left[p+\frac{1}{2}+\mu, p+\frac{1}{2}-\mu; p+1; 1-z\right] \\ &\quad= \frac{\Gamma(p)\,\Gamma(p+1)}{\Gamma\left(p+\frac{1}{2}+\mu\right)\Gamma\left(p+\frac{1}{2}-\mu\right)}z^{-p}\sum_{k=0}^{p-1}\frac{\left(\frac{1}{2}+\mu\right)_k\left(\frac{1}{2}-\mu\right)_k}{k!\,(1-p)_k}z^k \\ &\qquad-(-1)^p\frac{\Gamma(p+1)}{\Gamma\left(\frac{1}{2}+\mu\right)\Gamma\left(\frac{1}{2}-\mu\right)}\sum_{k=0}^{+\infty}\frac{\left(p+\frac{1}{2}+\mu\right)_k\left(p+\frac{1}{2}-\mu\right)_k}{k!(k+p)!} \\ &\qquad\qquad\times z^k\left[\Psi^{n=2p+2}(\mu,k)+\ln z\right], \end{aligned} \tag{4.105}$$

with

$$\Psi^{n=2p+2}(\mu,k) := -\psi(k+1)-\psi(k+p+1)+\psi\left(p+\tfrac{1}{2}+\mu+k\right)+\psi\left(p+\tfrac{1}{2}-\mu+k\right), \tag{4.106}$$

and where equation (4.105) is valid as $s \to 0$.

The results (4.93) and (4.105) combine to give

$$\begin{aligned}
&G^{n=2p+2}_{{\rm F}(D)}(z)\\
&= \frac{\boldsymbol{i}(-1)^{p+1}}{4^{p+\frac{3}{2}}\pi^{p+2}a^{2p}}\frac{\Gamma(\mu)\,\Gamma(1-\mu)\,\Gamma\left(\frac{1}{2}-\mu\right)\Gamma\left(\frac{1}{2}+\mu\right)}{\Gamma(-2\mu)\,\Gamma(2\mu+1)}\\
&\quad\times\Bigg\{\Gamma(p)\,z^{-p}\sum_{k=0}^{p-1}\frac{\left(\frac{1}{2}+\mu\right)_k\left(\frac{1}{2}-\mu\right)_k}{k!\,(1-p)_k}z^k-(-1)^p\left(\frac{1}{2}+\mu\right)_p\left(\frac{1}{2}-\mu\right)_p\\
&\qquad\qquad\times\sum_{k=0}^{+\infty}\frac{\left(p+\frac{1}{2}+\mu\right)_k\left(p+\frac{1}{2}-\mu\right)_k}{k!(k+p)!}\left[\Psi^{n=2p+2}(\mu,k)+\ln z\right]z^k\Bigg\},
\end{aligned}\tag{4.107}$$

exhibiting poles in the first term and a logarithmic divergence in the second term as $s\to 0$.

III. $n>2$, n ODD

When $n=2p+1$ with $p=1,2,\ldots$, the hypergeometric function in (4.57)

$$F\left[\frac{n-1}{2}+\mu,\frac{n-1}{2}-\mu;\frac{n}{2};1-z\right]=F\left[p+\mu,p-\mu;p+\frac{1}{2};1-z\right].\tag{4.108}$$

Therefore, formula §15.3.6 from [2] can be applied to (4.108) yielding

$$\begin{aligned}
&F\left[p+\mu,p-\mu;p+\frac{1}{2};1-z\right]\\
&\qquad=\frac{\Gamma\left(p+\frac{1}{2}\right)\Gamma\left(\frac{1}{2}-p\right)}{\Gamma\left(\frac{1}{2}+\mu\right)\Gamma\left(\frac{1}{2}-\mu\right)}F\left[p+\mu,p-\mu;p+\frac{1}{2};z\right]\\
&\qquad\quad+z^{\frac{1}{2}-p}\frac{\Gamma\left(p+\frac{1}{2}\right)\Gamma\left(p-\frac{1}{2}\right)}{\Gamma(p+\mu)\,\Gamma(p-\mu)}F\left[\frac{1}{2}-\mu,\frac{1}{2}+\mu;\frac{3}{2}-p;z\right],
\end{aligned}\tag{4.109}$$

which is valid as $s\to 0$.

The expressions (4.92) and (4.109) combine to give

$$G^{n=2p+1}_{\mathrm{F}(D)}(z) = \frac{(-1)^p}{4^{p+1}\pi^{p+\frac{3}{2}}a^{2p-1}}\frac{\Gamma(\mu)\,\Gamma(1-\mu)}{\Gamma(-2\mu)\,\Gamma(2\mu+1)} \times\left\{\Gamma\left(\tfrac{1}{2}-p\right)\Gamma(p-\mu)\,\Gamma(p+\mu)\,F\left[p+\mu,p-\mu;p+\frac{1}{2};z\right] + \Gamma\left(p-\tfrac{1}{2}\right)\Gamma\left(\tfrac{1}{2}-\mu\right)\Gamma\left(\tfrac{1}{2}+\mu\right)z^{\frac{1}{2}-p}F\left[\frac{1}{2}+\mu,\frac{1}{2}-\mu;\frac{3}{2}-p;z\right]\right\}. \tag{4.110}$$

The recurrence formulae §6.1.15 and §6.1.16 in [2] imply that

$$\Gamma(p\pm\mu+k) = (p\pm\mu)_k\,(\pm\mu)_p\,\Gamma(\pm\mu), \tag{4.111}$$

and the reflection formula §6.1.17 in [2] implies that

$$\Gamma(\mu)\,\Gamma(-\mu) = -\frac{\pi}{\mu}\operatorname{cosec}(\pi\mu). \tag{4.112}$$

Applying the results (4.111) and (4.86) to (4.110) allows the latter to also be written in the form,

$$G^{n=2p+1}_{\mathrm{F}(D)}(z) = \frac{(-1)^p}{4^{p+\frac{1}{2}}\pi^{p+\frac{3}{2}}a^{2p-1}}\left\{\Gamma\left(\tfrac{1}{2}-p\right)\frac{(\mu)_p\,(-\mu)_p}{\mu}\pi\cot(\pi\mu)F\left[p+\mu,p-\mu;p+\frac{1}{2};z\right] -\pi\Gamma\left(p-\tfrac{1}{2}\right)\sum_{k=0}^{+\infty}\frac{\left(\frac{1}{2}+\mu\right)_k\left(\frac{1}{2}-\mu\right)_k}{\left(\frac{3}{2}-p\right)_k}\frac{z^{k+\frac{1}{2}-p}}{k!}\right\}, [2pt]$$

the imaginary part of which is hidden in the $z^{\frac{1}{2}}$ factor in the sum over k (recalling (4.53)).

Now, applying (4.86)

$$\Gamma\left(\tfrac{1}{2}-p\right) = \frac{1}{\Gamma\left(p+\frac{1}{2}\right)}\pi\,\mathrm{cosec}\left(\pi\left(p+\tfrac{1}{2}\right)\right)$$
$$= \frac{(-1)^p}{\Gamma\left(p+\frac{1}{2}\right)}\pi. \tag{4.113}$$

Therefore

$$G^{n=2p+1}_{\mathrm{F}(D)}(z)$$
$$= \frac{(-1)^p}{(4\pi)^{p+\frac{1}{2}}a^{2p-1}}\left\{\frac{(-1)^p}{\Gamma\left(p+\frac{1}{2}\right)}\frac{(\mu)_p\,(-\mu)_p}{\mu}\pi\cot(\pi\mu)F\left[p+\mu,p-\mu;p+\frac{1}{2};z\right]\right.$$
$$\left.-\Gamma\left(p-\tfrac{1}{2}\right)\sum_{k=0}^{+\infty}\frac{\left(\frac{1}{2}+\mu\right)_k\left(\frac{1}{2}-\mu\right)_k}{\left(\frac{3}{2}-p\right)_k}\frac{z^{k+\frac{1}{2}-p}}{k!}\right\}. \tag{4.114}$$

4.3.3 The 'C-term' — $G_{\mathrm{F}(C)}(x,x')$

Recalling from (4.63) that the coefficient C in (4.55) is given by

$$C = (-1)^{\frac{n+1}{2}-\mu}D, \tag{4.115}$$

expansions of the C-term of $G_{\rm F}(z)$ for $n=2$, $n=2p+2$ and $n=2p+1$ (with $p=1,2,\ldots$) are respectively given below using the definition (4.56).

Expressions for $G_{\mathrm{F}(C)}(z)$ are simplified with the help of the relations:

$$\frac{\Gamma(\mu)\,\Gamma(1-\mu)}{\Gamma(-2\mu)\,\Gamma(2\mu+1)} = -2\cos(\pi\mu), \tag{4.116}$$

obtained by applying (4.112) to the numerator and denominator, for $n>2$; and for

$n \geq 2$:

$$(-1)^{-\mu} = \cos(\pi\mu) - \boldsymbol{i}\sin(\pi\mu), \tag{4.117}$$

obtained from Euler's formula.

I. $n = 2$

The result (4.88) and the hypergeometric function in (4.56) combine to give

$$G^{n=2}_{\mathrm{F}(C)}(z) = \frac{(-1)^{-\mu}}{4\pi}\sum_{k=0}^{+\infty}\frac{\Gamma\left(\frac{1}{2}+\mu+k\right)\Gamma\left(\frac{1}{2}-\mu+k\right)}{(k!)^2}z^k, \tag{4.118}$$

which can also be written in terms of Pochhammer symbols as

$$G^{n=2}_{\mathrm{F}(C)}(z) = \frac{(-1)^{-\mu}}{4}\sec(\pi\mu)\sum_{k=0}^{+\infty}\frac{\left(\frac{1}{2}+\mu\right)_k\left(\frac{1}{2}-\mu\right)_k}{(k!)^2}z^k. \tag{4.119}$$

Given (4.117),

$$G^{n=2}_{\mathrm{F}(C)}(z) = \frac{1}{4}\left[1 - \boldsymbol{i}\tan(\pi\mu)\right]\sum_{k=0}^{+\infty}\frac{\left(\frac{1}{2}+\mu\right)_k\left(\frac{1}{2}-\mu\right)_k}{(k!)^2}z^k. \tag{4.120}$$

II. $n > 2$, n EVEN

The result (4.93) and the hypergeometric function in (4.56) give

$$\begin{aligned} G^{n=2p+2}_{\mathrm{F}(C)}(z) = {} & \frac{(-1)^{1-\mu}}{4^{p+\frac{3}{2}}\pi^{p+2}a^{2p}}\frac{\Gamma(\mu)\Gamma(1-\mu)\Gamma\left(\frac{1}{2}-\mu\right)\Gamma\left(\frac{1}{2}+\mu\right)}{\Gamma(-2\mu)\Gamma(2\mu+1)} \\ & \times\sum_{k=0}^{+\infty}\frac{\Gamma\left(p+\frac{1}{2}+\mu+k\right)\Gamma\left(p+\frac{1}{2}-\mu+k\right)}{k!(p+k)!}z^k, \end{aligned} \tag{4.121}$$

which can also be written

$$G^{n=2p+2}_{{\rm F}(C)}(z) = \frac{(-1)^{-\mu}}{(4\pi)^{p+1}a^{2p}} \sum_{k=0}^{+\infty} \frac{\Gamma\left(p+\frac{1}{2}+\mu+k\right)\Gamma\left(p+\frac{1}{2}-\mu+k\right)}{k!\,(p+k)!} z^k, \tag{4.122}$$

using the results (4.116) and (4.85).

The recurrence formulae §6.1.15 and §6.1.16 in [2] imply that,

$$\Gamma\left(p+\tfrac{1}{2}\pm\mu+k\right) = \left(\tfrac{1}{2}\pm\mu+p\right)_k \left(\tfrac{1}{2}\pm\mu\right)_p \Gamma\left(\tfrac{1}{2}\pm\mu\right). \tag{4.123}$$

Given the results (4.85) and (4.117) and (4.123),

$$\begin{aligned} G^{n=2p+2}_{{\rm F}(C)}(z) = {} & \frac{\pi\left[1-\boldsymbol{i}\tan(\pi\mu)\right]}{(4\pi)^{p+1}a^{2p}} \left(\tfrac{1}{2}+\mu\right)_p \left(\tfrac{1}{2}-\mu\right)_p \\ & \times \sum_{k=0}^{+\infty} \frac{\left(p+\frac{1}{2}+\mu\right)_k \left(p+\frac{1}{2}-\mu\right)_k}{k!\,(p+k)!} z^k. \end{aligned} \tag{4.124}$$

III. $n > 2$, n ODD

The expressions (4.92) and the hypergeometric function in (4.56) yield

$$\begin{aligned} G^{n=2p+1}_{{\rm F}(C)}(z) = {} & \frac{(-1)^{1-\mu}}{4^{p+1}\pi^{p+\frac{3}{2}}a^{2p-1}} \frac{\Gamma(\mu)\,\Gamma(1-\mu)\,\Gamma\left(\frac{1}{2}-\mu\right)\Gamma\left(\frac{1}{2}+\mu\right)}{\Gamma(-2\mu)\,\Gamma(2\mu+1)} \\ & \times \sum_{k=0}^{+\infty} \frac{\Gamma(p+\mu+k)\,\Gamma(p-\mu+k)}{\Gamma\left(p+\frac{1}{2}+k\right)} \frac{z^k}{k!}, \end{aligned} \tag{4.125}$$

which can also be written

$$G^{n=2p+1}_{{\rm F}(C)}(z) = \frac{(-1)^{-\mu}}{(4\pi)^{p+\frac{1}{2}}a^{2p-1}} \sum_{k=0}^{+\infty} \frac{\Gamma(p+\mu+k)\,\Gamma(p-\mu+k)}{\Gamma\left(p+\frac{1}{2}+k\right)} \frac{z^k}{k!}, \tag{4.126}$$

using the results (4.116) and (4.85).

Applying (4.111) and (4.112) to (4.126) allows it also to be written in the form

$$G^{n=2p+1}_{\mathrm{F}(C)}(z) = \frac{\boldsymbol{i}}{(4\pi)^{p+\frac{1}{2}} a^{2p-1}\Gamma\left(p+\frac{1}{2}\right)} \frac{(\mu)_p\,(-\mu)_p}{\mu}\left[\boldsymbol{i}\pi\cot(\pi\mu)+\pi\right]$$
$$\times F\left[p+\mu, p-\mu; p+\frac{1}{2}; z\right]. \tag{4.127}$$

4.3.4 The series expansion

This section details the construction of the full Feynman Green function (4.55) as a series expansion for $n = 2$, $n > 2$, with n even and $n > 2$, with n odd. The procedure essentially adds the expressions in sections 4.3.2 and 4.3.3 for the 'C-term' and 'D-term' respectively.

The relations involving psi functions

$$\psi\left(k+1\right) = -\boldsymbol{\gamma} + \sum_{l=1}^{k} \frac{1}{l}, \qquad \text{§8.365.3 [45]}, \tag{4.128}$$

$$\psi\left(p+\tfrac{1}{2}\pm\mu+k\right) = \psi\left(\tfrac{1}{2}\pm\mu\right) + \sum_{l=0}^{p+k-1} \frac{1}{\frac{1}{2}\pm\mu+l}, \qquad \text{§8.365.4 [45]}, \tag{4.129}$$

$$\pi\tan(\pi\mu) = \psi\left(\tfrac{1}{2}+\mu\right) - \psi\left(\tfrac{1}{2}-\mu\right), \qquad \text{§8.365.9 [45]}, \tag{4.130}$$

(where $\boldsymbol{\gamma}$ is the Euler-Mascheroni constant), are referred to in the calculations that follow.

I. $\boldsymbol{n=2}$

Combining the C and D terms of the Feynman Green function (using (4.103) and (4.119) respectively) yields

$$G_{\mathrm{F}}^{n=2}(z)=\frac{1}{4\pi}\sum_{k=0}^{+\infty}\frac{\left(\frac{1}{2}+\mu\right)_k\left(\frac{1}{2}-\mu\right)_k}{(k!)^2}Z_{\log}^{n=2}(\mu,k,z)\,z^k, \tag{4.131}$$

where

$$Z_{\log}^{n=2}(\mu,k,z):=(-1)^{-\mu}\,\pi\sec(\pi\mu)+\boldsymbol{i}\Psi_{(2)}^{n=2}(\mu,k)-\boldsymbol{i}\ln z. \tag{4.132}$$

Inserting the result (4.117) and the definition for $\Psi_{(2)}^{n=2}(\mu,k)$ (4.102),

$$Z_{\log}^{n=2}(\mu,k,z)=\pi-\boldsymbol{i}\left[\pi\tan(\pi\mu)-2\psi(k+1)+\psi\left(\tfrac{1}{2}+\mu+k\right)+\psi\left(\tfrac{1}{2}-\mu+k\right)+\ln z\right], \tag{4.133}$$

which is simplified by applying (4.129) and (4.128) to the third term and both the fourth and fifth terms respectively giving

$$Z_{\log}^{n=2}(\mu,k,z)=\pi-\boldsymbol{i}\left[\pi\tan(\pi\mu)+2\boldsymbol{\gamma}-2\sum_{l=1}^{k}\frac{1}{l}+\psi\left(\tfrac{1}{2}+\mu\right)+\psi\left(\tfrac{1}{2}-\mu\right)+\sum_{l=0}^{k-1}\left\{\frac{1}{\frac{1}{2}+\mu+l}+\frac{1}{\frac{1}{2}-\mu+l}\right\}+\ln z\right]. \tag{4.134}$$

The expression for $Z_{\log}^{n=2}(\mu,k,z)$ above can be further simplied by applying (4.130)

on the $\pi\tan(\pi\mu)$ term such that

$$Z_{\log}^{n=2}(\mu,k,z)=\pi-\boldsymbol{i}\left[2\psi\left(\tfrac{1}{2}+\mu\right)+2\boldsymbol{\gamma}-2\sum_{l=1}^{k}\frac{1}{l}+\sum_{l=0}^{k-1}\left\{\frac{1}{\frac{1}{2}+\mu+l}+\frac{1}{\frac{1}{2}-\mu+l}\right\}+\ln z\right]. \tag{4.135}$$

II. $n>2$, n EVEN

Adding the C-term (4.124) and the D-term (4.107) gives

$$\begin{aligned}&G_{\mathrm{F}}^{n=2p+2}(z)\\&=\frac{1}{(4\pi)^{p+1}a^{2p}}\left[Z_{\mathrm{FLS}}^{n=2p+2}(\mu,k,z)+\left(\tfrac{1}{2}+\mu\right)_p\left(\tfrac{1}{2}-\mu\right)_p\right.\\&\qquad\left.\times\sum_{k=0}^{+\infty}\frac{\left(p+\frac{1}{2}+\mu\right)_k\left(p+\frac{1}{2}-\mu\right)_k}{k!\,(p+k)!}Z_{\log}^{n=2p+2}(\mu,k,z)\,z^k\right],\end{aligned} \tag{4.136}$$

where:

$$Z_{\log}^{n=2p+2}(\mu,k,z):=\pi-\boldsymbol{i}\left[\pi\tan(\pi\mu)+\Psi^{n=2p+2}(\mu,k)+\ln z\right]; \tag{4.137}$$

and

$$Z_{\mathrm{FLS}}^{n=2p+2}(\mu,k,z):=\boldsymbol{i}\,(-1)^p\,\Gamma(p)\sum_{k=0}^{p-1}\frac{\left(\frac{1}{2}+\mu\right)_k\left(\frac{1}{2}-\mu\right)_k}{k!\,(1-p)_k}z^{k-p}. \tag{4.138}$$

The object (4.137) is simplified using formula (4.130) and recalling the definition (4.106), applying (4.129) and (4.128) yielding

$$Z_{\log}^{n=2p+2}(\mu,k,z):=\pi-\boldsymbol{i}\left[2\psi\left(\tfrac{1}{2}+\mu\right)+2\boldsymbol{\gamma}+L(p,k)+\ln z\right], \tag{4.139}$$

where

$$L(p,k) := \sum_{l=0}^{p+k-1} \left\{ \frac{1}{\frac{1}{2}+\mu+l} + \frac{1}{\frac{1}{2}-\mu+l} \right\} - \sum_{l=1}^{k+p} \frac{1}{l} - \sum_{l=1}^{k} \frac{1}{l}. \tag{4.140}$$

III. $n > 2$, n ODD

Adding the C-term (4.127) and D-term (4.114) gives

$$G_{\rm F}^{n=2p+1}(z) = \frac{(-1)^p}{(4\pi)^{p+\frac{1}{2}} a^{2p-1}} \left\{ \frac{\boldsymbol{i}\pi}{\Gamma\left(p+\frac{1}{2}\right)} \frac{(\mu)_p \, (-\mu)_p}{\mu} F\left[p+\mu, p-\mu; p+\frac{1}{2}; z \right] + Z_{\rm FLS}^{n=2p+1}(\mu,k,z) \right\}, \tag{4.141}$$

where

$$Z_{\rm FLS}^{n=2p+1}(\mu,k,z) := -(-1)^p \, \Gamma\left(p-\tfrac{1}{2}\right) \sum_{k=0}^{+\infty} \frac{\left(\frac{1}{2}+\mu\right)_k \left(\frac{1}{2}-\mu\right)_k}{\left(\frac{3}{2}-p\right)_k} \frac{z^{k+\frac{1}{2}-p}}{k!}. \tag{4.142}$$

4.3.5 The singular part — $G_{\rm F,\,sing}(x,x')$

The expressions (4.131), (4.136) and (4.141) for the full series expansions of the Feynman Green function in (4.55) for $n = 2$, $n > 2$ for n even and n odd respectively, reveal clear singularity structures. This is good news for the point-splitting regularisation procedure as divergent terms can be easily gleaned. The focus of this section is extracting the singular parts of the Feynman Green function in preparation for later renormalisation.

I. $n = 2$

Recalling that $\bar{s}$ and $\bar{a}$ are the dimensionless versions of the radius of curvature a and geodetic interval s multiplied by the mass renormalisation scale M, then as $s \to 0$,

$$\ln z \to 2\ln\bar{s} - 2\ln 2 - 2\ln\bar{a} + \boldsymbol{i}\,\mathrm{csgn}\left(\boldsymbol{i}s^2\right)\pi + \mathcal{O}\left(s^2\right), \tag{4.143}$$

where

$$\mathrm{csgn}\, z' = \begin{cases} 1, & \mathrm{Re}\, z' > 0, \quad or \quad \mathrm{Re}\, z' = 0,\ \mathrm{Im}\, z' > 0, & \text{(4.144a)} \\ -1, & \mathrm{Re}\, z' < 0, \quad or \quad \mathrm{Re}\, z' = 0,\ \mathrm{Im}\, z' < 0, & \text{(4.144b)} \end{cases}$$

is the generalisation of the signum function to complex numbers (see e.g. [23]). For timelike intervals $s^2 < 0$, therefore, the term in π inside the expansion of $\ln z$ cancels out the $\boldsymbol{i}\pi$ in $Z^{n=2}_{\log}$ (4.133).

As $s \to 0$, only the $k = 0$ terms in (4.131) contribute. Therefore, the *non-vanishing* (indicated by the $\bigstar$ in the superscript) part of the Feynman Green function as $s \to 0$ (see (1.30)) is

$$G_{\mathrm{F}}^{n=2\bigstar}(s) = -\frac{\boldsymbol{i}}{2\pi}\left[\ln\bar{s} - \ln\bar{a} - \ln 2 + \psi\left(\tfrac{1}{2}+\mu\right) + \boldsymbol{\gamma}\right]. \tag{4.145}$$

Accordingly, the non-vanishing regular part of the Feynman Green function as $s \to 0$ is:

$$G_{\mathrm{F,\,reg}}^{n=2\bigstar}(s) = -\frac{\boldsymbol{i}}{2\pi}\left[\psi\left(\tfrac{1}{2}+\mu\right) + \boldsymbol{\gamma} - \ln\bar{a} - \ln 2\right], \tag{4.146}$$

and the non-vanishing singular part of the Feynman Green function as $s \to 0$ is

$$G_{\mathrm{F,\,sing}}^{n=2\bigstar}(s) = -\frac{\boldsymbol{i}}{2\pi}\ln\bar{s}. \tag{4.147}$$

II. $n > 2$, n EVEN

As $s \to 0$, only the $k = 0$ terms of the sum over the quantity $Z_{\log}^{n=2p+2}(\mu, k, z)$ in (4.136) contribute.

Therefore, the non-vanishing part of the Feynman Green function as $s \to 0$ is

$$G_{\rm F}^{n=2p+2\bigstar}(z) = \frac{1}{(4\pi)^{p+1}a^{2p}}\Bigg[Z_{\rm FLS}^{n=2p+2\bigstar}(\mu,0,z) + \frac{\left(\frac{1}{2}+\mu\right)_p\left(\frac{1}{2}-\mu\right)_p}{p!}Z_{\log}^{n=2p+2\bigstar}(\mu,0,z)\Bigg], \tag{4.148}$$

where from (4.139)

$$Z_{\log}^{n=2p+2}(\mu,0,z) = \pi - \boldsymbol{i}\left[\ln z + 2\psi\left(\tfrac{1}{2}+\mu\right) + 2\boldsymbol{\gamma} + L(p,0)\right], \tag{4.149}$$

with (4.140) giving

$$L(p,0) = \sum_{l=0}^{p-1}\left\{\frac{1}{\frac{1}{2}+\mu+l} + \frac{1}{\frac{1}{2}-\mu+l}\right\} - \sum_{l=1}^{p}\frac{1}{l}. \tag{4.150}$$

Therefore, recalling (4.143), the non-vanishing regular part of the Feynman Green function as $s \to 0$ is

$$G_{\rm F,\,reg}^{n=2p+2\bigstar}(s) = \frac{-\boldsymbol{i}}{4^{p+\frac{1}{2}}\pi^{p+1}a^{2p}p!}\left(\tfrac{1}{2}+\mu\right)_p\left(\tfrac{1}{2}-\mu\right)_p \times\left[\psi\left(\tfrac{1}{2}+\mu\right) + \boldsymbol{\gamma} + \frac{1}{2}L(p,0) - \ln 2 - \ln\bar{a}\right], \tag{4.151}$$

and the non-vanishing singular part of the Feynman Green function is

$$G^{n=2p+2\bigstar}_{\text{F, sing}}(z) = \frac{1}{4^{p+\frac{1}{2}}\pi^{p+1}a^{2p}} \times \left[-\boldsymbol{i}\frac{\left(\frac{1}{2}+\mu\right)_p\left(\frac{1}{2}-\mu\right)_p}{p!}\ln\bar{s} + \frac{1}{2}Z^{n=2p+2\bigstar}(\mu,0,z)\right]. \tag{4.152}$$

III. $n > 2$, n ODD

Referring to (4.141), as $s \to 0$, the hypergeometric function $F\left[p+\mu, p-\mu; p+\frac{1}{2}; z\right] \to 1$.

As a result, the non-vanishing Feynman Green function as $s \to 0$ is

$$G^{n=2p+1\bigstar}_{\text{F}}(z) = \frac{1}{(4\pi)^{p+\frac{1}{2}}a^{2p-1}}\left[\frac{\boldsymbol{i}\pi}{\Gamma\left(p+\frac{1}{2}\right)}\frac{(\mu)_p(-\mu)_p}{\mu} + Z^{n=2p+1\bigstar}_{\text{FLS}}(\mu,k,z)\right]. \tag{4.153}$$

Therefore, the non-vanishing regular part of the Feynman Green function as $s \to 0$ is

$$G^{n=2p+1\bigstar}_{\text{F, reg}}(s) = \frac{\boldsymbol{i}}{4^{p+\frac{1}{2}}\pi^{p-\frac{1}{2}}a^{2p-1}\Gamma\left(p+\frac{1}{2}\right)}\frac{(\mu)_p(-\mu)_p}{\mu}, \tag{4.154}$$

and the non-vanishing singular part of the Feynman Green function as $s \to 0$ is

$$G^{n=2p+1\bigstar}_{\text{F, sing}}(z) = \frac{1}{(4\pi)^{p+\frac{1}{2}}a^{2p-1}}Z^{n=2p+1\bigstar}_{\text{FLS}}(\mu,k,z). \tag{4.155}$$

4.4 The Hadamard form — $G_{\rm H}(x,x')$

4.4.1 Introduction

It is fortunate for renormalisation that there is a theorem due to Hadamard [47] which states exactly the form of the singularity structure of the Feynman Green function as the coincidence limit is approached in *any* space-time.

Generally, the Hadamard form is dependent on biscalar quantities. However, in the case of AdS_n and other maximally symmetic space-times calculations are significantly simplified. In particular, the key ingredients of the Hadamard expansion depend *only* on the geodetic interval s (or equivalently on the invariant distance σ).

Accordingly, the Hadamard form of the Feynman Green function for AdS_n is [31]

$$G_{\rm H}(\sigma) = \boldsymbol{i}\nu(n)\left[U(\sigma)\sigma^{1-\frac{n}{2}} + V(\sigma)\ln\bar{\sigma} + W(\sigma)\right], \qquad n \geq 2, \tag{4.156}$$

with

$$\nu(n) = \begin{cases} \dfrac{1}{4\pi}, & n = 2, \quad (4.157a) \\[2ex] \dfrac{\Gamma\left(\frac{n}{2}-1\right)}{2(2\pi)^{\frac{n}{2}}}, & n > 2, \quad (4.157b) \end{cases}$$

recalling that $\bar{\sigma}$ is a dimensionless variable (4.44) related to σ, through the mass renormalisation scale M, and where the Hadamard functions $U(\sigma)$, $V(\sigma)$ and $W(\sigma)$ are all regular in the coincidence limit.

The conventional *Ansatz* for the Hadamard functions are formal Laurent series (FLS)

expansions [31],

$$U(\sigma) = \begin{cases} 0, & n = 2, \quad (4.158a) \\ \sum_{l=0}^{+\infty} U_l(\sigma)\sigma^l, & n \text{ odd}, \quad (4.158b) \\ \sum_{l=0}^{\frac{n}{2}-2} U_l(\sigma)\sigma^l, & n > 2,\ n \text{ even}, \quad (4.158c) \end{cases}$$

$$V(\sigma) = \begin{cases} 0, & n \text{ odd}, \quad (4.159a) \\ \sum_{l=0}^{+\infty} V_l(\sigma)\sigma^l, & n \text{ even}, \quad (4.159b) \end{cases}$$

$$W(\sigma) = \sum_{l=0}^{+\infty} W_l(\sigma)\sigma^l, \qquad \forall\, n. \quad (4.160)$$

The Hadamard coefficients are given by [31]

$$U_l(\sigma) = u_l(x) + \sum_{k=1}^{+\infty} \frac{(-1)^k}{k!} u_{l(k)}, \qquad u_{l(k)} := u_{lp_1\cdots p_k}(x)\sigma^{;p_1}\cdots\sigma^{;p_k}, \quad (4.161)$$

$$V_l(\sigma) = v_l(x) + \sum_{k=1}^{+\infty} \frac{(-1)^k}{k!} v_{l(k)}, \qquad v_{l(k)} := v_{lp_1\cdots p_k}(x)\sigma^{;p_1}\cdots\sigma^{;p_k}, \quad (4.162)$$

$$W(\sigma) = w(x) + \sum_{k=1}^{+\infty} \frac{(-1)^k}{k!} w_{(k)}, \qquad w_{(k)} := w_{p_1\cdots p_k}(x)\sigma^{;p_1}\cdots\sigma^{;p_k}, \quad (4.163)$$

and also behave as regular scalar functions in the coincidence limit.

The Hadamard expansion (4.156) provides remarkable information on how the geometry of background space-time and the quantum state of the field propagating there separately influence the virtual particle population. In fact, the terms of (4.156) can be neatly separated into purely geometrical parts U and V and a state-dependent

part W.

Mathematically, this occurs due to the Ansatz (4.158a – 4.160) and the following recursion relations that respectively determine the Hadamard coefficients U_l, V_l and W_l [29] [31]:

$$0 = (2l+4-n)\left[(l+1)U_{l+1} + U_{l+1;\mu}\sigma^{;\mu} - U_{l+1}\Delta^{-\frac{1}{2}}\left(\Delta^{\frac{1}{2}}\right)_{;\mu}\sigma^{;\mu}\right] + \left(\Box_x - m_\xi^2\right)U_l, \tag{4.164}$$

$$0 = (l+1)\left[(2l+n)V_{l+1} + 2V_{l+1;\mu}\sigma^{;\mu} - 2V_{l+1}\Delta^{-\frac{1}{2}}\left(\Delta^{\frac{1}{2}}\right)_{;\mu}\sigma^{;\mu}\right] + \left(\Box_x - m_\xi^2\right)V_l, \tag{4.165}$$

$$\begin{aligned} 0 = (l+1)\left[(2l+n)W_{l+1} + 2W_{l+1;\mu}\sigma^{;\mu} - 2W_{l+1}\Delta^{-\frac{1}{2}}\left(\Delta^{\frac{1}{2}}\right)_{;\mu}\sigma^{;\mu}\right] + (4l+2+n)V_{l+1} \\ +2V_{l+1;\mu}\sigma^{;\mu} - V_{l+1}\Delta^{-\frac{1}{2}}\left(\Delta^{\frac{1}{2}}\right)_{;\mu}\sigma^{;\mu} + \left(\Box_x - m_\xi^2\right)W_l, \end{aligned} \tag{4.166}$$

with the associated boundary conditions for U_l and V_l [29] [31]:

$$U_0 = \quad \Delta^{\frac{1}{2}}, \qquad n > 2, \tag{4.167}$$

$$V_0 = \begin{cases} -\Delta^{\frac{1}{2}}, & n = 2, \qquad (4.168a) \\ \dfrac{1}{n-2}\left[-2V_{0;\mu}\sigma^{;\mu} + 2V_0\Delta^{-\frac{1}{2}}\left(\Delta^{\frac{1}{2}}\right)_{;\mu}\sigma^{;\mu} - \left(\Box_x - m_\xi^2\right)U_{\frac{n-4}{2}}\right], & \\ & n > 2, \qquad (4.168b) \end{cases}$$

where the conditions on l and n stated in (4.158a – 4.160) remain in force and where Δ is a quantity known as the Van Vleck-Morette determinant discussed in the next subsection.

Using these relations, the coefficients U_l and V_l can be determined by integrating along the *unique* geodesic separating the events x and x' [29]. The coefficients W_l

do not rely solely on the geometry nor are they uniquely defined. Once a solution for W_0 is picked, the remaining coefficients W_l are unambiguous.

4.4.2 The Van Vleck-Morette determinant — $\Delta(x, x')$

The Van-Vleck Morette determinant [57] [73] is defined in [74] as

$$\Delta(x, x') := -\frac{\det\left(-\sigma_{;\mu\nu'}(x, x')\right)}{\sqrt{(-g(x))(-g(x'))}}. \tag{4.169}$$

This quantity is a measure of the rate of geodetic convergence (or divergence) between fixed events $\{x, x'\}$ sharing a geodesic [32]. As AdS_n is maximally symmetric this measure depends only on σ, therefore,

$$\Delta = \Delta(\sigma). \tag{4.170}$$

An expression for the Van Vleck-Morette determinant as a function of σ on AdS_n may be calculated by first taking into account that it satisfies a partial differential equation [29],

$$\Box_x \sigma = n - 2\Delta^{-\frac{1}{2}}\left(\Delta^{\frac{1}{2}}\right)_{;\mu}\sigma^{;\mu}, \tag{4.171}$$

with the boundary condition

$$\lim_{\sigma\to 0}\Delta = 1. \tag{4.172}$$

In addition, a property of the geodetic distance that is useful in this calculation is

$$2\sigma = \sigma^{;\mu}\sigma_{;\mu}. \tag{4.173}$$

Using the chain rule, the right-hand side of (4.171) may be written as

$$n - 4\Delta^{-\frac{1}{2}}\left(\Delta^{\frac{1}{2}}\right)_{,\sigma}\sigma. \tag{4.174}$$

Moving now to the left-hand side of (4.171), the following relationship has been established by Allen & Jacobson [4]:

$$\Box_x s = \frac{(n-1)}{a}\coth\left(\frac{s}{a}\right). \tag{4.175}$$

Given the definition of the d'Alembertian acting on s and that s is a biscalar,

$$\begin{aligned}\Box_x s &= g_{\mu\nu}s^{;\mu\nu}\\ &= \sqrt{2}\,g_{\mu\nu}\left(\sqrt{\sigma}\right)^{;\mu\nu}\\ &= \sqrt{2}\left(\frac{1}{2}\sigma^{-\frac{1}{2}}\sigma_{;\mu}\right)^{;\mu}\\ &= \sqrt{2}\left(-\frac{1}{4}\sigma^{-\frac{3}{2}}\sigma^{;\mu}\sigma_{;\mu}+\frac{1}{2}\sigma^{-\frac{1}{2}}\sigma_{;\mu}{}^{;\mu}\right)\\ &= \frac{1}{\sqrt{2\sigma}}\left(\Box_x\sigma-1\right).\end{aligned} \tag{4.176}$$

It follows that

$$\Box_x\sigma = \sqrt{2\sigma}\,\Box_x s + 1. \tag{4.177}$$

Hence the left-hand side of (4.171) can be stated as

$$\Box_x\sigma = \sqrt{2\sigma}\,\frac{(n-1)}{a}\coth\left(\frac{\sqrt{2\sigma}}{a}\right)+1. \tag{4.178}$$

An explicit form for the Van Vleck-Morette determinant may now be found by solving the first order ordinary differential equation

$$\sqrt{2\sigma}\,\frac{(n-1)}{a}\coth\left(\frac{\sqrt{2\sigma}}{a}\right)+1 = n - 4\Delta^{-\frac{1}{2}}\left(\Delta^{\frac{1}{2}}\right)_{,\sigma}\sigma \tag{4.179}$$

for $\Delta^{\frac{1}{2}}$. The solution is

$$\Delta = \left[\boldsymbol{\kappa}_{\Delta} \frac{\sqrt{2\sigma}}{a} \operatorname{cosech} \left(\frac{\sqrt{2\sigma}}{a} \right) \right]^{n-1} \tag{4.180}$$

where $\boldsymbol{\kappa}_{\Delta}$ is the constant of integration. To fix $\boldsymbol{\kappa}_{\Delta}$, the behaviour of Δ in the coincidence limit is examined. Using the boundary condition (4.172),

$$\boldsymbol{\kappa}_{\Delta} = 1, \tag{4.181}$$

as

$$\operatorname{cosech} \left(\frac{\sqrt{2\sigma}}{a} \right) = \frac{a}{\sqrt{2\sigma}} + \mathcal{O}\left(\sqrt{\sigma}\right), \qquad \sigma \to 0. \tag{4.182}$$

Therefore the Van Vleck-Morette determinant on AdS_n is given by

$$\Delta = \left[\frac{\sqrt{2\sigma}}{a} \operatorname{cosech} \left(\frac{\sqrt{2\sigma}}{a} \right) \right]^{n-1}, \tag{4.183}$$

and is found to agree with the result of Allen, Folacci and Gibbons [3] for $n = 4$.

4.4.3 The singular part — $G_{\rm H,\,sing}(s)$

Expressions for the singular part of the Hadamard expansion of the Feynman Green function (4.156), $G_{\rm H,\,sing}(\sigma)$ are given below for $n=2$ and $n>2$, (for n even and then n odd). For later ease, $G_{\rm H,\,sing}(\sigma)$ is also expressed as a function of s in each case.

I. ——— $\boldsymbol{n=2}$ ———

$$G^{n=2}_{\rm H,\,sing}(\sigma) = \frac{\boldsymbol{i}}{4\pi} V(\sigma)\ln\bar{\sigma}, \tag{4.184}$$

$$G^{n=2}_{\rm H,\,sing}(\sigma(s)) = \frac{\boldsymbol{i}}{2\pi} V(s)\left[\ln\bar{s} - \frac{1}{2}\ln 2\right]. \tag{4.185}$$

II. ——— $\boldsymbol{n>2,\ n}$ **EVEN** ———

$$G^{n=2p+2}_{\rm H,\,sing}(\sigma) = \boldsymbol{i}\nu(n)\left\{U(\sigma)\sigma^{-p} + V(\sigma)\ln\bar{\sigma}\right\}, \tag{4.186}$$

$$G^{n=2p+2}_{\rm H,\,sing}(s) = \boldsymbol{i}\nu(n)\left\{2^p U(s)s^{-2p} + 2V(s)\left[\ln\bar{s} - \frac{1}{2}\ln 2\right]\right\}. \tag{4.187}$$

As the Hadamard functions $U(s)$ and $V(s)$ respectively multiply poles and logarithmically divergent terms in s, it is convenient to split $G^{n=2p+2}_{\rm H,\,sing}(s)$ into parts exhibiting these different behaviours. Accordingly,

$$G^{n=2p+2}_{\rm H,\,sing}(s) = G^{n=2p+2}_{{\rm H}(U)}(s) + G^{n=2p+2}_{{\rm H}(V)}(s), \tag{4.188}$$

where

$$G^{n=2p+2}_{\mathrm{H}(U)}(s) := \boldsymbol{i}\nu(n)2^p U(s)s^{-2p}, \tag{4.189}$$

$$G^{n=2p+2}_{\mathrm{H}(V)}(s) := 2\boldsymbol{i}\nu(n)V(s)\left[\ln\bar{s} - \frac{1}{2}\ln 2\right], \tag{4.190}$$

are the respective definitions of the 'U-part' and 'V-part' of the Hadamard expansion of the Feynman Green function.

III. ——— $n > 2$, n ODD ———

$$G^{n=2p+1}_{\mathrm{H,\,sing}}(\sigma) = \boldsymbol{i}\nu(n)U(\sigma)\sigma^{\frac{1}{2}-p}, \tag{4.191}$$

$$G^{n=2p+1}_{\mathrm{H,\,sing}}(s) = \boldsymbol{i}\nu(n)2^{p-\frac{1}{2}}U(s)s^{1-2p}. \tag{4.192}$$

4.4.4 The Hadamard function $U(x, x')$

I. ——— $n = 2$ ———

From the definition of the Hadamard expansion of the Feynman Green function (4.158a),

$$U = 0. \tag{4.193}$$

II. ——— $n > 2$, n EVEN ———

From (4.158c), the Hadamard function $U(s)$ has the Taylor series expansion

$$U = \sum_{l=0}^{p-1} 2^{-l}U_l s^{2l}. \tag{4.194}$$

For $n=4$, (i.e. $p=1$),

$$U = U_0 = \Delta^{\frac{1}{2}}, \tag{4.195}$$

from the boundary condition (4.167).

For this case, the dependence of the 'U-part' of the Hadamard expansion on s is found by expanding the cosech function in the definition of Δ (4.183) as a power series in s giving

$$G^{n=4}_{\mathrm{H}(U)}(s) \sim \Delta^{\frac{1}{2}} s^{-2} \sim \left[s \,\mathrm{cosech}\left(\frac{s}{a}\right)\right]^{\frac{3}{2}} s^{-2}, \qquad s \to 0, \tag{4.196}$$

$$= \sum_{j=0}^{+\infty} \delta^{n=4}_{2j} s^{2j-2}, \tag{4.197}$$

where the $\delta^{n=4}_{2j}$ are the expansion coefficients of $\Delta^{\frac{1}{2}}$ with

$$\delta^{n=4}_0 := 1. \tag{4.198}$$

For $n>4$, (i.e. $p>1$), it is necessary to calculate the Hadamard coefficients U_l (with $l>0$) exploiting the relevant recurrence relations (4.164) in σ:

$$\begin{aligned}&(l+1)(2l+4-n)U_{l+1} + U_{l+1;\mu}\sigma^{;\mu} \\ &\qquad -(2l+4-n)U_{l+1}\Delta^{-\frac{1}{2}}\left(\Delta^{\frac{1}{2}}\right)_{;\mu}\sigma^{;\mu} + \left(\Box_x - m^2_\xi\right)U_l = 0,\end{aligned} \tag{4.199}$$

with $l = 0, 1, 2, \ldots, \frac{n}{2}-3$ (for n even with $n>4$).

Defining

$$\widetilde{U}_l(\sigma) := -\frac{\Box_x - m^2 - \xi\mathcal{R}}{2l+4-n} U_l(\sigma), \tag{4.200}$$

and making use of (4.173), the recurrence relation may be written as

$$(l+1)U_{l+1} + 2U_{l+1,\sigma}\sigma - 2U_{l+1}\Delta^{-\frac{1}{2}}\left(\Delta^{\frac{1}{2}}\right)_{,\sigma}\sigma = \widetilde{U}_l. \tag{4.201}$$

The recurrence relation can then be recast in s as

$$(l+1)U_{l+1} + U_{l+1,s}s - U_{l+1}\Delta^{-\frac{1}{2}}\left(\Delta^{\frac{1}{2}}\right)_{,s}s = \widetilde{U}_l. \tag{4.202}$$

Multiplying through by $\Delta^{-\frac{1}{2}}s^l$, the left-hand side of (4.202) can be written as $\left(U_{l+1}\Delta^{-\frac{1}{2}}s^{l+1}\right)_{,s}$ and so the determination of each U_l (with $l > 0$) reduces to the integration along the geodesic between 0 and s

$$U_{l+1}\Delta^{-\frac{1}{2}}s^{l+1} = \int_0^s \widetilde{U}_l\Delta^{-\frac{1}{2}}\acute{s}^l d\acute{s} + \boldsymbol{\kappa}_U \tag{4.203}$$

$$\Rightarrow \qquad U_{l+1} = \frac{\boldsymbol{\kappa}_U\Delta^{\frac{1}{2}}}{s^{l+1}} + \frac{\Delta^{\frac{1}{2}}}{s^{l+1}}\int_0^s \widetilde{U}_l\Delta^{-\frac{1}{2}}\acute{s}^l d\acute{s}, \tag{4.204}$$

where the dummy integration variable is denoted as $\acute{s}$.

As U_l is regular as $s \to 0$, $\forall\, l$, but, in general $\Delta^{\frac{1}{2}}s^{-(l+1)}$ is *not*, then the constant of integration

$$\boldsymbol{\kappa}_U = 0. \tag{4.205}$$

Therefore

$$U_{l+1} = \frac{\Delta^{\frac{1}{2}}(s)}{s^{l+1}}\int_0^s \widetilde{U}_l\Delta^{-\frac{1}{2}}\acute{s}^l d\acute{s}, \qquad s > 0, \forall\, l. \tag{4.206}$$

III. $n > 2$, n ODD

From (4.158b), the Hadamard function U has the Taylor series expansion

$$U = \sum_{l=0}^{+\infty} 2^{-l} U_l s^{2l}. \tag{4.207}$$

For $n = 3$, (i.e. $p = 1$), just as for the $n = 4$ case, the dependence of the 'U-part' of the Hadamard expansion on s is found by expanding the cosech function in the definition of Δ (4.183) as a power series in s giving

$$G^{n=3}_{{\rm H}(U)}(s) \sim \Delta^{\frac{1}{2}} s^{-1} \sim \left[s \,\mathrm{cosech}\left(\frac{s}{a}\right)\right]^2 s^{-1}, \qquad s \to 0, \tag{4.208}$$

$$= \sum_{j=0}^{+\infty} \delta^{n=3}_{2j} s^{2j-1}, \tag{4.209}$$

where the $\delta^{n=3}_{2j}$ are the expansion coefficients of $\Delta^{\frac{1}{2}}$ with

$$\delta^{n=3}_0 := 1. \tag{4.210}$$

For $n > 3$, (i.e. $p > 1$), it is necessary to calculate the Hadamard coefficients U_l (with $l > 0$) using the relevant recurrence relations (4.164) where for n odd, $l = 0, 1, 2, \ldots$. Following the procedure outlined for n even with $n > 4$ above, these coefficients are also determined by the integration (4.206).

It is worth pointing out at this stage that the Hadamard coefficients U_l are *even* Taylor series in $s \;\forall\; n, l$. This can be seen by considering the first recurrence relation ($l = 0$), leading to an expression for U_1. In this case

$$\widetilde{U}_0 = -\frac{\Box_x - m^2 - \xi\mathcal{R}}{4-n}\Delta^{\frac{1}{2}}. \tag{4.211}$$

Now,

$$\Box_x \left(\Delta^{\frac{1}{2}}\right) = \left(\Delta^{\frac{1}{2}}\right)_{,ss} + \left(\Delta^{\frac{1}{2}}\right)_{,s} \Box_x s, \tag{4.212}$$

so $\Box_x(\Delta^{\frac{1}{2}})$ is an *even* Taylor series in s, and it follows that $\widetilde{U}_0$ and the integrand

$\widetilde{U}_0\Delta^{-\frac{1}{2}}$ are also expanded as even Taylor series in s . Finally, the power of s gained from the integration is then lost by the s^{-1} factor outside the integral, therefore the expansion of U_1 is also an even Taylor series in s.

By the same reasoning, in the second recurrence relation ($l = 1$), the integrand $\widetilde{U}_1\Delta^{-\frac{1}{2}}\acute{s}$ is expanded as an *odd* Taylor series in $\acute{s}$. However, the power of s gained by integration is cancelled by the s^{-2} outside the integral.

By induction, the integrand $\widetilde{U}_1\Delta^{-\frac{1}{2}}\acute{s}^l$ gains a power of s which is then cancelled by the $s^{-(l+1)}$ outside the integral leaving an even power series for all l. Therefore, the Hadamard coefficients U_l possess an even Taylor series in $s\ \forall\ n, l$,

$$U_l = \sum_{j=0}^{+\infty} u_{jl} s^{2j}, \tag{4.213}$$

with the expansion coefficients, u_{jl}.

4.4.5 The singular part of the 'U-part' — $G_{\mathrm{H}(U),\,\mathrm{sing}}(s)$

I. ——— $n = 2$ ———

Given (4.158a),

$$G^{n=2}_{\mathrm{H}(U)}(s) = 0. \tag{4.214}$$

II. ——— $n > 2$, n EVEN ———

Given (4.156), (4.194) and (4.213),

$$G^{n=2p+2}_{\mathrm{H}(U)}(s) \sim \sum_{l=0}^{p-1}\sum_{j=0}^{+\infty} 2^{-l} u_{jl} s^{2j+2l-2p}, \qquad s \to 0. \tag{4.215}$$

In this case, the Laurent series is *even*. Therefore, as $s \to 0$, $G^{n=2p+2}_{{\rm H}(U)}(s)$ diverges due to the principal part and will also *always* contain some finite non-vanishing terms of this Laurent series. These latter (i.e. zeroth-order) terms stem from powers of s in the expansion of the Hadamard coefficient (4.213) of $2j = 2p - 2l$.

The non-vanishing, singular part of the 'U-part' of the Hadamard expansion of the Feynman Green function is therefore

$$G^{n=2p+2\bigstar}_{{\rm H}(U),\,{\rm sing}}(s) := \boldsymbol{i}\nu(n)2^p \sum_{l=0}^{p-1}\sum_{j=0}^{p-l} 2^{-l} u_{jl} s^{2j+2l-2p}. \tag{4.216}$$

So, for each possible value of $l = 0, 1, \ldots, p-1$, the values $j = p, p-1, \ldots, 1$ contribute to the finite regular terms contained in $G^{n=2p+2}_{{\rm H}(U),\,{\rm sing}}(s)$.

III. $n > 2$, n ODD

As $G^{n=2p+1}_{\rm H}(s)$ has no logarithmic singularity, given (4.156), (4.207) and (4.213),

$$G^{n=2p+1}_{\rm H}(s) \sim \sum_{l=0}^{+\infty}\sum_{j=0}^{+\infty} 2^{-l} u_{jl} s^{2j+2l+1-2p}, \qquad s \to 0. \tag{4.217}$$

In this case, as the Laurent series is *odd*, there are no finite non-vanishing terms. Therefore as $s \to 0$, $G^{n=2p+1}_{\rm H}(s)$ diverges solely due to the terms in the principal part of this Laurent series. Such terms stem from powers of s in the expansion of the Hadamard coefficient (4.213) of $2j \leq 2p - 2l - 2$.

The non-vanishing, singular part of the Hadamard expansion of the Feynman Green function is therefore

$$G^{n=2p+1\bigstar}_{\rm H,\,sing}(s) := \boldsymbol{i}\nu(n)2^{p-\frac{1}{2}} \sum_{l=0}^{p-1}\sum_{j=0}^{p-l-1} 2^{-l} u_{jl} s^{2j+2l+1-2p}, \qquad s \to 0. \tag{4.218}$$

4.4.6 The Hadamard function $V(s)$

Given (4.17), the Feynman Green function $G_{\rm F}(s)$ is a solution to the *homogenous* scalar field wave equation

$$\left(\Box - m^2 - \xi\mathcal{R}\right) G_{\rm F}(\sigma) = 0, \qquad \sigma < 0, \tag{4.219}$$

and may be expressed as the linear combination of hypergeometric functions in (4.55).

From [31], as the Hadamard function V is also a solution to the *homogenous* scalar field wave equation

$$\left(\Box - m^2 - \xi\mathcal{R}\right) V = 0, \qquad \forall\, s, \tag{4.220}$$

it may also be expressed as a different linear combination of the same hypergeometric functions in (4.55), with constant coefficients A and B,

$$V = AF\left[\frac{n-1}{2}+\mu, \frac{n-1}{2}-\mu; \frac{n}{2}; -\left[\sinh\left(\frac{s}{2a}\right)\right]^2\right] + BF\left[\frac{n-1}{2}+\mu, \frac{n-1}{2}-\mu; \frac{n}{2}; \left[\cosh\left(\frac{s}{2a}\right)\right]^2\right]. \tag{4.221}$$

As $s \to 0$, the hypergeometric function in the second term of the solution above diverges $\forall\, n \geq 2$. This behaviour and the equation (4.220) impose a boundary condition

$$B = 0, \qquad \forall\, s. \tag{4.222}$$

Therefore

$$V = AF\left[\frac{n-1}{2}+\mu, \frac{n-1}{2}-\mu; \frac{n}{2}; -\left[\sinh\left(\frac{s}{2a}\right)\right]^2\right], \qquad \forall\, s. \tag{4.223}$$

4.4.7 The singular part of the 'V-part' — $G_{\mathrm{H}(V),\,\mathrm{sing}}(s)$

The Hadamard function $V(s)$ may be expressed as the Taylor series (4.159b)

$$V=\sum_{l=0}^{+\infty}2^{-l}V_l s^{2l}. \tag{4.224}$$

Therefore

$$G^{n\ \mathrm{even}}_{\mathrm{H}(V)}(s)\sim\sum_{l=0}^{+\infty}2^{-l}V_l s^{2l}\ln\bar{s},\qquad s\to 0. \tag{4.225}$$

Bearing in mind the left-hand side of (4.223) and (4.159b)

$$G^{n\ \mathrm{even}\bigstar}_{\mathrm{H}(V),\,\mathrm{sing}}(s)\sim V_0\ln\bar{s},\qquad s\to 0. \tag{4.226}$$

Given (4.223)

$$A=\lim_{s\to 0}V_0,\qquad \forall\, n \text{ even}. \tag{4.227}$$

I. ——— $\boldsymbol{n=2}$ ———

The Hadamard coefficient V_0 is obtained from the boundary condition (4.168a)

$$V_0=-\Delta^{\frac{1}{2}}. \tag{4.228}$$

Therefore

$$A=-1, \tag{4.229}$$

and so

$$G^{n=2\bigstar}_{\mathrm{H}(V),\,\mathrm{sing}}(s)=-\frac{\boldsymbol{i}}{2\pi}\left[\ln\bar{s}-\frac{1}{2}\ln 2\right]. \tag{4.230}$$

II. $n > 2$, n EVEN

The Hadamard coefficient V_0 is obtained from the recurrence relation in σ

$$(n-2)V_0 + 2V_{0;\mu}\sigma^{;\mu} - 2V_0\Delta^{-\frac{1}{2}}\left(\Delta^{\frac{1}{2}}\right)_{;\mu}\sigma^{;\mu} + \left(\Box_x - m_\xi^2\right)U_{\frac{n-4}{2}} = 0. \tag{4.231}$$

Exploiting (4.173), the equation may be written as

$$(n-2)V_0 + 4V_{0,\sigma}\sigma - 4V_0\Delta^{-\frac{1}{2}}\left(\Delta^{\frac{1}{2}}\right)_{,\sigma}\sigma + \left(\Box_x - m_\xi^2\right)U_{\frac{n-4}{2}} = 0, \tag{4.232}$$

which can then be recast in s as

$$(n-2)V_0 + 2V_{0,s}s - 2V_0\Delta^{-\frac{1}{2}}\left(\Delta^{\frac{1}{2}}\right)_{,s}s + \left(\Box_x - m_\xi^2\right)U_{\frac{n-4}{2}} = 0. \tag{4.233}$$

Therefore

$$A = -\lim_{s\to 0}\left\{\frac{\Box_x - m^2 - \xi\mathcal{R}}{n-2}U_{\frac{n-4}{2}}\right\}, \tag{4.234}$$

and so

$$G^{n\ \text{even}\bigstar}_{\mathrm{H}(V),\,\mathrm{sing}}(s) = A\ln\bar{s}, \qquad s\to 0. \tag{4.235}$$

5 | Hadamard renormalisation

5.1 Renormalisation of the quadratic fluctuations

In AdS_n, the Hadamard renormalised vacuum expectation value of the quadratic field fluctuations is defined as

$$\langle \Phi^2(x) \rangle_{\text{ren}} := -\boldsymbol{i} \lim_{s \to 0} \Big\{ G_{\text{F}}(s) - G_{\text{H, sing}}(s) \Big\} . \tag{5.1}$$

It amounts to the subtraction of divergent and vanishing terms in the expansion of the Feynman Green function. For even n, with $n > 2$, the definition (5.1) also involves the subtraction of some *finite* non-vanishing terms, resulting in 'finite renormalisation terms' (FRTs),

$$G_{\text{F, FRT}}(s) := \lim_{s \to 0} \Big\{ G_{\text{F, sing}}(s) - G_{\text{H, sing}}(s) \Big\} . \tag{5.2}$$

As mentioned in section 4.3.1, the *unrenormalised* vacuum expectation value of the quadratic field fluctuations '$\langle \Phi^2(x) \rangle$' (although undefined) can be formally viewed as special case of the Feynman Green function when $x = x'$. However, as this object is undefined, it is unphysical. For it to relate to a physical observable, divergences must be removed via the renormalisation scheme (5.1). Crucially, the divergences that appear in the full Feynman Green function must cancel *exactly* with those of $G_{\text{H, sing}}(s)$, stipulated by the Hadamard theorem (4.156).

The renormalised vacuum expectation value of the quadratic field fluctuations is an object of great significance to the physical content of any QFT. It is the prototype

of all physical observables as all such objects are quadratic in the fields and their derivatives, evaluated at the same space-time point. When $s = 0$, the loose interpretation of the Feynman Green function as a 'transition amplitude' of a virtual particle created at some event and destroyed at another is no longer appropriate. Instead, the coincidence limit brings with it an expectation value associated with the scalar field fluctuation population at some event x.

The regularisation of the full Feynman Green function $G_{\mathrm{F}}(s)$ carried out in section 4.3 and the Hadamard expansion (4.156) of the Feynman Green function dealt with in section 4.4 give the ingredients required to calculate $\langle\Phi^2(x)\rangle_{\mathrm{ren}}$ using the definition (5.1).

5.1.1 Computation of $\langle\Phi^2(x)\rangle_{\mathrm{ren}}$

A program has been written in MAPLE to compute expressions for $\langle\Phi^2(x)\rangle_{\mathrm{ren}}$ for $n = 2$ to $n = 11$ inclusive. In principle, with sufficient processing power and available time, the code could be easily altered to compute expressions of $\langle\Phi^2(x)\rangle_{\mathrm{ren}}$ for higher dimensions. The code for this program consists of four parts.

- **Part 1** computes expansions of the non-vanishing part of the Feynman Green function in s from the expressions (4.147), (4.152) and (4.155) for $n = 2$, and $n > 2$ with n even and n odd respectively. The key labour-intensive computations involved in this part are: that of the formal Laurent series in s in the expressions for $Z_{\mathrm{FLS}}^{n=2p+2}$ (4.138) and for $Z_{\mathrm{FLS}}^{n=2p+1}$ (4.142) (for $n > 2$ with n even and n odd respectively); and for n even with $n > 2$, the product of Pochhammer symbols in the coefficient of the term exhibiting logarithmic divergence in $\bar{s}$ in (4.152).

- **Part 2** computes the Hadamard expansions of the non-vanishing part of the Feynman Green function in s from the expressions (4.216) and (4.235) with (4.234)

for $n > 2$ with n even, and (4.218) for $n > 2$ with n odd. The bulk of processing in this part of the code is devoted to the computation of series expansions of the Hadamard functions $U(s)$ using the recurrence relation scheme outlined in section 4.4.4.II. To highlight the analogy with the development of previous part of the code, these $U(s)$ are then used to construct the formal Laurent series that comprise at least part of the singularity structure of the Feynman Green function for $n > 2$. Completing this analogy, for even n with $n > 2$, the coefficient A, of the term exhibiting logarithmic divergence in $\bar{s}$, in (4.190) is also computed.

- In **part 3** of the code, the different expansions of non-vanishing parts of the Feynman Green function are used to evaluate the FRTs using (5.2).

5.1.2 Results

The results generated by parts 1 – 3 of the code are as follows:

I. ——— $\boldsymbol{n = 2}$ ———

$$G^{n=2\bigstar}_{\mathrm{F,\ sing}}(s) = -\frac{\boldsymbol{i}}{2\pi} \ln \bar{s}, \tag{5.3}$$

$$G^{n=2\bigstar}_{\mathrm{H,\ sing}}(s) = -\frac{\boldsymbol{i}}{2\pi} \left\{ \ln \bar{s} - \frac{1}{2} \ln 2 \right\}, \tag{5.4}$$

$$\Rightarrow G^{n=2}_{\mathrm{F,\ FRT}}(s) = -\frac{\boldsymbol{i}}{2\pi} \left\{ -\frac{1}{2} \ln 2 \right\}. \tag{5.5}$$

II. $n = 3$

$$G^{n=3\bigstar}_{\mathrm{F,\ sing}}(s) = \frac{\boldsymbol{i}}{4\pi}\left\{\frac{1}{s}\right\}, \tag{5.6}$$

$$G^{n=3\bigstar}_{\mathrm{H,\ sing}}(s) = \frac{\boldsymbol{i}}{4\pi}\left\{\frac{1}{s}\right\}, \tag{5.7}$$

$$\Rightarrow G^{n=3}_{\mathrm{F,\ FRT}}(s) = 0. \tag{5.8}$$

III. $n = 4$

$$G^{n=4\bigstar}_{\mathrm{F,\ sing}}(s) = \frac{\boldsymbol{i}}{4\pi^2}\left\{\frac{1}{s^2} + \left[\frac{1}{2}m^2 + (1-6\xi)\frac{1}{a^2}\right]\ln\bar{s} - \frac{1}{12a^2}\right\}, \tag{5.9}$$

$$G^{n=4\bigstar}_{\mathrm{H,\ sing}}(s) = \frac{\boldsymbol{i}}{4\pi^2}\left\{\frac{1}{s^2} + \left[\frac{1}{2}m^2 + (1-6\xi)\frac{1}{a^2}\right]\ln\bar{s} - \frac{1}{4a^2}\right\} \tag{5.10}$$

$$G^{n=4}_{\mathrm{F,\ FRT}}(s) = \frac{\boldsymbol{i}}{4\pi^2}\left\{\frac{1}{6a^2}\right\}. \tag{5.11}$$

IV. $n = 5$

$$G^{n=5\bigstar}_{\mathrm{F,\ sing}}(s) = \frac{\boldsymbol{i}}{8\pi^2}\left\{\frac{1}{s^3} + \left(-\frac{1}{2}m^2 - \frac{2}{a^2} + 10\xi\frac{1}{a^2}\right)\frac{1}{s}\right\}, \tag{5.12}$$

$$G^{n=5\bigstar}_{\mathrm{H,\ sing}}(s) = \frac{\boldsymbol{i}}{8\pi^2}\left\{\frac{1}{s^3} + \left(-\frac{1}{2}m^2 - \frac{2}{a^2} + 10\xi\frac{1}{a^2}\right)\frac{1}{s}\right\}, \tag{5.13}$$

$$\Rightarrow G^{n=5}_{\mathrm{F,\ FRT}}(s) = 0. \tag{5.14}$$

V. $n = 6$

$$G^{n=6\bigstar}_{\mathrm{F,\,sing}}(s)$$

$$= \frac{\boldsymbol{i}}{4\pi^3}\left\{\frac{1}{s^4} + \left(-\frac{1}{4}m^2 - \frac{5}{3a^2} + \frac{15}{2}\xi\frac{1}{a^2}\right)\frac{1}{s^2} + \left[-\frac{1}{16}m^4 + \left(-\frac{5}{8} + \frac{15}{4}\xi\right)\frac{m^2}{a^2} + \left(-\frac{3}{2} + \frac{75}{4}\xi - \frac{225}{4}\xi^2\right)\frac{1}{a^4}\right]\ln\bar{s} + \frac{1}{48}\frac{m^2}{a^2} + \left(\frac{101}{720} - \frac{5}{8}\xi\right)\frac{1}{a^4}\right\}, \tag{5.15}$$

$$G^{n=6\bigstar}_{\mathrm{H,\,sing}}(s)$$

$$= \frac{\boldsymbol{i}}{4\pi^3}\left\{\frac{1}{s^4} + \left(-\frac{1}{4}m^2 - \frac{5}{3a^2} + \frac{15}{2}\xi\frac{1}{a^2}\right)\frac{1}{s^2} + \left[-\frac{1}{16}m^4 + \left(-\frac{5}{8} + \frac{15}{4}\xi\right)\frac{m^2}{a^2} + \left(-\frac{3}{2} + \frac{75}{4}\xi - \frac{225}{4}\xi^2\right)\frac{1}{a^4}\right]\ln\bar{s} + \frac{5}{48}\frac{m^2}{a^2} + \left(\frac{173}{288} - \frac{25}{8}\xi\right)\frac{1}{a^4}\right\}, \tag{5.16}$$

$$\Rightarrow G^{n=6}_{\mathrm{F,\,FRT}}(s)$$

$$= \frac{\boldsymbol{i}}{4\pi^3}\left\{-\frac{m^2}{12a^2} + \left(-\frac{221}{480} + \frac{5}{2}\xi\right)\frac{1}{a^4}\right\}. \tag{5.17}$$

VI. $n = 7$

$$G^{n=7\bigstar}_{\mathrm{F,\ sing}}(s)$$

$$= \frac{3\boldsymbol{i}}{16\pi^3}\left\{\frac{1}{s^5} + \left(\frac{8}{3a^4} + \frac{1}{24}m^4 + \frac{2}{3}\frac{m^2}{a^2} - 28\xi\frac{1}{a^4} - \frac{7}{2}\xi\frac{m^2}{a^2} + \frac{147}{2}\xi^2\frac{1}{a^4}\right)\frac{1}{s^3} + \left(-\frac{5}{3a^2} - \frac{1}{6}m^2 + 7\xi\frac{1}{a^2}\right)\frac{1}{s}\right\}, \tag{5.18}$$

$$G^{n=7\bigstar}_{\mathrm{H,\ sing}}(s)$$

$$= \frac{3\boldsymbol{i}}{16\pi^3}\left\{\frac{1}{s^5} + \left(\frac{8}{3a^4} + \frac{1}{24}m^4 + \frac{2}{3}\frac{m^2}{a^2} - 28\xi\frac{1}{a^4} - \frac{7}{2}\xi\frac{m^2}{a^2} + \frac{147}{2}\xi^2\frac{1}{a^4}\right)\frac{1}{s^3} + \left(-\frac{5}{3a^2} - \frac{1}{6}m^2 + 7\xi\frac{1}{a^2}\right)\frac{1}{s}\right\}, \tag{5.19}$$

$$\Rightarrow G^{n=7}_{\mathrm{F,\ FRT}}(s) = 0. \tag{5.20}$$

VII. $n = 8$

$$
\begin{aligned}
&G^{n=8\bigstar}_{\mathrm{F,\,sing}}(s) \\
&= \frac{\boldsymbol{i}}{2\pi^4}\Bigg\{\frac{1}{s^6} + \left(-\frac{1}{8}m^2 - \frac{7}{4a^2} + 7\xi\frac{1}{a^2}\right)\frac{1}{s^4} \\
&\qquad + \left(\frac{1}{64}m^4 + \frac{35}{96}\frac{m^2}{a^2} + \frac{259}{120a^4} - \frac{7}{4}\xi\frac{m^2}{a^2} - \frac{245}{12}\xi\frac{1}{a^4} + 49\xi^2\frac{1}{a^4}\right)\frac{1}{s^2} \\
&\qquad + \Bigg[\frac{1}{384}m^6 + \left(\frac{7}{96} - \frac{7}{16}\xi\right)\frac{m^4}{a^2} + \left(\frac{21}{32} - \frac{49}{6}\xi + \frac{49}{2}\xi^2\right)\frac{m^2}{a^4} \\
&\qquad\quad + \left(\frac{15}{8} - \frac{147}{4}\xi + \frac{686}{3}\xi^2 - \frac{1372}{3}\xi^3\right)\frac{1}{a^6}\Bigg]\ln\bar{s} \\
&\qquad - \frac{1}{768}\frac{m^4}{a^2} + \left(-\frac{11}{360} + \frac{7}{48}\xi\right)\frac{m^2}{a^4} + \left(-\frac{11027}{60480} + \frac{77}{45}\xi - \frac{49}{12}\xi^2\right)\frac{1}{a^6}\Bigg\},
\end{aligned}
\tag{5.21}
$$

$$
\begin{aligned}
&G^{n=8\bigstar}_{\mathrm{H,\,sing}}(s) \\
&= \frac{\boldsymbol{i}}{2\pi^4}\Bigg\{\frac{1}{s^6} + \left(-\frac{1}{8}m^2 - \frac{7}{4a^2} + 7\xi\frac{1}{a^2}\right)\frac{1}{s^4} \\
&\qquad + \left(\frac{1}{64}m^4 + \frac{35}{96}\frac{m^2}{a^2} + \frac{259}{120a^4} - \frac{7}{4}\xi\frac{m^2}{a^2} - \frac{245}{12}\xi\frac{1}{a^4} + 49\xi^2\frac{1}{a^4}\right)\frac{1}{s^2} \\
&\qquad + \Bigg[\frac{1}{384}m^6 + \left(\frac{7}{96} - \frac{7}{16}\xi\right)\frac{m^4}{a^2} + \left(\frac{21}{32} - \frac{49}{6}\xi + \frac{49}{2}\xi^2\right)\frac{m^2}{a^4} \\
&\qquad\quad + \left(\frac{15}{8} - \frac{147}{4}\xi + \frac{686}{3}\xi^2 - \frac{1372}{3}\xi^3\right)\frac{1}{a^6}\Bigg]\ln\bar{s} \\
&\qquad - \frac{7}{768}\frac{m^4}{a^2} + \left(-\frac{721}{3840} + \frac{49}{48}\xi\right)\frac{m^2}{a^4} + \left(-\frac{1373}{1440} + \frac{5047}{480}\xi - \frac{343}{12}\xi^2\right)\frac{1}{a^6}\Bigg\},
\end{aligned}
\tag{5.22}
$$

$n = 8$ (continued)

$$\Rightarrow G^{n=8}_{\mathrm{F,\ FRT}}(s) = \frac{\boldsymbol{i}}{2\pi^4}\left\{\frac{m^4}{128a^2} + \left(\frac{1811}{11520} - \frac{7}{8}\xi\right)\frac{m^2}{a^4} + \left(\frac{46639}{60480} - \frac{12677}{1440}\xi + \frac{49}{2}\xi^2\right)\frac{1}{a^6}\right\}. \tag{5.23}$$

VIII. $n = 9$

$$\begin{aligned} &G^{n=9\bigstar}_{\mathrm{F,\ sing}}(s) \\ &= \frac{15\boldsymbol{i}}{32\pi^4}\Bigg\{\frac{1}{s^7} + \left(-\frac{1}{10}m^2 - \frac{28}{15a^2} + \frac{36}{5}\xi\frac{1}{a^2}\right)\frac{1}{s^5} \\ &\quad + \left(\frac{1}{120}m^4 + \frac{4}{15}\frac{m^2}{a^2} + \frac{98}{45a^4} - \frac{6}{5}\xi\frac{m^2}{a^2} - \frac{96}{5}\xi\frac{1}{a^4} + \frac{216}{5}\xi^2\frac{1}{a^4}\right)\frac{1}{s^3} \\ &\quad + \Bigg(-\frac{1}{720}m^6 - \frac{1}{18}\frac{m^4}{a^2} - \frac{11}{15}\frac{m^2}{a^4} - \frac{16}{5a^6} + \frac{3}{10}\xi\frac{m^4}{a^2} + 8\xi\frac{m^2}{a^4} + \frac{264}{5}\xi\frac{1}{a^6} \\ &\quad - \frac{108}{5}\xi^2\frac{m^2}{a^4} - 288\xi^2\frac{1}{a^6} + \frac{2592}{5}\xi^3\frac{1}{a^6}\Bigg)\frac{1}{s}\Bigg\}, \end{aligned} \tag{5.24}$$

$$\begin{aligned} &G^{n=9\bigstar}_{\mathrm{H,\ sing}}(s) \\ &= \frac{15\boldsymbol{i}}{32\pi^4}\Bigg\{\frac{1}{s^7} + \left(-\frac{1}{10}m^2 - \frac{28}{15a^2} + \frac{36}{5}\xi\frac{1}{a^2}\right)\frac{1}{s^5} \\ &\quad + \left(\frac{1}{120}m^4 + \frac{4}{15}\frac{m^2}{a^2} + \frac{98}{45a^4} - \frac{6}{5}\xi\frac{m^2}{a^2} - \frac{96}{5}\xi\frac{1}{a^4} + \frac{216}{5}\xi^2\frac{1}{a^4}\right)\frac{1}{s^3} \\ &\quad + \Bigg(-\frac{1}{720}m^6 - \frac{1}{18}\frac{m^4}{a^2} - \frac{11}{15}\frac{m^2}{a^4} - \frac{16}{5a^6} + \frac{3}{10}\xi\frac{m^4}{a^2} + 8\xi\frac{m^2}{a^4} + \frac{264}{5}\xi\frac{1}{a^6} \\ &\quad - \frac{108}{5}\xi^2\frac{m^2}{a^4} - 288\xi^2\frac{1}{a^6} + \frac{2592}{5}\xi^3\frac{1}{a^6}\Bigg)\frac{1}{s}\Bigg\}, \end{aligned} \tag{5.25}$$

$$\Rightarrow G^{n=9}_{\mathrm{F,\ FRT}}(s) = 0. \tag{5.26}$$

IX. $n = 10$

$$
\begin{aligned}
&G^{n=10\bigstar}_{\text{F, sing}}(s) \\
&= \frac{3\boldsymbol{i}}{2\pi^5}\Bigg\{ \frac{1}{s^8} + \left(-\frac{1}{12}m^2 - \frac{2}{a^2} + \frac{15}{2}\xi\frac{1}{a^2}\right)\frac{1}{s^6} \\
&\quad + \left(\frac{1}{192}m^4 + \frac{7}{32}\frac{m^2}{a^2} + \frac{47}{20a^4} - \frac{15}{16}\xi\frac{m^2}{a^2} - \frac{315}{16}\xi\frac{1}{a^4} + \frac{675}{16}\xi^2\frac{1}{a^4}\right)\frac{1}{s^4} \\
&\quad + \Bigg(-\frac{1}{2304}m^6 - \frac{3}{128}\frac{m^4}{a^2} - \frac{203}{480}\frac{m^2}{a^4} - \frac{3229}{1260a^6} + \frac{15}{128}\xi\frac{m^4}{a^2} + \frac{135}{32}\xi\frac{m^2}{a^4} \\
&\qquad + \frac{609}{16}\xi\frac{1}{a^6} - \frac{675}{64}\xi^2\frac{m^2}{a^4} - \frac{6075}{32}\xi^2\frac{1}{a^6} + \frac{10125}{32}\xi^3\frac{1}{a^6}\Bigg)\frac{1}{s^2} \\
&\quad + \Bigg[-\frac{1}{18432}m^8 + \left(-\frac{5}{1536} + \frac{5}{256}\xi\right)\frac{m^6}{a^2} \\
&\qquad + \left(-\frac{109}{1536} + \frac{225}{256}\xi - \frac{675}{256}\xi^2\right)\frac{m^4}{a^4} \\
&\qquad + \left(-\frac{761}{1152} + \frac{1635}{128}\xi - \frac{10125}{128}\xi^2 + \frac{10125}{64}\xi^3\right)\frac{m^2}{a^6} \\
&\qquad + \left(-\frac{35}{16} + \frac{3805}{64}\xi - \frac{73575}{128}\xi^2 + \frac{151875}{64}\xi^3 - \frac{455625}{128}\xi^4\right)\frac{1}{a^8}\Bigg]\ln\bar{s} \\
&\quad + \frac{1}{27648}\frac{m^6}{a^2} + \left(\frac{271}{138240} - \frac{5}{512}\xi\right)\frac{m^4}{a^4} \\
&\quad + \left(\frac{51601}{1451520} - \frac{271}{768}\xi + \frac{225}{256}\xi^2\right)\frac{m^2}{a^6} \\
&\quad + \left(\frac{262349}{1209600} - \frac{51601}{16128}\xi + \frac{4065}{256}\xi^2 - \frac{3375}{128}\xi^3\right)\frac{1}{a^8}\Bigg\}, \qquad (5.27)
\end{aligned}
$$

$n = 10$ (CONTINUED)

$$
\begin{aligned}
&G^{n=10\bigstar}_{\mathrm{H,\,sing}}(s) \\
&= \frac{3\boldsymbol{i}}{2\pi^5}\Bigg\{\frac{1}{s^8} + \left(-\frac{1}{12}m^2 - \frac{2}{a^2} + \frac{15}{2}\xi\frac{1}{a^2}\right)\frac{1}{s^6} \\
&\quad + \left(\frac{1}{192}m^4 + \frac{7}{32}\frac{m^2}{a^2} + \frac{47}{20a^4} - \frac{15}{16}\xi\frac{m^2}{a^2} - \frac{315}{16}\xi\frac{1}{a^4} + \frac{675}{16}\xi^2\frac{1}{a^4}\right)\frac{1}{s^4} \\
&\quad + \Bigg(-\frac{1}{2304}m^6 - \frac{3}{128}\frac{m^4}{a^2} - \frac{203}{480}\frac{m^2}{a^4} - \frac{3229}{1260a^6} + \frac{15}{128}\xi\frac{m^4}{a^2} + \frac{135}{32}\xi\frac{m^2}{a^4} \\
&\qquad + \frac{609}{16}\xi\frac{1}{a^6} - \frac{675}{64}\xi^2\frac{m^2}{a^4} - \frac{6075}{32}\xi^2\frac{1}{a^6} + \frac{10125}{32}\xi^3\frac{1}{a^6}\Bigg)\frac{1}{s^2} \\
&\quad + \Bigg[-\frac{1}{18432}m^8 + \left(-\frac{5}{1536} + \frac{5}{256}\xi\right)\frac{m^6}{a^2} \\
&\qquad + \left(-\frac{109}{1536} + \frac{225}{256}\xi - \frac{675}{256}\xi^2\right)\frac{m^4}{a^4} \\
&\qquad + \left(-\frac{761}{1152} + \frac{1635}{128}\xi - \frac{10125}{128}\xi^2 + \frac{10125}{64}\xi^3\right)\frac{m^2}{a^6} \\
&\qquad + \left(-\frac{35}{16} + \frac{3805}{64}\xi - \frac{73575}{128}\xi^2 + \frac{151875}{64}\xi^3 - \frac{455625}{128}\xi^4\right)\frac{1}{a^8}\Bigg]\ln\bar{s} \\
&\quad + \frac{1}{3072}\frac{m^6}{a^2} + \left(\frac{97}{6144} - \frac{45}{512}\xi\right)\frac{m^4}{a^4} \\
&\quad + \left(\frac{48481}{193536} - \frac{1455}{512}\xi + \frac{2025}{256}\xi^2\right)\frac{m^2}{a^6} \\
&\quad + \left(\frac{464981}{358400} - \frac{242405}{10752}\xi + \frac{65475}{512}\xi^2 - \frac{30375}{128}\xi^3\right)\frac{1}{a^8}\Bigg\}, \qquad (5.28)
\end{aligned}
$$

$n = 10$ (CONTINUED)

$$\Rightarrow G^{n=10}_{\mathrm{F,\ FRT}}(s) = \frac{3\boldsymbol{i}}{2\pi^5}\Bigg\{-\frac{m^6}{3456a^2} + \left(-\frac{3823}{276480} + \frac{5}{64}\xi\right)\frac{m^4}{a^4} + \left(-\frac{624013}{2903040} + \frac{3823}{1536}\xi - \frac{225}{32}\xi^2\right)\frac{m^2}{a^6} + \left(-\frac{2091139}{1935360} + \frac{624013}{32256}\xi - \frac{57345}{512}\xi^2 + \frac{3375}{16}\xi^3\right)\frac{1}{a^8}\Bigg\}. \tag{5.29}$$

X. $n = 11$

$$\begin{aligned} &G^{n=11\bigstar}_{\mathrm{F,\ sing}}(s) \\ &= \frac{105\boldsymbol{i}}{64\pi^5}\Bigg\{\frac{1}{s^9} + \left(-\frac{1}{14}m^2 - \frac{15}{7a^2} + \frac{55}{7}\xi\frac{1}{a^2}\right)\frac{1}{s^7} \\ &\quad + \left(\frac{1}{280}m^4 + \frac{4}{21}\frac{m^2}{a^2} + \frac{13}{5a^4} - \frac{11}{14}\xi\frac{m^2}{a^2} - \frac{440}{21}\xi\frac{1}{a^4} + \frac{605}{14}\xi^2\frac{1}{a^4}\right)\frac{1}{s^5} \\ &\quad + \left(-\frac{1}{5040}m^6 - \frac{1}{72}\frac{m^4}{a^2} - \frac{103}{315}\frac{m^2}{a^4} - \frac{164}{63a^6} + \frac{11}{168}\xi\frac{m^4}{a^2} + \frac{55}{18}\xi\frac{m^2}{a^4}\right. \\ &\qquad \left. + \frac{2266}{63}\xi\frac{1}{a^6} - \frac{605}{84}\xi^2\frac{m^2}{a^4} - \frac{3025}{18}\xi^2\frac{1}{a^6} + \frac{33275}{126}\xi^3\frac{1}{a^6}\right)\frac{1}{s^3} \\ &\quad + \left(\frac{1}{40320}m^8 + \frac{1}{504}\frac{m^6}{a^2} + \frac{37}{630}\frac{m^4}{a^4} + \frac{16}{21}\frac{m^2}{a^6} + \frac{128}{35a^8}\right. \\ &\qquad - \frac{11}{1008}\xi\frac{m^6}{a^2} - \frac{55}{84}\xi\frac{m^4}{a^4} - \frac{814}{63}\xi\frac{m^2}{a^6} - \frac{1760}{21}\xi\frac{1}{a^8} \\ &\qquad + \frac{605}{336}\xi^2\frac{m^4}{a^4} + \frac{3025}{42}\xi^2\frac{m^2}{a^6} + \frac{44770}{63}\xi^2\frac{1}{a^8} \\ &\qquad \left. - \frac{33275}{252}\xi^3\frac{m^2}{a^6} - \frac{166375}{63}\xi^3\frac{1}{a^8} + \frac{1830125}{504}\xi^4\frac{1}{a^8}\right)\frac{1}{s}\Bigg\}, \end{aligned} \tag{5.30}$$

$n = 11$ (CONTINUED)

$$
\begin{aligned}
&G^{n=11\bigstar}_{\text{H, sing}}(s) \\
&= \frac{105\boldsymbol{i}}{64\pi^5}\Bigg\{\frac{1}{s^9} + \left(-\frac{1}{14}m^2 - \frac{15}{7a^2} + \frac{55}{7}\xi\frac{1}{a^2}\right)\frac{1}{s^7} \\
&\qquad + \left(\frac{1}{280}m^4 + \frac{4}{21}\frac{m^2}{a^2} + \frac{13}{5a^4} - \frac{11}{14}\xi\frac{m^2}{a^2} - \frac{440}{21}\xi\frac{1}{a^4} + \frac{605}{14}\xi^2\frac{1}{a^4}\right)\frac{1}{s^5} \\
&\qquad + \Bigg(-\frac{1}{5040}m^6 - \frac{1}{72}\frac{m^4}{a^2} - \frac{103}{315}\frac{m^2}{a^4} - \frac{164}{63a^6} + \frac{11}{168}\xi\frac{m^4}{a^2} + \frac{55}{18}\xi\frac{m^2}{a^4} \\
&\qquad\quad + \frac{2266}{63}\xi\frac{1}{a^6} - \frac{605}{84}\xi^2\frac{m^2}{a^4} - \frac{3025}{18}\xi^2\frac{1}{a^6} + \frac{33275}{126}\xi^3\frac{1}{a^6}\Bigg)\frac{1}{s^3} \\
&\qquad + \Bigg(\frac{1}{40320}m^8 + \frac{1}{504}\frac{m^6}{a^2} + \frac{37}{630}\frac{m^4}{a^4} + \frac{16}{21}\frac{m^2}{a^6} + \frac{128}{35a^8} \\
&\qquad\quad - \frac{11}{1008}\xi\frac{m^6}{a^2} - \frac{55}{84}\xi\frac{m^4}{a^4} - \frac{814}{63}\xi\frac{m^2}{a^6} - \frac{1760}{21}\xi\frac{1}{a^8} \\
&\qquad\quad + \frac{605}{336}\xi^2\frac{m^4}{a^4} + \frac{3025}{42}\xi^2\frac{m^2}{a^6} + \frac{44770}{63}\xi^2\frac{1}{a^8} \\
&\qquad\quad - \frac{33275}{252}\xi^3\frac{m^2}{a^6} - \frac{166375}{63}\xi^3\frac{1}{a^8} + \frac{1830125}{504}\xi^4\frac{1}{a^8}\Bigg)\frac{1}{s}\Bigg\}, \qquad (5.31)
\end{aligned}
$$

$$
\Rightarrow G^{n=11}_{\text{F, FRT}}(s) = 0. \qquad (5.32)
$$

Décanini & Folacci have published expressions for the Hadamard expansion of the non-vanishing part of the Feynman Green function for a *general* space-time for $n = 2$ to $n = 6$ inclusive [29] [31]. Although the computation of expansions for $n > 6$ are possible, the expressions grow greatly in length and complexity and have not been published explicitly.

Typically, for a general space-time the form of Hadamard expansions published by Décanini & Folacci involve biscalar functions and are rife with Riemann tensor polynomials. However, the maximal symmetry of AdS_n simplifies the task yielding expressions involving *scalar* functions only and reducing the possible types of Riemann tensor polynomials significantly.

The results for the non-vanishing part of the Hadamard expansion of the Feynman Green function for $n = 2$ to $n = 6$ above, (equations (5.4), (5.7), (5.10), (5.13) and (5.16)) agree with the corresponding expansions published by Décanini & Folacci [31].

It is crucial that the short-distance divergences in the counterpart expressions generated in the first two parts of the code do indeed cancel for each number of space-time dimensions. This requirement ensures that given the definition (5.1), $\langle\Phi^2(x)\rangle_{\rm ren}$ is finite and real and can therefore be associated with some physical quantity. It is particularly important to guarantee finiteness and reality for $\langle\Phi^2(x)\rangle_{\rm ren}$ as its determination acts as a basic template for the calculation *all* physical observables in a QFT.

Careful examination of these results reveals that for n odd with $n > 2$, the expressions for the expansion of the non-vanishing part of the Feynman Green function generated in parts 1 and 2 of the code are entirely singular and more importantly, *identical*. For n even, the expressions are seen to differ by *finite* terms only.

Returning to the final part of the code:

- **Part 4** computes expressions for $\langle\Phi^2(x)\rangle_{\text{ren}}$. Given that $G_{\text{F}}(s)$ can be written as the sum

$$G_{\text{F}}(s) = G_{\text{F, reg}}(s) + G_{\text{F, sing}}(s), \tag{5.33}$$

using definition (5.1), and the definition of FRTs (5.2), the computation of $\langle\Phi^2(x)\rangle_{\text{ren}}$ then boils down to

$$\langle\Phi^2(x)\rangle_{\text{ren}} = -\boldsymbol{i}\lim_{s\to 0} G_{\text{F, reg}}(s), \tag{5.34}$$

for n odd; and

$$\langle\Phi^2(x)\rangle_{\text{ren}} = -\boldsymbol{i}\left\{\lim_{s\to 0} G_{\text{F, reg}}(s) + G_{\text{F, FRT}}(s)\right\}, \tag{5.35}$$

for all n even.

Expressions for (5.34) are therefore computed using (4.154) for n odd. Similarly, for $n = 2$ and n even with $n > 2$, expressions for (5.35) are generated using (4.146) and (4.151) respectively combined with the finite renormalisation terms $G_{\text{F, FRT}}(s)$ computed in part 3 of the code.

The results of part 4 follow overleaf.

XI. $\langle \Phi^2 \rangle_{\rm ren}$ FOR $n = 2$ TO $n = 9$

$$\langle \Phi^2 \rangle_{\rm ren}^{n=2} = -\frac{1}{2\pi} \Upsilon(\mu, M, a), \tag{5.36}$$

$$\langle \Phi^2 \rangle_{\rm ren}^{n=3} = -\frac{1}{4\pi a}\, \mu, \tag{5.37}$$

$$\langle \Phi^2 \rangle_{\rm ren}^{n=4} = \frac{1}{8\pi^2 a^2} \left\{ \left(\mu^2 - \frac{1}{4} \right) \Upsilon(\mu, M, a) - \frac{1}{2}\mu^2 - \frac{1}{24} \right\}, \tag{5.38}$$

$$\langle \Phi^2 \rangle_{\rm ren}^{n=5} = \frac{1}{24\pi^2 a^3} \left\{ \mu^3 - \mu \right\}, \tag{5.39}$$

$$\langle \Phi^2 \rangle_{\rm ren}^{n=6} = -\frac{1}{64\pi^3 a^4} \left\{ \left(\mu^4 - \frac{5}{2}\mu^2 + \frac{9}{16} \right) \Upsilon(\mu, M, a) - \frac{3}{4}\mu^4 + \frac{29}{24}\mu^2 + \frac{107}{960} \right\}, \tag{5.40}$$

$$\langle \Phi^2 \rangle_{\rm ren}^{n=7} = -\frac{1}{240\pi^3 a^5} \left\{ \mu^5 - 5\mu^3 + 4\mu \right\}, \tag{5.41}$$

$$\langle \Phi^2 \rangle_{\rm ren}^{n=8} = \frac{1}{768\pi^4 a^6} \left\{ \left(\mu^6 - \frac{35}{4}\mu^4 + \frac{259}{16}\mu^2 - \frac{225}{64} \right) \Upsilon(\mu, M, a) - \frac{11}{12}\mu^6 + \frac{313}{48}\mu^4 - \frac{2471}{320}\mu^2 - \frac{11969}{16128} \right\}, \tag{5.42}$$

$$\langle \Phi^2 \rangle_{\rm ren}^{n=9} = \frac{1}{3360\pi^4 a^7} \left\{ \mu^7 - 14\mu^5 + 49\mu^3 - 36\mu \right\}, \tag{5.43}$$

XII. $\langle \Phi^2 \rangle_{\text{ren}}$ FOR $n = 10$ TO $n = 11$

$$\langle \Phi^2 \rangle_{\text{ren}}^{n=10} = -\frac{1}{12288\pi^5 a^8} \times \left\{ \left(\mu^8 - 21\mu^6 + \frac{987}{8}\mu^4 - \frac{3229}{16}\mu^2 + \frac{11025}{256} \right) \Upsilon(\mu, M, a) - \frac{25}{24}\mu^8 + \frac{461}{24}\mu^6 - \frac{87983}{960}\mu^4 + \frac{3854941}{40320}\mu^2 + \frac{288563}{30720} \right\}, \tag{5.44}$$

$$\langle \Phi^2 \rangle_{\text{ren}}^{n=11} = -\frac{1}{60480\pi^5 a^9} \left\{ \mu^9 - 30\mu^7 + 273\mu^5 - 820\mu^3 + 576\mu \right\}, \tag{5.45}$$

where for even n,

$$\Upsilon(\mu, M, a) := \psi\left(\tfrac{1}{2} + \mu\right) + \boldsymbol{\gamma} - \frac{1}{2}\ln 2 - \ln \bar{a}, \tag{5.46}$$

with $\bar{a}$ the dimensionless version of the radius of curvature resulting from the mass renormalisation scale M in (4.45).

Overall, the expressions for $\langle \Phi^2 \rangle_{\text{ren}}$ for $n = 2$ to $n = 11$ inclusive are essentially even or odd-powered polynomials in μ of leading-order $n - 2$. Physically interesting properties of these results include the fact that $\langle \Phi^2 \rangle_{\text{ren}}$ on AdS_n is *constant* throughout the space-time. Moreover, $\langle \Phi^2 \rangle_{\text{ren}}$ can be negative. Additionally, an immediate consequence of the Υ factor present in expressions for even n is that the scalar field fluctuations in AdS_n of even n are non-zero for $\mu = 0$.

Expressions for $\langle \Phi^2 \rangle_{\text{ren}}$ in AdS_n have already been computed using zeta-function regularisation methods by Caldarelli in [17], the results of which agree with the results (5.36) – (5.45) inclusive, up to the addition of a constant. The Euler-Mascheroni

constant $\boldsymbol{\gamma}$ and a term in $\ln 2$ is present in the expressions of $\langle\Phi^2\rangle_{\rm ren}$ for even n (equations (5.36), (5.38), (5.40), (5.42) and (5.44)). However these terms do not appear in Caldarelli's expressions. This difference may be interpreted as being due to the freedom in the choice of renormalisation mass scale. Therefore Caldarelli's effective choice of scale $M_{\rm C}$ is related to that arising naturally from the Hadamard renormalisation of the Feynman Green function, M by

$$M_{\rm C} = \sqrt{2}e^{-\gamma}M. \tag{5.47}$$

It follows that the appearance of such constants in expressions for even n is not a death-knell for validating the Hadamard renormalisation (or zeta-function regularisation for that matter) as these terms can be absorbed via a redefinition of M.

The results (5.36) – (5.45) are plotted below in figures 5.1 and 5.2 as functions of μ. To simplify the comparison of behaviour for different n, the radius of curvature of AdS_n, a has been set to unity and the renormalisation mass scale is fixed at

$$M = \frac{e^{\gamma}}{\sqrt{2}}, \tag{5.48}$$

so that the only remaining term in the Υ factor in equations (5.36), (5.38), (5.40), (5.42) and (5.44) is the (μ-dependent) psi function.

Figure 5.1 shows for different n, how the probability density of scalar fluctuations in the vacuum varies with the mass-coupling configuration, for relatively 'low' values of $0 \leq \mu \leq 4.5$. Each coloured curve in the plot describes this behaviour for a specific n. The curves associated with consecutive pairs of consecutive numbers of space-time dimensions alternate as to whether they are ultimately decreasing or increasing functions of μ.

Similarly, figure 5.2 displays the same relationships over a slightly extended range of

$0 \leq \mu \leq 7.5$. Although the fate of the curves for $n = 2$ to $n = 11$ (i.e. their respective polarity as μ increases) has already been determined by $\mu = 4.5$, the extended range in figure 5.2 reflects the rapidity of the predominance of the leading-order term as μ increases.

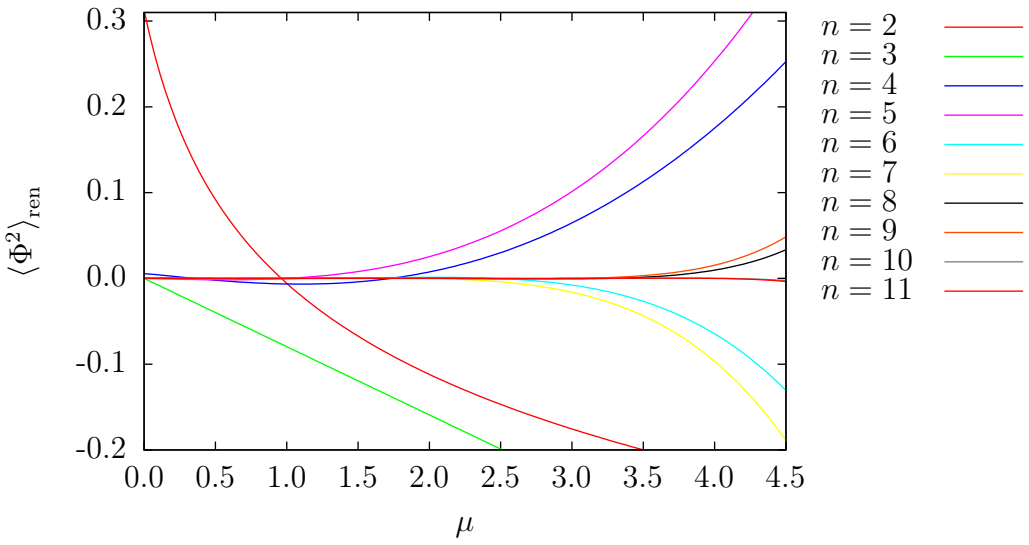

FIGURE 5.1 – $\langle \Phi^2 \rangle_{\text{ren}}$ as a function of $0 \leq \mu \leq 4.5$ for varying n with $a = 1$, $M = \dfrac{e^{\gamma}}{\sqrt{2}}$

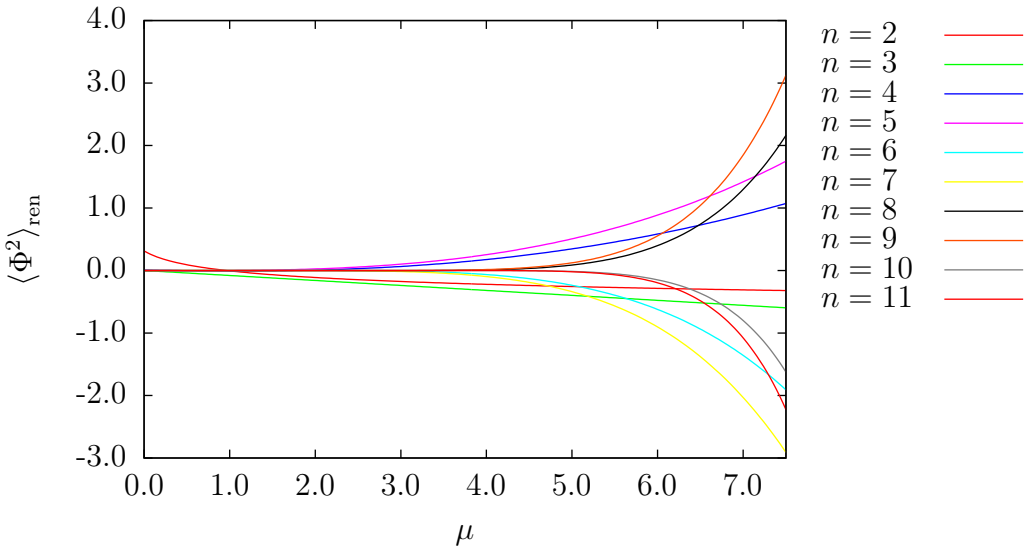

FIGURE 5.2 – $\langle \Phi^2 \rangle_{\text{ren}}$ as a function of $0 \leq \mu \leq 7.5$ for varying n with $a = 1$, $M = \dfrac{e^{\gamma}}{\sqrt{2}}$

In the case of the results for n even, the plots in figures 5.3 – 5.7 inclusive examine how the behaviour of $\langle\Phi^2\rangle_{\text{ren}}$ is influenced for varying values of μ by different values of the mass renormalisation scale $M(j) = \dfrac{e^{\gamma}}{\sqrt{2}}10^{j-6}$ with $j = -5, -4, \ldots, 5$ and $a = 1$.

The behaviour for $n = 2$ is unique, and can be expected from the form of the corresponding expression (5.36). In this situation,

$$\langle\Phi^2\rangle_{\text{ren}}^{n=2} \propto -\left[\psi\left(\mu + \tfrac{1}{2}\right) - (j-6)\ln 10\right]. \tag{5.49}$$

The parallel arrangement of curves can therefore be understood as a straightforward addition of a constant. Each curve above (or below) the $j = 0$ curve reflects successive increments (or decrements) to the value of j. The shape of the curves visible in the plot are due to the psi function being asymptotically logarithmic (see e.g. §6.3.18 [2]).

The dependence of $\langle\Phi^2(x)\rangle_{\text{ren}}$ for n even with $n > 2$ on M is shown in figures 5.4 – 5.7 inclusive. These plots share a common behaviour, namely a rapid 'fanning' following a stretch of 'hugging' the $\langle\Phi^2\rangle_{\text{ren}} = 0$ axis. The 'idle' phase, corresponds to the passage of the curves through their zeroes. The growth phase follows once the last zero is passed. For increasing values of n therefore, the wrapping is increasingly tighter round the $\langle\Phi^2\rangle_{\text{ren}} = 0$ axis, the initiation of the fanning is increasingly delayed, increasingly sudden and displaying a more rapid growth to infinity.

For $n = 2p + 2$, $p = 1, 2, \ldots$, the $j = 0$ curve will tend to $(-1)^{p+1}\infty$ as μ increases. Consequently, the curves corresponding to $j \gtrless 0$ will tend to $\pm(-1)^{p}\infty$.

5.2 Renormalisation of the stress-energy tensor

5.2.1 Introduction

The defining mathematical object of a QFT on a curved space-time is the renormalised expectation value of its stress-energy tensor. When evaluated with respect to the vacuum state,

$$\langle T_{\mu\nu}(x)\rangle_{\text{ren}} := \langle \mathbf{0}|\, T_{\mu\nu}(x)\, |\mathbf{0}\rangle_{\text{ren}}\,. \tag{5.50}$$

This object encapsulates all the information relating to the matter content of such theories, encoding the distribution and flows of energy of the associated fields propagating on the background space-time. By extension, $\langle T_{\mu\nu}(x)\rangle_{\text{ren}}$ also provides a local physical description of the matter fields at a given event x [36]. Be it global or local, as $\langle T_{\mu\nu}(x)\rangle_{\text{ren}}$ is computed from the Green function solution to (4.4), its physical description is influenced by the background geometry via the field equation (1.3). This influence is inevitable due to the presence of the background metric in the definition of the Laplace-Beltrami operator (3.18) and additionally through any non-minimal coupling ($\xi \neq 0$) present between the field and the space-time.

The renormalised expectation value of the stress-energy tensor is constructed from its classical counterpart. For a free classical scalar field $\Phi(x)$, the stress-energy tensor $T_{\mu\nu}(x)$ can be derived from the functional differentiation of the action $\mathcal{S}[\Phi, g_{\mu\nu}]$ (3.1) with respect to the background metric (see e.g. [11]) through the definition,

$$T_{\mu\nu} := \frac{2}{\sqrt{-g}}\frac{\delta}{\delta g^{\mu\nu}}\mathcal{S}[\Phi, g_{\mu\nu}], \tag{5.51}$$

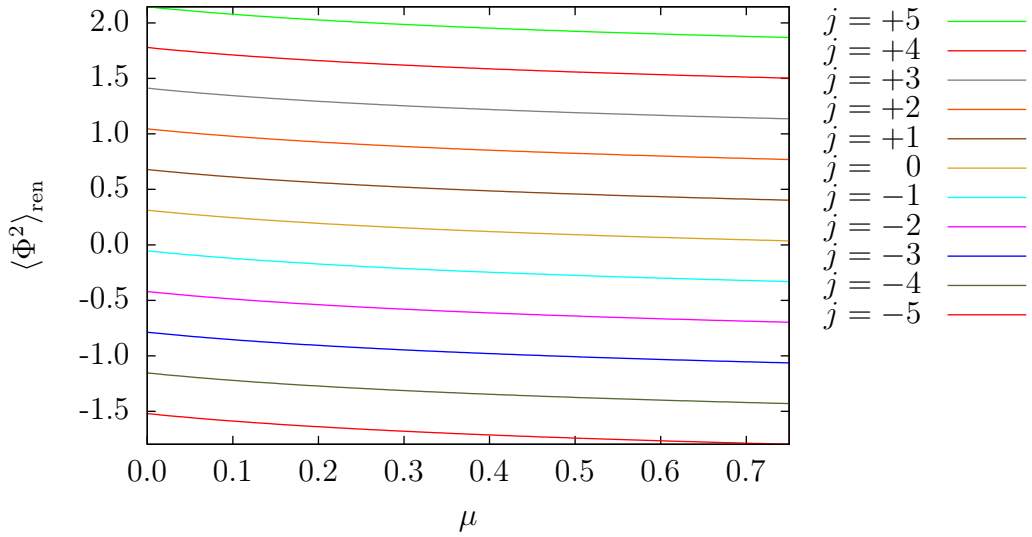

FIGURE 5.3 – $\langle\Phi^2\rangle_{\rm ren}$ as a function of μ for $n = 2$, $a = 1$ with varying $M(j) = \frac{e^\gamma}{\sqrt{2}}10^{j-6}$

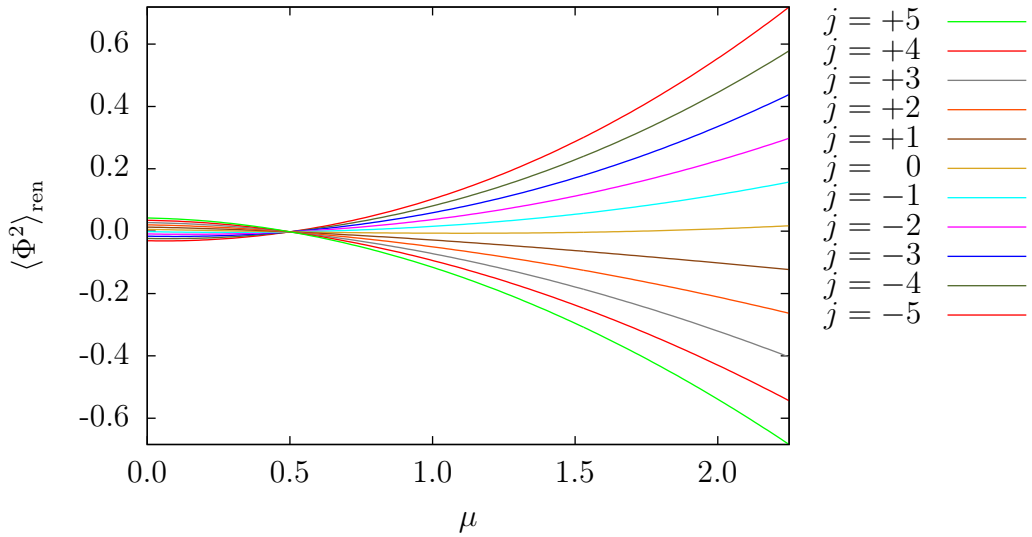

FIGURE 5.4 – $\langle\Phi^2\rangle_{\rm ren}$ as a function of μ for $n = 4$, $a = 1$ with varying $M(j) = \frac{e^\gamma}{\sqrt{2}}10^{j-6}$

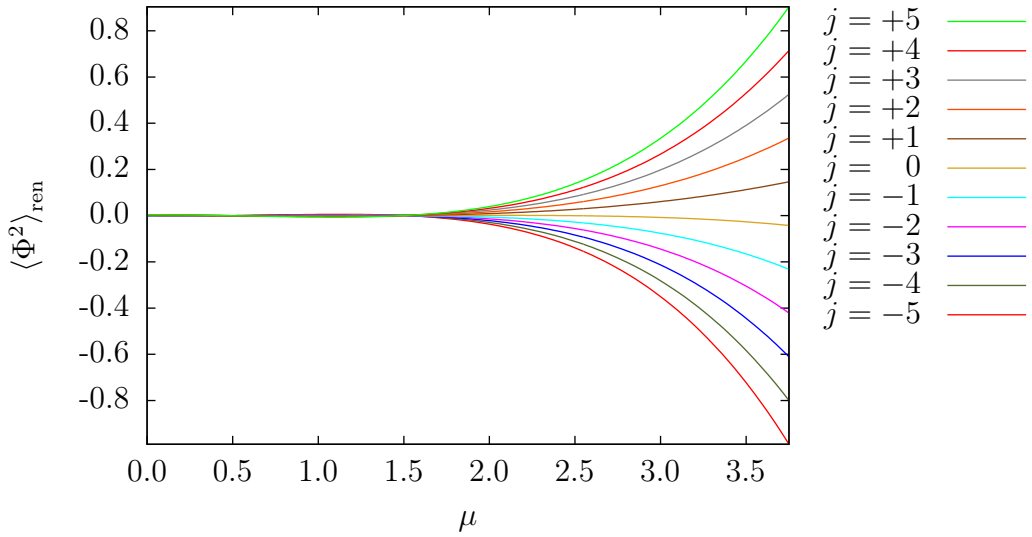

FIGURE 5.5 – $\langle\Phi^2\rangle_{\rm ren}$ as a function of μ for $n=6$, $a=1$ with varying $M(j)=\dfrac{e^{\gamma}}{\sqrt{2}}10^{j-6}$

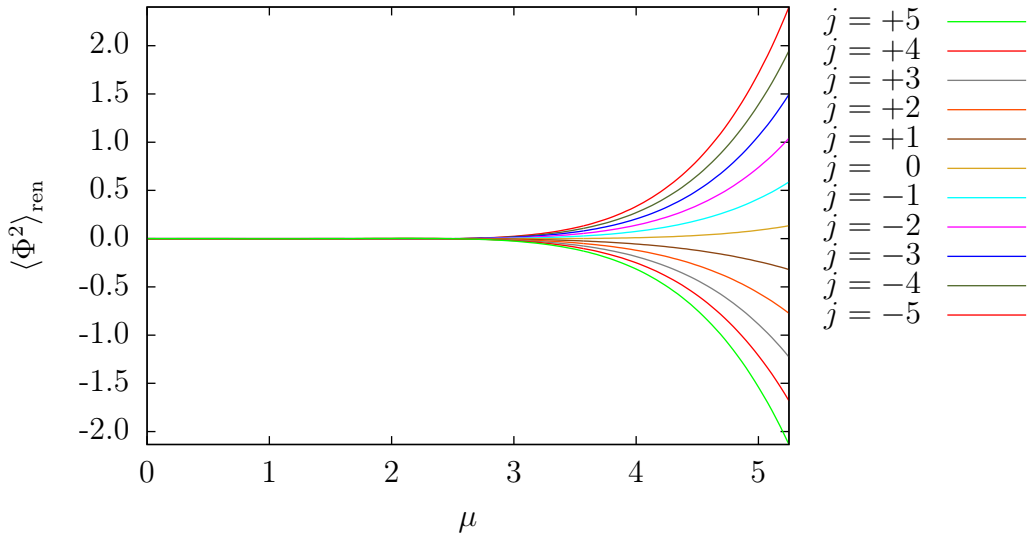

FIGURE 5.6 – $\langle\Phi^2\rangle_{\rm ren}$ as a function of μ for $n=8$, $a=1$ with varying $M(j)=\dfrac{e^{\gamma}}{\sqrt{2}}10^{j-6}$

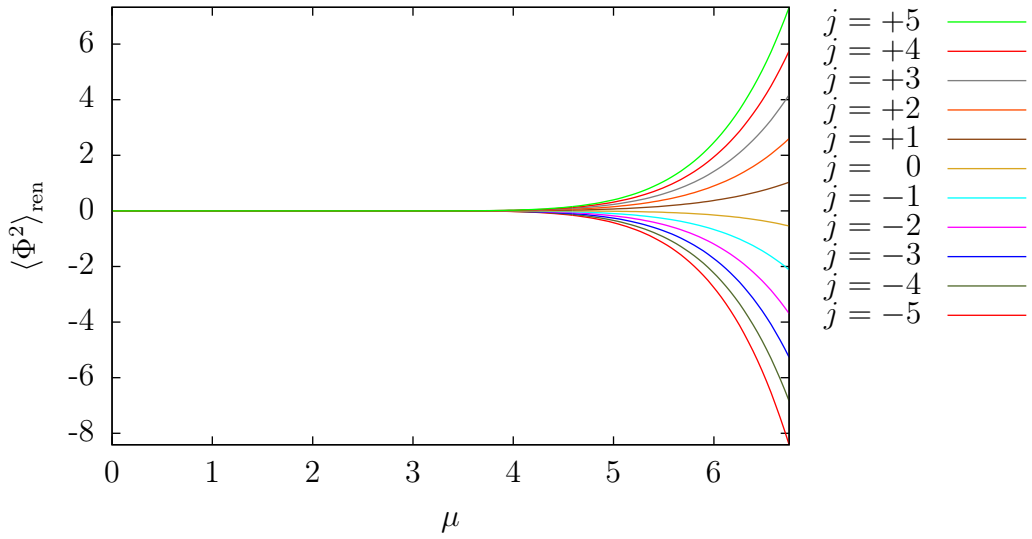

FIGURE 5.7 – $\langle\Phi^2\rangle_{\rm ren}$ as a function of μ for $n = 10$, $a = 1$ with varying $M(j) = \frac{e^\gamma}{\sqrt{2}}10^{j-6}$

resulting in the expression

$$T_{\mu\nu} = (1-2\xi)\Phi_{;\mu}\Phi_{;\nu} + \left(2\xi - \frac{1}{2}\right) g_{\mu\nu} g^{\rho\sigma}\Phi_{;\rho}\Phi_{;\sigma} - 2\xi\Phi\Phi_{;\mu\nu} + 2\xi g_{\mu\nu}\Phi\Box\Phi$$
$$+\xi\left(\mathcal{R}_{\mu\nu} - \frac{1}{2}g_{\mu\nu}\mathcal{R}\right)\Phi^2 - \frac{1}{2}g_{\mu\nu}m^2\Phi^2. \tag{5.52}$$

It is interesting to note, as Fulling remarks [43] for the $n = 4$ case, that given the Lagragian density $\mathcal{L}[\Phi, g_{\mu\nu}]$ associated with the action $\mathcal{S}[\Phi, g_{\mu\nu}]$ (3.1), in flat-space (5.52) is compatible with the definitions of the canonical stress-energy tensor and the 'new-improved stress-energy tensor' [18],

$$T^{\mathbb{M}^4}_{\mu\nu} := \Phi_{,\mu}\Phi_{,\nu} - g_{\mu\nu}\mathcal{L}, \qquad \xi = 0, \tag{5.53}$$

$$\bar{T}^{\mathbb{M}^4}_{\mu\nu} := T^{\mathbb{M}^4}_{\mu\nu} - \xi\left(\partial_\mu\partial_\nu - \eta_{\mu\nu}\Box\right)\Phi^2, \qquad \xi = \xi_{\rm c}, \tag{5.54}$$

respectively. This observation applies for all $n \geq 2$.

The procedure for computing expressions of the Hadamard renormalised vacuum

expectation value of the stress-energy tensor is very similar to that employed in the case of the quadratic field fluctuations. Practically, the difference for $\langle T_{\mu\nu}(x)\rangle_{\text{ren}}$ lies in the action of a second-order linear differential operator,

$$\boldsymbol{T}_{\mu\nu}(x,x') = (1-2\xi)g_{\nu}{}^{\nu'}\nabla_{\mu}\nabla_{\nu'} + \left(2\xi - \frac{1}{2}\right) g_{\mu\nu}g^{\rho\sigma'}\nabla_{\rho}\nabla_{\sigma'} - 2\xi g_{\mu}{}^{\mu'}g_{\nu}{}^{\nu'}\nabla_{\mu'}\nabla_{\nu'}$$

$$+2\xi g_{\mu\nu}\nabla_{\rho}\nabla^{\rho} + \xi\left(\mathcal{R}_{\mu\nu} - \frac{1}{2}g_{\mu\nu}\mathcal{R}\right) - \frac{1}{2}g_{\mu\nu}m^2, \tag{5.55}$$

to be applied to the Green function *before* renormalisation, and hence its point-split form (see e.g. [22] for a sketch of its derivation).

For a general space-time this leads to the definition [31]

$$\langle T_{\mu\nu}(x)\rangle_{\text{ren}} := \nu(n)\lim_{x'\to x}\left\{\boldsymbol{T}_{\mu\nu}(x,x')W(x,x')\right\} + \widetilde{\Theta}_{\mu\nu}(x). \tag{5.56}$$

The presence of the tensor $\widetilde{\Theta}_{\mu\nu}(x)$ is due to an ambiguity in the definition of $\langle T_{\mu\nu}(x)\rangle_{\text{ren}}$ that is a general characteristic of QFTs on curved space-times. This issue is discussed later in this section.

Recalling (4.156), the Hadamard function $W(x,x')$ takes the form

$$W(x,x') = -\frac{\boldsymbol{i}}{\nu(n)}\left[G_{\text{F}}(x,x') - G_{\text{H, sing}}(x,x')\right]. \tag{5.57}$$

It follows that given (5.55) and (5.56), the evaluation of $\langle T_{\mu\nu}(x)\rangle_{\text{ren}}$ will require expressions for the formal Laurent series expansions of $G_{\text{F, reg}}(x,x')$, $G_{\text{F, sing}}(x,x')$, and $G_{\text{H, sing}}(x,x')$ truncated to second order in s inclusive. These truncated expansions are respectively denoted by $G^{\mathbf{II}}_{\text{F,reg}}(x,x')$, $G^{\mathbf{II}}_{\text{F,sing}}(x,x')$ and $G^{\mathbf{II}}_{\text{H,sing}}(x,x')$.

From (5.56), Décanini & Folacci [31] outline the derivation of the convenient form,

$$\langle T_{\mu\nu}(x)\rangle_{\rm ren} = \nu(n)\left\{-w_{\mu\nu} + \frac{1}{2}(1-2\xi)w_{;\mu\nu} \right. \\ \left. + \frac{1}{2}\left(2\xi - \frac{1}{2}\right) g_{\mu\nu}\Box w + \xi\mathcal{R}_{\mu\nu}w - g_{\mu\nu}v_1\right\} + \Theta_{\mu\nu}. \tag{5.58}$$

Equation (5.58) simplifies the computation of $\langle T_{\mu\nu}(x)\rangle_{\rm ren}$ as it only relies on the five following coincidence limits of Hadamard functions, coefficients and their derivatives

$$w(x) = \lim_{x'\to x} W(x,x'), \tag{5.59}$$

$$w_{\mu\nu}(x) := \lim_{x'\to x} W(x,x')_{;\mu\nu}, \tag{5.60}$$

$$v_0(x) = \lim_{x'\to x} V_0(x,x'), \tag{5.61}$$

$$v_{0\mu\nu}(x) := \lim_{x'\to x} V_0(x,x')_{;\mu\nu}, \tag{5.62}$$

$$v_1(x) = \lim_{x'\to x} V_1(x,x'), \tag{5.63}$$

noticing from (5.57) that in fact, in the case of (5.59),

$$w(x) = -\frac{\boldsymbol{i}}{\nu(n)}\langle\Phi^2(x)\rangle_{\rm ren}. \tag{5.64}$$

The maximal symmetry of AdS_n makes life easier still as (5.36 - 5.45) state that w is independent of x, resulting in their derivatives vanishing from (5.58). This gives

$$\langle T_{\mu\nu}(x)\rangle_{\rm ren} = \nu(n)\left[-w_{\mu\nu} + \xi\mathcal{R}_{\mu\nu}w - g_{\mu\nu}v_1\right] + \Theta_{\mu\nu}, \tag{5.65}$$

remembering from (4.159a) that for n odd, the term in v_1 will disappear.

5.2.2 Second-order expansions of $G_{\mathbf{F}}(s)$

I. $\boldsymbol{n = 2}$

The second-order expansion in s of $G_{\mathrm{F}}^{n=2}(s)$ involves the $k = 0$ and $k = 1$ terms of the summation in (4.131). Using (4.135), these terms are,

$$Z_{\log}^{n=2}(\mu, 0, z) = \pi - 2\boldsymbol{i}\left[\psi\left(\tfrac{1}{2} + \mu\right) + \boldsymbol{\gamma} + \frac{1}{2}\ln z\right], \tag{5.66}$$

$$Z_{\log}^{n=2}(\mu, 1, z) = \pi - 2\boldsymbol{i}\left[\psi\left(\tfrac{1}{2} + \mu\right) + \boldsymbol{\gamma} + \frac{\frac{1}{4} + \mu^2}{\frac{1}{4} - \mu^2} + \frac{1}{2}\ln z\right]. \tag{5.67}$$

As $s \to 0$,

$$z \to -\frac{s^2}{4a^2} + \mathcal{O}\big(s^4\big), \tag{5.68}$$

$$\ln z \to 2\ln \bar{s} - 2\ln 2 - 2\ln \bar{a} - \boldsymbol{i}\pi + \frac{s^2}{12a^2} + \mathcal{O}\big(s^4\big). \tag{5.69}$$

The truncation of the expansion of the Feynman Green function to second order in s is therefore given by,

$$G_{\mathrm{F}}^{n=2\ \mathbf{II}}(s) = -\frac{\boldsymbol{i}}{2\pi}\left\{\left[\psi\left(\tfrac{1}{2} + \mu\right) + \boldsymbol{\gamma} + \ln \bar{s} - \ln 2 - \ln \bar{a} + \frac{s^2}{24a^2}\right]\left(1 - \frac{s^2}{4a^2}\right) - \left(\frac{\frac{1}{4} + \mu^2}{\frac{1}{4} - \mu^2}\right)\frac{s^2}{4a^2} - \frac{s^2}{48a^2}\right\}. \tag{5.70}$$

II. $n > 2$, n EVEN

To expand $G_{\mathrm{F}}^{n=2p+2}(s)$ to second order in s, it is convenient to split the expression (4.136) into a part containing the logarithmically divergent terms and another containing the formal Laurent series, and to examine them separately first. These parts are respectively defined as

$$G_{\mathrm{F,\,log}}^{n=2p+2}(z) := \frac{1}{(4\pi)^{p+1}\,a^{2p}}\left(\tfrac{1}{2}+\mu\right)_p\left(\tfrac{1}{2}-\mu\right)_p \times\sum_{k=0}^{+\infty}\frac{\left(p+\tfrac{1}{2}+\mu\right)_k\left(p+\tfrac{1}{2}-\mu\right)_k}{k!\,(p+k)!}Z_{\log}^{n=2p+2}(\mu,k,z)\,z^k, \tag{5.71}$$

and

$$G_{\mathrm{F,\,FLS}}^{n=2p+2}(z) = \frac{1}{(4\pi)^{p+1}\,a^{2p}}Z_{\mathrm{FLS}}^{n=2p+2}(\mu,k,z)\,. \tag{5.72}$$

For the summation present in (5.71), only the $k=0$ and $k=1$ terms contribute to a second-order expansion in s. From (4.139) and (4.140), the $Z_{\log}^{n=2p+2}(\mu,k,z)$ in these terms are

$$Z_{\log}^{n=2p+2}(\mu,0,z) = \pi - 2\boldsymbol{i}\left[\psi\left(\tfrac{1}{2}+\mu\right)+\boldsymbol{\gamma}-\frac{1}{2}\sum_{l=1}^{p}\frac{1}{l}+\frac{1}{2}\ln z + \frac{1}{2}\sum_{l=0}^{p-1}\left(\frac{1}{\frac{1}{2}+\mu+l}+\frac{1}{\frac{1}{2}-\mu+l}\right)\right], \tag{5.73}$$

and

$$Z_{\log}^{n=2p+2}(\mu,1,z) = Z_{\log}^{n=2p+2}(\mu,0,z) - \widetilde{L}, \tag{5.74}$$

where

$$\widetilde{L} := \boldsymbol{i}\left(\frac{1}{\frac{1}{2}+\mu+p}+\frac{1}{\frac{1}{2}-\mu+p}-\frac{1}{p+1}-2\right). \tag{5.75}$$

The logarithmic part is therefore given by,

$$G^{n=2p+2}_{F,\,\log} = \frac{1}{(4\pi)^{p+1}a^{2p}}\left(\tfrac{1}{2}+\mu\right)_p\left(\tfrac{1}{2}-\mu\right)_p \times\frac{(p+1)Z^{n=2p+2}_{\log}(\mu,0,z)+Z^{n=2p+2}_{\log}(\mu,1,z)\,z}{(p+1)!}. \tag{5.76}$$

Defining the second-order truncation

$$Z^{n=2p+2\,\mathbf{II}}_{\log}(\mu,0,z) := Z^{n=2p+2}_{\log}(\mu,0,z)-\mathcal{O}(s^4), \qquad s\to 0, \tag{5.77}$$

whilst being careful to note that the cancellation of terms in π arising from (5.68) and (5.69) gives,

$$Z^{n=2p+2}_{\log}(\mu,0,z) = -2\boldsymbol{i}\left[\psi\left(\tfrac{1}{2}+\mu\right)+\boldsymbol{\gamma}+\frac{1}{2}\sum_{l=0}^{p-1}\left(\frac{1}{\frac{1}{2}+\mu+l}+\frac{1}{\frac{1}{2}-\mu+l}\right) -\frac{1}{2}\sum_{l=1}^{p}\frac{1}{l}+\frac{1}{2}\ln\bar{s}-\ln 2-\ln\bar{a}+\frac{s^2}{4a^2}\right], \quad s\to 0, \tag{5.78}$$

leads to

$$Z^{n=2p+2\,\mathbf{II}}_{\log}(\mu,1,z) = Z^{n=2p+2\,\mathbf{II}}_{\log}(\mu,0,z)\left[\frac{s^2}{4a^2}-\frac{s^4}{96a^4}\right]-\widetilde{L}\frac{s^2}{4a^2}. \tag{5.79}$$

Recalling (4.138), the part (5.72) containing the Laurent series, $Z^{n=2p+2}_{\text{FLS}}$ is a *finite* sum whose k^{th} summands ($k=0,1,\ldots,p-1$) are respectively formal Laurent series of leading order $s^{-2p}, s^{2-2p},\ldots,s^2$. Therefore

$$Z^{n=2p+2\,\mathbf{II}}_{\text{FLS}} := Z^{n=2p+2}_{\text{FLS}}-\mathcal{O}(s^4), \qquad s\to 0. \tag{5.80}$$

Given (5.76) and (5.80), the truncation of the expansion of the Feynman Green function to second order in s is therefore given by,

$$G_{\mathrm{F}}^{n=2p+2\,\mathbf{II}}(s) = \frac{1}{(4\pi)^{p+1}\,a^{2p}}\left\{\frac{\left(\frac{1}{2}+\mu\right)_p\left(\frac{1}{2}-\mu\right)_p}{(p+1)!}\left[p+1+\frac{s^2}{4a^2}\left(1-\frac{s^2}{24a^2}\right)\right]\right.$$
$$\left.\times\, Z_{\log}^{n=2p+2\,\mathbf{II}}(\mu,0,z) - \widetilde{L}\frac{s^2}{4a^2} + Z_{\mathrm{FLS}}^{n=2p+2\,\mathbf{II}}\right\}. \quad (5.81)$$

III. ——— $n > 2$, n **ODD** ———

To expand $G_{\mathrm{F}}^{n=2p+1}(s)$ in (4.141) to second order in s, recall that (4.142), $Z_{\mathrm{FLS}}^{n=2p+1}$ is an *infinite* sum whose k^{th} summands ($k = 0, 1, \ldots$) are respectively formal Laurent series of leading order $s^{1-2p}, s^{3-2p}, \ldots$. Therefore,

$$Z_{\mathrm{FLS}}^{n=2p+1\,\mathbf{II}} := Z_{\mathrm{FLS}}^{n=2p+1} - \mathcal{O}(s^3), \qquad s \to 0,\ k = 0, 1, \ldots p, \quad (5.82)$$

where the optional condition on k sets an upper bound on the sum.

Given (5.82), the truncation of the expansion of the Feynman Green function to second order in s is therefore given by,

$$G_{\mathrm{F}}^{n=2p+1\,\mathbf{II}}(z)$$
$$= \frac{(-1)^p}{(4\pi)^{p+\frac{1}{2}}a^{2p-1}}\left\{\frac{\boldsymbol{i}\pi}{\Gamma\left(p+\frac{1}{2}\right)}\frac{(\mu)_p\,(-\mu)_p}{\mu}F\left[p+\mu, p-\mu; p+\frac{1}{2}; z\right] + Z_{\mathrm{FLS}}^{n=2p+1\,\mathbf{II}}(\mu,k,z)\right\}. \quad (5.83)$$

5.2.3 The validity of $\langle T_{\mu\nu}(x)\rangle_{\mathbf{ren}}$

The algebraic expressions generated for $\langle T_{\mu\nu}(x)\rangle_{\mathrm{ren}}$ (5.98 – 5.107) are finite – a promising start towards representing any physically acceptable matter content.

However, there was some debate in the infancy of QFTs on curved space-times as to how to rigorously stipulate what makes for a physically reasonable $\langle T_{\mu\nu}(x)\rangle_{\text{ren}}$. The viewpoint that is now widely accepted is that $\langle T_{\mu\nu}(x)\rangle_{\text{ren}}$ must satisfy a set of axioms established by Wald [75].

- **1. Conservation** (5.84)

  Given the semi-classical Einstein equations (1.3), and the fact that the Einstein tensor $\mathcal{G}_{\mu\nu}(x)$ is covariantly divergenceless, it is logical that a physically sensible $\langle T_{\mu\nu}(x)\rangle_{\text{ren}}$ should exhibit divergencelessness too.

- **2. Causality** (5.85)

  In the case of space-times that are asymptotically static in the remote past and remote future of x, the value of $\langle T_{\mu\nu}(x)\rangle_{\text{ren}}$ (with respect to a fixed in-state) should be immune to metric disturbances outside its causal past $\mathcal{J}^-(x)$ and (with respect to a fixed out-state) powerless to influence events outside its causal future $\mathcal{J}^+(x)$.

  Since AdS_n can be managed by way of the reflective boundary conditions (2.23) and moving to its covering space, the above requirement is satisfied. Moreover, AdS_n is maximally symmetric and therefore its metric is static.

- **3. Finite orthogonal matrix elements** (5.86)

  Despite the unrenormalised stress-energy tensor $T_{\mu\nu}(x)$ being a formal object, it can be shown [75] that it gives finite results when used to compute matrix elements between orthogonal states, i.e.

$$\langle \boldsymbol{\psi}' | \, T_{\mu\nu}(x) \, | \boldsymbol{\psi} \rangle \in \mathbb{R} \Leftrightarrow \langle \boldsymbol{\psi}' | \boldsymbol{\psi} \rangle = 0, \tag{5.87}$$

  which appears to be one way of literally 'making some sense' of $T_{\mu\nu}(x)$ without renormalising it.

  Nevertheless, since this type of computation does not feature in this research, it is a redundant criterion.

- **4. Normal-ordering on $\mathbb{M}^n$** (5.88)

  This is the requirement that $\langle T_{\mu\nu}(x) \rangle_{\text{ren}}$ computed on Minkowski space should coincide with the *normal-ordered* vacuum expectation value of the stress-energy tensor,

$$\langle T_{\mu\nu}(x) \rangle_{\text{ren}}^{\mathbb{M}^n} = : \langle T_{\mu\nu}(x) \rangle : . \tag{5.89}$$

- **Uniqueness theorem**

  Finally, there is a fundamental consequence of Wald's axiomatic approach [75] which in turn serves as a defining feature of QFTs on curved space-times. In particular, given two renormalised vacuum expectation values of the stress-energy tensor, $\langle T_{\mu\nu}(x) \rangle_{\text{ren A}}$ and $\langle T_{\mu\nu}(x) \rangle_{\text{ren B}}$ that both satisfy axioms **1** – **3** above, then it follows that

$$\Theta_{\mu\nu} = \langle T_{\mu\nu}(x) \rangle_{\text{ren A}} - \langle T_{\mu\nu}(x) \rangle_{\text{ren B}}, \tag{5.90}$$

  where $\Theta_{\mu\nu}$ is a local, conserved purely geometrical tensor.

Thus (5.90) implies a $\langle T_{\mu\nu}(x) \rangle_{\text{ren}}$ that satisfies (5.84 – 5.86) is *unique*, that is, it is

the *only* object that will fulfil Wald's axioms. However, a caveat follows naturally from (5.90) too, namely that the uniqueness of $\langle T_{\mu\nu}(x)\rangle_{\text{ren}}$ is only guaranteed up to the addition of a local conserved purely geometrical tensor $\Theta_{\mu\nu}(x)$.

From this it follows that if different renormalisation schemes are applied to the same curved space-time QFT yielding different results $\langle T_{\mu\nu}(x)\rangle_{\text{ren A}}$ and $\langle T_{\mu\nu}(x)\rangle_{\text{ren B}}$, and if version A satisfies Wald's axioms, then version B will only satisfy Wald's axioms if both versions satisfy (5.90). In this way, Wald's axioms act therefore as criteria for determining the suitability and uniqueness of the renormalisation prescription.

This general ambiguity manifests itself very specifically in Hadamard renormalisation. Firstly the direct computation of $\langle T_{\mu\nu}(x)\rangle_{\text{ren}}$ using the Hadamard recursion relations for W_l is not possible as they do not possess a boundary condition.

Secondly, the ambiguity is revealed by the freedom of choice that exists for the mass renormalisation scale M (for even n). This is noticeable from the results for $\Theta_{\mu\nu}(x)$ (5.108 – 5.111) which are non-zero only for even n. Therefore to rid the Hadamard $\langle T_{\mu\nu}(x)\rangle_{\text{ren}}$ of these ambiguities, the W_0 coefficient would need to be fixed, as would M.

This link between the ambiguity of M and the indeterminacy of W is explained clearly by Décanini & Folacci [31]. Following their discussion, for $G_{\text{H}}(x,x')$ to remain sensible for even n then (4.156) must be equivalent to

$$G_{\text{H}}(\sigma) = \boldsymbol{i}\nu(n)\left\{U(\sigma)\sigma^{1-\frac{n}{2}} + V(\sigma)\left[\ln\left(M^2\right) + \ln\sigma\right] + W(\sigma) - V(\sigma)\ln\left(M^2\right)\right\}. \tag{5.91}$$

In other words, introducing M to render the even-n logarithmic argument dimensionless,

$$\sigma \to \bar{\sigma} \Rightarrow W \to W + 2V\ln M, \tag{5.92}$$

especially since W is not uniquely determined.

Furthermore, the connection between this 'mass renormalisation ambiguity' associated with Hadamard renormalisation and the general statement of ambiguity by (5.90) is now apparent by considering that (5.56) and (5.92) result in the equality

$$\Theta_{\mu\nu} = -\nu(n) \lim_{x' \to x} \left\{ \boldsymbol{T}_{\mu\nu}(x, x') V(x, x') \ln\left(M^2\right) \right\}. \tag{5.93}$$

The definitions (5.59 – 5.63) and (5.92) mean that

$$w \to w - v_0 \ln\left(M^2\right), \tag{5.94}$$

$$w_{\mu\nu} \to w_{\mu\nu} - \left(v_{0\mu\nu} + g_{\mu\nu} v_1\right) \ln\left(M^2\right). \tag{5.95}$$

It follows naturally therefore that a convenient formula

$$\Theta_{\mu\nu} = -\nu(n) \left\{ -\left(v_{0\mu\nu} + g_{\mu\nu} v_1\right) + \frac{1}{2}(1 - 2\xi) v_{0;\mu\nu} \right.$$
$$\left. + \frac{1}{2}\left(2\xi - \frac{1}{2}\right) g_{\mu\nu} \Box v_0 + \xi \mathcal{R}_{\mu\nu} v_0 \right\} \ln\left(M^2\right), \tag{5.96}$$

akin to (5.56) can then be obtained for $\Theta_{\mu\nu}$, which also benefits from the maximal symmetry of AdS_n, resulting in the formula

$$\Theta_{\mu\nu} = \nu(n) \left[\left(v_{0\mu\nu} + g_{\mu\nu} v_1\right) - \xi \mathcal{R}_{\mu\nu} v_0 \right] \ln\left(M^2\right). \tag{5.97}$$

5.2.4 Computation of $\langle T_{\mu\nu}(x)\rangle_{\rm ren}$

Another program has been written in MAPLE to compute expressions for $\langle T_{\mu\nu}(x)\rangle_{\rm ren}$ for $n = 2$ to $n = 11$ inclusive. It has a similar structure to the code discussed in section 5.1.1 used to generate the expressions for $\langle\Phi^2(x)\rangle_{\rm ren}$ (5.36 – 5.45), and it too can be easily extended to generate expressions for $n > 11$ if necessary.

The code used to compute expressions for $\langle T_{\mu\nu}(x)\rangle_{\rm ren}$ differs from the previous code due to the presence of the differential operator $\boldsymbol{T}_{\mu\nu}(x, x')$ (5.55) in (5.56), and the consequent requirement to compute the quantities in (5.57) to second order in s.

The code consists of four parts:

- **Part 1** computes expansions of the Feynman Green function truncated to second order, $G_{\rm F}^{\mathbf{II}}(s)$ based on the results in section 5.2.2.
- **Part 2** computes expansions of the singular part of the Hadamard form of the Feynman Green function truncated to second order, $G_{\rm H,sing}^{\mathbf{II}}(s)$. As before, the recurrence relations (4.164) and (4.165) are used to obtain expansions of the $U(s)$ and $V(s)$ respectively. With a knowledge of the Hadamard coefficients generated in the process of constructing these expansions, the quantities v_0, $v_{0\mu\nu}$, and v_1, in equations (5.61 – 5.63) are also computed at this stage in order to assemble the ingredients required for the computation of $\Theta_{\mu\nu}(x)$ later.
- **Part 3** performs the subtraction (5.57) of the second-order expressions generated in the preceding parts of the code.
- In **part 4**, the objects w and $w_{\mu\nu}$ are computed from (5.59) and (5.60). Finally, expressions for $\langle T_{\mu\nu}(x)\rangle_{\rm ren}$ and $\Theta_{\mu\nu}(x)$ are generated using (5.65) and (5.97).

The results of this code follow overleaf.

I. $\langle T_{\mu\nu}\rangle_{\rm ren}$ **FOR** $n=2$ **TO** $n=7$

$$\langle T_{\mu\nu}\rangle^{n=2}_{\rm ren} = -\frac{1}{8\pi a^2}\left\{\left[-2\mu^2-4\xi+\frac{1}{2}\right]\Upsilon(\mu,M,a)+\mu^2+\frac{1}{12}\right\}g_{\mu\nu}+\Theta^{n=2}_{\mu\nu}. \tag{5.98}$$

$$\langle T_{\mu\nu}\rangle^{n=3}_{\rm ren} = -\frac{1}{12\pi a^3}\left\{\mu^3+(6\xi-1)\,\mu\right\}g_{\mu\nu}. \tag{5.99}$$

$$\begin{aligned}\langle T_{\mu\nu}\rangle^{n=4}_{\rm ren} = \quad & \frac{3}{128\pi^2 a^4}\left\{\left[-\frac{4}{3}\mu^4-\left(16\xi-\frac{10}{3}\right)\mu^2+4\xi-\frac{3}{4}\right]\Upsilon(\mu,M,a)\right.\\ & \left.+\,\mu^4+\left(8\xi-\frac{29}{18}\right)\mu^2+\frac{2}{3}\xi-\frac{107}{720}\right\}g_{\mu\nu}+\Theta^{n=4}_{\mu\nu}.\end{aligned} \tag{5.100}$$

$$\langle T_{\mu\nu}\rangle^{n=5}_{\rm ren} = \quad \frac{1}{120\pi^2 a^5}\left\{\mu^5+(20\xi-5)\,\mu^3-(20\xi-4)\,\mu\right\}g_{\mu\nu}. \tag{5.101}$$

$$\begin{aligned}\langle T_{\mu\nu}\rangle^{n=6}_{\rm ren} = -\frac{11}{4608\pi^3 a^6}\left\{\left[-\frac{12}{11}\mu^6-\left(\frac{360}{11}\xi-\frac{105}{11}\right)\mu^4\right.\right.\\ \left.+\left(\frac{900}{11}\xi-\frac{777}{44}\right)\mu^2-\frac{405}{22}\xi+\frac{675}{176}\right]\Upsilon(\mu,M,a)\\ +\mu^6+\left(\frac{270}{11}\xi-\frac{313}{44}\right)\mu^4-\left(\frac{435}{11}\xi-\frac{7413}{880}\right)\mu^2\\ \left.-\frac{321}{88}\xi+\frac{11969}{14784}\right\}g_{\mu\nu}+\Theta^{n=6}_{\mu\nu}.\end{aligned} \tag{5.102}$$

$$\langle T_{\mu\nu}\rangle^{n=7}_{\rm ren} = -\frac{1}{1680\pi^3 a^7}\left\{\mu^7+(42\xi-14)\,\mu^5-(210\xi-49)\,\mu^3+(168\xi-36)\,\mu\right\}g_{\mu\nu}. \tag{5.103}$$

II. $\langle T_{\mu\nu}\rangle_{\rm ren}$ **FOR** $n=8$ **&** $n=9$

$$\langle T_{\mu\nu}\rangle_{\rm ren}^{n=8} = \frac{25}{147456\pi^4 a^8}$$
$$\times\left\{\left[-\frac{24}{25}\mu^8-\left(\frac{1344}{25}\xi-\frac{504}{25}\right)\mu^6\right.\right.$$
$$+\left(\frac{2352}{5}\xi-\frac{2961}{25}\right)\mu^4-\left(\frac{21756}{25}\xi-\frac{9687}{50}\right)\mu^2+189\xi-\left.\frac{1323}{32}\right]$$
$$\times\,\Upsilon(\mu,M,a)$$
$$+\mu^8+\left(\frac{1232}{25}\xi-\frac{461}{25}\right)\mu^6-\left(\frac{8764}{25}\xi-\frac{87983}{1000}\right)\mu^4$$
$$\left.+\left(\frac{51891}{125}\xi-\frac{3854941}{42000}\right)\mu^2+\frac{11969}{300}\xi-\frac{288563}{32000}\right\}g_{\mu\nu}+\Theta_{\mu\nu}^{n=8}. \tag{5.104}$$

$$\langle T_{\mu\nu}\rangle_{\rm ren}^{n=9} = \frac{1}{30240\pi^4 a^9}$$
$$\times\left\{\mu^9+(72\xi-30)\,\mu^7-(1008\xi-273)\,\mu^5\right.$$
$$\left.+(3528\xi-820)\,\mu^3\,(2592\xi-576)\,\mu\right\}g_{\mu\nu}. \tag{5.105}$$

III. ——— $\langle T_{\mu\nu}\rangle_{\rm ren}$ **FOR** $n=10$ **&** $n=11$ ———

$$\langle T_{\mu\nu}\rangle_{\rm ren}^{n=10} = -\frac{137}{14745600\pi^5 a^{10}}$$
$$\times\left\{\left[-\frac{120}{137}\mu^{10} - \left(\frac{10800}{137}\xi - \frac{4950}{137}\right)\mu^8 + \left(\frac{226800}{137}\xi - \frac{65835}{137}\right)\mu^6\right.\right.$$
$$- \left(\frac{1332450}{137}\xi - \frac{1296075}{548}\right)\mu^4 + \left(\frac{2179575}{137}\xi - \frac{15858315}{4384}\right)\mu^2$$
$$\left.\left. - \frac{7441875}{2192}\xi + \frac{13395375}{17536}\right]\Upsilon(\mu, M, a) + \mu^{10}\right.$$
$$+ \left(\frac{11250}{137}\xi - \frac{20605}{548}\right)\mu^8 - \left(\frac{207450}{137}\xi - \frac{481133}{1096}\right)\mu^6$$
$$+ \left(\frac{3959235}{548}\xi - \frac{161437505}{92064}\right)\mu^4 - \left(\frac{57824115}{7672}\xi - \frac{418944187}{245504}\right)\mu^2$$
$$\left. - \frac{12985335}{17536}\xi + \frac{262292845}{1543168}\right\}g_{\mu\nu} + \Theta_{\mu\nu}^{n=10}. \qquad (5.106)$$

$$\langle T_{\mu\nu}\rangle_{\rm ren}^{n=11} = -\frac{1}{665280\pi^5 a^{11}}$$
$$\times\left\{\mu^{11} + (110\xi - 55)\,\mu^9 - (3300\xi - 1023)\,\mu^7\right.$$
$$+ (30030\xi - 7645)\mu^5 - (90200\xi - 21076)\,\mu^3$$
$$\left. + \ (63360\xi - 14400)\,\mu\right\}g_{\mu\nu}, \qquad (5.107)$$

where for even n, $\Upsilon(\mu, M, a)$ is given by (5.46).

The expressions for $\langle T_{\mu\nu} \rangle_{\text{ren}}$ for $n = 3$ to $n = 11$ inclusive (5.99 – 5.107) are even or odd-powered polynomials in μ of leading-order n, with an additional linear dependence on ξ.

Furthermore, these polynomials are proportional to the metric. It follows that $\langle T_{\mu\nu} \rangle_{\text{ren}}$ is conserved, which satisfies the remaining criterion (5.84) required to ensure its uniqueness.

As in the computation of $\langle \Phi^2 \rangle_{\text{ren}}$, expressions for $\langle T_{\mu\nu} \rangle_{\text{ren}}$ in AdS_n have already been computed using zeta-function regularisation methods by Caldarelli, the results of which corroborate those here bearing in mind (5.47). The simplifications made in the case of the plots for $\langle \Phi^2 \rangle_{\text{ren}}$, namely that $a = 1$ and $M = \dfrac{e^{\gamma}}{\sqrt{2}}$ also apply to the plots below.

The results (5.98 – 5.107) are plotted below in figure 5.8 as functions of μ. Since $\langle T_{\mu\nu} \rangle_{\text{ren}}$ depends on ξ as well as μ, ξ has been fixed (at $\xi = 0$) in order to allow an effective comparison of profiles. As before in the case of the plots of $\langle \Phi^2 \rangle_{\text{ren}}$ in figures 5.1 and 5.2, each coloured curve in figure 5.8 describes how the stress-energy varies with the mass-coupling configuration for a distinct value of n.

The distinction between profiles for even n and odd n is clear from this plot. Profiles for even n all decrease with increasing μ, whereas profiles for odd n alternate with increasing values of n as to whether they are ultimately increasing or decreasing functions of μ. In addition, profiles for even n have a slower rate of change with respect to μ. From the expressions for even n, it can be understood that the descent of their profiles is slowed by the $\psi\left(\frac{1}{2} + \mu\right)$-term present in $\Upsilon(\mu, M, a)$. Therefore, the profiles for even n are seen to occupy the right-hand side of the plot. The profiles for odd n exhibit rapid change with respect to μ and appear bunched towards the left-hand side of the plot.

In general, the order of final departure of each curve from the μ axis corresponds to increasing values of n. As the curves depict polynomials in μ, it follows that prior to their departure from the μ axis, they will have criss-crossed the the axis according to the function's number of zeroes. Figures 5.9 – 5.18 respectively display

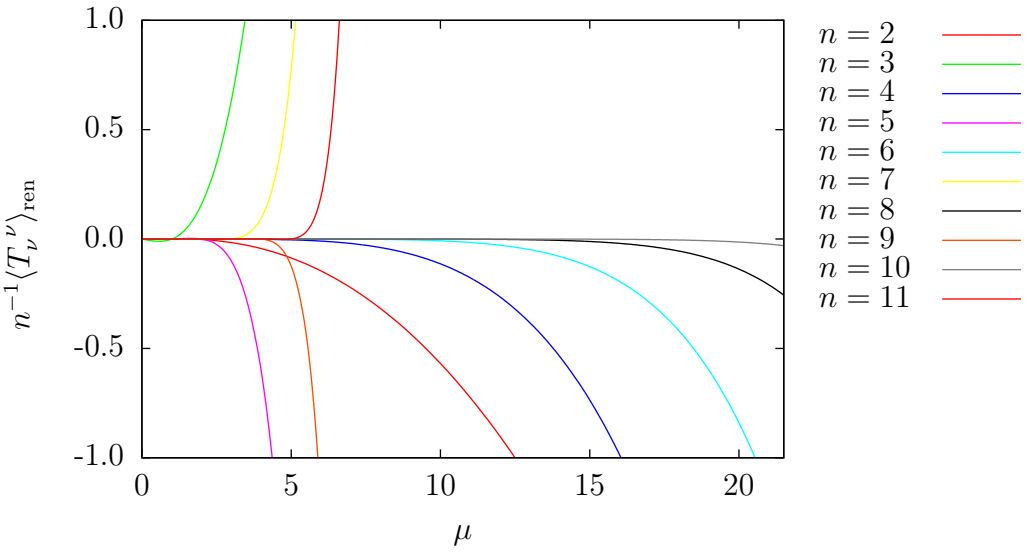

FIGURE 5.8 – $n^{-1}\langle T_\nu{}^\nu\rangle_{\rm ren}$ as a function of μ for $\xi = 0$ and varying n with $a = 1$ and $M = \dfrac{e^\gamma}{\sqrt{2}}$

the behaviour of each curve in figure 5.8 separately and now with ξ varying. These surface plots share a common footprint defined by the fixed ranges $\mu \in [0, 7.5]$ and $\xi \in [-0.25, 0.25]$. The order of departure from the $n^{-1}\langle T_\nu{}^\nu\rangle_{\rm ren} = 0$ plane determines the range of values covered by the vertical axis in the surface plots. Consequently, absolute values of $\langle T_\nu{}^\nu\rangle_{\rm ren}$ are progressively smaller with increasing values of n. Conversely, surface plots for odd n show increasingly rapid growth with increasing n and this is reflected by the much larger ranges of values available on the $n^{-1}\langle T_\nu{}^\nu\rangle_{\rm ren}$ axis.

The influence of ξ in the expressions (5.98) – (5.107) is particularly visible by the intersection of the plot's surface with the $\mu = 7.5$ plane, revealing the linear dependence on μ. For the ranges of values chosen, this dependence appears to strengthen with increasing n. Finally at lower values of μ, each plot seems to start off fairly

'level' (in the sense of its degree of parallelism with a constant $\langle T_\nu{}^\nu \rangle_{\text{ren}}$-planes), descending or ascending as μ increases, but also twisting as it does (and increasingly so with increasing n). The surface plots from about $n = 9$ upwards towards the $\xi = -0.25$ plane reveal regions of the surface whose dependence on μ differs in sign to that of higher values of ξ. From the point of view of figure 5.8, this is just a statement of the fact that the location of zeroes of the polynomials in μ depend on ξ.

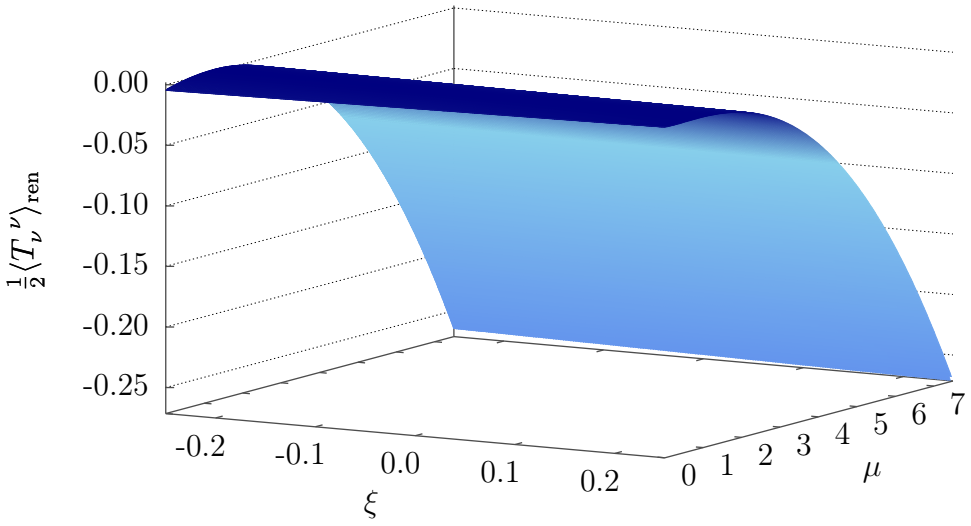

FIGURE 5.9 – $\frac{1}{2}\langle T_\nu{}^\nu \rangle_{\text{ren}}$ as a function of μ and ξ for $n = 2$ with $a = 1$ and $M = \dfrac{e^\gamma}{\sqrt{2}}$

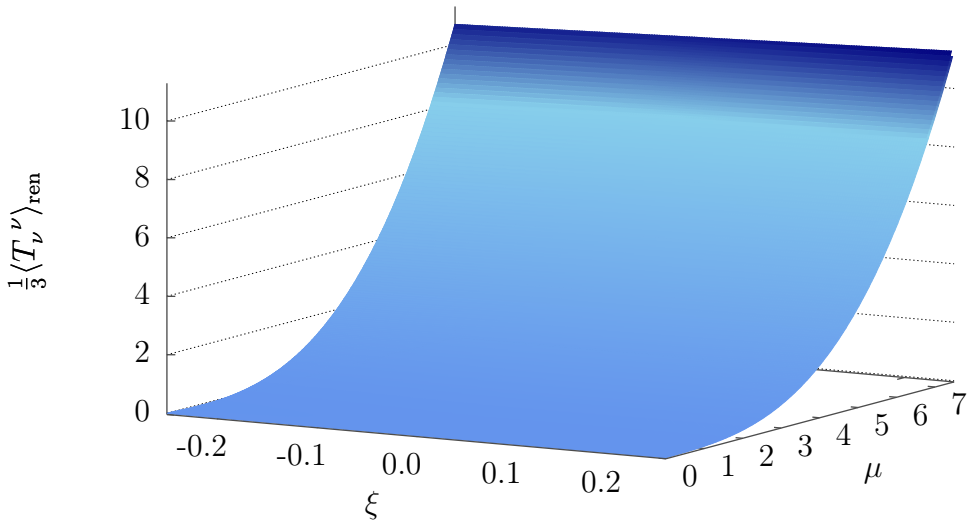

FIGURE 5.10 – $\frac{1}{3}\langle T_\nu{}^\nu \rangle_{\rm ren}$ as a function of μ and ξ for $n = 3$ with $a = 1$

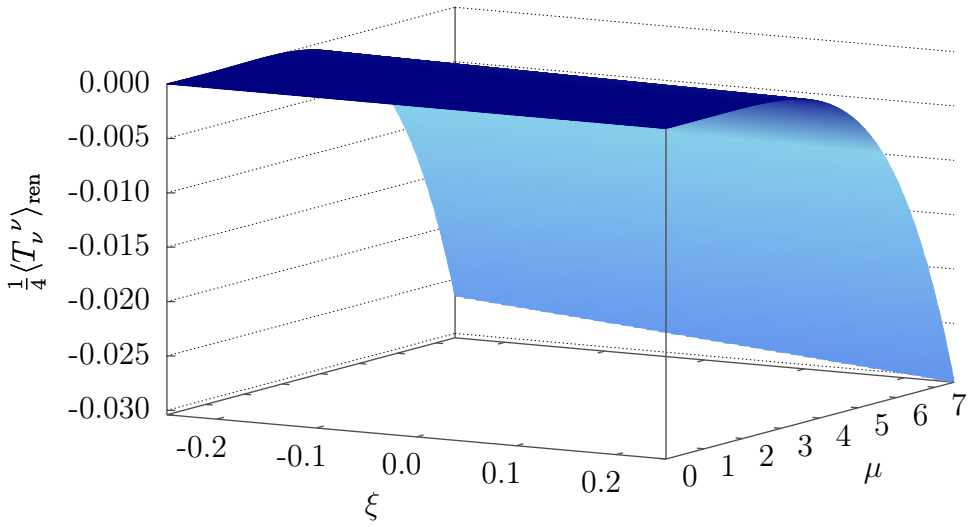

FIGURE 5.11 – $\frac{1}{4}\langle T_\nu{}^\nu \rangle_{\rm ren}$ as a function of μ and ξ for $n = 4$ with $a = 1$ and $M = \dfrac{e^\gamma}{\sqrt{2}}$

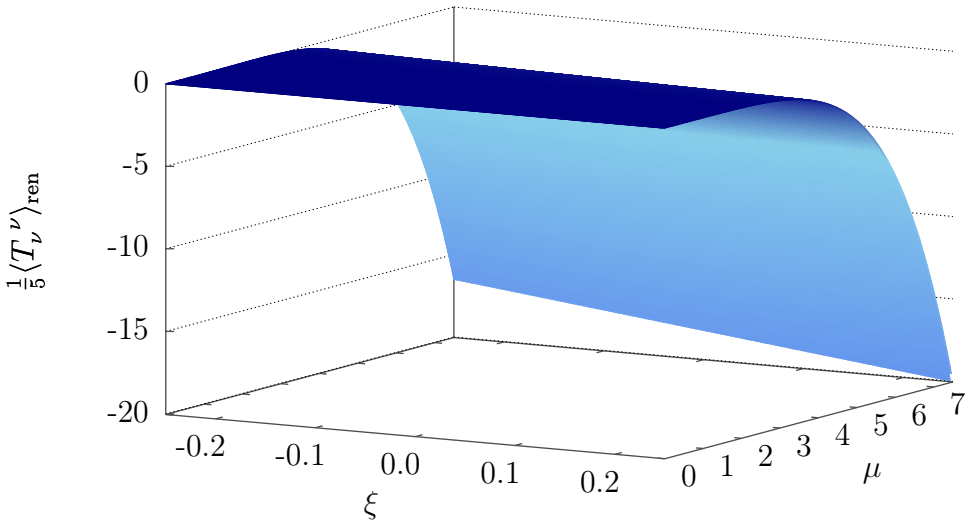

FIGURE 5.12 – $\frac{1}{5}\langle T_\nu{}^\nu\rangle_{\rm ren}$ as a function of μ and ξ for $n = 5$ with $a = 1$

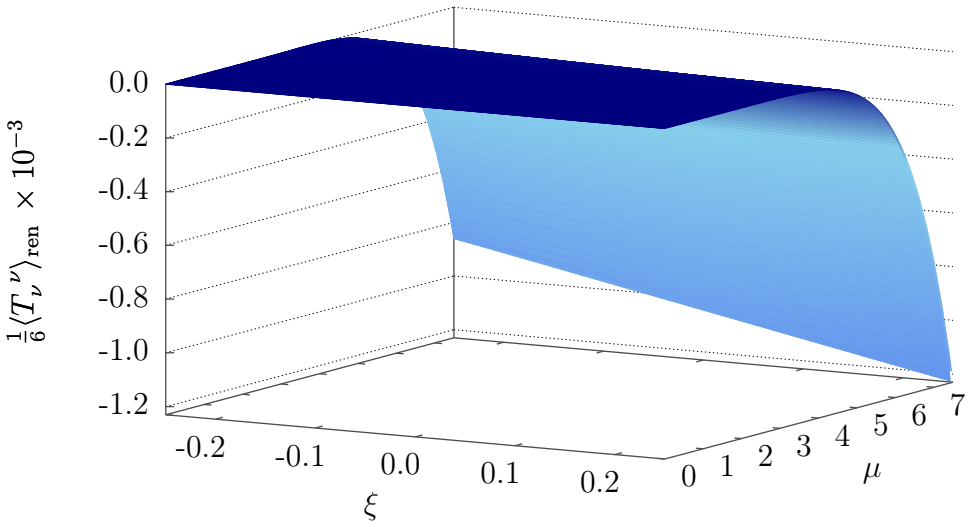

FIGURE 5.13 – $\frac{1}{6}\langle T_\nu{}^\nu\rangle_{\rm ren}$ as a function of μ and ξ for $n = 6$ with $a = 1$ and $M = \dfrac{e^\gamma}{\sqrt{2}}$

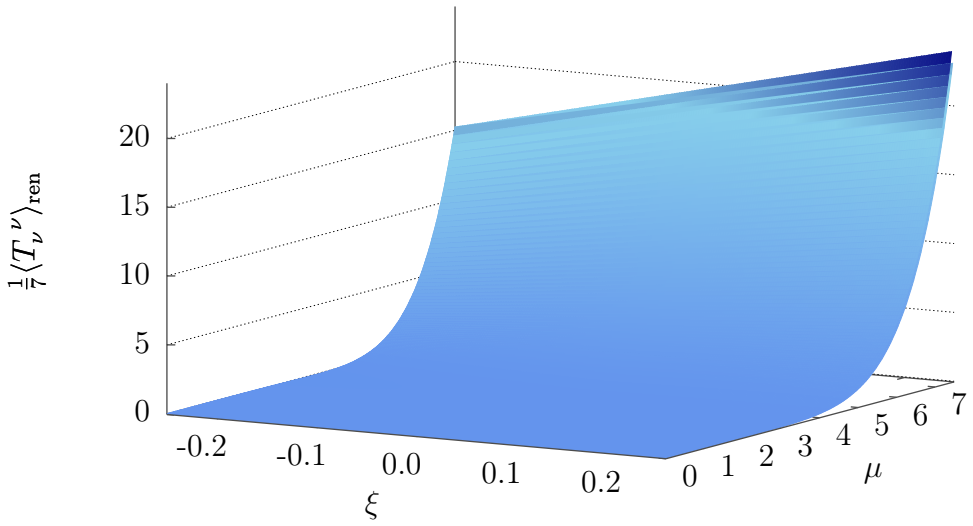

FIGURE 5.14 – $\frac{1}{7}\langle T_\nu{}^\nu \rangle_{\rm ren}$ as a function of μ and ξ for $n = 7$ with $a = 1$

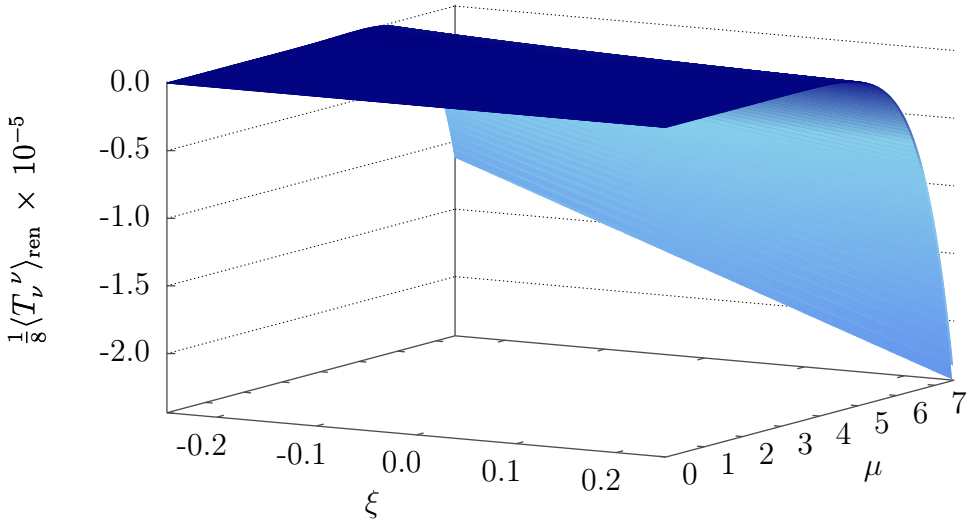

FIGURE 5.15 – $\frac{1}{8}\langle T_\nu{}^\nu \rangle_{\rm ren}$ as a function of μ and ξ for $n = 8$ with $M = \dfrac{e^\gamma}{\sqrt{2}}$

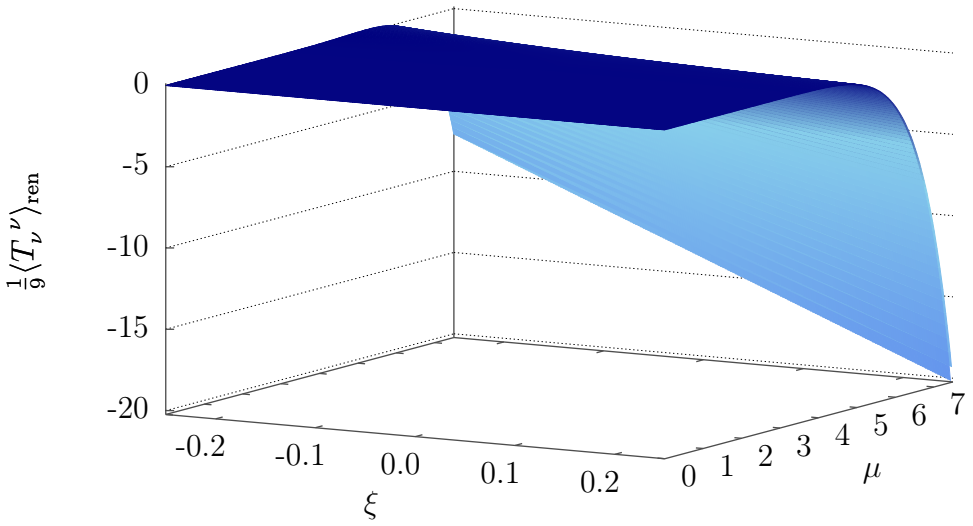

FIGURE 5.16 – $\frac{1}{9}\langle T_\nu{}^\nu\rangle_{\rm ren}$ as a function of μ and ξ for $n = 9$ with $a = 1$

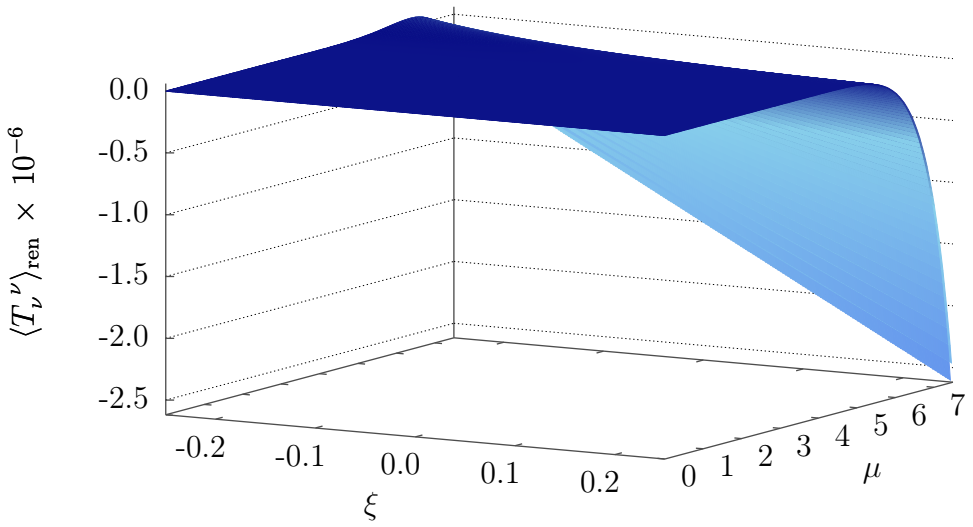

FIGURE 5.17 – $\langle T_\nu{}^\nu\rangle_{\rm ren}$ as a function of μ and ξ for $n = 10$ with $a = 1$ and $M = \dfrac{e^\gamma}{\sqrt{2}}$

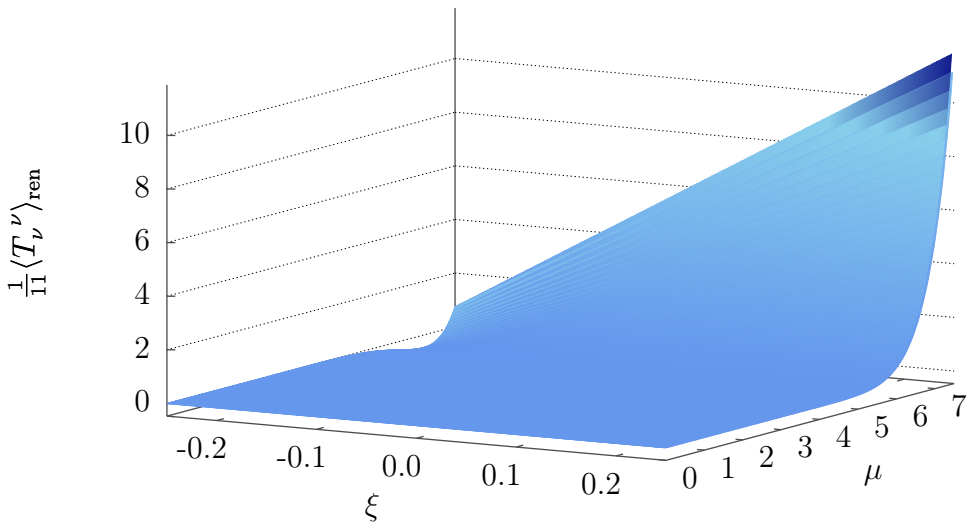

FIGURE 5.18 – $\frac{1}{11}\langle T_\nu{}^\nu\rangle_{\rm ren}$ as a function of μ and ξ for $n = 11$ with $a = 1$

Finally, figure 5.19 shows a plot of $\frac{1}{4}\langle T_\nu{}^\nu\rangle_{\rm ren}$ as a function of μ for a massive, conformally-coupled field for $n = 4$ and with varying M. The pattern of behaviour is qualitatively identical to the description given for the plots of $\langle\Phi^2\rangle_{\rm ren}$ in figures 5.3 – 5.7.

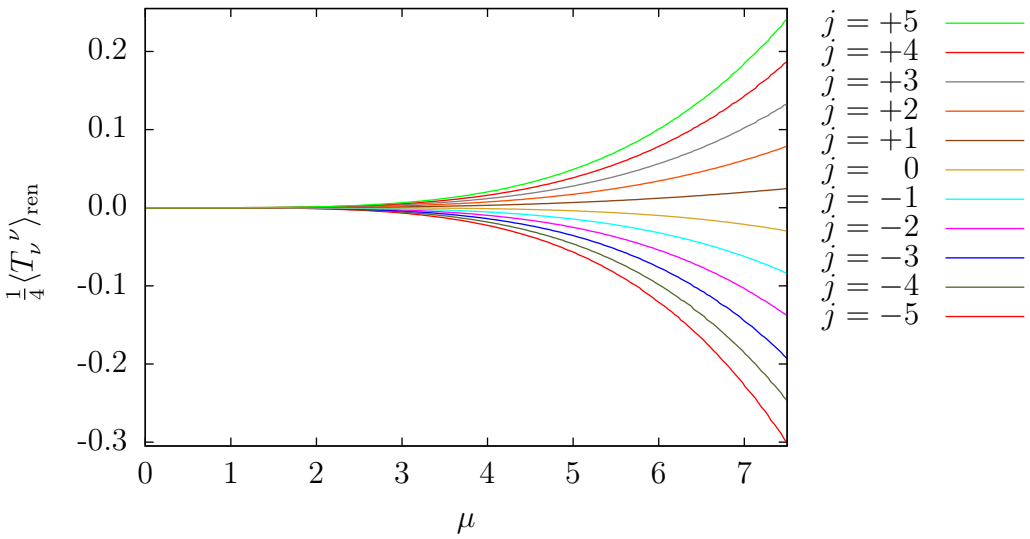

FIGURE 5.19 – $\frac{1}{4}\langle T_\nu{}^\nu\rangle_{\rm ren}$ as a function of μ for $\xi = \frac{1}{6}$, $n = 4$, $a = 1$ with $M(j) = \dfrac{e^\gamma}{\sqrt{2}}10^{j-6}$

IV. $\Theta_{\mu\nu}$ FOR $n = 2, 4, 6, 8$ & 10

From (5.97), results for the geometric tensor, $\Theta_{\mu\nu}$ are listed below.

$$\Theta_{\mu\nu}^{n=2} = -\frac{1}{8\pi a^2}\left\{\mu^2 + 2\xi - \frac{1}{4}\right\}\left(\ln M^2\right) g_{\mu\nu}. \tag{5.108}$$

$$\Theta_{\mu\nu}^{n=4} = \frac{1}{64\pi^2 a^4}\left\{\mu^4 + \left(12\xi - \frac{5}{2}\right)\mu^2 - 3\xi + \frac{9}{16}\right\}\left(\ln M^2\right) g_{\mu\nu}. \tag{5.109}$$

$$\begin{aligned}\Theta_{\mu\nu}^{n=6} = -\frac{1}{768\pi^3 a^6}\Bigg\{&\mu^6 + \left(30\xi - \frac{35}{4}\right)\mu^4 + \left(-75\xi + \frac{259}{16}\right)\mu^2 \\ &+\frac{135}{8}\xi - \frac{225}{64}\Bigg\}\left(\ln M^2\right) g_{\mu\nu}.\end{aligned}$$

$$\begin{aligned}\Theta_{\mu\nu}^{n=8} = &\frac{1}{12288\pi^4 a^8} \\ &\times\Bigg\{\mu^8 + (56\xi - 21)\,\mu^6 + \left(-490\xi + \frac{987}{8}\right)\mu^4 + \left(\frac{1813}{2}\xi - \frac{3229}{16}\right)\mu^2 \\ &- \frac{1575}{8}\xi + \frac{11025}{256}\Bigg\}\left(\ln M^2\right) g_{\mu\nu}.\end{aligned} \tag{5.110}$$

$$\begin{aligned}\Theta_{\mu\nu}^{n=10} = -&\frac{1}{245760\pi^5 a^{10}} \\ &\times\Bigg\{\mu^{10} + \left(90\xi - \frac{165}{4}\right)\mu^8 + \left(-1890\xi + \frac{4389}{8}\right)\mu^6 \\ &+ \left(\frac{44415}{4}\xi - \frac{86405}{32}\right)\mu^4 + \left(-\frac{145305}{8}\xi + \frac{1057221}{256}\right)\mu^2 \\ &+ \frac{496125}{128}\xi - \frac{893025}{1024}\Bigg\}\left(\ln M^2\right) g_{\mu\nu}.\end{aligned} \tag{5.111}$$

V. $\langle T_{\mathbf{mc}\ \mu}{}^{\mu}\rangle_{\rm ren}$ FOR $n = 2$ TO $n = 11$

Finally, results are given for the trace anomaly acquired through renormalisation for a conformally-invariant scalar field in even n.

$$\langle T_{\rm mc\ \mu}{}^{\mu}\rangle_{\rm ren}^{n=2} = -\frac{1}{12a^2\pi}. \tag{5.112}$$

$$\langle T_{\rm mc\ \mu}{}^{\mu}\rangle_{\rm ren}^{n=3} = 0. \tag{5.113}$$

$$\langle T_{\rm mc\ \mu}{}^{\mu}\rangle_{\rm ren}^{n=4} = -\frac{1}{240a^4\pi^2}. \tag{5.114}$$

$$\langle T_{\rm mc\ \mu}{}^{\mu}\rangle_{\rm ren}^{n=5} = 0. \tag{5.115}$$

$$\langle T_{\rm mc\ \mu}{}^{\mu}\rangle_{\rm ren}^{n=6} = -\frac{5}{4032a^6\pi^3}. \tag{5.116}$$

$$\langle T_{\rm mc\ \mu}{}^{\mu}\rangle_{\rm ren}^{n=7} = 0. \tag{5.117}$$

$$\langle T_{\rm mc\ \mu}{}^{\mu}\rangle_{\rm ren}^{n=8} = -\frac{23}{34560a^8\pi^4}. \tag{5.118}$$

$$\langle T_{\rm mc\ \mu}{}^{\mu}\rangle_{\rm ren}^{n=9} = 0. \tag{5.119}$$

$$\langle T_{\rm mc\ \mu}{}^{\mu}\rangle_{\rm ren}^{n=10} = -\frac{263}{506880a^{10}\pi^5}. \tag{5.120}$$

$$\langle T_{\rm mc\ \mu}{}^{\mu}\rangle_{\rm ren}^{n=11} = 0. \tag{5.121}$$

6 | Rotational vacuum states

6.1 Non-vacuum states

Having successfully renormalised the expectation value of the stress-energy tensor of the free scalar field with respect to its vacuum state, a foundation (albeit carrying an ambiguity in tow) is now available for research into 'other' states of the field.

A natural progression is to consider certain well-defined classes of states associated with an 'observer' or 'detector'. Such states are of key interest to QFTs in curved space-times as generally speaking, observers in different reference frames will disagree on their local descriptions of the state in question.

The remainder of the research presented in this thesis relates to the special case of the AdS_n vacuum state defined by a non-inertial observer. In fact, it could be said that such states are of interest to QFTs in curved space-time *because* of the ambiguity in the definition of the vacuum state.

Further weight is lent to this statement by the fact that when a discrepancy exists between observers' descriptions of the vacuum state, it implies that non-vacuum-like properties are observed, i.e. 'particle-like' descriptions.

The issue of what a particle is in this context is deliberately not broached here, as it is currently sufficient for the purposes of this research to use this terminology to heuristically distinguish vacuum states from non-vacuum states. Excellent formal discussions on aspects of the 'particle issue' in QFTs in curved space-times can be found for example (among many others) in the classic texts [11] [33] [78].

Nevertheless, there is a consequence of this 'particle' production induced by the background curvature that is of great significance to studies concerning states. The reflective boundary conditions on AdS_n (2.23) allow the space-time and the scalar field coupled to it to be considered as a closed thermodynamic system.

For example, the state of the scalar field described from the reference frame of a rigidly-rotating observer in pure AdS_n may also be interpreted as the description of the effects of a closed rotating system on a freely-falling observer's description of the irrotational vacuum state. Likewise, the state described from the reference frame of a uniformly accelerating (but not free-falling) observer may be perceived by a freely-falling observer's description of the vacuum state as a system at finite temperature.

A useful general starting-point that embodies this connection for all such states is how the dependent Green functions are related to their irrotational vacuum counterpart.

The present and following chapter (chapters 6 – 7 inclusive) respectively consider:

- Rotational vacuum states $\left|\mathbf{0}_{\mathbf{\Omega}}\right\rangle$;
- Irrotational thermal states $\left|\boldsymbol{\beta}\right\rangle$;
- Rotational thermal states $\left|\boldsymbol{\beta}_{\mathbf{\Omega}}\right\rangle$.

When considering the matter content developed from these states, given that it is only the vacuum expectation values that diverge in the coincidence limit, there is no need to renormalise *ever* again. However, this blessing comes at a cost as these classes of states are accompanied by their own brand of problems. These difficulties and their management are discussed separately in each relevant chapter.

As mentioned in [28], significantly more attention has been given in the literature

to the study of the effects on a detector that is linearly accelerating than to the investigation of the effects on a rigidly-rotating detector.

6.2 Rotational anti-commutator function — $G^{\mathbf{\Omega}}_{(1)}(x,x')$

Since this study of rotational vacuum states is intended to lead to rotational thermal states, it is convenient to develop the matter content from the anti-commutator Green function (4.8) in keeping with common practice in the literature on thermal states.

The explicit form of the anti-commutator function for the *irrotational* vacuum state can be found by first inserting the field mode expansion (3.6) into the definition of the anti-commutator function (4.8). Dropping the space-time dependence temporarily for clarity, and defining

$$\Phi_{j'} := \Phi_j(x'), \tag{6.1}$$

it follows that,

$$\begin{aligned}
G_{(1)}(x,x') &= \sum_{j,j'} \langle \mathbf{0}| \left(a_j\Phi_j + a_j^\dagger\Phi_j^*\right)\left(a_{j'}\Phi_{j'} + a_{j'}^\dagger\Phi_{j'}^*\right) \\
&\qquad\qquad + \left(a_{j'}\Phi_{j'} + a_{j'}^\dagger\Phi_{j'}^*\right)\left(a_j\Phi_j + a_j^\dagger\Phi_j^*\right)|\mathbf{0}\rangle \\
&= \sum_{j,j'} \langle \mathbf{0}|\, a_j\Phi_j a_{j'}^\dagger\Phi_{j'}^* + a_{j'}\Phi_{j'}a_j^\dagger\Phi_j^*\,|\mathbf{0}\rangle \\
&= \sum_{j,j'} \langle \mathbf{0}|\, a_j a_{j'}^\dagger\Phi_j\Phi_{j'}^* + a_{j'}a_j^\dagger\Phi_{j'}\Phi_j^*\,|\mathbf{0}\rangle \\
&= \sum_{j,j'} \langle \mathbf{0}|\, [a_j, a_{j'}^\dagger]\Phi_j\Phi_{j'}^* + a_{j'}^\dagger a_j\Phi_j\Phi_{j'}^* + [a_{j'}, a_j^\dagger]\Phi_{j'}\Phi_j^* + a_j^\dagger a_{j'}\Phi_{j'}\Phi_j^*\,|\mathbf{0}\rangle\,,
\end{aligned} \tag{6.2}$$

where the factors annihilating the vacuum are discounted in the second line, and where the commutation relations

$$[a_j, a^\dagger_{j'}] = \delta_{jj'}, \tag{6.3}$$

have been applied to the fourth line.

Reinstating space-time dependence explicitly yields

$$G_{(1)}(x, x') = \sum_j \Phi_j(x)\Phi^*_j(x') + \Phi_j(x')\Phi^*_j(x). \tag{6.4}$$

Relaxing the requirement that $\mathcal{k}$ (and therefore also that $\mathcal{w}_n$) be an integer (see (3.61) and (3.71) respectively), results in the positive-frequency field modes

$$\Phi_{n\ell}(x) = N_{r\ell} e^{-i\omega\tau} Y_\ell(\theta, \varphi) (\sin\rho)^\ell (\cos\rho)^k \; P_r^{\left(\ell+\frac{n-3}{2}, k-\frac{n-1}{2}\right)} (\cos 2\rho), \tag{6.5}$$

that may be defined on $CAdS_n$. The omission of the quantisation condition (3.62) is reflected in the change of notation from the AdS_n field modes (3.71). In (6.5), the integers $\mathcal{k}$, $\mathcal{w}_n$ have been replaced with k, ω, where

$$\omega = k + \ell + 2r. \tag{6.6}$$

At this stage, it proves convenient to make the following definition:

$$r(\rho) := (\sin\rho)^\ell (\cos\rho)^k P_r^{\left(\ell+\frac{n-3}{2}, k-\frac{n-1}{2}\right)} (\cos 2\rho). \tag{6.7}$$

Therefore the expressions (3.38), (3.41), (3.57) and (3.67) from section 3.4 show that

$$r = (N_{r\ell})^{-1} \widetilde{R}. \tag{6.8}$$

where

$$r := r(\rho). \tag{6.9}$$

Finally, defining

$$r' := r(\rho'), \qquad Y_\ell := Y_\ell(\theta,\varphi) \qquad Y'_\ell := Y_\ell(\theta',\varphi'), \tag{6.10}$$

allows (6.5) to be written more compactly as

$$G_{(1)}(x,x') = \sum_{\ell,\, r} |N_{r\ell}|^2 \left(e^{i\omega(\tau-\tau')} + e^{-i\omega(\tau-\tau')}\right) rr' \sum_{m_i} Y_\ell \, (Y_\ell)^* \,, \qquad n \geq 3, \tag{6.11}$$

recalling (2.105).

A set of coordinates appropriate for an observer rotating rigidly with angular speed $\mathbf{\Omega}$ in pure AdS_n is obtained via the transformation of (2.5) as

$$\tau \mapsto \widetilde{\tau}, \tag{6.12}$$

$$\varphi \mapsto \widetilde{\varphi} := \varphi - \mathbf{\Omega} a \tau. \tag{6.13}$$

Recalling (2.86) and (2.103), the set of modes in this coordinate system look like

$$\widetilde{\Phi}_{n\ell}(x) = N_{r\ell} e^{-i\widetilde{\omega}\widetilde{\tau}} r e^{im\widetilde{\varphi}} \Theta_{m_i}. \tag{6.14}$$

Defining

$$\widetilde{\omega} := \omega - \mathbf{\Omega} a m, \tag{6.15}$$

and bearing in mind (6.12) and (6.13), it is clear that the expressions (6.5) and (6.14) are *formally* equivalent under the exchange of tildes.

It is tempting to assume that because of this formal equivalence, the irrotational and rotational vacuum states coincide, and that an equivalent QFT can thus be defined based on either of the mode expansions. However, it is wise to heed something of a mantra in the literature on rotational states: '*it is the modes not the frequencies that determine the commutation relations*' [28] [34] (based on material in [54]). Accordingly, as indicated in the discussion in section 3.1, identical QFTs require identical commutation relations. To verify whether this is the case here, it is now necessary to check whether

$$\widetilde{\omega} \gtrless 0 \quad \Leftrightarrow \quad \|\Phi^{(\pm)}_{n\ell}\|_{\mathrm{KG}} \gtrless 0, \tag{6.16}$$

holds.

Given that $k > 0$ and ℓ, $r = 0, 1, \ldots$, it follows from (6.6) that

$$\omega > 0. \tag{6.17}$$

Also, recalling (2.79),

$$\ell \geq m, \qquad m = 0, 1, \ldots. \tag{6.18}$$

Therefore

$$\omega > m. \tag{6.19}$$

From (6.15),

$$\widetilde{\omega} > 0 \Leftrightarrow \omega > \mathbf{\Omega} a m. \tag{6.20}$$

Therefore,

$$\widetilde{\omega} > 0 \Leftrightarrow \begin{cases} \mathbf{\Omega} a < 1, & m > 0, \quad (6.21a) \\ \mathbf{\Omega} a \in \mathbb{R}, & m = 0. \quad (6.21b) \end{cases}$$

The conditions for (6.21a – 6.21b) constrain the candidate modes for a rigidly-rotating observer (6.14) to,

$$\Phi^{\mathbf{\Omega}}_{n\ell} := N_{r\ell} e^{-i\omega\widetilde{\tau}} r e^{im\widetilde{\varphi}} \Theta_{m_i}, \qquad \mathbf{\Omega}a < 1, \qquad m > 0, \tag{6.22}$$

effectively confirming the existence of a timelike Killing vector $\partial_{\widetilde{\tau}}$ associated with the symmetries of the coordinate transformation (6.12) such that

$$\partial_{\widetilde{\tau}} \Phi^{\mathbf{\Omega}(\pm)}_{n\ell} \propto \mp i\omega \Phi^{\mathbf{\Omega}(\pm)}_{n\ell}, \qquad \omega > 0. \tag{6.23}$$

The anti-commutator function with respect to a rotational vacuum state (in terms of the coordinate transformations (6.12), (6.13) and the definition (6.15)) can be found by inserting the modes (6.22) into the definition (6.4) and evaulating the sum. This results in the now unsurprising expression

$$G^{\mathbf{\Omega}}_{(1)}(x,x') = \sum_{\ell,\, r} |N_{r\ell}|^2 \left(e^{i\widetilde{\omega}(\tau-\tau')} + e^{-i\widetilde{\omega}(\tau-\tau')} \right) r r' \sum_{m_i} Y_\ell(\theta,\widetilde{\varphi}) \left(Y_\ell(\theta',\widetilde{\varphi}') \right)^* \quad n \geq 3, \tag{6.24}$$

and thus that

$$G^{\mathbf{\Omega}}_{(1)}(x,x') = G_{(1)}(x,x'), \qquad \mathbf{\Omega}a < 1; \widetilde{\omega}, \widetilde{\varphi} \leftrightarrow \omega, \varphi. \tag{6.25}$$

In summary, the notion of the vacuum state for an observer rigidly-rotating with angular speed $\mathbf{\Omega} < a^{-1}$ coincides with that of a static observer. Ultimately therefore, the associated field theory can be defined in view of the fact that the renormalised rotational vacuum expectation value of the stress-energy tensor,

$$\langle T_{\mu\nu} \rangle^{\mathbf{\Omega}}_{\text{ren}} := \left\langle \mathbf{0}_{\mathbf{\Omega}} \right| T_{\mu\nu} \left| \mathbf{0}_{\mathbf{\Omega}} \right\rangle_{\text{ren}} = \langle T_{\mu\nu} \rangle_{\text{ren}}, \qquad \mathbf{\Omega}a < 1. \tag{6.26}$$

7 | Irrotational thermal states

7.1 Introduction

The consideration of thermal states is of intrinsic interest to QFT in curved space-time, as their characterisation is connected to the ambiguity in the definition of the vacuum state. In short, a uniformly accelerated observer may describe the vacuum state (as described by an inertial observer) as a finite, non-zero temperature thermal state.

Thermal states are also particularly significant in the treatment of black-hole space-times due to the thermal (Hawking) radiation [49] [50] that emanates naturally from their horizons. Therefore, as black holes are inherently thermal objects, the study of thermal states on AdS_n is a sensible foundation for intended research into asymptotically-AdS_n black-hole space-times mentioned in section 1.4.

This chapter concentrates on *irrotational* thermal states of the scalar field on AdS_n. This state of affairs can be interpreted as pure AdS_n filled with a free bosonic radiation field at finite temperature [3].

In order to set the scene for the discussion of the calculation of expectation values with respect to thermal states later in the chapter, it is useful to first review some basic theory. Much of the background material presented in this section and the next (sections 7.1 and 7.2) can be found in Birrell & Davies [11] and the seminal work by Allen, Folacci & Gibbons [3], who studied the effects of finite temperature associated with a conformally-invariant scalar field on AdS_4.

The associated presence of a non-zero finite temperature introduces a degree of disorder to the space-time. Accordingly, a key consequence of the thermalisation of AdS_n is a symmetry-breaking. Tolman's investigations of thermal equilibrium in gravitational fields [71] [35] revealed that the inverse temperature measured by a local observer $\boldsymbol{\beta}_{\mathrm{T}}$ depends on the gravitational field at the site of measurement [71].

For a static metric, this relationship gives the Tolman relation

$$\boldsymbol{\beta}_{\mathrm{T}} \left(-g_{00}\right)^{\frac{1}{2}} = \boldsymbol{K}, \tag{7.1}$$

where $\boldsymbol{K}$ is a *constant*. Therefore for AdS_n, (7.1) implies that

$$\boldsymbol{\beta}_{\mathrm{T}} \propto \cos\rho, \tag{7.2}$$

breaking the maximal symmetry previously enjoyed by the vacuum state, by clearly distinguishing a privileged origin [3] at which radiation will pool. The resulting distribution of radiation in thermal equilibrium vanishes at spatial infinity and therefore does not require the imposition of the reflective boundary conditions (2.23) [51] to prevent leakage at spatial infinity.

The thermal expectation values computed in this chapter are expectation values relative to the vacuum expectation values discussed in chapter 5

7.2 Thermal Green functions

Thermal Green functions are the state-dependent Green functions of the scalar field in thermodynamic equilibrium, with inverse (non-zero) temperature $\boldsymbol{\beta}$. The form of such thermal expectation values hinges on the fact that the related field configuration is appropriately described by a Bose-Einstein distribution of states $\left|\boldsymbol{\beta}_j\right\rangle$,

($j = 1, 2, \ldots$). Since the particle number for fluctuations is not conserved, this distribution is simplified as the chemical potential vanishes.

The Hamiltonian $\mathcal{H}$ of the thermal state space has the spectrum $\{\omega_j\}$ which may be obtained via the usual eigenvalue equation,

$$\mathcal{H} \left|\boldsymbol{\beta}_j\right\rangle = \omega_j \left|\boldsymbol{\beta}_j\right\rangle . \tag{7.3}$$

The explicitly indexed notation of the energy eigenvalues ω_j appears temporarily for clarity, with the understanding that $\omega_j = \omega$.

Given their statistical nature, thermal states are represented by *mixed* states $|\boldsymbol{\beta}\rangle$, which may be thought of as probability distributions of all possible pure states weighted by ϱ_j forming a partition of unity. The probability of the field lying in the state $\left|\boldsymbol{\beta}_j\right\rangle$ is therefore

$$\varrho_j = Z^{-1} e^{-\boldsymbol{\beta}\omega_j}, \tag{7.4}$$

where

$$Z = \sum_j e^{-\boldsymbol{\beta}\omega_j}, \tag{7.5}$$

is the canonical partition function.

In view of (7.3), the probability (7.4) is also the diagonal matrix element of the operator representation of the mixed state $|\boldsymbol{\beta}\rangle$, i.e.

$$\varrho_j = \langle \boldsymbol{\beta}_j \left|\varrho\right| \boldsymbol{\beta}_j \rangle, \qquad \varrho = Z^{-1} e^{-\boldsymbol{\beta}\mathcal{H}}. \tag{7.6}$$

It then follows that the thermal expectation value of an operator O is the ensemble

average

$$\langle O\rangle_{\boldsymbol{\beta}} := \langle \boldsymbol{\beta}\,|O|\,\boldsymbol{\beta}\rangle = Z^{-1}\sum_j \varrho_j \langle \boldsymbol{\beta}_j\,|O|\,\boldsymbol{\beta}_j\rangle$$
$$= Z^{-1}\,\mathrm{tr}\{\varrho O\}. \tag{7.7}$$

Thus the *thermal* Wightman functions $G^{\boldsymbol{\beta}}_{\pm}(x,x')$, may be expressed as

$$G^{\boldsymbol{\beta}}_{+}\left(t',\underline{x}';t,\underline{x}\right) = \langle\boldsymbol{\beta}|\,\Phi\left(t,\underline{x}\right)\Phi\left(t',\underline{x}'\right)|\boldsymbol{\beta}\rangle = Z^{-1}\,\mathrm{tr}\left\{\Phi\left(t,\underline{x}\right)\Phi\left(t',\underline{x}'\right)e^{-\boldsymbol{\beta}\mathcal{H}}\right\}, \tag{7.8}$$

$$G^{\boldsymbol{\beta}}_{-}\left(t,\underline{x};t',\underline{x}'\right) = \langle\boldsymbol{\beta}|\,\Phi\left(t',\underline{x}'\right)\Phi\left(t,\underline{x}\right)|\boldsymbol{\beta}\rangle = Z^{-1}\,\mathrm{tr}\left\{\Phi\left(t',\underline{x}'\right)\Phi\left(t,\underline{x}\right)e^{-\boldsymbol{\beta}\mathcal{H}}\right\}. \tag{7.9}$$

Exploiting Heisenberg's equations of evolution

$$\Phi\left(t,\underline{x}\right) = e^{\boldsymbol{i}\mathcal{H}(t-t'')}\Phi\left(t'',\underline{x}\right)e^{-\boldsymbol{i}\mathcal{H}(t-t'')}, \tag{7.10}$$

and the cyclic property of the trace in (7.8) and (7.9) leads to

$$G^{\boldsymbol{\beta}}_{\pm}\left(t,\underline{x};t',\underline{x}'\right) = G^{\boldsymbol{\beta}}_{\mp}\left(t\pm\boldsymbol{i}\boldsymbol{\beta},\underline{x};t',\underline{x}'\right). \tag{7.11}$$

For the discrete case of $CAdS_n$ the respective Fourier decompositions of the commutator (4.15), the anti-commutator (4.8) and the thermal Wightman functions (7.8 – 7.9) are

$$\boldsymbol{i}G(x,x') = \sum_{\omega>0}\left\{\boldsymbol{c}(+)e^{-\boldsymbol{i}\omega(\tau-\tau')} + \boldsymbol{c}(-)e^{\boldsymbol{i}\omega(\tau-\tau')}\right\}, \tag{7.12}$$

$$G_{(1)}(x,x') = \sum_{\omega>0}\left\{\boldsymbol{c}_{(1)}(+)e^{-\boldsymbol{i}\omega(\tau-\tau')} + \boldsymbol{c}_{(1)}(-)e^{\boldsymbol{i}\omega(\tau-\tau')}\right\}, \tag{7.13}$$

$$G^{\boldsymbol{\beta}}_{\pm}(x,x') = \sum_{\omega>0}\left\{\boldsymbol{c}^{\boldsymbol{\beta}}_{\pm}(+)e^{-\boldsymbol{i}\omega(\tau-\tau')} + \boldsymbol{c}^{\boldsymbol{\beta}}_{\pm}(-)e^{\boldsymbol{i}\omega(\tau-\tau')}\right\}, \tag{7.14}$$

with respective Fourier coefficients $\boldsymbol{c}(\pm)$, $\boldsymbol{c}_{(1)}(\pm)$, and $\boldsymbol{c}^{\boldsymbol{\beta}}_{\pm}(\pm)$ where,

$$f(\pm) := f(\pm\omega; \underline{x}, \underline{x}'), \tag{7.15}$$

and the notation ω for the energy levels has been reinstated.

Applying the addition theorem (2.110) to the expansion of the anti-commutator function (6.4) gives

$$G_{(1)}(x, x') = \sum_{\ell,\, r} N \left(e^{\boldsymbol{i}\omega(\tau-\tau')} + e^{-\boldsymbol{i}\omega(\tau-\tau')} \right) rr' C^{\alpha}_{\ell}(z)\,, \qquad n \geq 3, \tag{7.16}$$

where

$$z \overset{(7.16)}{\longmapsto} \hat{x} \cdot \hat{x}', \tag{7.17}$$

$$\alpha \overset{(7.16)}{\longmapsto} \frac{n-3}{2}, \tag{7.18}$$

and

$$N := \begin{cases} \dfrac{\Gamma\left(\frac{n-1}{2}\right)}{2\pi^{\frac{n-1}{2}}} \dfrac{2\ell + n - 3}{n-3} \left| N_{r\ell} \right|^2, & n \geq 4, \qquad \text{(7.19a)} \\[2ex] \dfrac{1}{\pi} \left| N_{r\ell} \right|^2, & n = 3. \qquad \text{(7.19b)} \end{cases}$$

It follows that the thermal commutator function given by,

$$G(x, x') = -\boldsymbol{i} \left\langle \boldsymbol{\beta} \right| \left[\Phi(x), \Phi(x') \right] \left| \boldsymbol{\beta} \right\rangle, \tag{7.20}$$

may also be expressed explicitly as

$$G(x, x') = -\boldsymbol{i} \sum_{\ell,\, r} N \left(e^{\boldsymbol{i}\omega(\tau-\tau')} - e^{-\boldsymbol{i}\omega(\tau-\tau')} \right) rr' C^{\alpha}_{\ell}(z)\,, \qquad n \geq 3. \tag{7.21}$$

Since the commutation relations for the free scalar field mean that the associated commutator function is a c-number and is therefore state-independent, then

$$G(x,x') = G^{\boldsymbol{\beta}}(x,x'). \tag{7.22}$$

As

$$\boldsymbol{i}G(x,x') = G_{+}(x,x') - G_{-}(x,x'), \tag{7.23}$$

$$G_{(1)}(x,x') = G_{+}(x,x') + G_{-}(x,x'), \tag{7.24}$$

then

$$\boldsymbol{i}G^{\boldsymbol{\beta}}(x,x') = G^{\boldsymbol{\beta}}_{+}(x,x') - G^{\boldsymbol{\beta}}_{-}(x,x'), \tag{7.25}$$

$$G^{\boldsymbol{\beta}}_{(1)}(x,x') = G^{\boldsymbol{\beta}}_{+}(x,x') + G^{\boldsymbol{\beta}}_{-}(x,x'). \tag{7.26}$$

Therefore,

$$\boldsymbol{ic} = \boldsymbol{c}^{\boldsymbol{\beta}}_{+} - \boldsymbol{c}^{\boldsymbol{\beta}}_{-}. \tag{7.27}$$

$$\boldsymbol{c}^{\boldsymbol{\beta}}_{(1)} = \boldsymbol{c}^{\boldsymbol{\beta}}_{+} + \boldsymbol{c}^{\boldsymbol{\beta}}_{-}. \tag{7.28}$$

Furthermore, given (7.11),

$$\boldsymbol{ic}(\pm) = \pm\left(e^{\boldsymbol{\beta}\omega} - 1\right)\boldsymbol{c}^{\boldsymbol{\beta}}_{\mp}(\pm). \tag{7.29}$$

Therefore we have

$$\boldsymbol{c}^{\boldsymbol{\beta}}_{(1)} = \frac{\boldsymbol{c}_{(1)}}{e^{\boldsymbol{\beta}\omega} - 1}. \tag{7.30}$$

which finally gives the thermal anti-commutator function, defined as the difference

between the anti-commutator functions of zero and finite temperature states:

$$G^{\boldsymbol{\beta}}_{(1)}(x,x') = \sum_{\ell,\,r} N^{\boldsymbol{\beta}} \left(e^{\boldsymbol{i}\omega(\tau-\tau')} + e^{-\boldsymbol{i}\omega(\tau-\tau')} \right) rr' C^{\alpha}_{\ell}(z)\,, \qquad n \geq 3, \tag{7.31}$$

where

$$N^{\boldsymbol{\beta}} := \frac{N}{e^{\boldsymbol{\beta}\omega} - 1}. \tag{7.32}$$

7.3 Thermal quadratic field fluctuations

The thermal expectation value of the quadratic field fluctuations is found by evaluating (7.31) in the coincidence limit, yielding

$$\begin{aligned} \langle \Phi^2(x) \rangle^{\boldsymbol{\beta}} &= \lim_{x' \to x} G^{\boldsymbol{\beta}}_{(1)}(x,x') \\ &= 2 \sum_{\ell,\,r} N^{\boldsymbol{\beta}} r^2 C^{\alpha}_{\ell}(1)\,, \qquad n \geq 3. \end{aligned} \tag{7.33}$$

The expression on the right-hand side of (7.33) has been evaluated numerically using code written in MATHEMATICA. In summary, the objects evaluated are approximations based on explicit forms of (7.33). Recalling (3.58), (3.88) and (3.61) (with $\not{k} \mapsto k$), these expressions are given by

$$\begin{aligned} \langle \Phi^2(\rho) \rangle^{\boldsymbol{\beta}} = \frac{\Gamma\left(\frac{n-1}{2}\right)}{(n-3)!\pi^{\frac{n-1}{2}} a^{n-2}} \sum_{\ell} \frac{(2\ell+n-3)(\ell+n-4)!}{\ell!} \\ \times \sum_{r} \frac{1}{e^{\boldsymbol{\beta}(k+2r+\ell)} - 1} \left| N_{r\ell} \right|^2 r^2(\rho), \qquad n \geq 4; \end{aligned} \tag{7.34}$$

$$\langle \Phi^2(\rho) \rangle^{\boldsymbol{\beta}} = \frac{2}{\pi a} \sum_{\ell} \epsilon_{\ell} \sum_{r} \frac{1}{e^{\boldsymbol{\beta}(k+2r+\ell)} - 1} \left| N_{r\ell} \right|^2 r^2(\rho), \qquad n = 3, \tag{7.35}$$

where the definition

$$\epsilon_{\ell} := \begin{cases} \frac{2}{\ell}, & \ell > 0, \quad (7.36a) \\ 1, & \ell = 0, \quad (7.36b) \end{cases}$$

has been made to reflect the properties of the Gegenbauer polynomial in the coincidence limit (see (2.113) and (2.114)).

Essentially, the numerical approximation of (7.34) and (7.35) relies on the determination of the upper bounds $\ell_{\max}$ and $r_{\max}$ of the infinite summations over ℓ and r respectively, such that precision reaches a user-defined, predetermined threshold δ.

The Planck factor present in thermal expectation values inhibits simplification by mixing the summation variables in the exponential term, such that (7.34) and (7.35) are inseparable in these variables. This represents a double-edged sword. Inevitably, this mixing forces a numerical approach that is overwhelmingly sensitive to $\boldsymbol{\beta}$. By the same token though, the Planck factor furnishes a single, overriding agent for a rapid (and stable) convergence, which in turn ensures tractable evaluation.

With this in mind, preliminary analyses revealed an approximate practical working range of $\boldsymbol{\beta} \in [1, 10]$, which is more than sufficient to gain some useful qualitative insight into the behaviour of $\langle \Phi^2(\rho) \rangle^{\boldsymbol{\beta}}$ as a function of the parameters ρ, μ, $\boldsymbol{\beta}$, n and specific combinations of interest. Accordingly a representative selection of profiles follows, accompanied by discussion/observations.

Figure 7.1 gives the radial profiles of $\langle \Phi^2(\rho) \rangle^{\boldsymbol{\beta}}$ for different values of n with μ corresponding to the massless, minimally-coupled case

$$\mu_{\text{mm}} := \mu, \qquad m = 0, \, \xi = 0. \quad (7.37)$$

The effect of the Planck factor and the Tolman relation (7.2) is evident from the

plot. For a given n, the value of $\langle\Phi^2(\rho)\rangle^{\boldsymbol{\beta}}$ is strictly positive and maximal at the origin. Physically, this profile is expected as it suggests an accumulation of thermal radiation at the origin, and a vanishing field at spatial infinity.

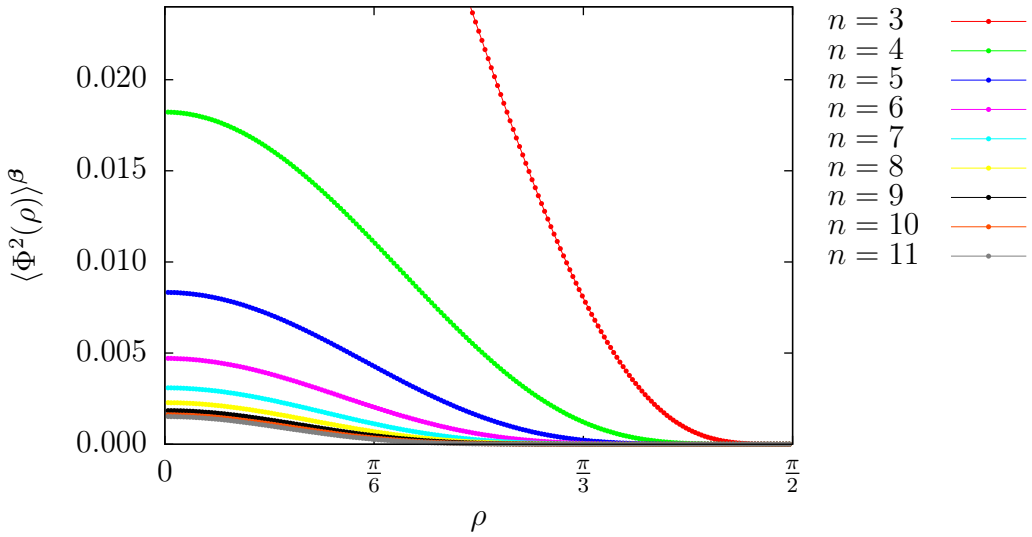

FIGURE 7.1 – $\langle\Phi^2(\rho)\rangle^{\boldsymbol{\beta}}$ for varying n with $\mu = \mu_{\text{mm}}$, $a = \boldsymbol{\beta} = 1$

Figures 7.2 and 7.3 are semi-log plots showing the effect of varying $\boldsymbol{\beta}$ on radial profiles for $n = 6$ and $n = 7$ respectively. Once again, the maxima at the origin and the vanishing at spatial infinity are suggestive of the Tolman relation (7.2).

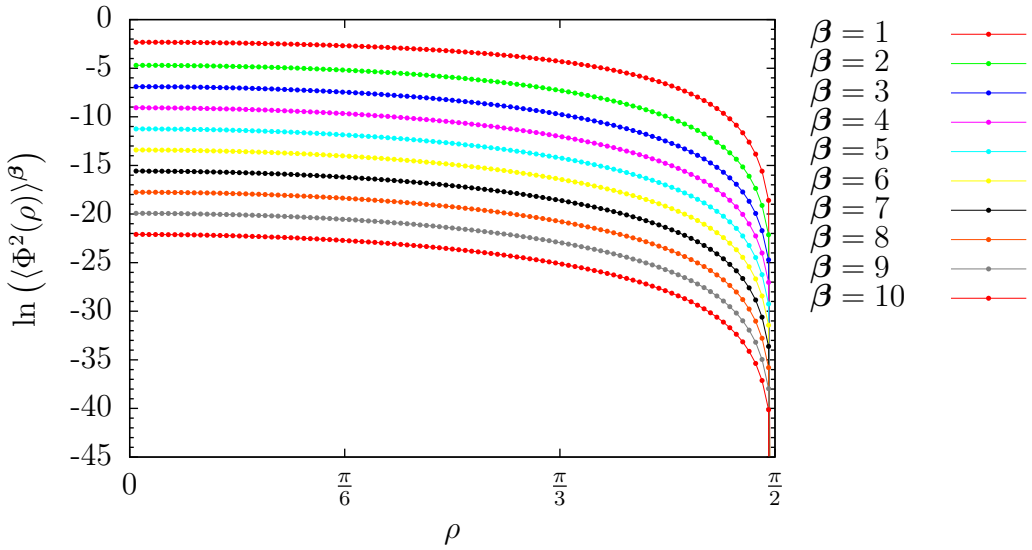

FIGURE 7.2 – $\ln\left(\langle\Phi^2(\rho)\rangle^{\boldsymbol{\beta}}\right)$ for $n = 6$ with $\mu = \mu_{\text{mm}}$, and varying $\boldsymbol{\beta}$

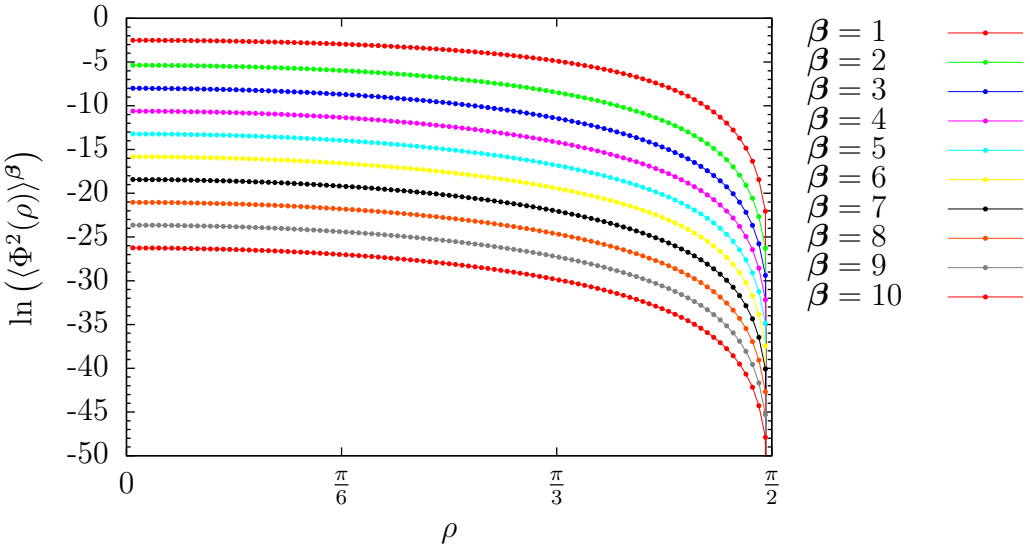

FIGURE 7.3 – $\ln\left(\langle\Phi^2(\rho)\rangle^{\boldsymbol{\beta}}\right)$ for $n = 7$ with $\mu = \mu_{\text{mm}}$, and varying $\boldsymbol{\beta}$

Finally figure 7.4 overleaf displays the dependence of $\langle\Phi^2(\rho)\rangle^{\boldsymbol{\beta}}$ on μ, (for the particular value of $\rho = \frac{\pi}{4}$). The general behaviour is an exponential decay from $\mu = 0$, which is expected from the presence of μ in the Planck factor. The value of $\langle\Phi^2(\rho)\rangle^{\boldsymbol{\beta}}$ is seen to increase with increasing n, a feature most visible at $\mu = 0$.

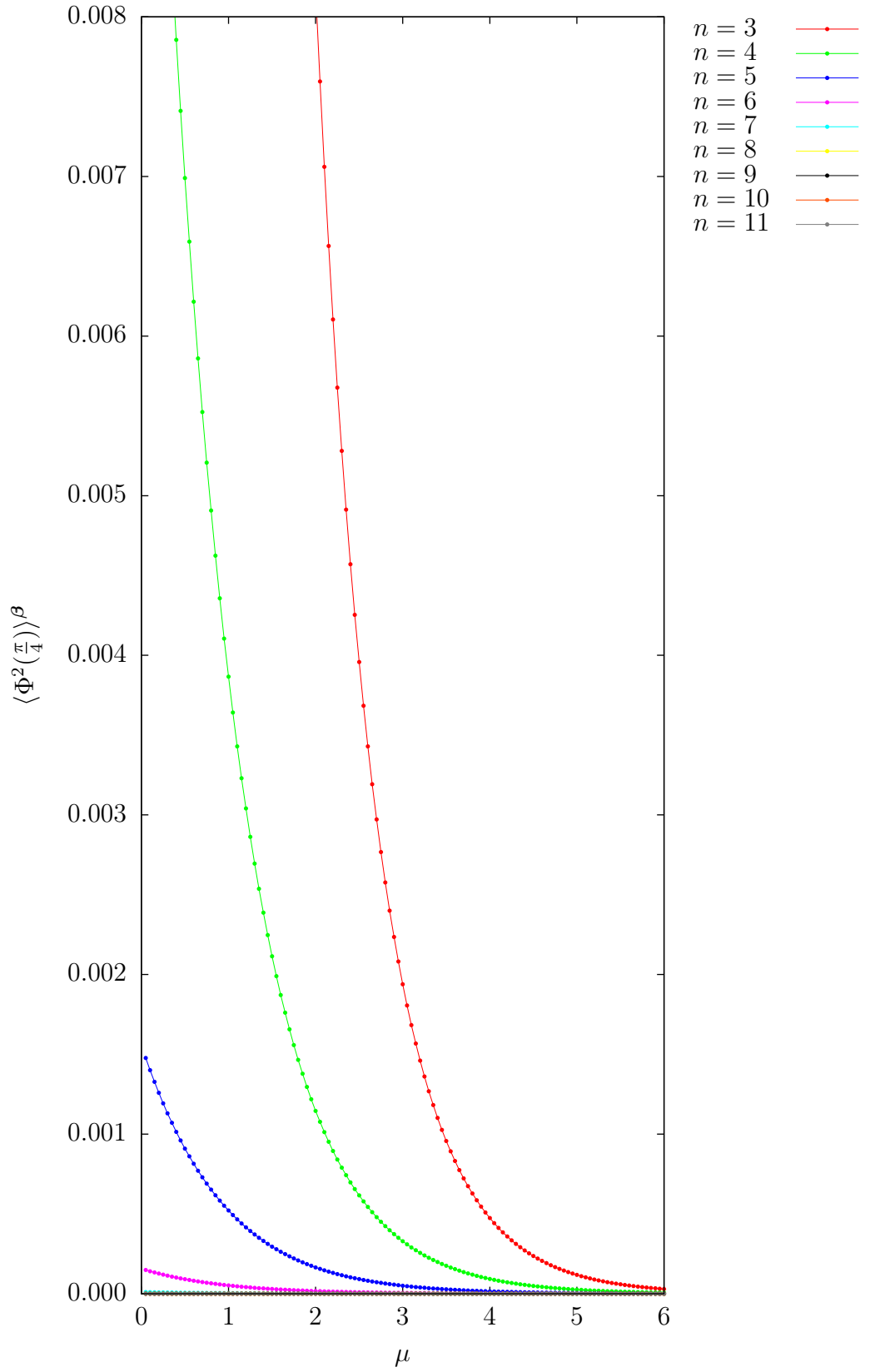

Figure 7.4 – $\langle\Phi^2(\frac{\pi}{4})\rangle^{\beta}$ for varying n and μ with $a = \beta = 1$

7.4 Thermal stress-energy tensor

7.4.1 Components

A scalar field in AdS_n in thermal equilibrium suffers from a broken radial symmetry. Therefore the thermal expectation value of the stress-energy tensor is no longer simply proportional to the metric. Therefore, to verify that $\langle T_{\mu\nu}(\rho)\rangle^{\boldsymbol{\beta}}$ is conserved, it is necessary to explicitly compute its components.

The calculations throughout section 7.4 can apply to vacuum or thermal states. To allow for this fact and for clarity, the following temporary notation is adopted.

$$\text{if } |\boldsymbol{\psi}\rangle = \begin{cases} |\mathbf{0}\rangle\,, & \text{then} \quad \boldsymbol{N} := N, \quad T_{\mu\nu} := \langle T_{\mu\nu}\rangle_{\text{ren}}, & \text{(7.38a)} \\ |\boldsymbol{\beta}\rangle\,, & \text{then} \quad \boldsymbol{N} := N^{\boldsymbol{\beta}}, \quad T_{\mu\nu} := \langle T_{\mu\nu}\rangle^{\boldsymbol{\beta}}, & \text{(7.38b)} \end{cases}$$

Given (5.65) and the fact that

$$W(x,x') = \frac{1}{2\nu(n)} G_{(1)}(x,x'), \tag{7.39}$$

the components of $T_{\mu\nu}$ are constructed as linear combinations of w and the components of $w_{;\mu\nu}$, $g_{\mu\nu}\Box w$, $w_{\mu\nu}$ and $\mathcal{R}_{\mu\nu}$. Each of these ingredients is derived respectively below, leading to expressions for $T_{\tau\tau}$, $T_{\rho\rho}$ and $T_{\theta_i\theta_i}$.

From (5.59)

$$w = \frac{1}{\nu(n)} \sum_{\ell,\, r} \boldsymbol{N} C_\ell^\alpha(1)\, r^2, \tag{7.40}$$

which only depends on ρ. Therefore, its double covariant derivative has the form

$$w_{;\mu\nu} = w_{,\mu\nu} - \Gamma^\rho_{\mu\nu} w_{,\rho}, \tag{7.41}$$

resulting in

$$w_{;\tau\tau} = -\Gamma^{\rho}_{\tau\tau} w_{,\rho}, \tag{7.42}$$

$$w_{;\rho\rho} = w_{,\rho\rho} - \Gamma^{\rho}_{\rho\rho} w_{,\rho}, \tag{7.43}$$

$$w_{;\theta_i\theta_i} = -\Gamma^{\rho}_{\theta_i\theta_i} w_{,\rho}. \tag{7.44}$$

Now

$$w_{,\rho} = \frac{2}{\nu(n)} \sum_{\ell,\, r} \boldsymbol{N} C^{\alpha}_{\ell}(1)\, r r_{,\rho}, \tag{7.45}$$

$$w_{,\rho\rho} = \frac{2}{\nu(n)} \sum_{\ell,\, r} \boldsymbol{N} C^{\alpha}_{\ell}(1) \left[\left(r_{,\rho} \right)^2 + r_{,\rho\rho} r \right]. \tag{7.46}$$

Therefore the definition,

$$\mathcal{C} := r_{,\rho} r^{-1}, \tag{7.47}$$

gives the expressions,

$$w_{,\rho} = \frac{2}{\nu(n)} \sum_{\ell,\, r} \boldsymbol{N} C^{\alpha}_{\ell}(1)\, r^2\, \mathcal{C}, \tag{7.48}$$

$$w_{,\rho\rho} = \frac{2}{\nu(n)} \sum_{\ell,\, r} \boldsymbol{N} C^{\alpha}_{\ell}(1)\, r^2 \left[\mathcal{C}^2 + r_{,\rho\rho} r^{-1} \right]. \tag{7.49}$$

Furthermore, recalling (3.35 - 3.37) and with (6.7) in mind, it follows that

$$r_{,\rho\rho} + \mathcal{A} r_{,\rho} + \mathcal{B} r = 0, \tag{7.50}$$

leading to the results,

$$w_{,\rho\rho} = \frac{2}{\nu(n)} \sum_{\ell,\, r} \boldsymbol{N} C_\ell^\alpha(1)\, r^2 \left[\mathcal{C}^2 - \mathcal{A}\mathcal{C} - \mathcal{B}\right], \tag{7.51}$$

$$w_{;\tau\tau} = -\frac{2}{\nu(n)} \sum_{\ell,\, r} \boldsymbol{N} C_\ell^\alpha(1)\, r^2\, \mathcal{C} \tan\rho, \tag{7.52}$$

$$w_{;\rho\rho} = \frac{2}{\nu(n)} \sum_{\ell,\, r} \boldsymbol{N} C_\ell^\alpha(1)\, r^2 \left[\mathcal{C}^2 - \mathcal{A}\mathcal{C} - \mathcal{C}\tan\rho - \mathcal{B}\right], \tag{7.53}$$

$$w_{;\theta_i\theta_i} = -\frac{2}{\nu(n)} \sum_{\ell,\, r} \boldsymbol{N} C_\ell^\alpha(1)\, r^2\, \mathcal{C} \tan\rho \prod_{l=1}^{i-1} (\sin\theta_l)^2 . \tag{7.54}$$

Turning now to the calculation of $g_{\mu\nu}\Box w$,

$$\begin{aligned}
\Box w &= g^{\mu\nu} w_{;\mu\nu} \\
&= g^{\tau\tau} w_{;\tau\tau} + g^{\rho\rho} w_{;\rho\rho} + g^{\theta_i\theta_i} w_{;\theta_i\theta_i} \\
&= -g^{\tau\tau}\Gamma^\rho_{\tau\tau} w_{,\rho} + g^{\rho\rho} w_{,\rho\rho} - g^{\rho\rho}\Gamma^\rho_{\rho\rho} w_{,\rho} - g^{\theta_i\theta_i}\Gamma^\rho_{\theta_i\theta_i} w_{,\rho} \\
&= g^{\rho\rho} w_{,\rho\rho} - g^{\theta_i\theta_i}\Gamma^\rho_{\theta_i\theta_i} w_{,\rho} \\
&= g^{\rho\rho} w_{,\rho\rho} + (n-2) g^{\theta_i\theta_i} \tan\rho \prod_{l=1}^{i-1} (\sin\theta_l)^2\, w_{,\rho},
\end{aligned} \tag{7.55}$$

given that

$$g^{\tau\tau} = -g^{\rho\rho}, \tag{7.56}$$

$$\Gamma^\rho_{\tau\tau} = \Gamma^\rho_{\rho\rho}. \tag{7.57}$$

Hence,

$$g_{\tau\tau}\Box w = -w_{,\rho\rho} - \mathcal{A}w_{,\rho}$$

$$= -\frac{1}{\nu(n)}\sum_{\ell,\,r}\boldsymbol{N}C_\ell^\alpha(1)\,r^2\left[\mathcal{C}^2-\mathcal{B}\right], \tag{7.58}$$

$$g_{\rho\rho}\Box w = -g_{\tau\tau}\Box w, \tag{7.59}$$

$$g_{\theta_i\theta_i}\Box w = (\sin\rho)^2\prod_{l=1}^{i-1}(\sin\theta_l)^2\,w_{,\rho\rho} + (n-2)\tan\rho\prod_{l=1}^{i-1}(\sin\theta_l)^2\,w_{,\rho}$$

$$= \frac{2}{\nu(n)}\sum_{\ell,\,r}\boldsymbol{N}C_\ell^\alpha(1)\,r^2\Big\{(\sin\rho)^2\left[\mathcal{C}^2-\mathcal{A}\mathcal{C}-\mathcal{B}\right]$$

$$+(n-2)\,\mathcal{C}\tan\rho\Big\}\prod_{l=1}^{i-1}(\sin\theta_l)^2,$$

$$= \frac{2}{\nu(n)}\sum_{\ell,\,r}\boldsymbol{N}C_\ell^\alpha(1)\,r^2\,(\sin\rho)^2\left[\mathcal{C}^2-\mathcal{B}\right]\prod_{l=1}^{i-1}(\sin\theta_l)^2. \tag{7.60}$$

From (7.39):

$$W_{,\tau} = \frac{1}{2\nu(n)} \sum_{\ell,\, r} \boldsymbol{N} \boldsymbol{i} \omega \left(e^{\boldsymbol{i}\omega(\tau-\tau')} - e^{\boldsymbol{i}\omega(\tau-\tau')} \right) r r' C_\ell^\alpha(z) \tag{7.61}$$

$$W_{,\tau\tau} = -\frac{1}{2\nu(n)} \sum_{\ell,\, r} \boldsymbol{N} \omega^2 \left(e^{\boldsymbol{i}\omega(\tau-\tau')} + e^{\boldsymbol{i}\omega(\tau-\tau')} \right) r r' C_\ell^\alpha(z)\,, \tag{7.62}$$

$$W_{,\rho} = \frac{1}{2\nu(n)} \sum_{\ell,\, r} \boldsymbol{N} \left(e^{\boldsymbol{i}\omega(\tau-\tau')} + e^{-\boldsymbol{i}\omega(\tau-\tau')} \right) r_{,\rho} r' C_\ell^\alpha(z) \tag{7.63}$$

$$W_{,\rho\rho} = \frac{1}{2\nu(n)} \sum_{\ell,\, r} \boldsymbol{N} \left(e^{\boldsymbol{i}\omega(\tau-\tau')} + e^{-\boldsymbol{i}\omega(\tau-\tau')} \right) r_{,\rho\rho} r' C_\ell^\alpha(z)\,, \tag{7.64}$$

$$W_{,\theta_i} = \frac{1}{2\nu(n)} \sum_{\ell,\, r} \boldsymbol{N} \left(e^{\boldsymbol{i}\omega(\tau-\tau')} + e^{-\boldsymbol{i}\omega(\tau-\tau')} \right) r r' C_\ell^\alpha(z)_{,z}\, z_{,\theta_i} \tag{7.65}$$

$$\begin{aligned} W_{,\theta_i\theta_i} = \frac{1}{2\nu(n)} \sum_{\ell,\, r} \boldsymbol{N} \left(e^{\boldsymbol{i}\omega(\tau-\tau')} + e^{-\boldsymbol{i}\omega(\tau-\tau')} \right) r r' \\ \times \left[C_\ell^\alpha(z)_{,zz} \left(z_{,\theta_i}\right)^2 + C_\ell^\alpha(z)_{,z}\, z_{,\theta_i\theta_i} \right]. \end{aligned} \tag{7.66}$$

Before calculating the components of $w_{\mu\nu}$, the angular derivatives of W require some extra care before proceding to take limits. Considering,

$$\begin{aligned} z = &\cos\theta_1\cos\theta_1' + \sin\theta_1\sin\theta_1'\cos\theta_2\cos\theta_2' + \sin\theta_1\sin\theta_1'\sin\theta_2\sin\theta_2'\cos\theta_3\cos\theta_3' \\ &+ \ldots + \sin\theta_1\sin\theta_1'\ldots\sin\theta_{k-1}\sin\theta_{k-1}'\cos\theta_k\cos\theta_k' \\ &+ \ldots + \sin\theta_1\sin\theta_1'\ldots\sin\theta_{n-3}\sin\theta_{n-3}' \\ &\times\left(\cos\theta_{n-2}\cos\theta_{n-2}' + \sin\theta_{n-2}\sin\theta_{n-2}'\right), \end{aligned} \tag{7.67}$$

$$\begin{aligned} z_{,\theta_k} = &\sin\theta_1\sin\theta_1'\cdots(-\sin\theta_k\cos\theta_k' + \cos\theta_k\sin\theta_k' \\ &\times\left(\cos\theta_{k+1}\cos\theta_{k+1}' + \sin\theta_{k+1}\sin\theta_{k+1}'(\cdots\right. \\ &\left.\times\left(\cos\theta_{n-2}\cos\theta_{n-2}' + \sin\theta_{n-2}\sin\theta_{n-2}'\right)\right)\right), \end{aligned} \tag{7.68}$$

$$\begin{aligned} z_{,\theta_k\theta_k} = &\sin\theta_1\sin\theta_1'\cdots(-\cos\theta_k\cos\theta_k' - \sin\theta_k\sin\theta_k' \\ &\times\left(\cos\theta_{k+1}\cos\theta_{k+1}' + \sin\theta_{k+1}\sin\theta_{k+1}'(\cdots\right. \\ &\left.\times\left(\cos\theta_{n-2}\cos\theta_{n-2}' + \sin\theta_{n-2}\sin\theta_{n-2}'\right)\right)\right), \end{aligned} \tag{7.69}$$

it follows that

$$\begin{aligned} \lim_{x'\to x} z_{,\theta_i} = &\quad \prod_{l=1}^{i-1}(\sin\theta_l)^2\,(\cos\theta_k\sin\theta_k(1-1(1(\cdots(1))))) = 0, \\ \lim_{x'\to x} z_{,\theta_i\theta_i} = &-\prod_{l=1}^{i-1}(\sin\theta_l)^2\,(1(1(\cdots(1)))) = -\prod_{l=1}^{i-1}(\sin\theta_l)^2\,. \end{aligned} \tag{7.70}$$

Also, the Gegenbauer polynomials obey the second-order linear differential equation

given by formula §22.6.5 in [2],

$$\left(1-z^2\right) C_\ell^\alpha(z)_{,zz} - (2\alpha+1)\, z C_\ell^\alpha(z)_{,z} + \ell(\ell+2\alpha) C_\ell^\alpha(z) = 0, \tag{7.71}$$

yielding

$$C_\ell^\alpha(z)_{,z} = \mathcal{D}\, C_\ell^\alpha(z)\,, \qquad x' \to x, \tag{7.72}$$

where

$$\mathcal{D} := \frac{\ell(\ell+2\alpha)}{2\alpha+1}. \tag{7.73}$$

Therefore,

$$\lim_{x'\to x} W_{,\tau} = 0, \tag{7.74}$$

$$\lim_{x'\to x} W_{,\tau\tau} = -\frac{1}{\nu(n)} \sum_{\ell,\, r} \boldsymbol{N} C_\ell^\alpha(1)\, r^2 \omega^2. \tag{7.75}$$

$$\lim_{x'\to x} W_{,\rho} = \quad \frac{1}{\nu(n)} \sum_{\ell,\, r} \boldsymbol{N} C_\ell^\alpha(1)\, r^2\, \mathcal{C}, \tag{7.76}$$

$$\lim_{x'\to x} W_{,\rho\rho} = -\frac{1}{\nu(n)} \sum_{\ell,\, r} \boldsymbol{N} C_\ell^\alpha(1)\, r^2 [\mathcal{A}\mathcal{C} + \mathcal{B}]. \tag{7.77}$$

$$\lim_{x'\to x} W_{,\theta_i} = 0, \tag{7.78}$$

$$\lim_{x'\to x} W_{,\theta_i\theta_i} = -\frac{1}{\nu(n)} \sum_{\ell,\, r} \boldsymbol{N} C_\ell^\alpha(1)\, r^2\, \mathcal{D} \prod_{l=1}^{i-1} (\sin\theta_l)^2\,. \tag{7.79}$$

Now given that

$$w_{\mu\nu} = \lim_{x'\to x} \left[W_{,\mu\nu} - \Gamma^\sigma_{\mu\nu} W_{,\sigma} \right], \tag{7.80}$$

where

$$\Gamma^\tau_{\tau\tau} = \Gamma^{\theta_i}_{\tau\tau} = \Gamma^\tau_{\rho\rho} = \Gamma^{\theta_i}_{\rho\rho} = \Gamma^\tau_{\theta_i\theta_i} = \Gamma^{\theta_i}_{\theta_i\theta_i} = 0, \tag{7.81}$$

it follows that

$$w_{\tau\tau} = \lim_{x'\to x}\left[W_{,\tau\tau} - \Gamma^{\rho}_{\tau\tau}W_{,\rho}\right]$$

$$= -\frac{1}{\nu(n)}\sum_{\ell,\,r}\boldsymbol{N}C^{\alpha}_{\ell}(1)\,r^2\left[\omega^2 + \mathcal{C}\tan\rho\right]. \tag{7.82}$$

$$w_{\rho\rho} = \lim_{x'\to x}\left[W_{,\rho\rho} - \Gamma^{\rho}_{\rho\rho}W_{,\rho}\right]$$

$$= -\frac{1}{\nu(n)}\sum_{\ell,\,r}\boldsymbol{N}C^{\alpha}_{\ell}(1)\,r^2\left[\mathcal{A}\mathcal{C} + \mathcal{B} + \mathcal{C}\tan\rho\right]. \tag{7.83}$$

$$w_{\theta_i\theta_i} = \lim_{x'\to x}\left[W_{,\theta_i\theta_i} - \Gamma^{\rho}_{\theta_i\theta_i}W_{,\rho}\right]$$

$$= -\frac{1}{\nu(n)}\sum_{\ell,\,r}\boldsymbol{N}C^{\alpha}_{\ell}(1)\,r^2\left[\mathcal{D} - \mathcal{C}\tan\rho\right]\prod_{l=1}^{i-1}\left(\sin\theta_l\right)^2. \tag{7.84}$$

Finally, the Ricci tensor components can be found using

$$\mathcal{R}_{\mu\nu} = -a^{-2}(n-1)g_{\mu\nu}, \tag{7.85}$$

where the metric components can be found from (2.10) to give

$$\mathcal{R}_{\tau\tau} = (n-1)(\sec\rho)^2, \tag{7.86}$$

$$\mathcal{R}_{\rho\rho} = -\mathcal{R}_{\tau\tau}, \tag{7.87}$$

$$\mathcal{R}_{\theta_i\theta_i} = -(n-1)(\tan\rho)^2\prod_{l=1}^{i-1}\left(\sin\theta_l\right)^2. \tag{7.88}$$

Now let

$$T_{\tau\tau} = \sum_{\ell,\, r} \boldsymbol{N} C_\ell^\alpha(1)\, r^2 t_{\tau\tau}, \tag{7.89}$$

$$T_{\rho\rho} = \sum_{\ell,\, r} \boldsymbol{N} C_\ell^\alpha(1)\, r^2 t_{\rho\rho}, \tag{7.90}$$

$$T_{\theta_i\theta_i} = \sum_{\ell,\, r} \boldsymbol{N} C_\ell^\alpha(1)\, r^2 t_{\theta_i\theta_i} \prod_{l=1}^{i-1} (\sin\theta_l)^2\,, \tag{7.91}$$

where

$$\begin{aligned} t_{\tau\tau} &= \omega^2 + \mathcal{C}\tan\rho - (1-2\xi)\,\mathcal{C}\tan\rho - \left(2\xi - \frac{1}{2}\right)\left[\mathcal{C}^2 - \mathcal{B}\right] + \xi(n-1)(\sec\rho)^2 \\ &= 2\xi\left[\mathcal{C}\tan\rho - \mathcal{C}^2 + \mathcal{B} + \frac{n-1}{2}(\sec\rho)^2\right] + \omega^2 + \frac{1}{2}\left[\mathcal{C}^2 - \mathcal{B}\right], \end{aligned} \tag{7.92}$$

$$\begin{aligned} t_{\rho\rho} &= \mathcal{A}\mathcal{C} + \mathcal{B} + \mathcal{C}\tan\rho + (1-2\xi)\left[\mathcal{C}^2 - \mathcal{A}\mathcal{C} - \mathcal{C}\tan\rho - \mathcal{B}\right] \\ &\quad + \left(2\xi - \frac{1}{2}\right)\left[\mathcal{C}^2 - \mathcal{B}\right] - \xi(n-1)(\sec\rho)^2 \\ &= 2\xi\left[\mathcal{A}\mathcal{C} + \mathcal{C}\tan\rho - \frac{n-1}{2}(\sec\rho)^2\right] + \frac{1}{2}\left[\mathcal{C}^2 + \mathcal{B}\right], \end{aligned} \tag{7.93}$$

$$\begin{aligned} t_{\theta_i\theta_i} &= \mathcal{D} - \mathcal{C}\tan\rho + (1-2\xi)\,\mathcal{C}\tan\rho \\ &\qquad + \left(2\xi - \frac{1}{2}\right)(\sin\rho)^2\left[\mathcal{C}^2 - \mathcal{B}\right] - \xi(n-1)(\tan\rho)^2 \\ &= 2\xi\left\{(\sin\rho)^2\left[\mathcal{C}^2 - \mathcal{B}\right] - \mathcal{C}\tan\rho - \frac{n-1}{2}(\tan\rho)^2\right\} \\ &\qquad + \mathcal{D} - \frac{1}{2}(\sin\rho)^2\left[\mathcal{C}^2 - \mathcal{B}\right]. \end{aligned} \tag{7.94}$$

7.4.2 Conservation

The conservation of $T_{\mu\nu}$ is a direct consequence of the scalar field wave equation (3.4). As a supplementary consistency check this property can be verified explicitly by evaluating the right-hand side of each of the n equations,

$$T_{\mu\nu}{}^{;\mu} = g^{\mu\lambda}\left(T_{\mu\nu,\lambda} - \Gamma^{\sigma}_{\mu\lambda}T_{\sigma\nu} - \Gamma^{\sigma}_{\nu\lambda}T_{\sigma\mu}\right), \tag{7.95}$$

individually. To do so requires a knowledge of the metric elements in (2.10), the non-zero Christoffel connections (2.11 - 2.16), and the components of $T_{\mu\nu}$ (7.89 - 7.94), stated at the end of the previous section.

With these relations in hand, when $\nu = \tau$

$$\begin{aligned} T_{\mu\tau}{}^{;\mu} &= g^{\mu\lambda}\left(T_{\mu\tau,\lambda} - \Gamma^{\sigma}_{\mu\lambda}T_{\sigma\tau} - \Gamma^{\sigma}_{\tau\lambda}T_{\sigma\mu}\right) \\ &= g^{\tau\tau}T_{\tau\tau,\tau} - g^{\mu\lambda}\Gamma^{\tau}_{\mu\lambda}T_{\tau\tau} - g^{\mu\lambda}\Gamma^{\sigma}_{\tau\lambda}T_{\sigma\mu} \\ &= g^{\tau\tau}T_{\tau\tau,\tau}, \end{aligned} \tag{7.96}$$

and as $t_{\tau\tau}$ depends on ρ alone,

$$T_{\mu\tau}{}^{;\mu} = 0. \tag{7.97}$$

When $\nu = \rho$,

$$\begin{aligned} T_{\mu\rho}{}^{;\mu} &= g^{\mu\lambda}\left(T_{\mu\rho,\lambda} - \Gamma^{\sigma}_{\mu\lambda}T_{\sigma\rho} - \Gamma^{\sigma}_{\rho\lambda}T_{\sigma\mu}\right) \\ &= g^{\rho\rho}T_{\rho\rho,\rho} - g^{\mu\lambda}\Gamma^{\rho}_{\mu\lambda}T_{\rho\rho} - g^{\mu\lambda}\Gamma^{\sigma}_{\rho\lambda}T_{\sigma\mu} \\ &= g^{\rho\rho}T_{\rho\rho,\rho} - g^{\tau\tau}\Gamma^{\rho}_{\tau\tau}T_{\rho\rho} - g^{\rho\rho}\Gamma^{\rho}_{\rho\rho}T_{\rho\rho} \\ &\quad - g^{\theta_i\theta_i}\Gamma^{\rho}_{\theta_i\theta_i}T_{\rho\rho} - g^{\tau\tau}\Gamma^{\tau}_{\rho\tau}T_{\tau\tau} - g^{\rho\rho}\Gamma^{\rho}_{\rho\rho}T_{\rho\rho} - g^{\theta_i\theta_i}\Gamma^{\rho}_{\theta_i\theta_i}T_{\theta_i\theta_i}, \end{aligned} \tag{7.98}$$

and given the relations (7.56) and (7.57),

$$g_{\rho\rho}T_{\mu\rho}{}^{;\mu} = T_{\rho\rho,\rho} + \Gamma^{\rho}_{\rho\rho}\left(T_{\tau\tau} - T_{\rho\rho}\right) - g_{\rho\rho}g^{\theta_i\theta_i}\left(\Gamma^{\rho}_{\theta_i\theta_i}T_{\rho\rho} + \Gamma^{\rho}_{\theta_i\theta_i}T_{\theta_i\theta_i}\right). \tag{7.99}$$

Recalling (7.47), consider

$$\left(r^2 t_{\rho\rho}\right)_{,\rho} = 2rr_{,\rho}t_{\rho\rho} + r^2 t_{\rho\rho,\rho} \tag{7.100}$$

$$= r^2\left[2\mathcal{C}t_{\rho\rho} + t_{\rho\rho,\rho}\right], \tag{7.101}$$

and so, from (7.99), each summand in (7.90) (multiplied by $r^{-2}g_{\rho\rho}$) can be written as

$$\begin{aligned} r^{-2}g_{\rho\rho}t_{\mu\rho}{}^{;\mu} &= t_{\rho\rho,\rho} + 2\mathcal{C}t_{\rho\rho} + \left(t_{\tau\tau} - t_{\rho\rho}\right)\tan\rho \\ &\quad -(n-2)(\operatorname{cosec}\rho)^2\left[-t_{\rho\rho}\tan\rho + t_{\theta_i\theta_i}\sec\rho\operatorname{cosec}\rho\right] \\ &= t_{\rho\rho,\rho} + 2\mathcal{C}t_{\rho\rho} + \left(t_{\tau\tau} - t_{\rho\rho}\right)\tan\rho + \mathcal{A}\left[t_{\rho\rho} + t_{\theta_i\theta_i}\operatorname{cosec}\rho\right]. \end{aligned} \tag{7.102}$$

The terms in $t_{\rho\rho,\rho}$ and $(t_{\tau\tau} - t_{\rho\rho})$ on the right-hand side of (7.102) are now found

from the relations (7.92) and (7.93), as the first steps towards the simplification of $T_{\mu\rho}{}^{;\mu}$. To begin with,

$$t_{\rho\rho,\rho} = 2\xi\left[\mathcal{A}_{,\rho}\mathcal{C} + \mathcal{A}\mathcal{C}_{,\rho} + \mathcal{C}(\sec\rho)^2 + \mathcal{C}_{,\rho}\tan\rho - (n-1)(\sec\rho)^2\tan\rho\right] + \mathcal{C}\mathcal{C}_{,\rho} + \frac{1}{2}\mathcal{B}_{,\rho}. \tag{7.103}$$

From the definitions of $\mathcal{C}$ and r, (equations (7.47) and (6.7) respectively),

$$\begin{aligned}\mathcal{C}_{,\rho} &= r_{,\rho\rho}r^{-1} - \left[r_{,\rho}r^{-1}\right]^2 \\ &= -\mathcal{A}\mathcal{C} - \mathcal{B} - \mathcal{C}^2.\end{aligned} \tag{7.104}$$

Therefore,

$$\begin{aligned}t_{\rho\rho,\rho} = 2\xi\Big[&\mathcal{A}_{,\rho}\mathcal{C} - \mathcal{A}^2\mathcal{C} - \mathcal{A}\mathcal{B} - \mathcal{A}\mathcal{C}^2 + \mathcal{C}(\sec\rho)^2 - \mathcal{A}\mathcal{C}\tan\rho - \mathcal{B}\tan\rho - \mathcal{C}^2\tan\rho \\ &-(n-1)(\sec\rho)^2\tan\rho\Big] + \mathcal{A}\mathcal{C}^2 - \mathcal{B}\mathcal{C} - \mathcal{C}^3 + \frac{1}{2}\mathcal{B}_{,\rho}.\end{aligned} \tag{7.105}$$

Subtracting (7.93) from (7.92),

$$t_{\tau\tau} - t_{\rho\rho} = 2\xi\left[-\mathcal{C}^2 - \mathcal{A}\mathcal{C} + \mathcal{B} + (n-1)(\sec\rho)^2\right] + \omega^2 - \mathcal{B}, \tag{7.106}$$

equation (7.102) now becomes

$$\begin{aligned}r^{-2}g_{\rho\rho}t_{\mu\rho}{}^{;\mu} &= t_{\rho\rho,\rho} + 2\mathcal{C}t_{\rho\rho} + \left(t_{\tau\tau} - t_{\rho\rho}\right)\tan\rho + \mathcal{A}\left[t_{\rho\rho} - t_{\theta_i\theta_i}(\operatorname{cosec}\rho)^2\right] \\ &= 2\xi\left[\mathcal{A}_{,\rho}\mathcal{C} - (n-2)\mathcal{C}(\sec\rho)^2 + \mathcal{A}\mathcal{C}\sec\rho\operatorname{cosec}\rho - \mathcal{A}\mathcal{C}\tan\rho\right] \\ &\quad + \omega^2\tan\rho - \mathcal{B}\tan\rho + \frac{1}{2}\mathcal{B}_{,\rho} - \mathcal{A}\mathcal{D}(\operatorname{cosec}\rho)^2.\end{aligned} \tag{7.107}$$

Next, recalling (3.36) and (3.37)

$$\mathcal{A}_{,\rho} = (n-2)\left[(\sec\rho)^2 + (\operatorname{cosec}\rho)^2\right], \tag{7.108}$$

$$\mathcal{B}_{,\rho} = -2a^2 m_\xi^2 (\sec\rho)^2 \tan\rho - 2\lambda(\operatorname{cosec}\rho)^2 \cot\rho. \tag{7.109}$$

Therefore

$$\begin{aligned} r^{-2} g_{\rho\rho} t_{\mu\rho}{}^{;\mu} &= 2\xi(n-2)\mathcal{C}(\sec\rho)^2 \left\{\left[1-(\cot\rho)^2\right] - 1 + (\operatorname{cosec}\rho)^2 - 1\right\} \\ &\quad + \omega^2\tan\rho + a^2 m_\xi^2 (\sec\rho)^2\tan\rho - \lambda(\operatorname{cosec}\rho)^2\tan\rho - \omega^2\tan\rho \\ &\quad - a^2 m_\xi^2 (\sec\rho)^2\tan\rho - \lambda(\operatorname{cosec}\rho)^2\cot\rho - \mathcal{A}\mathcal{D}(\operatorname{cosec}\rho)^2 \\ &= -(\operatorname{cosec}\rho)^2\left[\lambda(\tan\rho+\cot\rho) + \mathcal{A}\mathcal{D}\right] \\ &= -\sec\rho\operatorname{cosec}\rho\left\{\lambda\left[1+(\cot\rho)^2\right] + \mathcal{A}\mathcal{D}(\cot\rho)\right\}. \end{aligned} \tag{7.110}$$

Using (3.34) and

$$\mathcal{D} \overset{(7.17)}{\longmapsto} \frac{\ell(\ell+n-3)}{n-2}, \tag{7.111}$$

results in

$$\begin{aligned} r^{-2} g_{\rho\rho} t_{\mu\rho}{}^{;\mu} &= -\left\{-\ell(\ell+n-3)\left[(1+\cot\rho)^2\right] + \ell(\ell+n-3)(\operatorname{cosec}\rho)^2\right\}\sec\rho\operatorname{cosec}\rho \\ &= -\ell(\ell+n-3)\left[1+(\cot\rho)^2 - (\operatorname{cosec}\rho)^2\right]\sec\rho\operatorname{cosec}\rho \\ &= 0. \end{aligned} \tag{7.112}$$

Therefore, given (7.90)

$$T_{\mu\rho}{}^{;\mu} = 0. \tag{7.113}$$

Finally, when $\nu = \theta_i$,

$$\begin{aligned} T_{\mu\theta_i}{}^{;\mu} &= g^{\mu\lambda}\left(T_{\mu\theta_i,\lambda} - \Gamma^{\sigma}_{\mu\lambda}T_{\sigma\theta_i} - \Gamma^{\sigma}_{\theta_i\lambda}T_{\sigma\mu}\right) \\ &= g^{\theta_i\theta_i}T_{\theta_i\theta_i,\theta_i} - g^{\mu\lambda}\Gamma^{\theta_i}_{\mu\lambda}T_{\theta_i\theta_i} - g^{\mu\lambda}\Gamma^{\sigma}_{\theta_i\lambda}T_{\sigma\mu}. \\ &= g^{\theta_i\theta_i}T_{\theta_i\theta_i,\theta_i} - g^{\theta_j\theta_j}\Gamma^{\theta_i}_{\theta_j\theta_j}T_{\theta_i\theta_i} - g^{\theta_j\theta_j}\Gamma^{\theta_i}_{\theta_i\theta_j}T_{\theta_j\theta_j}. \end{aligned} \tag{7.114}$$

Recalling (7.94) and that $t_{\theta_i\theta_i}$ only depends on ρ,

$$-g_{\theta_j\theta_j}t_{\mu\theta_i}{}^{;\mu} = (n-2)\left[-\cot\theta_i\prod_{l=1}^{j-1}(\sin\theta_l)^2\,t_{\theta_i\theta_i} + (\cot\theta_i)\,t_{\theta_j\theta_j}\right]. \tag{7.115}$$

where

$$t_{\theta_j\theta_j} = \prod_{l=1}^{j-1}(\sin\theta_l)^2\,t_{\theta_i\theta_i}. \tag{7.116}$$

Therefore from (7.91),

$$T_{\mu\theta_i}{}^{;\mu} = 0. \tag{7.117}$$

7.4.3 Trace

In the massless, conformally coupled case,

$$m_\xi^2 := m^2_{\xi,\,\mathrm{mc}} = -\frac{n(n-2)}{4a^2}, \tag{7.118}$$

$$\mathcal{B} := \ \mathcal{B}_{\mathrm{mc}} \ = \frac{1}{4}n(n-2)(\sec\rho)^2 + \lambda(\mathrm{cosec}\,\rho)^2 + \omega^2, \tag{7.119}$$

(where the subscript 'mc' denotes 'massless, conformally-coupled'). Defining

$$\tilde{t}_{\mathrm{mc}\,\mu\nu} := 2a^2(n-1)t_{\mathrm{mc}\,\mu\nu}, \tag{7.120}$$

$$\tilde{\tilde{t}}_{\mathrm{mc}\,\mu}{}^{\mu} := \tilde{t}_{\mathrm{mc}\,\tau}{}^{\tau} + \tilde{t}_{\mathrm{mc}\,\rho}{}^{\rho} + \prod_{l=1}^{i-1} (\sin\theta_l)^2\, \tilde{t}_{\mathrm{mc}\,\theta_i}{}^{\theta_i}, \tag{7.121}$$

Examining each term on the right-hand side of (7.121), the following expressions are obtained:

$$\tilde{t}_{\mathrm{mc}\,\tau}{}^{\tau} = -(n-2)\mathcal{C}\sin\rho\cos\rho - \mathcal{C}^2(\cos\rho)^2 - \frac{1}{4}(n-2)^2$$
$$+\lambda(\cot\rho)^2 - (2n-3)\omega^2(\cos\rho)^2, \tag{7.122}$$

$$\tilde{t}_{\mathrm{mc}\,\rho}{}^{\rho} = (n-1)(\cos\rho)^2\mathcal{C}^2 + (n-2)^2\mathcal{C}\cot\rho + (n-2)\mathcal{C}\cos\rho\sin\rho$$
$$+(n-1)\lambda(\cot\rho)^2 + (n-1)\omega^2(\cos\rho)^2 + \frac{1}{4}(n-1)(n-2)^2, \tag{7.123}$$

$$\prod_{l=1}^{i-1} (\sin\theta_l)^2\, \tilde{t}_{\mathrm{mc}\,\theta_i}{}^{\theta_i} = -(n-2)(\cos\rho)^2\mathcal{C}^2 - (n-2)^2\mathcal{C}\cot\rho + (n-2)(\cot\rho)^2\lambda$$
$$+(n-2)(\cos\rho)^2\omega^2 + 2(n-1)(n-2)(\cot\rho)^2\mathcal{D} - \frac{1}{4}(n-2)^3. \tag{7.124}$$

Bearing in mind (7.89 – 7.91) and the relations (7.120 – 7.124),

$$T_{\mu}{}^{\mu} = \sum_{l,\,r} \boldsymbol{N} C_l^{\alpha}(1)\, r^2 2a^2(n-1)\tilde{\tilde{t}}_{\mu}{}^{\mu}, \tag{7.125}$$

and therefore that

$$\tilde{\tilde{t}}_{\mathrm{mc}\,\mu}{}^{\mu} = 2(n-1)(\cot\rho)^2[\lambda + (n-2)\mathcal{D}]. \tag{7.126}$$

Finally, recalling (3.34) and (7.111)

$$T_{\mathrm{mc}\ \mu}{}^{\mu} = 0. \tag{7.127}$$

This is as expected – the conformal anomaly for a thermal expectation value relative to the vacuum is zero.

7.4.4 Results

Plots of the physically meaningful components $\langle T_{\tau}{}^{\tau}(\rho)\rangle^{\boldsymbol{\beta}}$, $\langle T_{\rho}{}^{\rho}(\rho)\rangle^{\boldsymbol{\beta}}$ and $\langle T_{\theta_i}{}^{\theta_i}(\rho)\rangle^{\boldsymbol{\beta}}$ using (7.89 – 7.91) have been generated using code written in MATHEMATICA. Figures 7.5 – 7.7 show radial profiles of each component for $n = 4$ to $n = 11$. Figures 7.5 and 7.6 for $\langle T_{\tau}{}^{\tau}(\rho)\rangle^{\boldsymbol{\beta}}$ and $\langle T_{\rho}{}^{\rho}(\rho)\rangle^{\boldsymbol{\beta}}$ display the expected decay with increasing ρ.

For these plots the dependence on n is of interest. In the case of $\langle T_{\tau}{}^{\tau}(\rho)\rangle^{\boldsymbol{\beta}}$, there is a progression in the shape of each curve with increasing n. For low values of n, the minima are relatively low values compared with those at high n. Also this increase in values at the origin is monotonic with increasing n. As the profiles taper to zero, the lower their minima, the more rapid are their ascents to the $\langle T_{\tau}{}^{\tau}(\rho)\rangle^{\boldsymbol{\beta}} = 0$ axis.

For the radial profiles of $\langle T_{\rho}{}^{\rho}(\rho)\rangle^{\boldsymbol{\beta}}$, the description of their behaviour with increasing n can be made in similar terms. Here the pattern is slightly different. The maxima at the origin start off relatively high, but this time for *low* values of n with modest points of inflection. As n increases the maxima at the origin decrease until settling around $n = 8$ before beginning to rise again. As they do so, the points of inflection become more prominent.

The next set of plots in figures 7.8 – 7.10 show the behaviour of the components with respect to μ with a fixed value of ξ at a fixed value of ρ. In the cases of the

plots of $\langle T_{\rho}{}^{\rho}(\rho)\rangle^{\boldsymbol{\beta}}$ and $\langle T_{\theta_i}{}^{\theta_i}(\rho)\rangle^{\boldsymbol{\beta}}$, it is simply the overwhelming effect of the Planck factor on everything else inside the respective summations (7.90) and (7.91). For the angular component for $n = 3$, there appears to be a slight dip into negative values between approximately $\mu = 2$ and $\mu = 3.5$.

In the case of figure 7.8, the situation is qualitatively similar, with the exception that the profiles suggest that

$$\left.\frac{d}{d\mu}\right|_{\mu=0} \langle T_{\tau}{}^{\tau}(\rho)\rangle^{\boldsymbol{\beta}} > 0, \tag{7.128}$$

briefly.

Finally, figures 7.11 – 7.13 show the behaviour of $\langle T_{\nu}{}^{\nu}(\rho)\rangle^{\boldsymbol{\beta}}$ for $n = 4$, $a = 1$, $\mu = \mu_{\mathrm{mc}}$ with varying $\boldsymbol{\beta}$ – a case also studied by Allen, Folacci & Gibbons [3]. The data for each component are presented in semi-log plots; all of which exhibit the Tolman relation through the observed decay from the origin and vanishing at spatial infinity.

In the case of $\langle T_{\tau}{}^{\tau}(\rho)\rangle^{\boldsymbol{\beta}}$ and $\langle T_{\theta_i}{}^{\theta_i}(\rho)\rangle^{\boldsymbol{\beta}}$, the data have been manipulated to aid comparison of behaviour at different $\boldsymbol{\beta}$ by taking the logarithm of the absolute values of these components. In the angular case, there are noticeable discontinuities in each of the profiles. The 'bounces' that follow these discontinuities correspond to when the decay of $\langle T_{\theta_i}{}^{\theta_i}(\rho)\rangle^{\boldsymbol{\beta}}$ dips briefly into negative values before rising again to zero at spatial infinity.

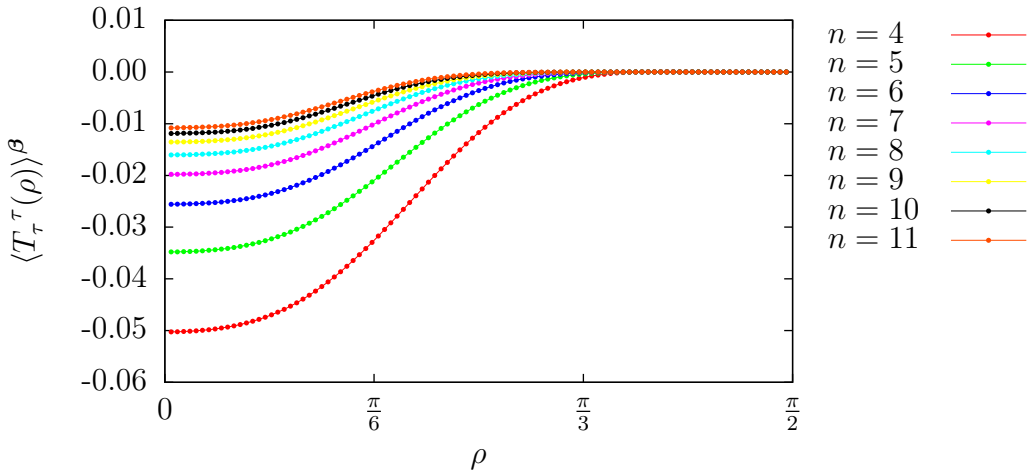

Figure 7.5 – $\langle T_\tau{}^\tau(\rho)\rangle^{\boldsymbol{\beta}}$ for varying n with $\mu = \mu_{\text{mc}}$ and $a = \boldsymbol{\beta} = 1$

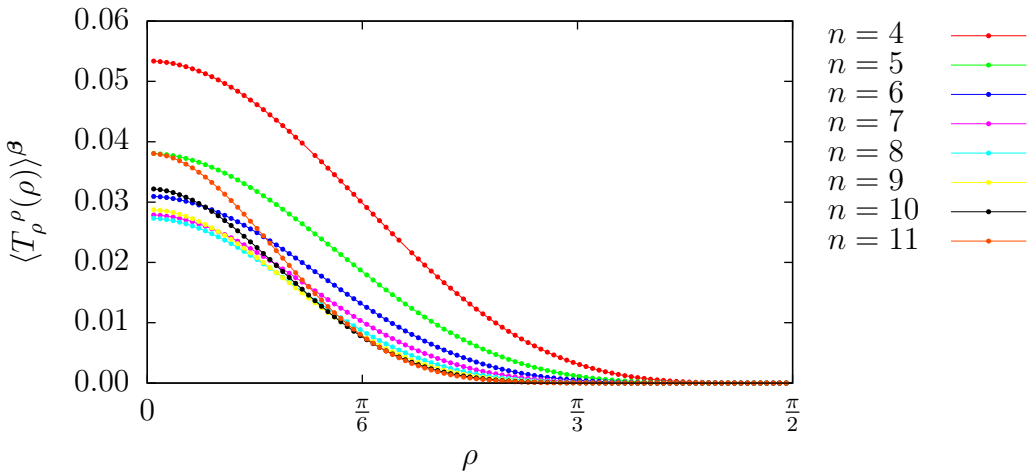

Figure 7.6 – $\langle T_\rho{}^\rho(\rho)\rangle^{\boldsymbol{\beta}}$ for varying n with $\mu = \mu_{\text{mc}}$ and $a = \boldsymbol{\beta} = 1$

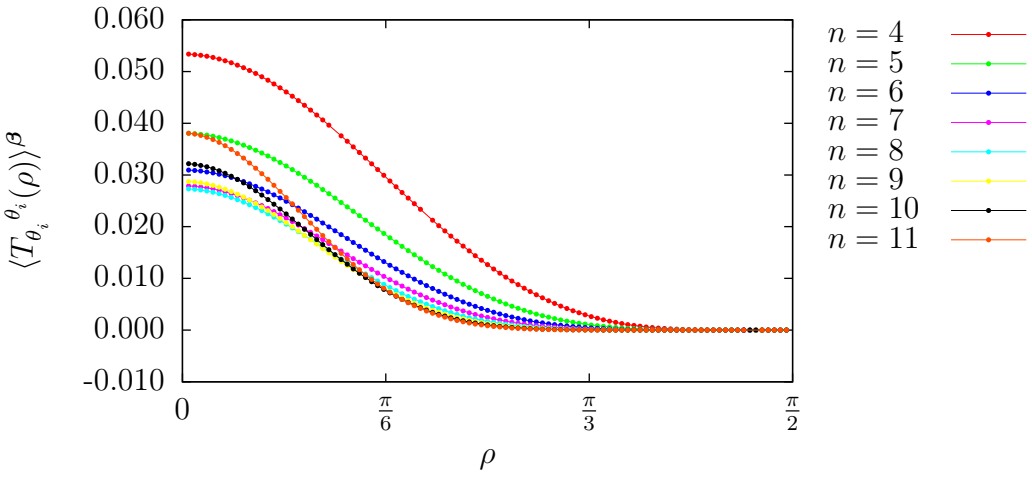

Figure 7.7 – $\langle T_{\theta_i}{}^{\theta_i}(\rho)\rangle^{\boldsymbol{\beta}}$ for varying n with $\mu = \mu_{\text{mc}}$ and $a = \boldsymbol{\beta} = 1$

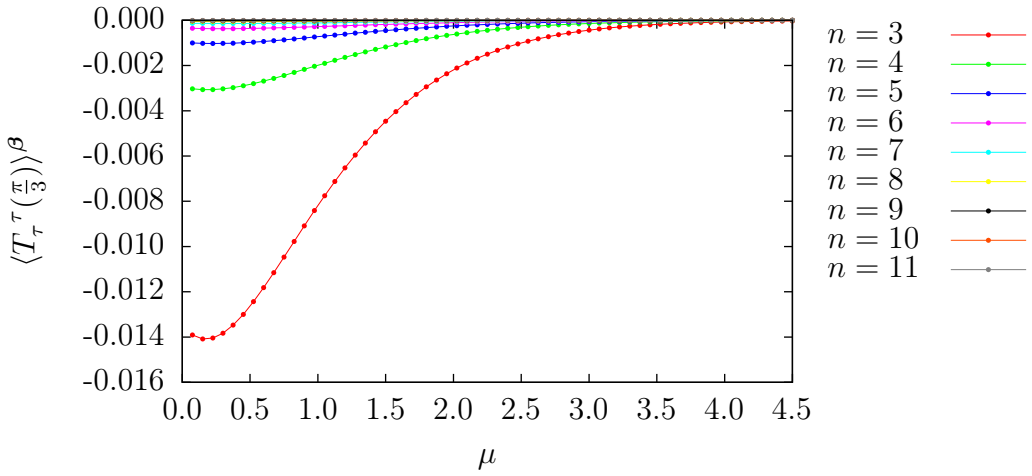

FIGURE 7.8 – $\langle T_\tau{}^\tau(\rho)\rangle^{\boldsymbol{\beta}}$ for varying n and μ with $\rho = \frac{\pi}{3}$, $\xi = 0.1$ and $a = \boldsymbol{\beta} = 1$

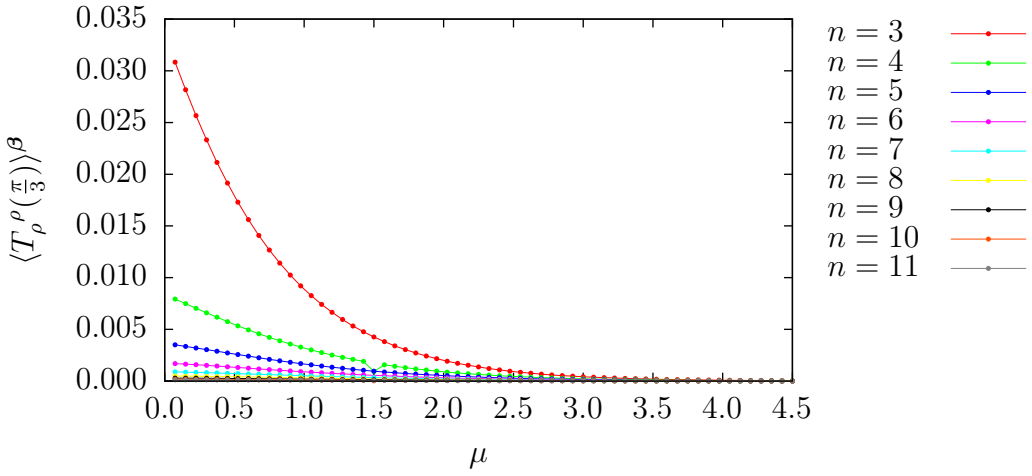

FIGURE 7.9 – $\langle T_\rho{}^\rho(\rho)\rangle^{\boldsymbol{\beta}}$ for varying n and μ with $\rho = \frac{\pi}{3}$, $\xi = 0.1$ and $a = \boldsymbol{\beta} = 1$

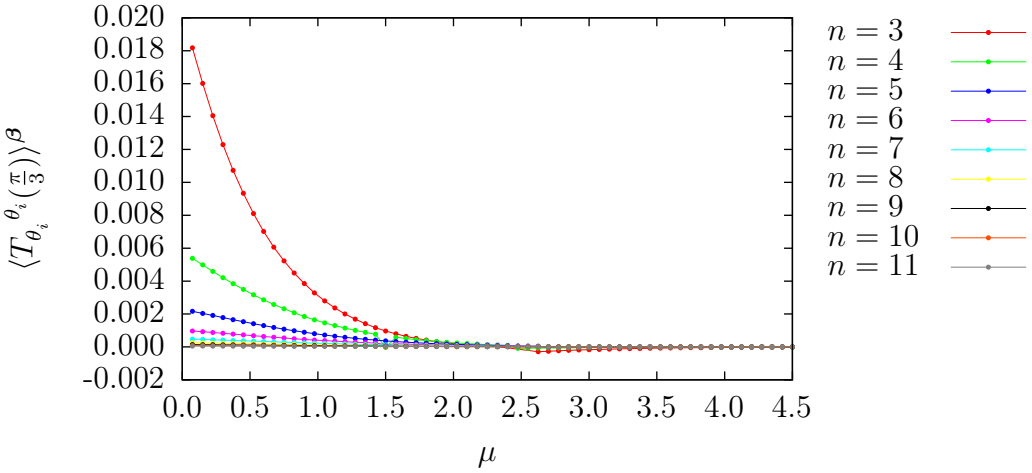

FIGURE 7.10 – $\langle T_{\theta_i}{}^{\theta_i}(\rho)\rangle^{\boldsymbol{\beta}}$ for varying n and μ with $\rho = \frac{\pi}{3}$, $\xi = 0.1$ and $a = \boldsymbol{\beta} = 1$

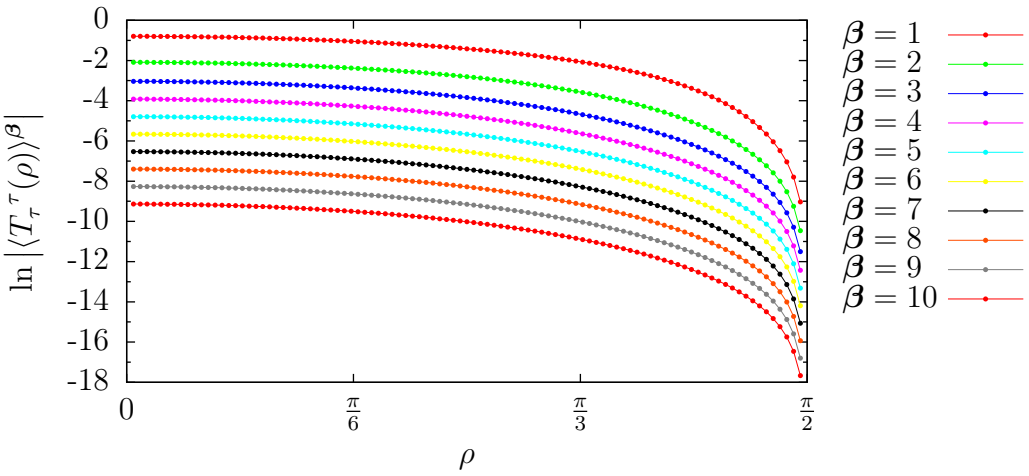

FIGURE 7.11 – $\ln\left|\langle T_\tau{}^\tau(\rho)\rangle^{\boldsymbol{\beta}}\right|$ for varying $\boldsymbol{\beta}$ with $n = 4$, $\mu = \mu_{\text{mc}}$, and $a = 1$

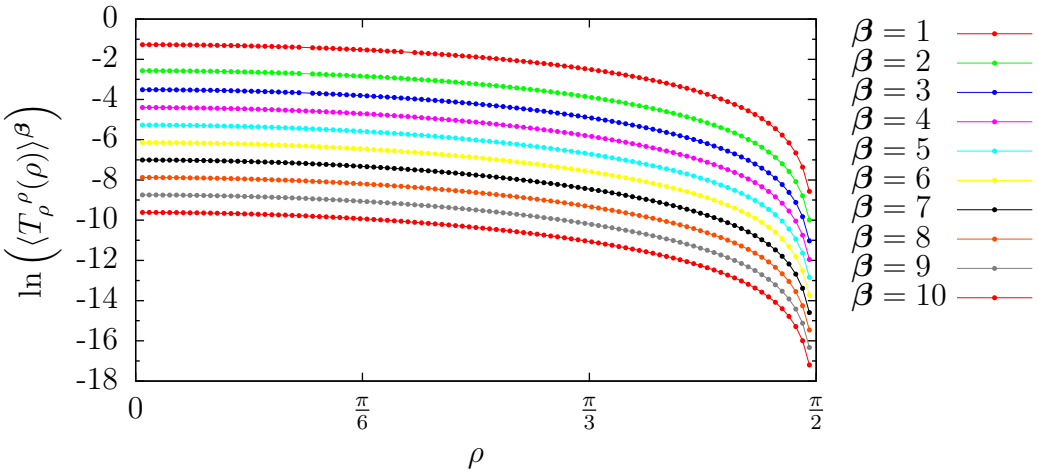

FIGURE 7.12 – $\ln\left(\langle T_\rho{}^\rho(\rho)\rangle^{\boldsymbol{\beta}}\right)$ for varying $\boldsymbol{\beta}$ with $n = 4$, $\mu = \mu_{\text{mc}}$, and $a = 1$

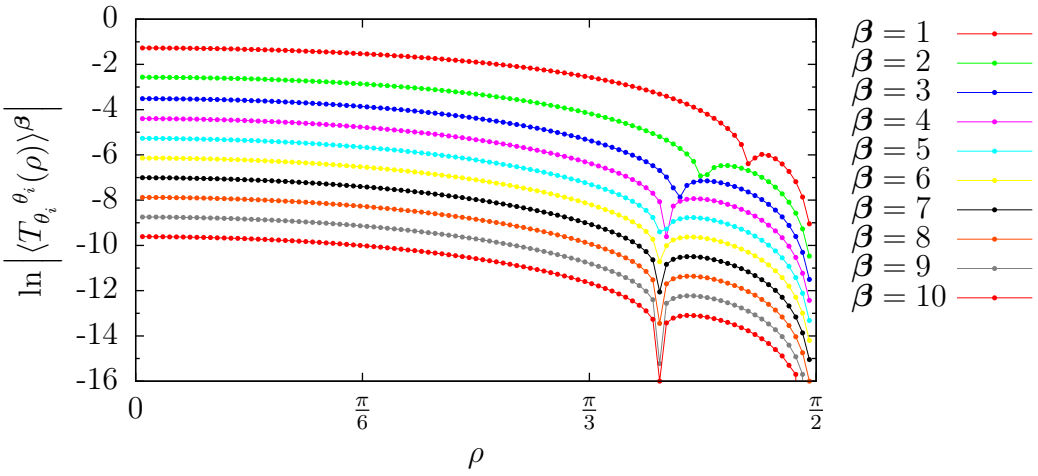

FIGURE 7.13 – $\left|\langle T_{\theta_i}{}^{\theta_i}(\rho)\rangle^{\boldsymbol{\beta}}\right|$ for varying $\boldsymbol{\beta}$ with $n = 4$, $\mu = \mu_{\text{mc}}$, and $a = 1$

8 | Conclusions

This thesis covers recent research into a free, massive quantum scalar field generally-coupled to AdS_n. Accordingly, the practical goals of this effort have been to determine:

- the Hadamard renormalised vacuum expectation values of the quadratic fluctuations $\langle\Phi^2\rangle_{\text{ren}}$ and stress-energy tensor $\langle T_{\mu\nu}\rangle_{\text{ren}}$;
- the Hadamard renormalised rotational vacuum expectation values of the quadratic fluctuations $\langle\Phi^2\rangle^{\boldsymbol{\Omega}}_{\text{ren}}$ and stress-energy tensor $\langle T_{\mu\nu}\rangle^{\boldsymbol{\Omega}}_{\text{ren}}$;
- the thermal expectation values of the quadratic fluctuations $\langle\Phi^2(x)\rangle^{\boldsymbol{\beta}}$ the stress-energy tensor $\langle T_{\mu\nu}(x)\rangle^{\boldsymbol{\beta}}$;
- the rotational thermal expectation values of the quadratic fluctuations $\langle\Phi^2(x)\rangle^{\boldsymbol{\Omega\beta}}$ and stress-energy tensor $\langle T_{\mu\nu}(x)\rangle^{\boldsymbol{\Omega\beta}}$.

Analytical expressions for the Hadamard renormalised vacuum expectation values $\langle\Phi^2\rangle_{\text{ren}}$ and $\langle T_{\mu\nu}\rangle_{\text{ren}}$ have been obtained explicitly using code written in MAPLE for $n = 2$ to $n = 11$ – see (5.36 – 5.45) and (5.98 – 5.107) respectively. In principle this code can be extended to any n with sufficient computational power. Since there appears to be no published results on higher-dimensional Hadamard renormalised expectation values, the results present in this thesis are possibly the first examples of such work.

Before renormalising, a significant amount of time and effort was spent on verifying the published methods for the calculation of the n-dimensional Feynman Green function on AdS_n – see chapters 3 and 4. Allen & Jacobson's method (see section 4.2.2.I.)

solves the scalar field wave equation on AdS_n (4.4) by exploiting maximal symmetry, reducing the problem to a second-order ODE given by (4.17). The other method (see section 4.2.1) constructs the Feynman Green function, $G_{\rm F}(s)$ by summing over the field modes.

The verification of these results was motivated by a slight discrepancy in the literature between Burgess & Lütken and Cotăescu [16] [25] relating to the form of the modes. Since Hadamard renormalisation is performed with $G_{\rm F}(s)$, which may be constructed directly by summing over the field modes, it has been necessary to resolve this discrepancy first.

Having validated Cotăescu's modes [25] (see (3.71)), the expression for $G_{\rm F}(s)$ in [4] has been found to agree with its counterpart in [16] (when summing over Cotăescu's modes).

Camporesi's derivation of $G_{\rm F}(s)$ for $n = 4$ [19], has then been generalised to $n \geq 2$ (see 4.2.2.II.), having noticed its form lends itself well to renormalisation by affording a clear singularity structure. Properties of hypergeometric functions present in the expression (4.55) have then been exploited to generate expansions in s (or some function $z(s)$) near $s = 0$ for the regularisation of $G_{\rm F}(s)$ (see section 4.3).

The Hadamard form of $G_{\rm F}(s)$ has also been obtained explicitly following Décanini & Folacci [31] (see section 4.4). The subsequent Hadamard renormalisation (see chapter 5) has resulted in expressions for $\langle T_{\mu\nu} \rangle_{\rm ren}$ in (5.98 – 5.107) that are shown to satisfy Wald's axioms for uniqueness (5.90) and to exhibit the trace anomaly for even n – see (5.112 – 5.121).

In the case of rotational vacuum states, a condition has been established on the angular velocity of the rigidly rotating reference frame to ensure that the associated rotational modes (6.22) are consistent with the commutation relations determined by

the irrotational modes. Under this constraint, the rotational anti-commutator function $G^{\mathbf{\Omega}}_{(1)}(s)$ has been found to coincide formally with the anti-commutator function for a static observer $G_{(1)}(s)$ (7.16).

The irrotational thermal anti-commutator function, $G^{\boldsymbol{\beta}}_{(1)}(x, x')$ has been found using standard results (see e.g. [11]). Finite temperature breaks the radial symmetry of AdS_n and furnishes a Planck factor which renders it necessary to evaluate the thermal expectation values numerically.

Explicit results for $\langle \Phi^2(x) \rangle^{\boldsymbol{\beta}}$ and $\langle T_{\mu\nu}(x) \rangle^{\boldsymbol{\beta}}$ have been plotted for $n = 3$ to $n = 11$ inclusive, for a variety of parameters (see figures 7.1 – 7.9) and corroborate results in [3] for the massless, conformally-coupled case for $n = 4$. The data used was generated by code written in MATHEMATICA.

At present, work on rotational thermal expectation values is ongoing. The preceding studies of rotation and temperature suggest a straightforward extension of the numerics used to obtain the irrotational thermal expectation values.

Since each expectation value of the stress-energy tensor obtained relates to the matter content of a *free* field theory, it follows that they each determine the semi-classical Einstein equations (1.3) completely, effectively defining a self-consistent theory of quantum gravity by providing the necessary 'one-loop' quantum correction to the cosmological constant.

This research is intended in part as a precursor to research into asymptotically AdS_n black hole space-times, focusing at first on Schwarzschild black holes, with the aim of introducing rotation as a further complication.

In particular, it is known that for a scalar field propagating on some static, spherically symmetric space-time that is asymptotically equivalent to some maximally symmetric space-time, $\langle \Phi^2(x) \rangle_{\text{ren}}$ has a part which can be expressed analytically

and a part which has to be evaluated numerically.

Breen & Ottewill have developed numerical techniques for calculating $\langle \Phi^2(x) \rangle$ for general spherically symmetric black holes [13], a refinement of an approach due to Anderson, Hiscock & Samuel [5]. However, these techniques fail for asymptotically AdS_n black holes, because at spatial infinity *all* modes of the scalar field contribute.

It is therefore hoped that the research presented in this thesis will contribute to the study of the analytical part of renormalised objects in Schwarzschild-anti de Sitter space-time.

References

[1] Abbiendi, G. *et al.* Precise determination of the Z resonance parameters at LEP: 'Zedometry'. *Eur. Phys. J.* (2001), 587–661.

[2] Abramowitz, M., and Stegun, I. A. *Handbook of mathematical functions.* U.S. Government Printing Office, Washington D.C., 1972. Tenth printing (with corrections).

[3] Allen, B., Folacci, A., and Gibbons, G. W. Anti-de Sitter space at finite temperature. *Phys. Lett. B 189* (1987), 304–310.

[4] Allen, B., and Jacobson, T. Vector two-point functions in maximally symmetric spaces. *Commun. Math. Phys. 103* (1986), 669–692.

[5] Anderson, P. A., Hiscock, W., and Samuel, D. Stress-energy tensor of quantized scalar fields in static black hole spacetimes. *Phys. Rev. Lett. 70* (1993), 1739.

[6] Arkani–Hamed, N., Dimopoulos, S., and Dvali, G. The hierarchy problem and new dimensions at a millimeter. *Phys. Lett. B 429* (1998), 263–272.

[7] Ashby, N. Relativity in the Global Positioning System. *Living Rev. Relativity 1* (2003), 1–42.

[8] ATLAS Collaboration. Observation of a new particle in the search for the Standard Model Higgs boson with the ATLAS detector at the LHC. *Phys. Lett. B 716* (2012), 1–29.

[9] Avis, S. J., Isham, C. J., and Storey, D. Quantum field theory in anti-de Sitter space-time. *Phys. Rev. D 18* (1978), 3565–3576.

[10] Bengtsson, I. Anti-de Sitter space. *http://www.physto.se/~ingemar/Kurs.ps*, 2009.

[11] Birrell, N. D., and Davies, P. C. W. *Quantum fields in curved space.* Cambridge Monographs on Mathematical Physics. Cambridge University Press, Cambridge, 1984. First paperback edition (with corrections).

[12] Breen, C., and Ottewill, A. C. Extended Green-Liouville asymptotics and vacuum polarization for lukewarm black holes. *Phys. Rev. D 82* (2010), 084019.

[13] Breen, C., and Ottewill, A. C. Hadamard renormalization of the stress energy tensor on the horizons of a spherically symmetric black hole space-time. *Phys. Rev. D 85* (2012), 064026.

[14] Breitenlohner, P., and Freedman, D. Z. Stability in gauge extended supergravity. *Ann. Phys. (N. Y.) 144* (1982), 249–281.

[15] Burges, C. J. C., Davis, S., Freedman, D. Z., and Gibbons, G. W. Supersymmetry in anti-de Sitter space. *Ann. Phys. (N.Y.) 167* (1986), 285–316.

[16] Burgess, C. P., and Lütken, C. A. Propagators and effective potentials in anti-de Sitter space. *Phys. Lett. 153B* (1985), 137–141.

[17] Caldarelli, M. M. Quantum scalar fields on anti-de Sitter space-time. *Nucl. Phys. B 549* (1999), 499–515.

[18] Callan, C. G., Coleman, S., and Jackiw, R. A new improved energy-momentum tensor. *Ann. Phys. 59* (1970), 42–73.

[19] Camporesi, R. ζ-function regularization of one-loop effective potentials in anti-de Sitter spacetime. *Phys. Rev. D 43* (1991), 3958–3965.

[20] Candelas, P., and Raine, D. D. Feynmann propagator in curved spacetime. *Phys. Rev. D 15* (1977), 1494–1500.

[21] Casimir, H. B. G. On the attraction between two perfectly conducting plates. *Proc. Kon. Nederland. Akad. Wetensch. B 51* (1948), 793–795.

[22] Christensen, S. M. Vacuum expectation value of the stress tensor in an arbitrary curved background: The covariant point-separation method. *Phys. Rev. D 10* (1976), 2490–2501.

[23] Cornil, J., and Testud, P. *An Introduction to Maple V.* Springer-Verlag, Berlin, 2001.

[24] Cotăescu, I. I. Comment on the quantum modes of the scalar field on AdS_{d+1} spacetime. *arXiv:gr-qc/9903.029v1* (1999).

[25] Cotăescu, I. I. Remarks on the quantum modes of the scalar field on AdS_{d+1} spacetime. *Phys. Rev. D 60* (1999), 107504.

[26] Cummins, C. J., Fulling, S. A., King, R. C., and Wybourne, B. G. Normal forms for tensor polynomials: I. The Riemann tensor. *Class. Quantum Grav. 9* (1992), 1151–1197.

[27] Davies, P. C. W. Scalar production in Schwarzschild and Rindler metrics. *J. Phys. A 8* (1975), 609–616.

[28] Davies, P. C. W., Dray, T., and Manogue, C. A. Detecting the rotating quantum vacuum. *Phys. Rev. D 53* (1996), 4382–4387.

[29] Décanini, Y., and Folacci, A. Off-diagonal coefficients of the DeWitt-Schwinger and Hadamard representations of the Feynman propagator. *Phys. Rev. D 73* (2006), 044027.

[30] Décanini, Y., and Folacci, A. FKWC-bases and geometrical identities for classical and quantum field theories in curved spacetimes. *arXiv:gr-qc/0805.1595v1* (2008).

[31] Décanini, Y., and Folacci, A. Hadamard renormalization of the stress-energy tensor for a quantized scalar field in a general spacetime of arbitrary dimension. *Phys. Rev. D 78* (2008), 044025.

[32] DeWitt, B. S. *Dynamical theory of groups and fields*. Documents on Modern Physics. Blackie & Son Ltd., London, 1965.

[33] DeWitt, B. S. Quantum field theory in curved spacetime. *Phys. Rep. 19* (1975), 295–357.

[34] Duffy, G., and Ottewill, A. C. Rotating quantum thermal distribution. *Phys. Rev. D 67* (2003), 044002.

[35] Ehrenfest, P., and Tolman, R. C. Temperature equilibrium in a static gravitational field. *Phys. Rev. 36* (1930), 1791–1798.

[36] Ellis, G. F. R., and Hawking, S. W. *The large scale structure of space-time*. Cambridge Monographs on Mathematical Physics. Cambridge University Press, Cambridge, 1973.

[37] Erdélyi, A., Ed. *Higher transcendental functions*, vol. 2. McGraw-Hill, New York, 1953.

[38] Erdélyi, A., Ed. *Higher transcendental functions*, vol. 1. McGraw-Hill, New York, 1953.

[39] Fewster, C. J., and Roman, T. A. On wormholes with arbitrarily small quantities of exotic matter. *Phys. Rev. D 72* (2005), 044023.

[40] Fogwell, S., Gabrielse, G., and Hanneke, D. New measurement of the electron magnetic moment and the fine structure constant. *Phys. Rev. Lett. 100* (2008), 120801.

[41] Ford, L. H. Quantum coherence effects and the second law of thermodynamics. *Proc. R. Soc. Lond. A 364* (1978), 227–236.

[42] Fulling, S. A. Nonuniqueness of canonical field quantization in Riemannian space-time. *Phys. Rev. D 7* (1973), 2850–2862.

[43] Fulling, S. A. *Aspects of quantum theory in curved space-time*. Cambridge University Press, Cambridge, 1989.

[44] Gell-Mann, M. A schematic model of baryons and mesons. *Phys. Lett. 8* (1964), 214–215.

[45] Gradsteyn, I. M., and Ryzhik, I. S. *Table of integrals, series, and products*. Academic Press, New York, 2000. Sixth edition, revised.

[46] Griffiths, J. B., and Podolskỳ, J. *Exact space-times in Einstein's general relativity*. Cambridge Monographs on Mathematical Physics. Cambridge University Press, Cambridge, 2009.

[47] Hadamard, J. S. *Lectures on Cauchy's problem in linear partial differential equations*. Dover Publications, Mineola, New York, 2003.

[48] Hansen, E. R. *A table of series and products*. Prentice-Hall, Englewood Cliffs, N. J., 1975.

[49] Hawking, S. W. Black hole explosions? *Nature 248* (1974), 30–31.

[50] Hawking, S. W. Particle creation by black holes. *Commun. Math. Phys. 43* (1975), 199–220.

[51] Hawking, S. W., and Page, D. N. Thermodynamics of black holes in anti-de Sitter space. *Commun. Math. Phys. 87* (1983), 577–588.

[52] Kanti, P. Black holes in theories with large extra dimensions: A review. *Int. J. Mod. Phys. A 19* (2004), 4899–4951.

[53] Kiefer, C. *Quantum gravity.* No. 136 in International Series of Monographs of Physics. Oxford University Press, Oxford, 2007. Second edition.

[54] Letaw, J. R., and Pfautsch, J. D. Quantized scalar field in the stationary coordinate systems of flat spacetime. *Phys. Rev. D 24* (1981), 1491–1498.

[55] Maldacena, J. M. The large n limit of superconformal field theories and supergravity. *Adv. Theor. Math. Phys. 2* (1998), 231–252.

[56] Misner, C. W., Thorne, K. S., and Wheeler, J. A. *Gravitation.* W. H. Freeman, 1973. Second printing edition.

[57] Morette, C. On the definition and approximation of Feynman's path integrals. *Phys. Rev. 81* (1951), 848–852.

[58] Moretti, V. Comments on the stress-energy tensor operator in curved spacetime. *Commun. Math. Phys. 232* (2003), 189–221.

[59] Moschella, U. *Seminaire Poincaré 2005: Einstein, 1905–2005*, vol. 47 of *Progress in Mathematical Physics.* Birkhäuser Verlag, Basel, 2006, ch. 4. 'The de Sitter and anti-de Sitter sightseeing tour', pp. 120–133.

[60] Mukhanov, V. F., and Winitzki, S. *Introduction to quantum effects in gravity.* Cambridge University Press, Cambridge, 2007.

[61] Müller, C. *Spherical harmonics.* Lecture notes in mathematics. Springer-Verlag, Berlin/ Heidelberg, 1966.

[62] Padmanabhan, T. Semiclassical approximations for gravity and the issue of backreaction. *Class. Quantum Grav. 6* (1989), 533–555.

[63] Pöschl, G., and Teller, E. Bemerkungen zur Quantenmechanik des anharmonischen Oszilltators. *Z. Phys. 83* (1933), 143–151.

[64] Rovelli, C. *Quantum gravity.* Cambridge Monographs on Mathematical Physics. Cambridge University Press, Cambridge, 2004.

[65] Schwarz, J. H. Introduction to superstring theory. *arXiv:hep-ex/0008017* (2000).

[66] Schwinger, J. On gauge invariance and vacuum polarization. *Phys. Rev. 82* (1951), 664–679.

[67] Stephani, H. *Relativity.* Cambridge University Press, Cambridge, 2004. Third edition.

[68] Synge, J. L. *Relativity: the general theory.* North-Holland Publishing Company, Amsterdam, 1960.

[69] Taylor, J. H., and Weisberg, J. M. The relativistic binary pulsar B1913+16: Thirty years of observations and analysis. *Binary Radio Pulsars 328* (2005), 25–32.

[70] Tian, W. J. Bound states of Klein-Gordon and Dirac equations with type-I vector and scalar Pöschl-Teller potentials. *Sciencepaper Online DOI: 200910-186* (2009).

[71] Tolman, R. C. On the weight of heat and thermal equilibrium in general relativity. *Phys. Rev. 35* (1930), 904–924.

[72] Unruh, W. G. Notes on black-hole evaporation. *Phys. Rev. D 14* (1976), 870–892.

[73] VAN VLECK, J. H. The correspondence principle in the statistical interpretation of quantum mechanics. *Proc. Nat. Acad. Sci. 14* (1928), 178–188.

[74] VISSER, M. van Vleck determinants: Geodesic focusing in Lorentzian spacetimes. *Phys. Rev. D 47* (1993), 2395–2402.

[75] WALD, R. M. The back reaction effect in particle creation in curved spacetime. *Commun. Math. Phys. 54* (1977), 1–19.

[76] WALD, R. M. On the Euclidean approach to quantum field theory in curved spacetime. *Commun. Math. Phys. 70* (1979), 221–242.

[77] WALD, R. M. *General relativity.* Chicago University Press, Chicago, 1984.

[78] WALD, R. M. *Quantum field theory in curved spacetime and black hole thermodyamics.* Chicago Lectures in Physics. Chicago University Press, Chicago, 1994.

[79] WITTEN, E. Anti de Sitter space and holography. *Adv. Theor. Math. Phys 2* (1998), 253–291.

[80] ZWEIG, G. An $SU(3)$ model for strong interaction symmetry and its breaking. *CERN 8181-TH-401* (1964).